

NUREG/CR-6100
INEL-94/0156

Gate Valve and Motor-Operator Research Findings

Prepared by
R. Steele, Jr., K. G. DeWall, J. C. Watkins, M. J. Russell, D. Bramwell

Idaho National Engineering Laboratory
Lockheed Idaho Technologies Company

Prepared for
U.S. Nuclear Regulatory Commission

9510060250 950930
PDR NUREG
CR-6100 R PDR

AVAILABILITY NOTICE

Availability of Reference Materials Cited in NRC Publications

Most documents cited in NRC publications will be available from one of the following sources:

1. The NRC Public Document Room, 2120 L Street, NW., Lower Level, Washington, DC 20555-0001
2. The Superintendent of Documents, U.S. Government Printing Office, P. O. Box 37082, Washington, DC 20402-9328
3. The National Technical Information Service, Springfield, VA 22161-0002

Although the listing that follows represents the majority of documents cited in NRC publications, it is not intended to be exhaustive.

Referenced documents available for inspection and copying for a fee from the NRC Public Document Room include NRC correspondence and internal NRC memoranda; NRC bulletins, circulars, information notices, inspection and investigation notices; licensee event reports; vendor reports and correspondence; Commission papers; and applicant and licensee documents and correspondence.

The following documents in the NUREG series are available for purchase from the Government Printing Office: formal NRC staff and contractor reports, NRC-sponsored conference proceedings, international agreement reports, grantee reports, and NRC booklets and brochures. Also available are regulatory guides, NRC regulations in the *Code of Federal Regulations*, and *Nuclear Regulatory Commission Issuances*.

Documents available from the National Technical Information Service include NUREG-series reports and technical reports prepared by other Federal agencies and reports prepared by the Atomic Energy Commission, forerunner agency to the Nuclear Regulatory Commission.

Documents available from public and special technical libraries include all open literature items, such as books, journal articles, and transactions, *Federal Register* notices, Federal and State legislation, and congressional reports can usually be obtained from these libraries.

Documents such as theses, dissertations, foreign reports and translations, and non-NRC conference proceedings are available for purchase from the organization sponsoring the publication cited.

Single copies of NRC draft reports are available free, to the extent of supply, upon written request to the Office of Administration, Distribution and Mail Services Section, U.S. Nuclear Regulatory Commission, Washington, DC 20555-0001.

Copies of industry codes and standards used in a substantive manner in the NRC regulatory process are maintained at the NRC Library, Two White Flint North, 11545 Rockville Pike, Rockville, MD 20852-2738, for use by the public. Codes and standards are usually copyrighted and may be purchased from the originating organization or, if they are American National Standards, from the American National Standards Institute, 1430 Broadway, New York, NY 10018-3308.

DISCLAIMER NOTICE

This report was prepared as an account of work sponsored by an agency of the United States Government. Neither the United States Government nor any agency thereof, nor any of their employees, makes any warranty, expressed or implied, or assumes any legal liability or responsibility for any third party's use, or the results of such use, of any information, apparatus, product, or process disclosed in this report, or represents that its use by such third party would not infringe privately owned rights.

Gate Valve and Motor-Operator Research Findings

Manuscript Completed: April 1995
Date Published: September 1995

Prepared by
R. Steele, Jr., K. G. DeWall, J. C. Watkins, M. J. Russell, D. Bramwell

Idaho National Engineering Laboratory
Managed by the U.S. Department of Energy

Lockheed Idaho Technologies Company
Idaho Falls, ID 83415

G. H. Weidenhamer, NRC Project Manager

Prepared for
Division of Engineering Technology
Office of Nuclear Regulatory Research
U.S. Nuclear Regulatory Commission
Washington, DC 20555-0001
NRC Job Code A6857

ABSTRACT

This report provides an update on the valve research being sponsored by the U.S. Nuclear Regulatory Commission (NRC) and conducted at the Idaho National Engineering Laboratory (INEL). The research addresses the need to provide assurance that motor-operated valves are able to perform their intended safety function, usually to open or close against specified (design basis) flow and pressure loads. This report describes several important developments:

- Two methods for estimating or bounding the design basis stem factor (in rising-stem valves), using data from tests less severe than design basis tests
- A new correlation for evaluating the opening responses of gate valves and for predicting opening requirements
- An extrapolation method that uses the results of a best effort flow test to estimate the design basis closing requirements of a gate valve that exhibits atypical responses (peak force occurs before flow isolation)
- The extension of the original INEL closing correlation to include low-flow and low-pressure loads.

The report also includes a general approach, presented in step-by-step format, for determining operating margins for rising-stem valves (gate valves and globe valves) as well as quarter-turn valves (ball valves and butterfly valves).

CONTENTS

ABSTRACT	iii
LIST OF FIGURES	vii
LIST OF TABLES	xi
EXECUTIVE SUMMARY	xiii
ACKNOWLEDGMENTS	xv
1. INTRODUCTION	1-1
1.1 Research Methods	1-1
1.2 Research Objectives	1-1
1.3 Research Results	1-1
2. MOTOR-OPERATED VALVE OPERATING MARGINS	2-1
2.1 Understanding How Valve Operators Work	2-1
2.2 Getting the Information Necessary for Determining MOV Margins	2-2
2.3 An Approach to Determining Operating Margins	2-4
2.3.1 Gather Specific Information	2-4
2.3.2 Initial Calculations	2-5
2.3.3 In Situ Test at Static Conditions.	2-10
2.3.4 In Situ Test at Dynamic Conditions.	2-10
2.3.5 Final Calculations for Estimating MCV Margins.	2-11
2.3.6 Overstress Margins.	2-14
2.4 Changes in the Operating Margin	2-14
2.4.1 Changes in the Calculated Margin	2-14
2.4.2 Changes in the Actual Margin.	2-15
2.5 Conclusions	2-15
3. DISC LOAD	3-1
3.1 Typical Valve Responses During Closure Against Lower Loads	3-2
3.1.1 Test Data From a Utility Valve Test Program.	3-2
3.1.2 Extending the Original INEL Closing Correlation.	3-6
3.1.3 Applying the Extended INEL Closing Correlation.	3-8
3.1.4 Preconditioning.	3-10
3.2 Closing Requirements of Valves with an Atypical Response	3-10

3.2.1	The Cause of Atypical MOV Responses.	3-12
3.2.2	Best Effort Flow Test.	3-18
3.2.3	Extrapolation of Atypical Responses.	3-19
3.3	Opening Requirements	3-21
3.3.1	Analysis of Full-Scale Test Results.	3-22
3.3.2	A Correlation for Evaluating MOV Opening Requirements.	3-25
3.3.3	Estimating an Atypical Opening Response.	3-33
3.4	Conclusions	3-33
4.	STEM FACTOR	4-1
4.1	Results of Full-Scale Valve Testing	4-2
4.2	Testing on the MOVLS	4-3
4.3	The Threshold Method	4-8
4.4	The Fold Line Method	4-10
4.5	Conclusions	4-25
5.	ELECTRIC MOTOR TESTING	5-1
5.1	Motor Performance Curves	5-1
5.2	Degraded Voltage	5-4
5.3	Elevated Temperatures	5-10
5.4	Motor-Operator Gearbox Performance	5-15
5.5	Conclusions	5-18
6.	GENERAL CONCLUSIONS	6-1
7.	REFERENCES	7-1
	Appendix A—Nebula EP-1 Lubricant Analyses for the Eight Tested Stems	A-1

LIST OF FIGURES

2-1.	Simplified diagram of the key components of a Limitorque motor operator	2-1
2-2.	Flow chart illustrating the process for determining the torque margins for quarter-turn and rising-stem valves	2-6
2-3.	Flow chart illustrating the process for determining the thrust margins for rising-stem valves	2-7
3-1.	Results from testing a 14-in. 600-lb-class valve at a utility	3-2
3-2.	Disc factor plotted against differential pressure for the 14-in. utility valve. Tests at higher differential pressure show a more consistent disc factor	3-3
3-3.	Disc load versus dynamic stem load; data fit for tests performed with the valve in the vertical position	3-4
3-4.	Disc load versus dynamic stem load; data fit for tests performed with the valve in the horizontal position	3-4
3-5.	Same plot as Figure 3-3, modified to show one of the causes of the data scatter shown in Figure 3-2	3-5
3-6.	Same plot as Figure 3-4, modified to show one of the causes of the data scatter shown in Figure 3-2	3-6
3-7.	INEL closing correlation extended to include low disc loadings	3-7
3-8.	Extended INEL closing correlation with data from utility testing	3-9
3-9.	Stem thrust trace for a closure test, showing the classic, typical response. The peak thrust before wedging is at flow isolation	3-11
3-10.	Stem thrust trace for a closure test showing an atypical response. The peak thrust before wedging is before flow isolation	3-12
3-11.	A guide-restrained tipped disc	3-14
3-12.	A seat-restrained tipped disc	3-14
3-13.	Stem thrust trace showing a jagged shape, indicating valve damage	3-15
3-14.	Stem thrust trace showing a hook shape in the response and showing evidence of valve damage	3-15
3-15.	Stem thrust trace from testing of a 6-in. service water valve closing against design basis flow. The trace shows an atypical response, but no damage occurred	3-16
3-16.	Valve disc cross-section showing horizontal and vertical forces acting on the disc and stem, as identified by the standard industry equation	3-16

3-17. Valve disc cross-section showing additional vertical forces acting on the disc, identified as F_{top} and F_{bot} in the INEL correlation	3-17
3-18. Disc areas that the various pressures act on; as the disc tips, these areas and pressures change	3-18
3-19. Stem thrust trace for partial opening and reclosing. The closing trace shows evidence of a bent guide	3-19
3-20. Stem thrust traces showing how the hook shape was less pronounced during the second test (upper plot, closing stroke) than during the first test (lower plot). Note also that during the partial opening stroke (upper plot), the peak thrust occurs after unwedging and unseating	3-20
3-21. Stem thrust trace recorded during an opening test, showing the classic, typical response	3-22
3-22. Valve 5 stem thrust traces compared to calculations for both opening and closing	3-24
3-23. Valve 6 stem thrust traces compared to calculations for both opening and closing	3-24
3-24. Valve 2 stem thrust traces compared to calculations for both opening and closing for a single phase fluid, cold water	3-26
3-25. Valve 2 stem thrust traces compared to calculations for both opening and closing for a single phase fluid, steam	3-26
3-26. Valve 2 stem thrust traces compared to calculations for both opening and closing for 10°F subcooled water	3-27
3-27. Valve 2 stem thrust traces compared to calculations for both opening and closing for 100°F subcooled water	3-28
3-28. Valve 2 stem thrust traces compared to calculations for both opening and closing for 100°F subcooled water	3-28
3-29. Valve 2 stem thrust traces compared to calculations for both opening and closing for 100°F subcooled water	3-29
3-30. Valve 2 stem thrust traces compared to calculations for both opening and closing for 100°F subcooled water	3-29
3-31. Valve 3 stem thrust traces compared to calculations for both opening and closing for 10°F subcooled water	3-30
3-32. Valve 3 stem thrust traces compared to calculations for both opening and closing for 10°F subcooled water	3-30
3-33. Normalized sliding loads versus normalized normal loads for the opening stroke for gate valves	3-31

3-34.	Stem thrust trace from testing a 6-in. service water valve opening against design basis flow; the trace shows indications of an atypical response just after flow initiation	3-34
4-1.	Four valve tests at the same torque switch setting. At the design basis flow and pressure loads, the valve failed to completely close	4-2
4-2.	The INEL's load simulator for testing valve stems (the MOVLS)	4-4
4-3.	Load-sensitive behavior is simulated on the MOVLS	4-5
4-4.	Simplified diagram showing the key components of a Limitorque motor-operator	4-5
4-5.	Coefficient of friction versus stem load for tests with Moly 101 lubricant; the data scatter decreases as the load increases	4-9
4-6.	Friction data plotted against a normalized load, with coefficient of friction versus stem thread pressure for tests with Moly 101 lubricant	4-9
4-7.	Coefficient of friction versus stem thread pressure for tests with EP-1 lubricant	4-11
4-8.	Coefficient of friction versus load comparing two greases on the same stem	4-11
4-9.	Running coefficients of friction (just before wedging) versus stem thread pressure for three representative stems	4-12
4-10.	Running and wedging (torque switch trip) coefficients of friction versus stem thread pressure for three stems	4-13
4-11.	Wedging transient for Stem 6 (static test, high torque switch setting), with coefficient of friction plotted against thread pressure	4-15
4-12.	Coefficient of friction during the wedging transient for Stem 6, compared to individual data points for running and for torque switch trip	4-15
4-13.	Wedging transients for three representative stems	4-16
4-14.	Stem 6 data compared with Stem 8 data	4-17
4-15.	The fold line method demonstrated in three successive plots of Stem 6 data	4-19
4-16.	The fold line method bounds the performance of Stems 1 and 2	4-20
4-17.	The fold line method bounds the performance of Stems 3 and 4	4-21
4-18.	The fold line method bounds the performance of Stems 7 and 8	4-22
4-19.	The behavior of Stem 5 is different from that of the other stems, but the fold line method still bounds its response	4-23
4-20.	The fold line method bounds the performance of Stem 3 in tests using EP-1 lubricant instead of Moly 101	4-24

4-21. Real-time coefficient of friction data from two pairs of tests at two torque switch settings for Stem 3	4-24
5-1. Manufacturer's motor performance curves for the 5 ft-lb 460-volt ac motor	5-3
5-2. Actual motor performance curves for the 5 ft-lb 460-volt ac motor	5-3
5-3. Manufacturer's motor performance curves for the 25 ft-lb 460-volt ac motor	5-5
5-4. Actual motor performance curves for the 25 ft-lb 460-volt ac motor	5-5
5-5. Manufacturer's motor performance curves for the 60 ft-lb 460-volt ac motor	5-6
5-6. Actual motor performance curves for the 60 ft-lb 460-volt ac motor	5-6
5-7. Actual motor speed versus torque, derived from testing of the 5 ft-lb motor at degraded voltage	5-7
5-8. Actual motor speed versus torque, derived from testing of the 25 ft-lb motor at degraded voltage	5-7
5-9. Actual motor speed versus torque, derived from testing of the 60 ft-lb motor at degraded voltage	5-8
5-10. Actual motor current versus torque, derived from testing of the 5 ft-lb motor at degraded voltage	5-8
5-11. Actual motor current versus torque, derived from testing of the 25 ft-lb motor at degraded voltage	5-9
5-12. Actual motor current versus torque, derived from testing of the 60 ft-lb motor at degraded voltage	5-9
5-13. Actual motor speed versus torque, derived from elevated temperature testing of the 5 ft-lb motor at 100% voltage	5-11
5-14. Actual motor speed versus torque, derived from elevated temperature testing of the 5 ft-lb motor at 80% voltage	5-11
5-15. Actual motor speed versus torque, derived from elevated temperature testing of the 25 ft-lb motor at 100% voltage	5-12
5-16. Actual motor speed versus torque, derived from elevated temperature testing of the 25 ft-lb motor at 80% voltage	5-12
5-17. Actual motor speed versus torque, derived from elevated temperature testing of the 60 ft-lb motor at 100% voltage	5-13
5-18. Actual motor speed versus torque, derived from elevated temperature testing of the 60 ft-lb motor at 80% voltage	5-13
5-19. Actual motor current versus torque, derived from elevated temperature testing of the 60 ft-lb motor at 100% voltage	5-14

5-20. Actual motor current versus torque, derived from elevated temperature testing of the 60 ft-lb motor at 80% voltage	5-14
5-21. Motor torque versus elevated temperature at 100% voltage and 80% voltage, compared with the Limitorque Part 21 prediction	5-16
5-22. Motor current versus elevated temperature at 100% voltage and 80% voltage, compared with the Limitorque Part 21 prediction	5-16
5-23. Actual gearbox efficiency measured during stall testing of the SMB-00 motor operator	5-17
5-24. Actual gearbox efficiency measured during stall testing of the SMB-0 motor operator	5-17
5-25. Actual gearbox efficiency measured during stall testing of the SMB-1 motor operator	5-18

LIST OF TABLES

4-1. Technical data for eight stems and three operators used in the MOVLS test program	4-7
5-1. Matrix for testing of operators and stems on the MOVLS	5-2
5-2. Limitorque Part 21 predictions for loss in performance with increased temperature	5-10

EXECUTIVE SUMMARY

The U.S. Nuclear Regulatory Commission (NRC) is supporting valve research at the Idaho National Engineering Laboratory (INEL). The following objectives provided guidance for the research subjects documented in this report:

- Develop a consistent and uniform approach for evaluating motor-operated valve (MOV) margins
- Determine if the stem factor (the efficiency of the conversion of motor-operator torque to stem thrust) can be predicted and bounded from something less than a design basis test for margins determinations purposes
- Determine how degraded voltage and ambient temperature influence motor stall torques and MOV margins for both ac and dc motors
- Ascertain if there is method for determining whether a gate valve will exhibit atypical behavior.

The authors have conducted original research, reviewed past research results, and reviewed the research results of others to address these objectives.

The research has produced some new findings:

- We discovered that the primary cause of atypical gate valve behavior (stem force peaks before flow isolation in the closing direction or after flow initiation in the opening direction) is tilting of the valve disc in response to flow through the partially open valve. This finding provided the insights for developing new equations for evaluating and extrapolating in situ atypical gate valve performance in both the opening and closing directions.
- Through the review of the test programs of others, we found data that supports extend-

ing the applicability of our original gate valve closing correlation (for valves with typical performance) to loads lower than the previous 400-psi lower limit.

- We have developed two methods for determining the design basis stem factor (efficiency of torque/thrust conversion) from test loads less than design basis loads. These methods address what is known as the rate-of-loading issue. When validated, these methods will support efforts to determine the operating margins of rising-stem motor-operated valves.
- We have completed about 60% of our MOV electric motor and operator performance testing. We have not performed an in-depth analysis of the data, but the preliminary results question some of the design rules used in the past.

We have continued to provide independent review of the Electric Power Research Institute (EPRI) MOV Performance Prediction Program. This program is industry's initiative for predicting valve responses from a prediction model. Through interaction at the regular program status meeting with the NRC, the EPRI program has moved away from a strictly analytical approach and more towards a performance-based program. EPRI has also taken the results of the INEL stem factor work as part of a technology transfer. Battelle Columbus has been commissioned to expand the research sample size and to coordinate with industry how to implement the final product.

Our ASME involvement was successful on two fronts: the qualification of mechanical equipment (QME), and operation and maintenance (OM). The QME family of consensus standards made their way through the comment and approval processes and are expected to be published in 1994.

We are processing the enhanced in situ test data and detailed design information on 12 identical valves. The data are from industry testing

conducted at a domestic nuclear power plant. This effort is part of our grouping study.

We continued our involvement with the MOV Users Group (MUG). We made technical presentations of the results of the NRC research at both the summer and winter sessions. We partici-

pated at the subcommittee level, where NRC research results have helped form the basis for the MUG MOV in situ test acceptance criteria guidance document. This document provides a consensus position on the important elements for both static and dynamic testing of MOVs.

ACKNOWLEDGMENTS

The authors acknowledge the contributions of the following INEL staff who assisted in making this project a success. We thank Geraldine S. Reilly and Christine W. White for their efforts to produce the high quality graphics contained in this report. Technical editing expertise was provided by Julie Steffes and Dave Pack. Typing and layout duties were aptly handled by Cyndie Diehl, Pam Grant, Cathy Willis, Mindy Renfro, and Sandy Criddle. Experimenters need someone to build their toys, and we thank Jim Hall for turning our sometimes less-than-complete drawings into high caliber experimental tools. We thank Jerry Edson for his help with the electrical modifications on the motor-operated valve load simulator and power supply, and Gay Gilbert for her dedication to the laborious task of data collection and reduction. Thanks also to Mark Holbrook for keeping us in touch with reality, and to Mike Nitzel for performing quality control engineering self-assessment.

We also acknowledge the following industry researchers for providing technical review, counsel, and insights, helping to make this work a success. Cooperation extended by Ken Wolfe of the Electric Power Research Institute (EPRI) and EPRI's stem factor researcher Jim Gleeson of Battelle Columbus helped enormously on a number of occasions. Counsel provided by Dr. Claude Thibault of Wyle Laboratories was well taken and very beneficial. Drs. Schauki, Rauffmann, and Simon, and Herren Muser and Knoedler of Siemens provided guidance based on their work in Germany. Steve Bryant and Bob Hough from the Sizewell B nuclear plant in the United Kingdom furnished information from their qualification testing, providing invaluable insights to a number of qualification issues. We thank Doug Jones of Grand Gulf Nuclear Power Station, and Tom Rak and Lee Kelly of Trojan Nuclear Power Plant for sharing their test loop and in-plant test data with us.

We thank Mark Smith and Mike Bailey from Limitorque, who provided valuable technical information and reviewed our research, providing comments and insights.

We also thank Dr. G. H Weidenhamer and his NRC Valve Review Group; they patiently labored through our development of the various elements of this report, providing guidance, council, and suggestions that helped us stay on track.

Gate Valve and Motor-Operator Research Findings

1. INTRODUCTION

The Idaho National Engineering Laboratory (INEL) is performing motor-operated valve (MOV) research in support of the U.S. Nuclear Regulatory Commission's (NRC) efforts regarding the implementation of Generic Letter 89-10, "Safety-Related Motor-Operated Valve Testing and Surveillance." This report updates the research reported in NUREG/CR-5720, *Motor-Operated Valve Research Update*, published in June 1992.

1.1 Research Methods

The research methods used to meet the objectives stated below include literature review, field and laboratory testing, engineering analysis, peer review, and NRC Program Manager review.

1.2 Research Objectives

Research objectives included:

- Develop a consistent and uniform approach for evaluating MOV operating margins
- Determine if the stem factor (the efficiency of the conversion of motor-operator torque to stem thrust) can be predicted and bounded from the results of tests conducted at conditions less severe than a design basis test
- Determine how degraded voltage and ambient temperature influence motor stall torques and MOV margins for both ac and dc motors
- Ascertain if there is method for determining whether a gate valve will exhibit atypical behavior.

1.3 Research Results

Our work this past year has produced some important breakthroughs in two research areas identified in the research objectives. One of these

areas is the stem factor issue (the stem factor represents the conversion of operator torque to stem thrust in rising-stem valves), and the other is atypical behavior in gate valves (the occurrence in some valves of a peak stem force response before flow isolation in the closing direction and after flow initiation in the opening direction, formerly described as nonpredictable behavior). In addition, we completed 60% of our electric motor, under-voltage, and operator testing; a preliminary look at the results of that work is included in this report. Our work in these three research areas supports the first objective, the development of a consistent and uniform method to evaluate motor-operated valve margins. These three issues (stem factor, typical/atypical responses, electric motor capability and operator efficiency) represent some of the most troublesome variables in evaluations of valve operability margins. The research results have helped us toward defining the margins issue.

In addition to that work, we provided an independent review of a large, full-scale valve test program, the Electric Power Research Institute (EPRI) MOV Performance Prediction Program. We also completed the second iteration of the Isolation Valve Assessment (IVA) software package to the point where it is in the external test phase. This software package (Watkins et al. 1994) brings together all the important findings from our research and presents them in a user-friendly format to provide guidance and perform calculations in MOV evaluations. Also, we started to process the enhanced in situ test data and detailed design information on about a dozen like valves tested by industry; this work was part of a grouping study to develop criteria that might be used to group similar valves for the purpose of testing only a sample of the group to meet the intent of the recommendations of Generic Letter 89-10. Our ASME involvement was successful on both fronts: the qualification of mechanical equipment (QME), and operation and maintenance (OM). The QME family of qualification consensus standards made

their way through the comment and approval processes and were issued in June 1994. Interaction with the Motor-Operated Valve Users Group (MUG) continued; we made technical presentations to audiences of more than 300 people at the summer and winter MUG meetings. We were heavily involved at the MUG subcommittee level in the development of the MOV in situ test acceptance criteria guidance document, which includes a consensus position on the important elements for evaluation of both static and dynamic MOV test results. NRC research results contributed to several sections of that document.

The following sections of this report address four of the objectives listed above. Section 2

discusses operating margins for MOVs and presents a method for evaluating margins. Section 3 addresses typical versus atypical responses in the disc load of gate valves in both the opening and closing directions, and proposes methods for predicting or bounding the design basis responses. Section 4 addresses the stem factor issue and proposes two methods for using the results of tests conducted at conditions less severe than design basis conditions to predict or bound the design basis stem factor. Section 5 addresses the motor capability issue and presents a preliminary look at the results of our electric motor tests. Section 6 presents conclusions, and Section 7 lists references.

2. MOTOR-OPERATED VALVE OPERATING MARGINS

For rising-stem valves (gate valves, globe valves, etc.), the operating margin is the difference between the design basis required thrust and the thrust that the motor-operator can deliver at its control switch setting, with consideration given to the worst-case design-basis ambient temperature and degraded voltage conditions. (Operating margin equals available thrust minus required thrust.) The definition for quarter-turn valves (butterfly valves, ball valves, etc.) is the same, except that the parameter of concern is torque instead of thrust. (Operating margin equals available torque minus required torque.)

2.1 Understanding How Valve Operators Work

Motor-operators produce torque. Their operation is controlled by limit switches, torque switches, or both. Some valves controlled by

limit switches also have a torque switch in the circuit to serve as a safety device, and some do not. Limit switches are gear-driven, and their operation is based on position. Torque switches are displacement-driven, and their operation is based on compression of the torque spring as it responds to the increasing torque load experienced by the operator. In a motor-operator with a torque switch, the output torque can be limited either by the torque switch or by the electric motor torque at its worst case ambient temperature and degraded voltage conditions. If the electric motor torque rather than the torque switch is the limiting factor, it is possible that when subjected to high loadings, the motor will slow down to a stall without tripping the torque switch.

Figure 2-1 is a simplified sketch of a rising-stem application of the Limitorque motor-operator, showing the important features. There is one input path, and there are two output paths. There are no

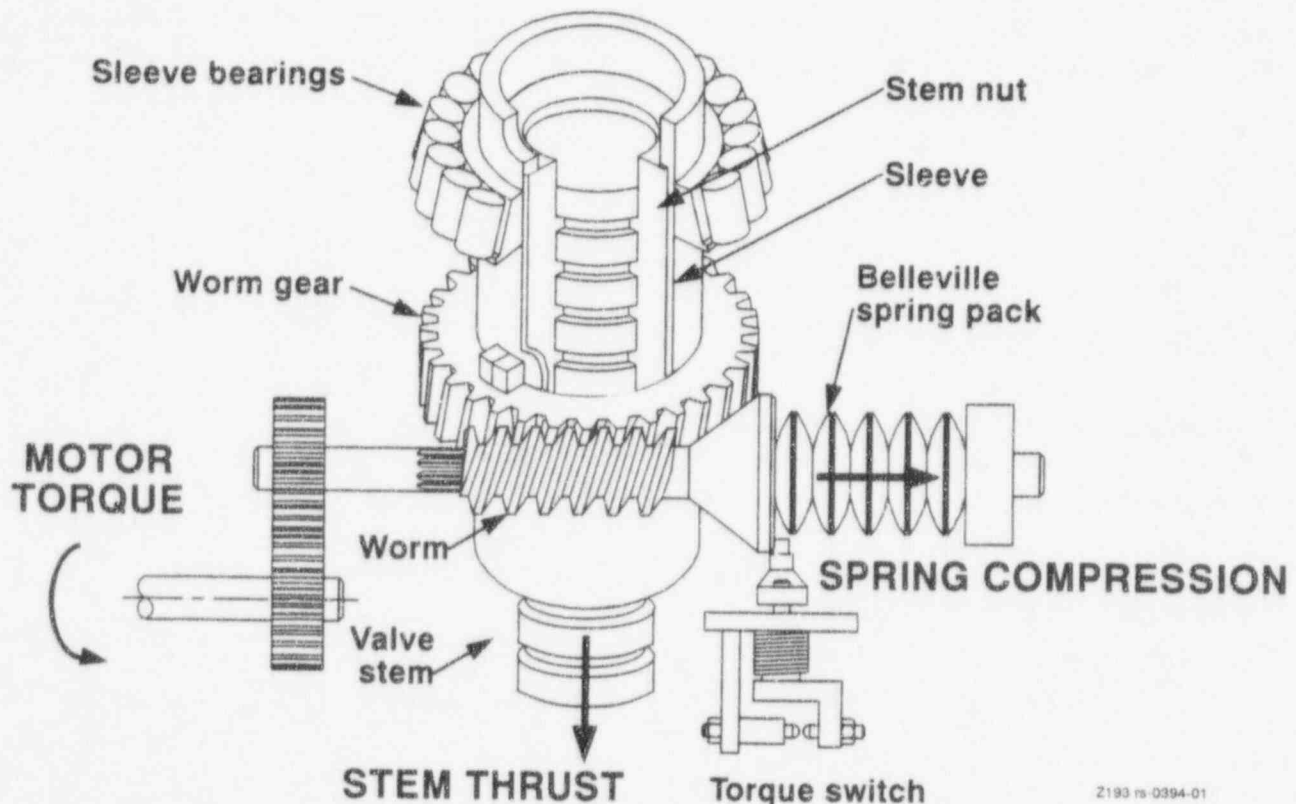


Figure 2-1. Simplified diagram of the key components of a Limitorque motor operator.

clutches in the device. Every revolution of the electric motor either turns the stem nut around the stem or causes the worm to compress the torque spring. The more resistance there is to rotation of the stem nut on the stem, the farther the worm compresses the torque spring, until the torque switch trips, interrupting the power to the motor. Whether the torque switch serves as a control device or a safety device, it limits the maximum output torque of the operator.

In quarter-turn applications there is usually a second gearbox mounted on the operator to effect another gear reduction. Many quarter-turn valves are limit-controlled, and these may or may not have a torque switch in the circuit. Limit-controlled valves without a torque switch or other safety features (for example, an overload relay) can be subject to the full stall capacity of the electric motor. The disadvantages of this arrangement are the risk of structural overload and the risk of motor burn-out. If for some reason the motor is not capable of moving the valve to the place where the limit switch causes the power to the motor to be interrupted, the motor will stall, overheat, and probably burn out.

The rising-stem and rotating rising-stem valves, whether limit- or torque-controlled, are a bit more complicated than quarter-turn valves. In these designs, operator torque in the stem nut is converted to thrust in the stem. This conversion takes place at the stem/stem-nut interface, and the efficiency of the conversion is evaluated by dividing stem torque by stem thrust (torque divided by thrust equals stem factor). With rotating rising-stems valves, it is necessary also to account for rotating packing friction.

Regardless of whether the valve is torque-controlled or limit-controlled, the operator is a device that delivers torque. The delivered torque is limited either by the torque switch or by the motor capacity. The conversion of that torque to thrust is outside the control of the operator. The efficiency of the conversion must be accounted for when setting the torque switch or calculating the required motor capacity. In this discussion of MOV margins, this conversion of torque to thrust

is the primary difference between quarter-turn valves operated on torque and rising-stem valves operated on thrust. Except for this conversion of torque to thrust, the other considerations for operating margins are basically the same for the two operating schemes. Design basis valve load, low voltage conditions, ambient temperature conditions, etc. are considerations for both.

2.2 Getting the Information Necessary for Determining MOV Margins

A consistent and uniform method for evaluating MOV operating margins would include a list of the major considerations and an indication of whether the individual considerations are valve-specific or whether they can be determined from some other source (utility design documents, prototypical testing, vendor manuals, or government or industry research reports).

Consideration	Source of Information
Design requirements for the MOV	Utility design documents
Motor size (output torque), less degraded voltage, ambient temperature losses	Vendor manuals
Operator overall gear ratio, structural strength, torque output capability, etc.	Vendor manuals
Operator efficiencies	Vendor manuals
Stem diameter, pitch, and lead (for rising-stem valves)	Vendor manuals
Stem factor (for rising-stem valves)	Valve specific
Design basis valve load	Valve specific, prototypical testing, research reports
Diagnostic test equipment accuracy	Vendor manuals

As stated earlier, a valve's operating margin is the difference between the operator's available output and the valve's requirements at design basis conditions. The evaluation of available output starts with the output torque of the electric motor; the evaluation of the valve's design basis requirements begins with the design basis stem load (a thrust load in a rising-stem valve, a torque load in a quarter-turn valve). Most of the calculations involved in these evaluations are fairly straightforward, but there are some variables, and three of the most important variables have been particularly troublesome in the past.

The first of those troublesome but important variables is the stem load (stem torque in quarter-turn valves such as butterfly valves, stem thrust in rising-stem valves such as gate valves). The methods used in the past by valve manufacturers for determining these loads have made margins determination quite difficult. Relatively recent government and industry research has found that the variables and in some cases the equations themselves were incorrect or inadequate for modeling a valve's response to actual loads. This is true for both butterfly valves and gate valves. Industry research has recently found some of the same kinds of problems with the industry's standard equations for evaluating stem thrust in globe valves. Section 3 of this report presents our most recent findings on stem load evaluations of wedge-type gate valves.

The second of these variables is the stem factor (in rising-stem valves). In the past, the stem factor was always calculated as a constant; in fact, two very early diagnostic systems were based on the notion that stem factor remained constant with load. We know now that the stem factor tends to change with changes in the load, a phenomenon we call load-sensitive behavior (also known as the rate-of-loading effect). In addition, the stem factor is valve-specific. Valves of the same size and model do not necessarily have the same stem factor. Using constants as default values for the stem factor in the calculations was considered acceptable until diagnostic testing showed that in many cases the actual stem factor can be considerably lower than the default values. As a result of using

the default values to calculate the required torque and set the torque switches, many valves experienced higher than anticipated thrusts. Quite often these high thrusts may have exceeded structural allowables on the weak link component of the valve. On the other hand, plant experience shows that in some instances the actual stem factor can be as high as the default values. Using a stem factor that is lower than the actual value can result, for example, in too low a torque switch setting, such that the valve might fail to fully close at design basis loadings. Thus, it is important to determine the actual stem factor for a specific valve. Section 4 of this report presents our most recent findings on stem factor evaluations for rising-stem valves.

The third variable is electric motor/operator output. The output torque of the electric motor is limited by the available torque at the most degraded conditions. Motor voltage degradation was thought to be fairly well understood, but the added degradation due to elevated ambient temperature was not. Limitorque (Limitorque Corporation, Lynchburg, VA) only recently published some data on the effect of ambient temperature on ac motor output. Section 5 of this report presents our preliminary findings on electric motor evaluations.

Although we now know how to go about calculating MOV operating margins, we do not always know what the specific values are for each of the variables in the calculations. Of course, the best method for determining the correct values for the stem load and the stem factor would be to test the valve at design basis conditions. This is not always possible, for a number of reasons. The design basis load for some valves is pipe break flow, and it is not possible to simulate pipe break flow in the plant. Other in situ design basis tests would require that the plant be defueled. For a number of valves, design basis testing in the plant is either very difficult or simply impossible. For those valves, operating margins are determined analytically, using the results of laboratory testing, type testing, or in situ testing at conditions less severe than design basis conditions. Of necessity, margins determined analytically include conservatism in the calculations.

2.3 An Approach to Determining Operating Margins

Based on the results of our research, we suggest that MOVs be evaluated as described in the following discussion. The approach presented here is only one of several possible ways that this issue could be addressed. Another approach might work just as well. We have tried to make this approach complete enough that it will guide the analyst to cover all the important parameters and all the possible variables. The discussion is presented in procedure format to aid the user in completing the process step by step.

The most complicated analysis is probably that of the torque-controlled rising-stem flex-wedge gate valve. We use this valve type as our model for this discussion, but when one of the other valve designs requires different considerations, we note them at that step in the process.

For quarter-turn valves (butterfly valves, ball valves), we define the operating margin in terms of torque (available torque minus required torque equals margin). For rising-stem valves (gate valves, globe valves), the definition can be based on either torque or thrust (available thrust minus required thrust equals margin). We prefer the definition based on torque, because focusing on the torque is consistent with our understanding that except for the conversion of torque to thrust, the margins evaluations for rising-stem valves and quarter-turn valves are basically the same. Also, this approach acknowledges that motor-operators mounted on rising-stem valves deliver torque, not thrust.

A definition based on thrust would work just as well. Both definitions account for the effects of the stem factor, one in evaluating available thrust, the other in evaluating required torque. The following discussion addresses both methods of determining margins for rising-stem valves. Most of the steps are the same for the two methods.

The discussion is written to apply to any MOV that needs a margins evaluation. It is written to be

as comprehensive as possible without being cumbersome. We acknowledge that not all the steps apply to all valves in all instances, and that where this procedure calls for data from in situ tests, it might be possible to use information from other sources.

The following discussion uses six steps to determine a valve's operating margin at design basis conditions:

- Gather specific information
- Make initial calculations using specified defaults for the variables in the equations
- Compare the calculations to the results of an in situ static test (a test without a flow load)
- Compare the calculations to the results of an in situ dynamic test (a test with a flow load)
- Make a final calculation that uses the results of the tests to specify the variables and to confirm or challenge the appropriateness of the torque switch setting and the capability of the motor
- Calculate the overstress margins to ensure that the motor-operator will not damage itself or the valve.

2.3.1 Gather Specific Information

2.3.1.1 Design Basis Requirement (Plant Specific). Determine the MOV's design basis requirements for the parameters listed below. There may be more than one design basis requirement, depending on the load scenario or the accident scenario. If so, use the one that specifies the most severe fluid flow, pressure, ambient temperature, and degraded voltage conditions.

- System fluid temperature, pressure, flow, and subcooling
- Differential pressure across the valve
- Worst case ambient temperature conditions
- Worst case degraded voltage conditions.

2.3.1.2 The Valve (Valve Specific). Obtain the design documentation for the MOV. Determine the following parameters.

- Valve type and size
- Valve internal specifics
- Gate valve mean seat diameter and wedge angle
- Globe valve controlling area (a disc guide area or a seat area)
- Butterfly valve disc geometry (symmetric/asymmetric, aspect ratio)
- Stem diameter and thread pitch and lead (rising-stem valves)
- Packing type and anticipated packing friction load.

Standard packing friction loads for most packing types and stem diameters are specified in the literature, and except for live-loaded (spring-loaded) packing, actual packing loads in tests are typically lower than the specified packing loads.

2.3.1.3 The Operator (Operator Specific). Determine the following specific information for the operator.

- Operator size
- Torque spring part number
- Motor size (speed, output torque, and stall characteristics)
- Overall gear ratio (including second gear box for butterfly valves)
- Operator efficiencies (running, pullout, and stall efficiencies).

2.3.2 Initial Calculations. Figures 2-2 and 2-3 are flow diagrams that outline the important steps in either the initial calculations or the final calculations. In Figure 2-2, the margin is defined in terms

of available torque versus required torque. This flow diagram applies to rising-stem valves as well as quarter-turn valves. In Figure 2-3, the margin is defined in terms of available thrust versus required thrust. This flow diagram applies to rising-stem valves only. With a few exceptions, the numbered paragraphs in the following discussion correspond to the boxes in the flow diagrams.

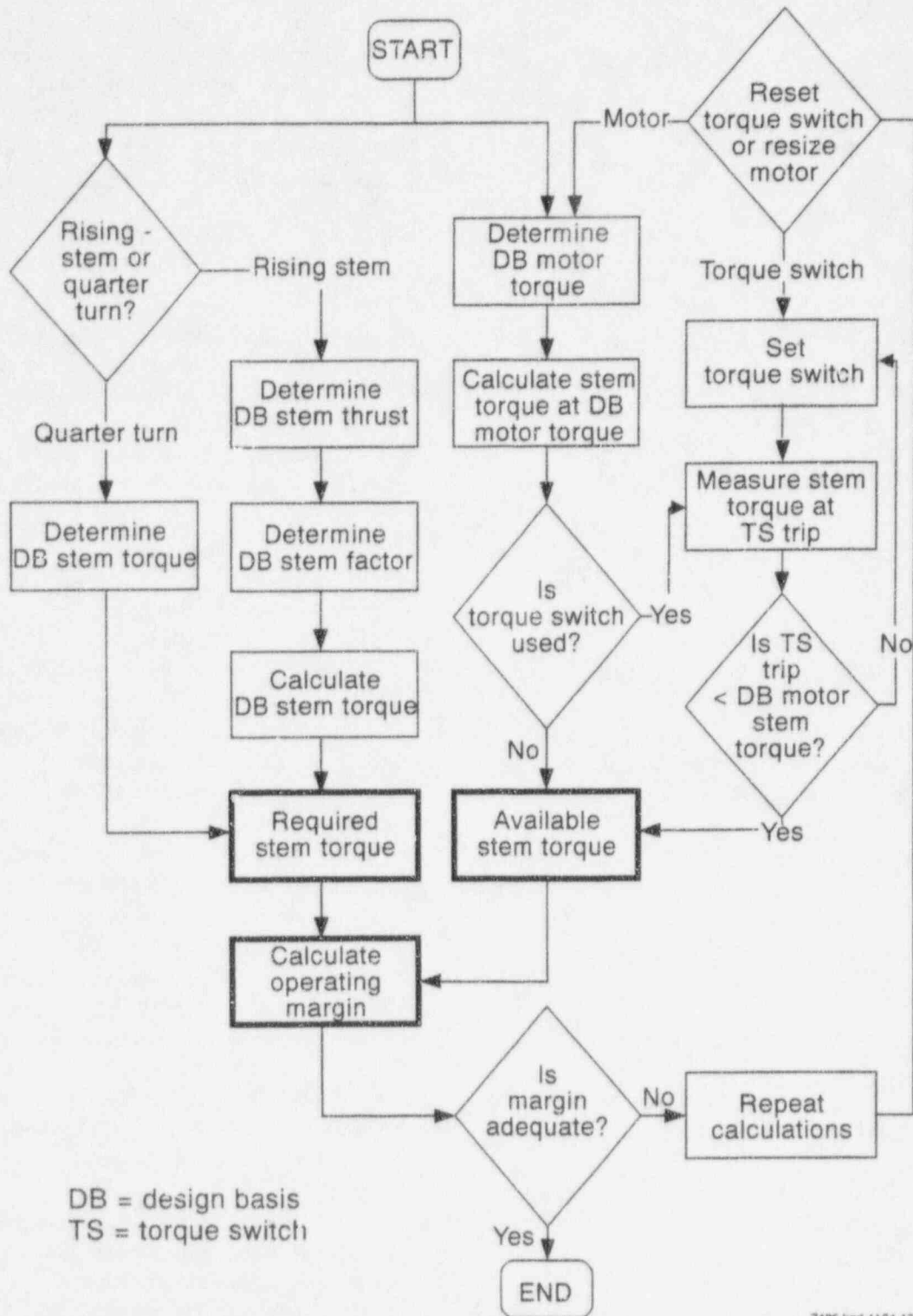
The purpose of the initial calculations is to provide

- Sufficient information to evaluate the torque switch setting and make an initial estimate of the operating margin
- Estimates that can be compared to the actual valve responses recorded during in situ testing at nominal motor voltage
- Assurance that the valve's structural limits will not be exceeded.

The purpose of comparing the results of these initial calculations with the results of the in situ tests is to assist in the analysis. Gross inconsistencies can alert the analyst to calculation errors or measurement errors. After the in situ tests are performed, the results of the tests can be used in the final calculation to provide more specific information on the valve's requirements and the operator's capabilities. If the initial calculation was accurate enough to provide for an adequate torque switch setting, as confirmed by the final calculation, then it will not be necessary to reset the torque switch and repeat the procedure.

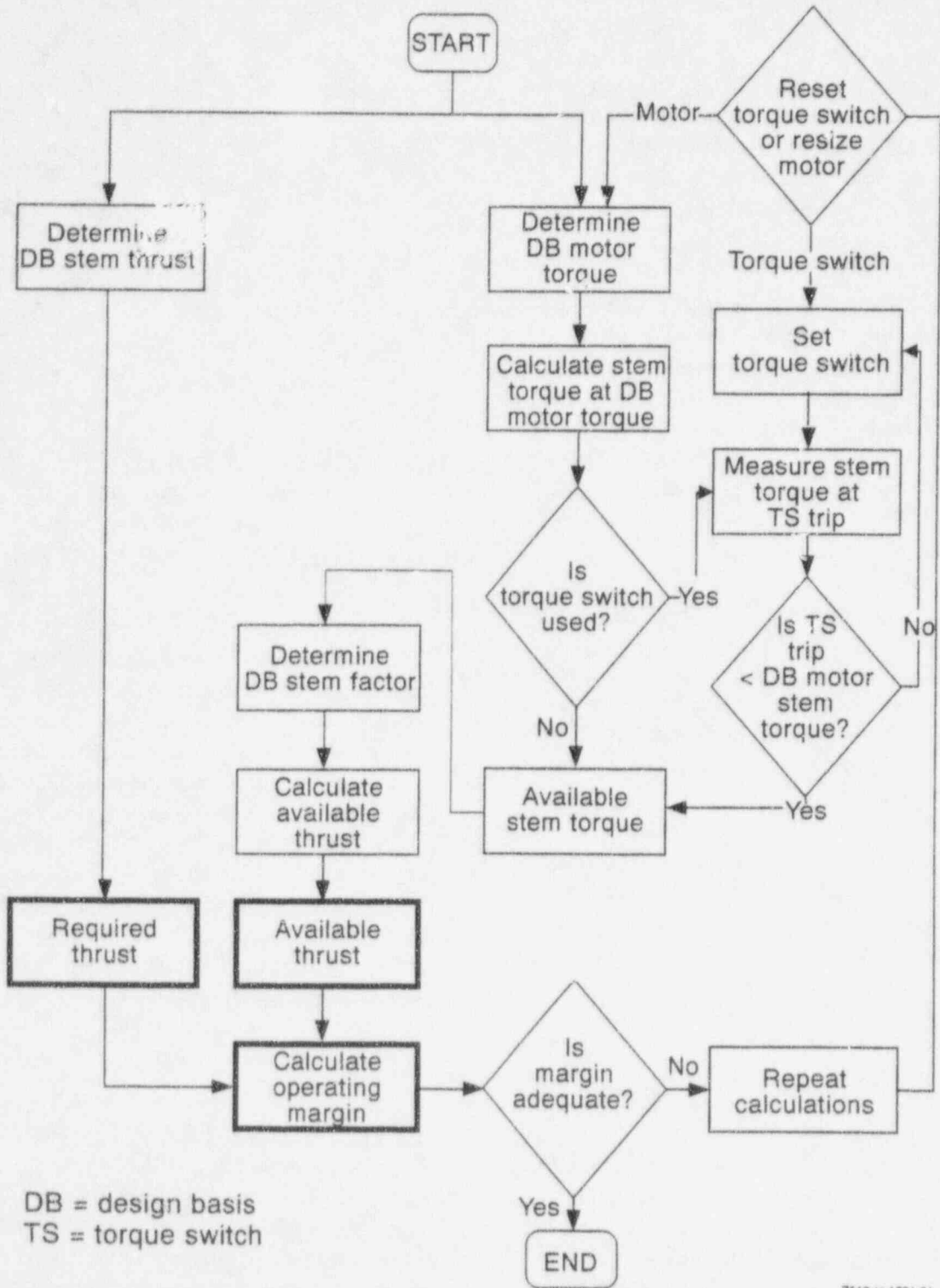
2.3.2.1 Determine the Design Basis Stem Thrust Requirement (Rising-Stem Valves).

Typically, this is the thrust necessary to close the valve and isolate flow. (However, some valves have a design basis opening requirement, and some have both.) This calculation involves an equation that converts the differential pressure and flow loads on the gate (or the plug on a globe valve) to a thrust load in the stem. It also considers the packing friction and the stem rejection loads. There are several equations available for performing this calculation. The variables for disc factor or disc friction factor and the basis for their



2496 kgd-1194-17

Figure 2-2. Flow chart illustrating the process for determining the torque margins for quarter-turn and rising-stem valves.



Z512 rs-1294-01

Figure 2-3. Flow chart illustrating the process for determining the thrust margins for rising-stem valves.

use are typically found with the equations. We recommend that one of the modern equations be used, one that is based on recent valve research. For example, the Isolation Valve Assessment (IVA) software (Watkins et al. 1994) includes a method based on the INEL correlation. The disc factors and stem factors that served as default values in the old equations originally published by the valve manufacturers are out of date and might produce estimates that are not appropriate. Section 3 of this report presents a discussion on disc loads in gate valves.

2.3.2.2 Determine the Design Basis Stem Factor (Rising-Stem Valves). For this initial calculation, a stem factor based on an upper bounding stem/stem-nut coefficient of friction should be used. (A lower, more accurate value based on the results of the in situ tests may be used in the final calculation. Section 4 of this report presents a discussion on stem factors in rising-stem valves.)

For margins evaluations based on torque (Figure 2-2), the stem factor is used along with the required thrust to determine the required torque. For margins evaluations based on thrust (Figure 2-3), the stem factor is used along with the available torque to determine the available thrust.

2.3.2.3 Determine the Design Basis Torque Requirement (All Valves). For rising-stem valves, this value is a straightforward calculation using the design basis stem thrust and the stem factor, determined in the previous steps (torque equals thrust times stem factor). For quarter-turn valves, this calculation can be made using an acceptable validated method for butterfly valves or ball valves, as appropriate. This step does not apply to rising-stem valves that are being evaluated according to the method shown in Figure 2-3 (thrust margin).

2.3.2.4 Determine the Design Basis Available Torque Based on Motor Output (All Valves, Worst Case Motor Conditions). This calculation includes an evaluation of the available output of the electric motor at its worst-

case design basis conditions. Considerations should include

- Rated motor torque
- Minimum voltage conditions
- Design basis ambient temperature conditions
- Application factor (Limitorque SEL term)
- Pullout efficiency of the gearbox (Limitorque SEL term).

This calculation determines the available torque based on the minimum capability of the motor. Section 5 of this report presents some preliminary findings on motor and operator performance.

2.3.2.5 Determine the Available Torque Based on the Torque Switch Setting. This step applies to valves equipped with torque switches, regardless of whether the torque switch serves as a control device or a safety device. The available torque depends on the torque switch setting and on the torque spring installed in the operator. Typically, a given operator size might be fitted with one of several different torque springs, each with a different stiffness. Generic torque spring calibration data are available from the operator manufacturer. One can get specific information by removing and calibrating the torque spring.

2.3.2.6 Determine Available Torque (All Valves). Ideally, the available torque as determined by the torque switch setting should be less than the available torque based on minimum motor capability; otherwise, the motor might slow down at high loadings and stall without tripping the torque switch. Regardless of which is less, the lesser of the two is the value used in the calculation of the operability margin.

2.3.2.7 Determine the Design Basis Available Thrust (Rising-Stem Valves). This step applies only to rising-stem valves that are being evaluated according to the method shown in Figure 2-3, where the margin is defined in terms of thrust. This step is a straightforward calculation using the available torque and the design basis stem factor, determined in previous steps (thrust equals torque divided by stem factor).

2.3.2.8 Estimate the Valve's Operating Margin (All Valves). For margins defined in terms of torque (Figure 2-2), compare the design basis torque requirement with the available torque. For margins defined in terms of thrust (Figure 2-3), compare the design basis thrust requirement with the design basis available thrust. If the available torque (or thrust) is larger than the required value, the operator has a positive margin. If the available torque (or thrust) is less than the required value, the operator has a negative margin. A negative margin suggests a need for corrective action (changing the torque switch setting, replacing the motor, etc., as applicable). If the negative margin is small, the analyst might want to recommend testing the valve and repeating the margins evaluation, this time using actual values instead of default values or estimates for some of the variables.

2.3.2.9 Calculate the Operator Torque (and Thrust) at Expected Test Conditions (All Valves). The purpose of this calculation is to provide information that can be compared to the results of the in situ tests. The comparison can provide insights on how to prepare the final calculations. In addition, discrepancies in the comparison can alert the analyst to measurement errors or calculation errors. This calculation should be performed for both the dynamic test and the static test. Conditions for this calculation should be carefully considered and best estimate values used. Expected packing friction loads should be used rather than design basis packing loads. For rising-stem valves, use the pressures and differential pressures expected in the in situ tests to estimate the expected peak stem thrust before seating, and use a best estimate (instead of an upper bound value) for the stem factor to calculate the corre-

sponding operator torque. Use the estimate of the available torque based on torque switch setting (see above), together with a best estimate of the stem factor, to estimate the expected stem thrust at torque switch trip. For quarter-turn valves, use the pressures and differential pressures expected in the in situ tests to estimate the expected peak stem torque. Considerations include

- Best estimate motor torque
- Nominal motor voltage
- Gearbox efficiency
- Expected packing friction loads
- Static test conditions
- Dynamic test conditions
- Best estimate stem factor for dynamic test
- Realistically low stem factor for static test.

2.3.2.10 Determine the Maximum Expected Stem Load (Overstress Calculation). This is the maximum stem torque and thrust (if applicable) that can be expected. The purpose of this calculation is to determine that this maximum expected stem load will not overstress any of the valve or operator components. The conditions that should be considered are

- Maximum motor voltage (overvoltage conditions)
- Maximum motor torque
- Operator torque at torque switch trip
- Minimum stem factor (most likely to occur in a static test with packing friction load only)
- Effects of motor controller dropout time
- Effects of motor momentum
- Gearbox stall efficiency.

Static test conditions with a minimum running load (little or no stem rejection load) will typically provide the highest stem thrust in rising-stem valves, because at these conditions the coefficient of friction in the stem/stem-nut interface tends to be at its lowest at the point of interest (that is, after seating). This is the reason that, for the maximum thrust calculation, we recommend using a stem factor based on the minimum expected (lower bounding) stem/stem-nut coefficient of friction; use of the minimum stem factor will result in the maximum possible thrust expected for a given torque. Finally, the effects of motor controller dropout time and motor momentum (considering operator stall efficiency) should be added to the torque and thrust at torque switch trip (if applicable) to determine the maximum final stem load after torque switch trip.

2.3.3 In Situ Test at Static Conditions. A static test is a test conducted with a packing load only, or with a packing load and a pressure load, but without differential pressure or flow loads. We recommend that the following parameters be measured continuously, at a sample rate consistent with the timing needs. For example, one millisecond resolution requires a minimum of 1000 samples per second. The recommended measurements include

- Stem torque or operator torque (on all valve configurations)
- Stem thrust (on rising-stem valves)
- Motor current and voltage
- Control switch position (open or closed)
- Stem position (optional).

Direct measurements of stem torque are better than indirect measurements that are based on spring pack measurements, because indirect measurements introduce uncertainties that must be accounted for in the analysis; however, indirect measurements are better than no measurements. Stem position (vertical position for a rising-stem valve, rotational position for a quarter-turn valve) is an optional measurement on all valve configura-

tions, but it is a very valuable measurement if any kind of trouble-shooting is required.

The static test provides data that can be used to determine the actual packing load. This information is useful in the analysis of the results from the dynamic tests of all valve types. [Generally, in order to determine the stem load attributable to flow and differential pressure, it is necessary to subtract the packing friction load and the stem rejection load (if applicable) from the total measured load.]

Generally, in torque-controlled rising-stem valves, static test conditions tend to produce lower stem/stem-nut friction at torque switch trip than will be experienced under dynamic test conditions. Thus, the static test normally produces the highest stem thrust that is possible with the present torque switch setting. The actual stem factor at torque switch trip in the static test is useful for checking the value used in the structural analysis.

For valves that cannot be tested in situ with a flow load, such that margins must be determined by analysis, it might be possible to use the results of the static test to estimate a stem factor that can be used in a design basis analysis. Section 4 of this report proposes a method that, when validated, can be used to make such an estimate. (See the subsection describing the *fold line method*.) A stem factor thus estimated likely will be less accurate (higher) than one determined from a test with a higher running load, but more accurate than default values.

For those limit-controlled valves that cannot be seated or tested, we suggest dynamometer testing the operator to provide some assurance of the operator's capability. In dynamometer tests of operators used in thrust applications (rising-stem valves), the test should include appropriate thrust loads. Otherwise, the calculations must consider torque losses that may occur when thrust is applied to the stem.

2.3.4 In Situ Test at Dynamic Conditions. Next, the valve should be subjected to a diagnostically monitored dynamic test. The dynamic test provides data for more precisely determining the values for the variables used in the margins

calculations. In addition to the parameters recorded in the static test, the following parameters should be recorded:

- Valve inlet line pressure
- Valve flow rate
- Valve differential pressure
- Fluid temperature.

If possible, the test should be conducted at design basis flows, fluid temperatures, fluid pressures, and differential pressures. If the fluid pressure and differential pressure are at least 95% of the design basis conditions, the test is considered representative of a full-scale design basis test; extrapolation can be used to compensate for shortfalls of 5% or less. If the test conditions are less than 95% of design basis conditions, some form of analysis or extrapolation will be necessary to relate the test results to valve operability at design basis conditions.

Extrapolation of both disc factor and stem factor is discussed in other sections of this report, but a summary is presented here for continuity. For a gate valve that exhibits typical responses (peak stem force occurs at flow isolation), there are a number of models that can be used to extrapolate the results. If the test differential pressure exceeds either 200 psid or 50% of the design basis differential pressure, the original INEL correlation can be used. As presented in the IVA software (Watkins et al. 1994), this correlation provides a typicality test and some guidance in predicting the design basis stem load. The research that produced the correlation is documented in NUREG/CR-5720 (1992).

For gate valves with atypical behavior but no evidence of valve damage, Section 3 of this report proposes a linear extrapolation method for evaluating the results and predicting the stem load. This method, too, is included in the IVA software.

As for the stem/stem-nut coefficient of friction, Section 4 of this report proposes two methods for determining a design basis friction coefficient

from the results of tests conducted at conditions less severe than design basis conditions. One uses the results of a dynamic test, the other uses the results of a static test.

2.3.5 Final Calculations for Estimating MOV Margins. The process for the final calculations is very similar to the process for the initial calculations. The main difference is that instead of using bounding values or default values for some of the variables, the final calculations use more accurate values based, for example, on the results of the in situ tests.

The values used in the final calculation of MOV operating margins can be based on one or more of the following:

- Direct measurements from in situ tests conducted at design basis conditions
- Extrapolations or estimates based on the results of in situ tests conducted at conditions less severe than design basis conditions
- Calculations based on the best available test data
- Calculations based on analysis.

We recommend values based on test results over values determined by analysis.

The purpose of the final calculations (as compared to that of the initial calculations) is to use data obtained from the in situ tests (or data from other sources) to verify the initial assessment of the valve's operating margin. Again, the margin can be defined in terms of torque (all valves), as shown in Figure 2-2, or it can be defined in terms of thrust (rising-stem valves), as shown in Figure 2-3. The margin is the difference between what is available and what is required for the valve to overcome its design basis loadings (available minus required equals margin).

2.3.5.1 Determine the Required Design Basis Stem Thrust (Rising-Stem Valves).

The design basis stem thrust calculation typically considers some or all of the following:

- Peak stem thrust measured before seating in a dynamic test
- Actual packing friction load (measured in a static test)
- Design basis packing friction load
- Design basis stem rejection load (design basis pressure times stem area)
- Design basis disc (or plug) load (total thrust minus actual packing friction load minus stem rejection load)
- Effective disc (or plug) area
- Design basis differential pressure
- Disc angle (wedge-type gate valves).

Even if actual values are determined from a design basis dynamic test, the calculation of the required thrust typically uses the design basis packing load rather than the actual packing load. This saves recalculating the design basis load every time the packing is adjusted. [This may not be a concern with valves equipped with live-loaded (spring-loaded) packing.] Where any of the values were determined from a dynamic test at conditions less severe than design basis conditions, each of the design basis values may have to be calculated independently, depending on the method and the equations one uses. Normally, methods cannot be mixed. For gate valves, the design basis disc load should be determined from the peak stem thrust before wedging, whether that peak occurs at flow isolation or before flow isolation. Section 3 of this report presents a discussion on disc loads in gate valves.

2.3.5.2 Determine the Design Basis Stem Factor (Rising-Stem Valves). The design basis stem factor can be determined directly from test results, if the dynamic test was a design basis

test, or if the test meets the threshold requirements defined in Section 4 of this report. The stem factor should be determined from the peak stem thrust measurement in the running portion of the stroke before seating and from the corresponding torque measurement (torque divided by thrust equals the stem factor).

The stem factor should *not* be directly determined from measurements of torque and thrust recorded at torque switch trip; stem factors recorded at torque switch trip can be much lower than the running stem factor. The low stem factor at torque switch trip is typical of a phenomenon we call load-sensitive behavior, sometimes referred to as the rate-of-loading effect. It is very important that the design basis stem factor used in margins calculations be a value that has not been compromised by load-sensitive behavior. The running stem factor at the peak thrust before seating is the point of interest for determining design basis requirements. This subject is discussed further in Section 4 of this report. For the final value of the design basis stem factor, use the stem factor determined from a test, plus a margin to account for degradation due to lubricant dry-out, etc.

2.3.5.3 Determine the Required Operator Torque.

This step does not apply to rising-stem valves that are being evaluated according to the method shown in Figure 2-3 (thrust margin). The final calculation to determine the required operator torque in a rising-stem valve typically considers the following variables, determined in previous steps:

- Required stem thrust
- Design basis stem factor.

Multiply the design basis stem factor times the required stem thrust to calculate the design basis operator torque. For rising-stem valves, this value is the *required operator torque* that is used in the margins calculation.

For quarter-turn valves, the *required operator torque* is the peak stem torque measured during operation in a design basis test, minus the actual packing load (determined in the static test), plus

the design basis packing load specified in the design documents. In the absence of a design basis test, the required operator torque might be a value extrapolated or estimated from the results of dynamic tests at lower loads or from the results of testing of similar valves. For some low-pressure applications, the seating torque may exceed the dynamic torque. Where this is the case, the seating torque is the required operator torque. The seating torque can be determined from a static test.

2.3.5.4 Determine the Available Operator Torque Based on Motor Output. For operators that have a torque switch in the control circuit (whether the torque switch is used as a safety device or a control device), the available operator torque may be limited by either (a) the motor capacity at the motor's design basis conditions of reduced voltage and elevated ambient temperature, or (b) the torque switch setting. For operators without a torque switch, motor capacity at design basis conditions is the single limiting factor.

The purpose of the reduced-voltage calculations is to determine if the motor operating at reduced torque output can operate the valve at the design basis flow and pressure loads. In a successful dynamic test of a torque-controlled valve, the torque switch limits the operator output to a certain value. Generally, the test is conducted at normal conditions, so the output torque of the motor is likely to be near its nominal output. The undervoltage calculation ensures that even at its reduced output, the motor is still capable of producing enough operator torque to successfully close (or open) the valve at design basis loads. The calculation also needs to determine that the motor will not stall before it trips the torque switch. If the calculation shows that the motor at reduced output is not capable of producing sufficient torque to trip the torque switch, it will be necessary to either lower the torque switch setting or replace the motor with a more powerful one.

To determine the available operator torque based on motor capacity, determine the maximum torque developed by the motor with the output

downgraded to account for degraded voltage and high ambient temperature. (For more information, see Section 5 of this report.) Use the standard equations and the applicable values for the operator overall gear ratio (sometimes called the unit ratio), the application factor, and the operator pullout efficiency to estimate the available operator torque.

2.3.5.5 Determine the Available Torque Based on the Torque Switch Setting. This value is simply the torque recorded at torque switch trip in either a static test or a dynamic test. In the absence of a test that trips the torque switch, one can calculate this value using spring pack data and the effective moment arm (the distance between the centerline of the worm/worm-gear interface and the centerline of the stem). Ideally, this value (the available operator torque based on torque switch setting) should limit the torque developed by the operator so that the stem torque, stem thrust, and motor stall limits of the valve and operator are not exceeded (see the discussion of overstress margin, below). The torque switch should be set low enough to avoid such overloads, yet high enough to provide positive margin at the valve's design basis conditions.

For rising-stem valves, the torque switch setting must also account for the stem factor, including the effects of load-sensitive behavior (rate-of-loading). The available torque must produce the design basis thrust required to perform the valve's safety function. For margins evaluated as shown in Figure 2-2 (torque margins), the stem factor is accounted for in the calculation of the required operator torque (the torque required to deliver the thrust needed to operate the valve). For margins evaluated as shown in Figure 2-3 (thrust margin), the stem factor is accounted for in the calculation of the available thrust (the thrust available at a given torque switch setting or a given motor output).

2.3.5.6 Determine the Available Operator Torque. For valves equipped with a torque switch, the available operator torque is either the available torque based on motor output or the available torque based on the torque switch setting, whichever is lower. For valves not equipped

with a torque switch, the available operator torque is the available torque based on motor output.

2.3.5.7 Determine the Available Stem Thrust (Rising-Stem Valves). This step applies only to rising-stem valves that are being evaluated according to the method shown in Figure 2-3, where the margin is defined in terms of thrust. This is a straightforward calculation using values determined in previous steps, namely the design basis stem factor, and the available torque based on either the motor output or the torque switch setting, whichever value is lower. (Thrust equals torque divided by stem factor.)

2.3.5.8 Operating Margin. For margins evaluated in terms of torque (Figure 2-2), the operating margin is the difference between *available operator torque* and *required operator torque* (available torque minus required torque equals margin). For margins evaluated in terms of thrust (Figure 2-3), the operating margin is the difference between *available stem thrust* and *required stem thrust*. If the margin is inadequate, raise the torque switch setting or resize the motor etc., as appropriate, and repeat the procedure.

2.3.6 Overstress Margins. The purpose of calculating the overstress margins is to ensure that the operator will not damage itself or the valve during normal operation or under certain abnormal conditions. One calculation evaluates the overstress margin related to the torque switch setting, and another calculation evaluates the overstress margin related to the maximum output of the electric motor at over-voltage conditions.

For a valve that has been subjected to a static test, one can use the results to estimate the overstress margin for the torque switch setting. The conditions most likely to produce maximum thrust and torque at a given torque switch setting are static test conditions, where in many valve stems, the coefficient of friction in the stem/stem-nut interface tends to be quite low after seating, and where the effects of motor momentum are greatest. For the calculation of this margin,

use the recorded values for final torque and final thrust. Compare these values to the stress limits of the valve and operator components. The component with the smallest margin (the weak link) determines the overstress margin for that torque switch setting. If that margin is not adequate, set the torque switch at a lower setting and repeat the procedure. Consider also that small overstress margins indicate a possibility that some valve and operator components might experience unnecessary wear and fatigue during normal operation and in-service testing.

For a valve that has not been subjected to a static test, a calculation based on the recommendations given in Section 2.3.2.10 might be used.

The purpose of the over-voltage calculations is to determine if the higher torque produced by the motor at design basis high voltage exceeds any of the valve and operator structural limitations. The over-voltage calculations assume that the entire output of the motor at over-voltage conditions goes through the operator to the valve. (This might occur, for example, if the torque switch were to fail.) This calculation should use a stem factor determined from measurements taken after seating in a static test, or a lower-bounding estimate. The calculation needs to determine that the motor will stall before the operator compromises a containment boundary by breaking the valve housing, for example, or by pushing the disc beyond the seat so that fluid passes over the top of the disc.

2.4 Changes in the Operating Margin

The following discussion distinguishes between the actual operating margin and the calculated operating margin of an MOV.

2.4.1 Changes in the Calculated Margin. The intent of any method for evaluating MOV margins is to arrive at a calculated value that is appropriate, that is, the actual margin is larger than the calculated one. Many assumptions are inherent in the calculations. In some instances, these assumptions stack up in such a way that the

calculation shows that little or no margin exists, when in fact the actual margin is adequate.

When a margins evaluation determines that the margin is inadequate, the analyst may choose to recalculate the margin rather than declare the valve inoperative. Such a recalculation would allow the analyst to reexamine some of the values used as variables in the calculation and perhaps identify and reduce unwanted conservatism. Note that in any such effort, the analyst must be very careful not to introduce nonconservatisms. The following are suggestions that the analyst might consider in the effort to reduce unwanted conservatism.

- Conduct a best-effort dynamic test to determine whether a gate valve's response is typical (peak thrust occurs at flow isolation) or atypical (peak thrust occurs before flow isolation in the closing direction or after flow initiation in the opening direction); if the response is typical, conservatism to account for a possible atypical response might be eliminated.
- Use a disc factor (or a disc friction factor) determined from a best effort dynamic test instead of a higher default value
- Use a stem factor determined from a best effort dynamic test instead of a higher default value
- Use a bounding stem factor derived from the results of a static test instead of a higher default value.

Sections 3 and 4 of this report provide additional information on the use of test results to determine disc factors and stem factors.

2.4.2 Changes in the Actual Margin. It is possible that characteristics of the components of the valve and operator can change over time in

such a way as to change their behavior during valve operation. Such changes may be due, for example, to aging. Under some conditions, these changes can affect the actual operating margin of the MOV. The following is a partial list of such potential changes.

- Disc friction characteristics (due, for example, to corrosion)
- Stem/stem-nut lubrication (dirt, lubrication dry-out)
- Stem/stem-nut characteristics (pitting, wear)
- Torque spring fatigue
- Overtightening of the packing gland nut
- Motor degradation
- Bearing failure
- Inadequate lubrication.

It might be useful to monitor changes that occur in the MOV operating margin over time. Such monitoring would make it possible to anticipate future changes and to schedule MOV tests in such a way as to ensure that the actual margin does not become inadequate before the next test.

2.5 Conclusions

Logical methods exist for evaluating the design-basis capabilities and requirements of MOVs. This section describes one such method. The operating margin is the difference between what is available and what is required. For valves that cannot be tested at design basis loads, in situ testing at lower loads can make it possible to reduce the conservatisms required in the calculations.

3. DISC LOAD

This section of the report addresses our latest research findings regarding dynamic loads in flexible-wedge gate valves. The dynamic load is defined as that portion of the stem load that results from the effects of flow and differential pressure on the disc. Thus, we sometimes call it the disc load, to distinguish it from the other loads (stem rejection load, packing friction load, etc.) that contribute to the total stem load. The disc load includes the frictional load as well as the hydraulic load. These latest research findings address valve disc load requirements not already addressed by the INEL closing correlation published in NUREG/CR-5720, *Motor-Operated Valve Research Update*, published in June 1992.

For this discussion, it may be instructive to begin by discussing disc friction and making a distinction between the terms *disc factor* and *friction factor*. The materials of construction for disc, guide, and seat surfaces have been the subject of a number of studies to investigate *friction factors*. The effects of temperature and load on the hard-facing material of the seat and disc (typically Stellite 6) have been noted in evaluations of the results of laboratory friction tests; generally, higher temperature and higher loads tend to lower the friction factor. When evaluating the results of actual valve tests, where the valves were subjected to flow and pressure loads (in tests where damage or mechanical interference do not occur), we have observed that the resulting friction factors are lower than the friction factors obtained in the laboratory from material samples. This result is particularly evident in tests conducted at higher temperature. In general, test results show that temperature, pressure, fluid type, and differential pressure, independently and in combination, all have an effect on the friction factor.

In analyses of the results of valve tests with flow and pressure, it is often difficult to separate the various components that make up the net load on the stem. In such cases, instead of extracting a *friction factor* from the test results, the analysis might simply extract a *disc factor*. In such a calculation, the disc factor converts the horizontal

force against the disc (differential pressure times disc area) into a vertical force resisting the vertical movement of the stem. Thus, the disc factor is a multiplier like the friction factor, but it does not represent a calculation of a normal versus sliding load; it includes other variables besides the actual friction. Generally, the results of test analyses or calculations using a disc factor cannot be compared with those where the actual friction factor was determined.

During previously reported research, in our development of the original INEL closing correlation and the model that supports it, we endeavored to account for all the identifiable pressure forces that contribute to the net stem load, so that what was extracted from the analysis was a normal versus sliding calculation that was as close a representation as possible of actual disc-to-seat friction. The closing correlation provides a useful tool for evaluating the on-the-seat closing requirements of valves that exhibit typical responses (peak stem thrust is achieved at flow isolation) where the differential pressure exceeds 400 psid. However, the original correlation does not address opening requirements, atypical closing requirements, or differential pressures below 400 psid. These limitations on the applicability of the original INEL correlation left a serious need to extend the method or to develop new methods to include

- Typical valve responses during closing at pressures below 400 psid
- Atypical valve responses in the closing direction
- Valve opening responses (both typical and atypical).

This section of the report is presented in three subsections that discuss our latest efforts in addressing these three kinds of valve responses. These responses represent areas where, until now, we were unable to provide any technical support. For the first of these three areas, we extended the applicability of the INEL closing correlation. We

did this by evaluating available low-load test data and enhancing the INEL closing correlation to address data scatter in the friction factor at these lower loads. For the other two areas, we developed new approaches. We completed the initial development of a method that uses a disc factor for directly extrapolating the results of a best effort dynamic test to bound the design basis closing requirements of a gate valve with an atypical response. We also completed the initial development of a correlation (similar to the INEL closing correlation) that uses a friction factor for predicting the opening requirements of gate valves.

3.1 Typical Valve Responses During Closure Against Lower Loads

Our analysis of the closing requirements of valves with typical responses and our development of the INEL correlation are documented in NUREG/CR-5720 (1992). So far, the applicability of the INEL correlation has been limited to medium- to high-flow applications, where the dif-

ferential pressure is about 400 psid or greater. One of the reasons for this is because at the time, we simply did not have the data to extend applicability of the INEL correlation to lower loads. Another reason is because in many valves tested at low pressures and low flows, the analysis of the test results tends to produce a large amount of data scatter, regardless of the model used in the analysis. The following discussion first takes a look at this kind of low-load data scatter, as evidenced in the results from utility testing of a valve, then presents an updated version of the INEL closing correlation. This updated version has been extended to include valve operation at loads lower than the 400 psid limit. A brief discussion of valve preconditioning and its effect on data scatter is also presented in this subsection of the report.

3.1.1 Test Data From a Utility Valve Test Program. A classic example of the data scatter usually seen at low loads is the evaluation of a 14-in. 600-lb-class valve tested recently by a nuclear utility. A quick look at the test results provided by the utility is presented in Figure 3-1, which shows the calculated disc factor by stroke

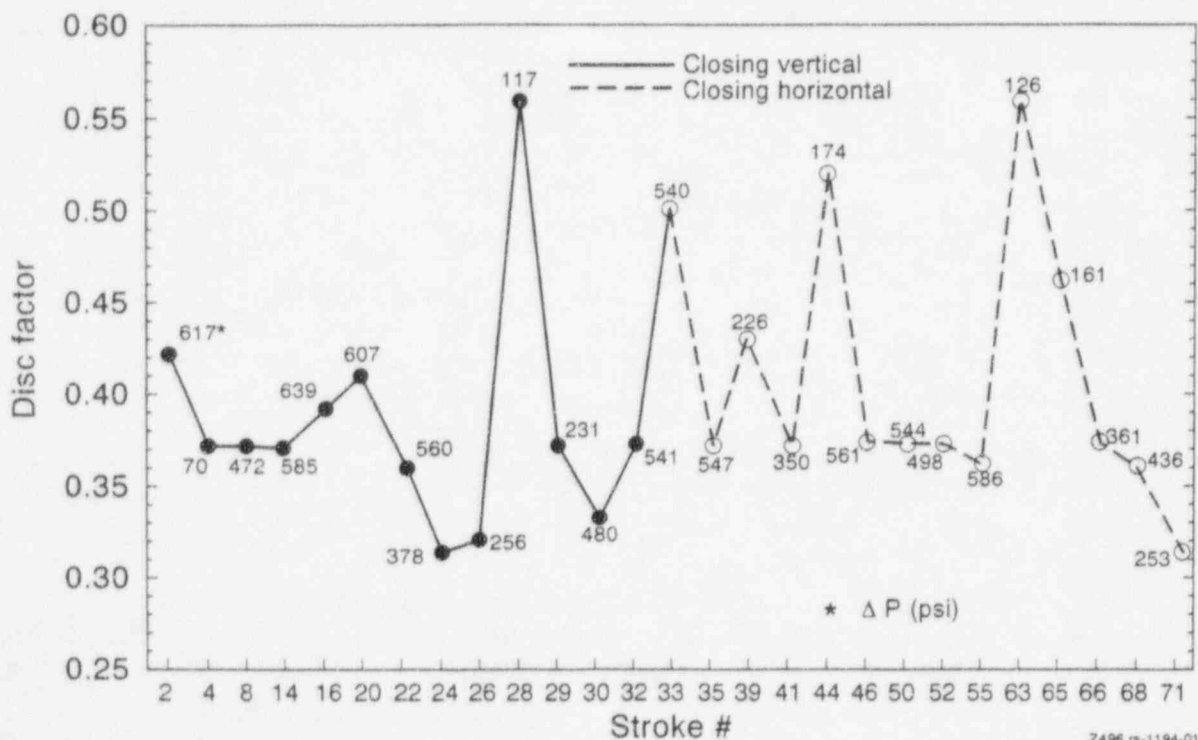


Figure 3-1. Results from testing a 14-in. 600-lb-class valve at a utility.

number. These test results are all from the same valve. Each of the circles represents the results of a closing test, and the number next to the circle is the differential pressure for that test at flow isolation. The solid circles represent tests with the valve mounted in the vertical position, and the clear circles represent tests with the valve mounted in the horizontal position. This preliminary view of the test results shows the data scatter mentioned earlier.

Presenting these data as the disc factor plotted against the differential pressure, as shown in Figure 3-2, gives a better indication of the data scatter. This comparison is the result of the utility analyzing the data with the NMAC stem thrust equation, which includes terms that account for the wedge angle. [The NMAC equation (Grant and Keating, 1990) was developed by the EPRI Nuclear Maintenance Application Center.] The plot also shows the bounding limits of the INEL correlation. As a general trend, the tests at a higher differential pressure show less scatter in the disc factor than do the tests at a lower differential pressure. With this much scatter in the data, as pres-

ented in this format, it is very difficult to define a trend that would be useful for evaluating the performance of the valve at low loads.

Looking at the data using a simplified analysis that is similar to the INEL methodology, we see a much better correlation of the data. This simplified analysis, also provided by the utility, is shown in Figures 3-3 and 3-4. Figure 3-3 presents data from tests with the valve oriented in the vertical position; data for the horizontal position are presented in Figure 3-4. These plots represent a relationship between the dynamic stem thrust and the horizontal disc load, such that the disc factor is represented by the slope of the line. (The dynamic stem thrust equals the total stem thrust minus the stem rejection load minus the packing friction load; the disc load equals the disc area times the differential pressure.) The effect of this simplified analysis is that both the dynamic stem thrust and the disc load have been divided by the disc area term; the vertical axis, though labeled differently, is equal to the dynamic stem thrust divided by the disc area, and the horizontal axis,

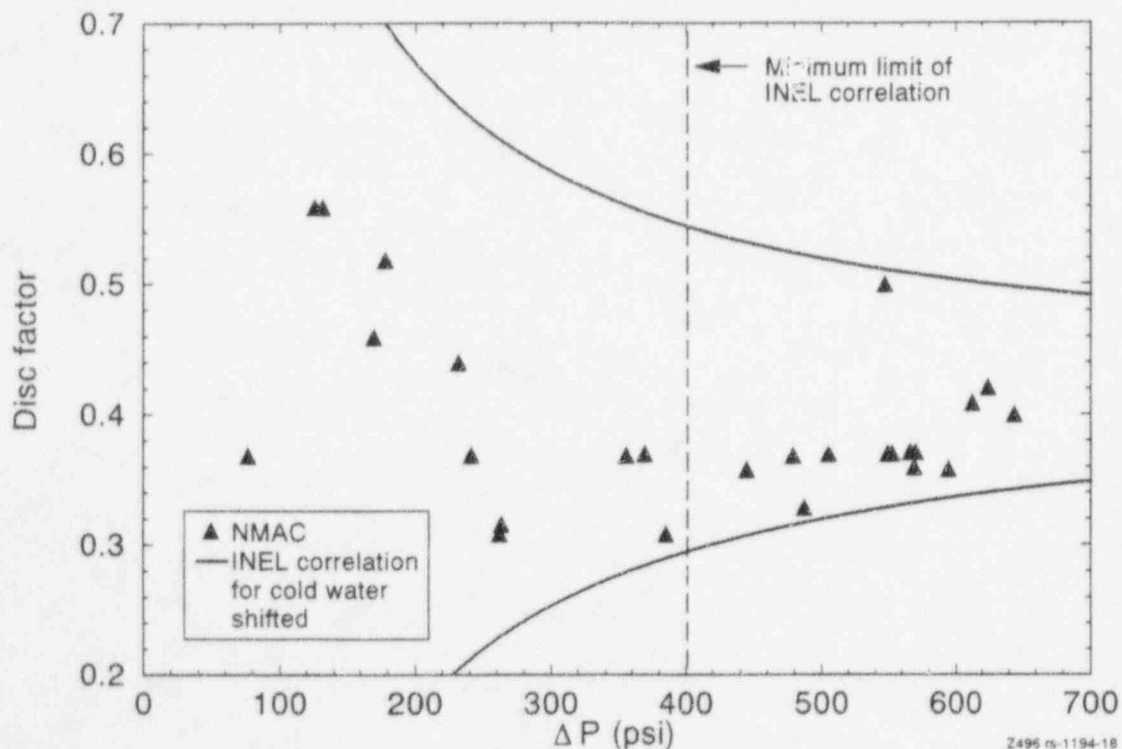


Figure 3-2. Disc factor plotted against differential pressure for the 14-in. utility valve. Tests at higher differential pressure show a more consistent disc factor.

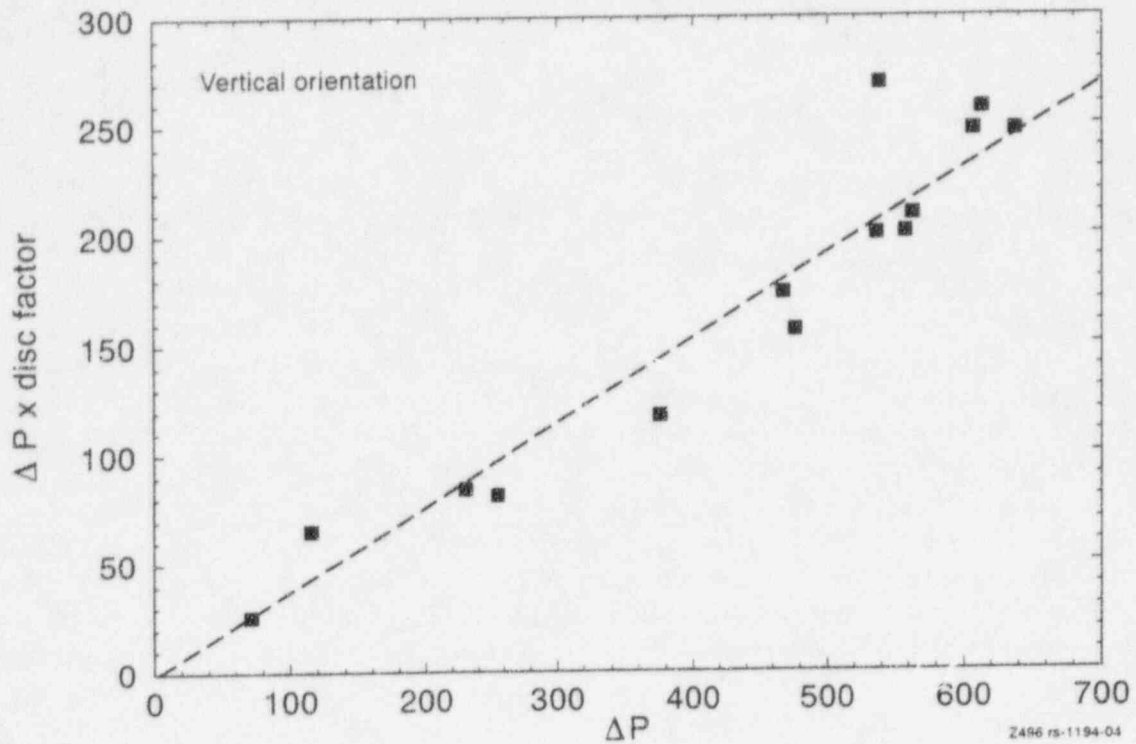


Figure 3-3. Disc load versus dynamic stem load; data fit for tests performed with the valve in the vertical position.

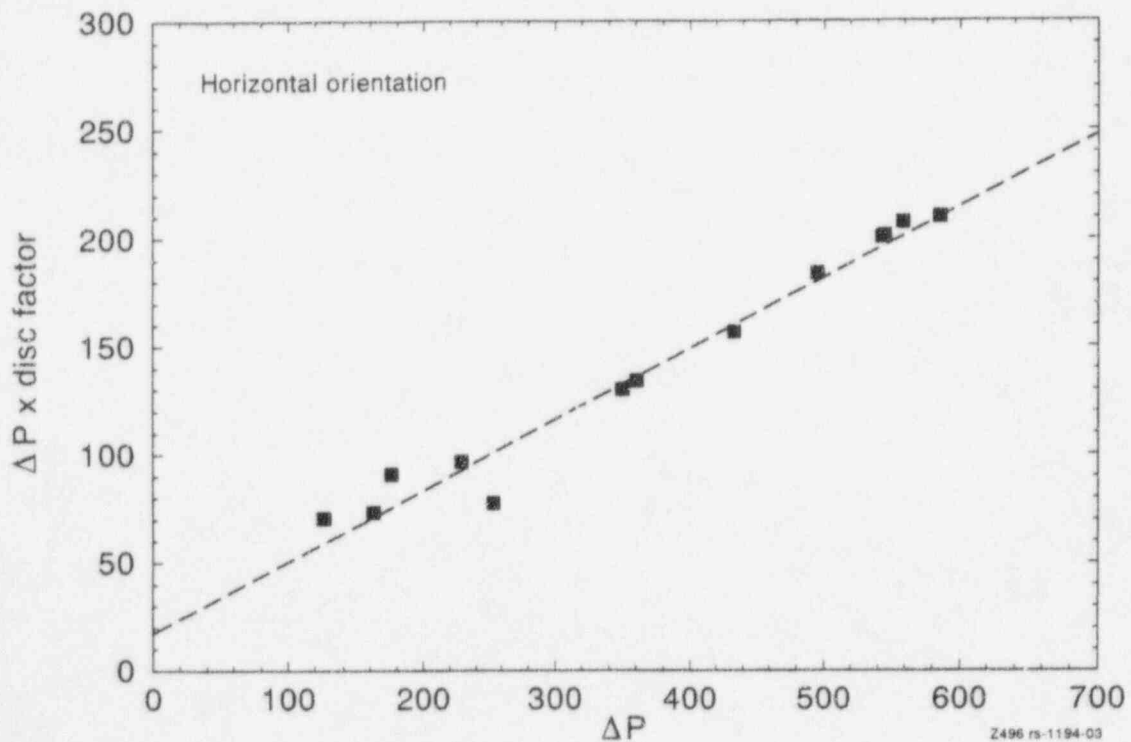


Figure 3-4. Disc load versus dynamic stem load; data fit for tests performed with the valve in the horizontal position.

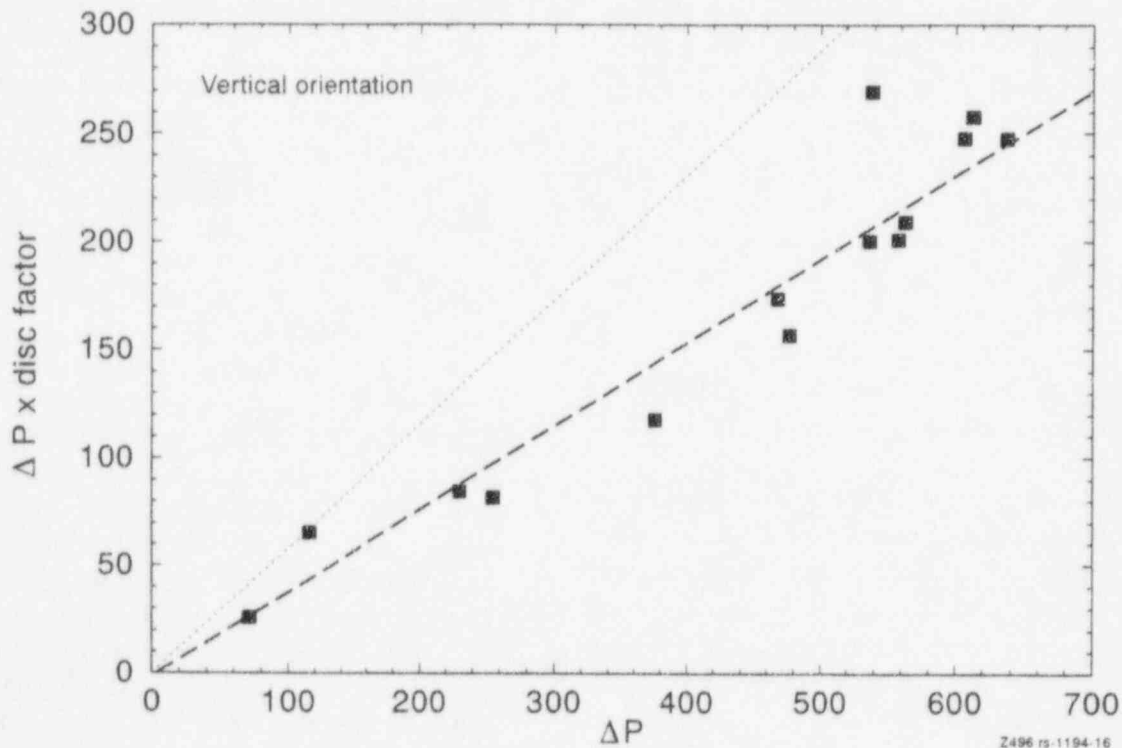
also labeled differently, is equal to the disc load divided by the disc area. In practice, the value for the vertical axis is calculated as the differential pressure times the disc factor, and the value for the horizontal axis is simply the differential pressure. This simplified approach is useful where the value for the disc factor is already known, and where it will not be necessary to compare the results of testing of different valves.

With the data arranged in this manner, what originally appeared to be a lot of scatter in the data now appears as a more linear relationship between the dynamic stem thrust and the disc load, with most of the individual data points falling fairly close to the trace representing a best linear fit.

There are several reasons that the data points appear to be more scattered in Figure 3-2 than in Figures 3-3 and 3-4. Figure 3-5, adapted from Figure 3-3, shows one of these reasons. The slope of the dashed line in Figure 3-5 represents a disc factor of 0.39. This represents the best fit for all of the tests shown on the data plot. In contrast, the

slope of the dotted line represents the disc factor in a single low-load test, the one conducted at 117 psid. The disc factor represented by this slope is 0.58. Compared to the best fit of 0.39, the magnitude of this disc factor, as indicated by the steepness of the slope of the trace, is partly a result of a small variation from the best fit but mostly the result of the low magnitude of the differential pressure load. At lower loads, a certain amount of variation in the data represents a larger portion of the total than the same amount of variation would represent at higher loads.

Figure 3-6, adapted from Figure 3-4, shows another reason. In this figure, the slope of the dashed line represents a disc factor of 0.33, and the slope of the dotted line represents a disc factor of 0.44 for a test conducted at 161 psid. Even though this data point falls very near the best linear fit for tests conducted with the valve in the horizontal orientation, the corresponding data points, as viewed in Figures 3-1 and 3-2, appear more like outliers. In this instance, the main reason for the difference is that Figures 3-1 and 3-2, as well as



2496 rs-1194-16

Figure 3-5. Same plot as Figure 3-3, modified to show one of the causes of the data scatter shown in Figure 3-2.

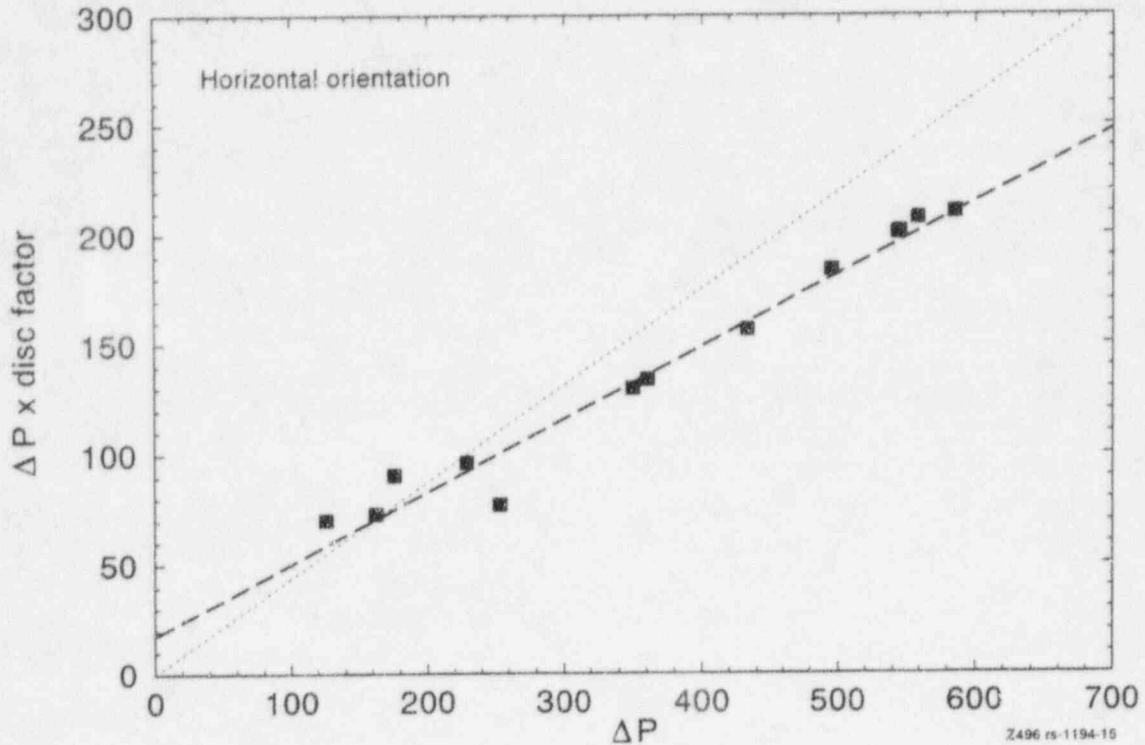
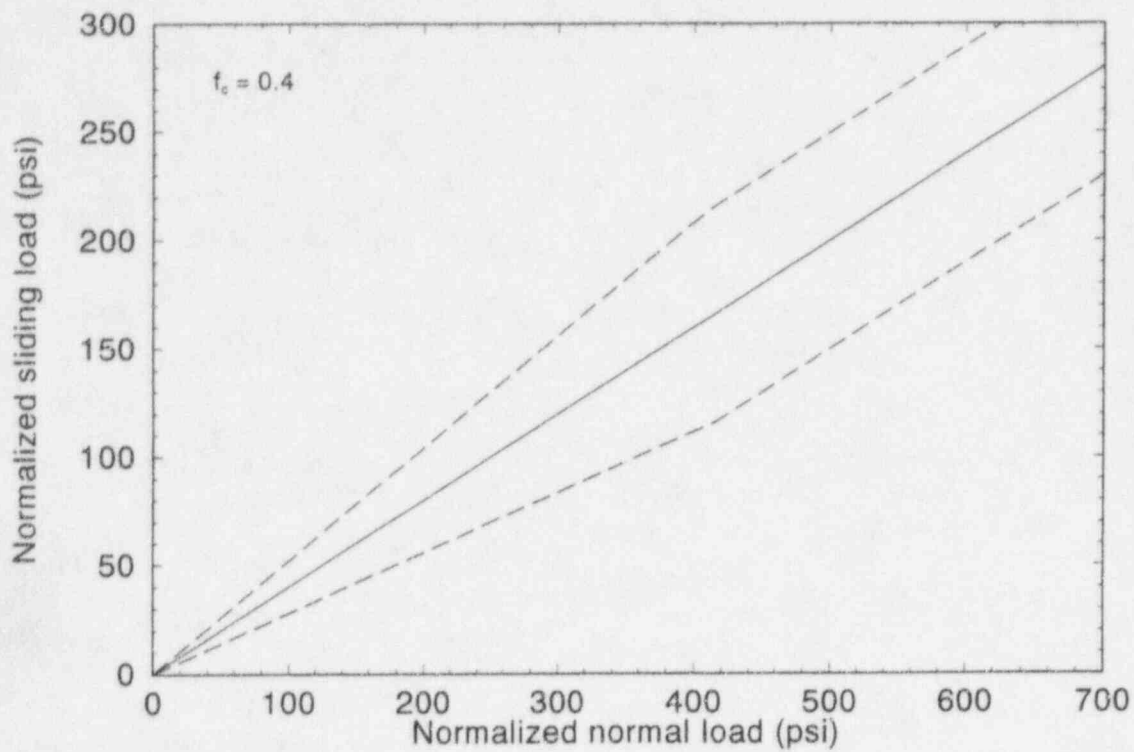


Figure 3-6. Same plot as Figure 3-4, modified to show one of the causes of the data scatter shown in Figure 3-2.

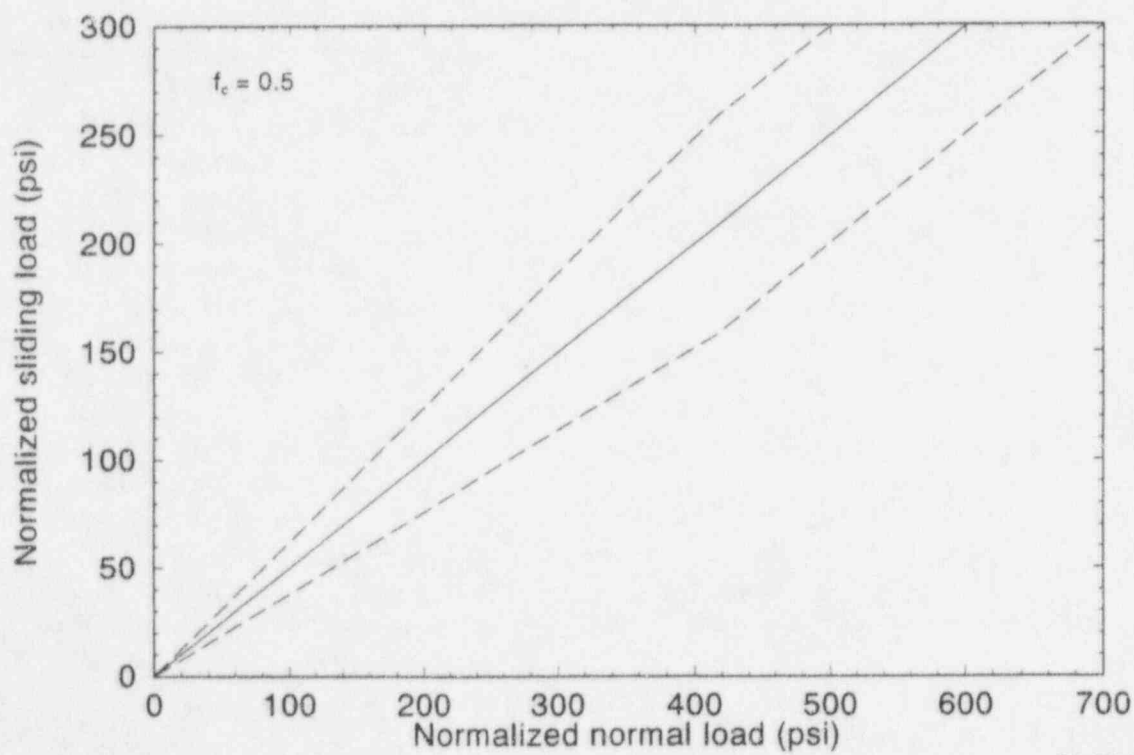
the dotted line in Figure 3-6, fail to account for the offset shown in Figure 3-6, where the dashed line representing the best linear fit does not intersect the vertical axis at zero.

These comparisons demonstrate that in evaluations of a single valve or a population of valves, particularly with tests conducted at low loads, it is more useful to derive a relationship between the dynamic stem thrust and the horizontal disc load than it is to simply plot the disc factor against the differential pressure load. These comparisons also show that for valves with typical responses (highest load before wedging occurs after flow isolation), it is not appropriate to use a single value for the disc factor to perform a linear extrapolation. The results of such an extrapolation can be very inaccurate, as shown, for example, by the dotted lines in Figures 3-5 and 3-6, where a linear extrapolation would predict a stem thrust much higher than the stem thrusts actually experienced in the tests conducted at higher differential pressure loads.

3.1.2 Extending the Original INEL Closing Correlation. Like the utility tests described in the previous discussion, the low-load tests that we performed as part of our full-scale testing showed a significant degree of scatter in the disc factor data. For this reason, we initially limited the application of the INEL correlation to loads above about 400 psid. The data we had at the time did not support extending the correlation any lower. However, from what we now see in the INEL data, the utility data described above, and other data we have looked at, it is evident that there is a linear trend running through a set of data scatter, even at lower loads. Based on these observations, we have extended the INEL correlation below the 400 psid lower limit. The extended correlation is shown in Figure 3-7. The equations that support the extended correlation are presented on page 3-8. Above a normalized normal load of approximately 415 psi, the first equation should be used, whereas below this load, the second equation should be used. The methods that produced the original correlation, including the equations that define the normalized normal and sliding loads, are explained in NUREG/CR-5720 (1992).



2512 rs-1294-03



2512 rs-1294-02

Figure 3-7. INEL closing correlation extended to include low disc loadings.

Disc Load

For $F_n \geq 415$ psi:

$$F_{stem} = F_{packing} + F_{sr} - F_{top} + F_{bot} + \frac{(\sin \alpha + f_c \cos \alpha) (F_{up} - F_{dn}) \pm 50 A_{ms}}{(\cos \alpha - f_c \sin \alpha)}$$

For $F_n < 415$ psi:

$$F_{stem} = F_{packing} + F_{sr} - F_{top} + F_{bot} + \frac{[\sin \alpha + (1.0 \pm 0.3) f_c \cos \alpha] (F_{up} - F_{dn})}{[\cos \alpha - (1.0 \pm 0.3) f_c \sin \alpha]}$$

where

$$F_n = \frac{(F_{up} - F_{dn}) \cos \alpha + (F_{stem} - F_{packing} - F_{sr} + F_{top} - F_{bot}) \sin \alpha}{A_{ms}}$$

F_{stem} = stem thrust

$F_{packing}$ = packing drag

F_{sr} = stem rejection load
= $P_{up} * A_{stem}$

F_{top} = $P_{up} * A_{ms} * \tan \alpha$

F_{bot} = $P_{dn} * A_{ms} * \tan \alpha$

α = valve seat angle

F_{up} = $P_{up} * A_{ms}$

F_{dn} = $P_{dn} * A_{ms}$

A_{ms} = mean seat area
= $1/4 \pi (\text{mean seat diameter})^2$

A_{stem} = stem area
= $1/4 \pi (\text{stem diameter})^2$

P_{up} = upstream pressure

P_{dn} = downstream pressure

f_c = 0.400 (less than 70°F fluid subcooling)
0.500 (70°F or more fluid subcooling)

With the normal load plotted against the sliding load, as shown in Figure 3-7, the resulting correlation is a very close representation of actual disc/seat friction. The upper and lower bounds of the INEL correlation are also shown on the figure.

These limits bound the test data that were used to develop the correlation.

Figure 3-8 shows the utility data described above, analyzed using the INEL methodology, and plotted in the extended INEL closing correlation (with $f_c = 0.400$). These utility data are included in the figure as an example to illustrate the concept, not to defend the validity of the extended correlation. In this analysis, we see that the data still vary somewhat, but the variation falls quite well within the limits of the INEL correlation. This analysis, too, helps us understand the scatter observed in the disc factor results shown in Figure 3-2. The slope of the solid line in Figure 3-8 represents a friction factor of 0.4. Below a normalized normal load of 415 psi, the upper and lower bounds of the INEL correlation are equivalent to friction factors of 0.52 and 0.28. The data at the very low normal loadings are scattered within these limits, but the amount of scatter appears to be much less than the scatter depicted in Figure 3-2. Some of the scatter shown in Figure 3-2 is simply the result of the method used to plot the data, and some is an artifact of using a disc factor instead of a true friction factor to assess the valve's response. Using the INEL methodology and viewing the data in terms of normal load versus sliding load accounts for the inherent data scatter and provides a more stable basis of viewing and assessing the data and predicting valve responses at higher loads.

3.1.3 Applying the Extended INEL Closing Correlation. It is our opinion that if a valve cannot be tested at its design basis differential

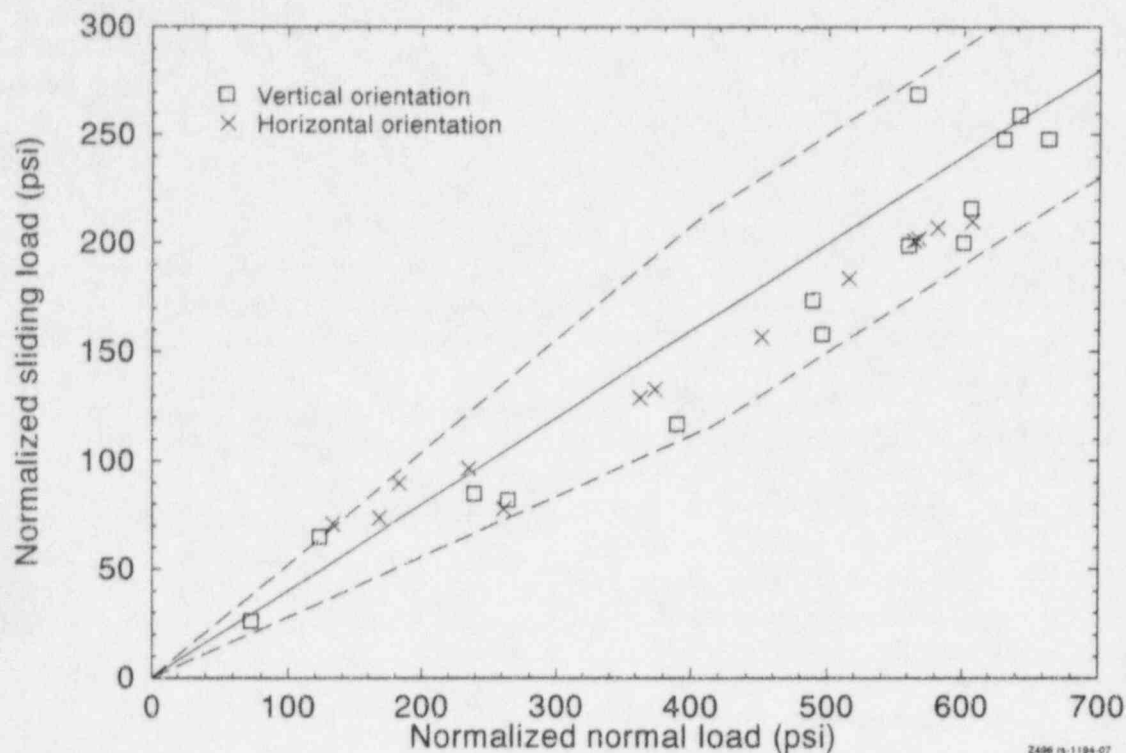


Figure 3-8. Extended INEL closing correlation with data from utility testing.

pressure, the valve should be set up using the best information available and using a justifiable friction factor or disc factor for the design basis loads. Then the valve should be tested at the highest differential pressure possible and the results checked for atypical behavior and for calculation and measurement errors.

We present the INEL correlation as one of several possible means of determining a justifiable friction factor. The use of the extended correlation for evaluating a valve's closing requirements is the same as for the original INEL closing correlation. The evaluation requires that a test be performed for verification purposes. If a test cannot be conducted at design basis differential pressure, we recommend that a test be conducted at the highest differential pressure possible, but at a minimum of either 200 psid or 50% of the design basis load, whichever is lower. Thus, 200 psid is the minimum test pressure for valves with a design basis differential pressure of 400 psid or greater. The flow rate must produce the necessary differential pressures at flow isolation before

wedging. Differential pressures developed after wedging do not load the valve disc properly and will not validate the evaluation. The results of a properly executed test can be used to check the tested valve's performance against the extended INEL correlation. If the results of the low-load test fall within the expected bounds, shown in Figure 3-7, the extended INEL correlation is considered applicable. This evaluation verifies that the response of the valve is typical of the valve responses used to develop the correlation. If the less-than-design-basis test results fall within the bounds of the correlation shown in Figure 3-7, then the correlation is applicable for design basis calculations for the specific valve.

The effect of the extended INEL correlation is to establish a nominal friction factor of either 0.4 or 0.5, depending on fluid conditions, and then to establish an upper bound for making predictions. For the correlation shown in Figure 3-8, where the nominal friction factor is 0.4, the slope of this upper bound represents a friction factor of 0.52 at lower loads, that is, normalized normal loads less

than 415 psi. At higher loads, the upper bound friction factor determined by the upper bound becomes a load-dependant friction factor that decreases toward 0.4 as the load increases. In effect, the friction factor used to predict the stem load varies from 0.52 to a little more than 0.4, depending on the load. For the correlation with the nominal friction factor of 0.5, the friction factor varies from 0.65 to a little more than 0.5. For more information on the concept of a load-dependent friction factor, see NUREG/CR-5720, page 51, Section 3.3.5.

This model considers disc/seat sliding friction only; the effects of mechanical interference on thrust are outside of the basis of this formula. The upper bound on the extended correlation represents the upper limit on what we consider sliding friction. Disc friction factors above 0.65 are outside the bounds of the data that support the correlation. This 0.65 limit applies to valves operating in colder fluids (more than 70°F subcooling). For valves operating in hotter fluids (less than 70°F subcooling), the limit is the 0.52 friction factor mentioned in the previous paragraph. Friction factors higher than these limits may represent valve performance from designs not included in our research base, or they may represent mechanical interference and possible valve damage rather than sliding friction alone. Evaluation of valves that experience mechanical interference is discussed in Section 3.2 of this report.

Note that with either the original INEL correlation or the extended correlation, the procedure for making the prediction is not a true extrapolation, though it appears to be such and though it is sometimes referred to as such. The prediction of the design basis stem force requirements is a straightforward calculation using a friction factor provided by the correlation and using known values for the valve dimensions and the design basis conditions. The calculation itself is independent of the low-load test results. The low-load test results do not provide a base from which to extrapolate; instead, they provide justification for using the methodology.

3.1.4 Preconditioning. Some of the scatter in the disc factor data from the utility valve test

program described in Section 3.1.1 (Figure 3-1) can be attributed to a lack of preconditioning. Preconditioning refers to the breaking-in of a new valve or a recently overhauled valve. New gate valves and gate valves that have recently been overhauled might temporarily have lower-than-normal disc friction coefficients.

Tribology experts who are currently investigating this phenomenon disagree as to its cause. The phenomenon may be the result, for example, of a residue of machining oil left on the disc and seat surfaces, or it may be the result of some other yet to be explained cause. Regardless of the cause, this phenomenon occurs, and it must be accounted for. This lack of preconditioning is seen as a general trend in the results of industry testing; tests run earlier in a test series tend to produce lower disc factors than those run later in the series. This explains why in Figure 3-1, the disc factors for stroke numbers 28 and 33 (at differential pressures of 117 and 540 psid) appear to be abnormally high; they were run out of turn, later in the test series.

Data scatter due to lack of preconditioning has appeared in other test results as well. Following the NRC/INEL Phase 2 MOV testing (reported in NUREG/CR-5558, 1990), it was observed that exposing a new or overhauled valve to hot water or steam conditions stabilized the friction coefficient immediately. In recent industry tests, researchers observed that under ambient temperature water conditions, many cycles were necessary to age the friction surfaces enough to yield a stable friction coefficient. It appears that disc friction values derived from recently overhauled valves operated in ambient temperature water may not be reliable. When such valves are tested in situ and the results are evaluated, it may be better to use the friction values obtained before the overhaul, or values from similar valves with aged surfaces.

3.2 Closing Requirements of Valves with an Atypical Response

There are several models currently used in the industry to evaluate gate valve responses and requirements. All of these models, including the

original INEL model, are applicable only after flow isolation and before wedging, when the disc is riding fully on the downstream seat, and when the upstream, bonnet, and downstream pressures have stabilized. The underlying assumption in the use of these models is that flow isolation is the part of the closing stroke that produces the highest load (before wedging). Experience shows that this assumption does not always hold true. However, it appears to be a valid assumption, since this is the part of the closing stroke where the differential pressure is the highest and the disc area exposed to the differential pressure is at its maximum. For this reason, we call this the classic or typical valve response. In typical valve responses, the increase in the stem load is approximately proportional with the increase in differential pressure and the increase in exposed disc area. Figure 3-9 is a stem thrust trace from a closing test showing the typical valve response. The peak thrust before wedging is at flow isolation, where the disc is riding on the seat.

Over the past few years, as more and more valve testing has been completed, we have

observed a substantial number of cases where the peak thrust during valve closure occurred before flow isolation. We call this an atypical valve response. This atypical valve response involves forces that may not be trivial; some of these atypical valve responses included a stem force before flow isolation that was 20 to 50% more than the subsequent thrust required at flow isolation. An atypical response is shown in Figure 3-10, a stem thrust trace from a valve closure. This response is sometimes called a hooked response, because the thrust history appears to have a hook shape just before the plateau that indicates flow isolation. Atypical responses can occur in either the opening direction or the closing direction. Closing responses are discussed here; opening responses are discussed later in this report.

The appearance of this atypical response would not be so serious if all valves could be tested in the plant at their design basis conditions, but this is not the case. If the hook response is noted in a design basis test, a check for damage should be performed. The stem thrust history provides an

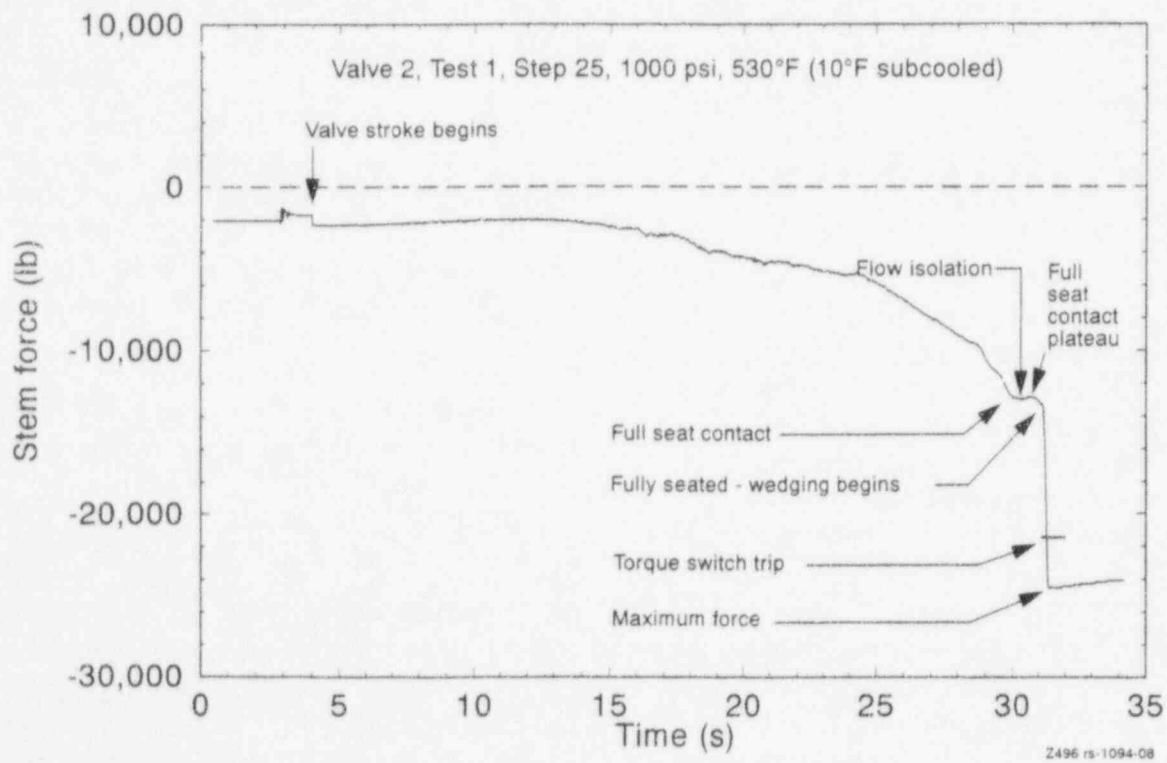


Figure 3-9. Stem thrust trace for a closure test, showing the classic, typical response. The peak thrust before wedging is at flow isolation.

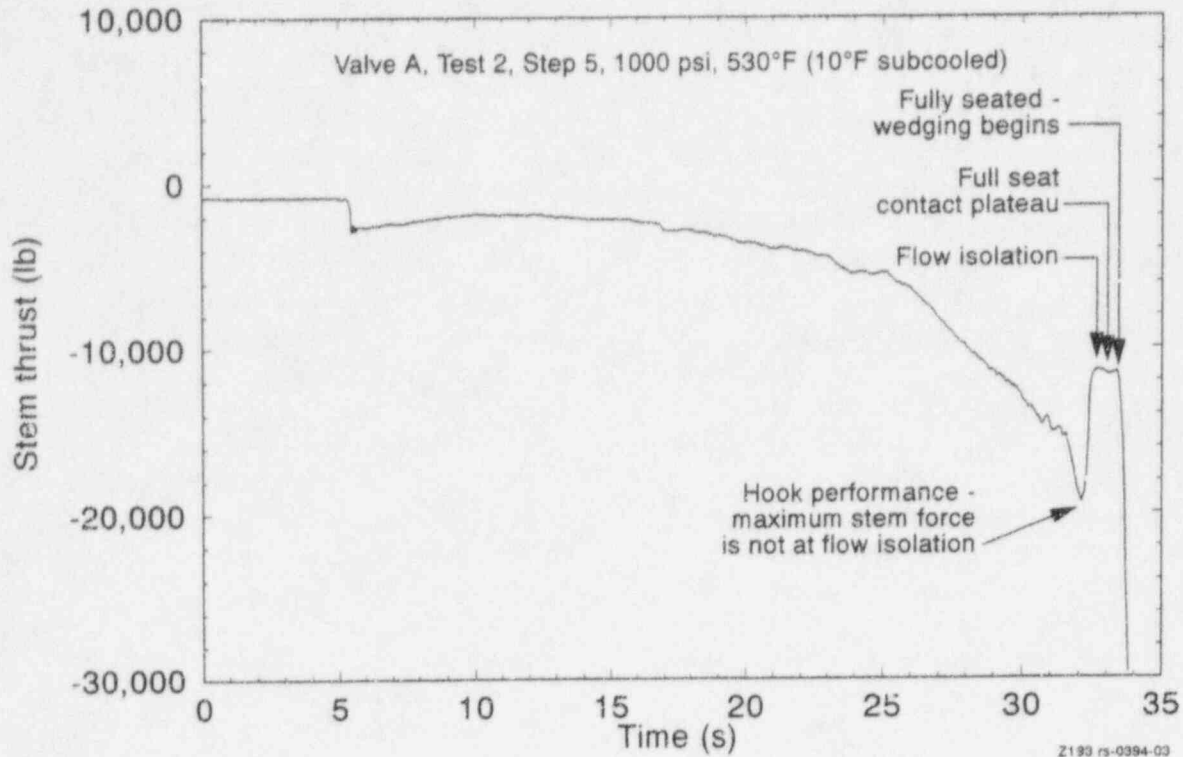


Figure 3-10. Stem thrust trace for a closure test showing an atypical response. The peak thrust before wedging is before flow isolation.

excellent tool for looking for damage. A jagged appearance in the stem thrust response is often an indicator of internal valve damage. An atypical response in a test conducted at conditions less severe than design basis conditions presents a problem in the evaluation of the valve's performance.

None of the current models used to evaluate valve responses and to predict or extrapolate valve closing stem force requirements apply to an atypical valve response, where the peak stem force occurs before flow isolation. All of these models rely on the pressures being uniform on the upstream and downstream sides of the disc after flow isolation. In an atypical response, flow is still taking place and the pressures are not uniform.

With so many valve responses showing evidence of atypical behavior, there was a serious need for a method to evaluate atypical behavior. Testing is the only feasible way to determine which valves perform with typical responses and which ones perform with atypical responses. For

this reason, the methodology presented here applies only to valves that can be subjected to a best effort flow test.

Our analysis of atypical responses includes data from NRC full-scale test programs [reported in NUREG/CR-5558 (1990) and NUREG/CR-5406 (1989)] and from industry testing. The following discussion presents our understanding of the cause of the atypical response, then recommends a best effort flow test to determine the typicality of the response. The discussion then proposes a method for using the best effort flow test as a basis for evaluating the valve's response and then performing an extrapolation to calculate a value that will bound the stem thrust expected at the valve's design basis conditions.

3.2.1 The Cause of Atypical MOV Responses. From our analysis of data from our test programs and from other data available to us, we have determined that the primary cause of this atypical response is tipping of the disc in response to flow forces as the valve closes. This tipping is primarily a result of large clearances between the

disc guide slots and the valve body guides (unsupported lower portions of welded-in body guides can also bend in response to flow forces, allowing the disc to tip). Figure 3-11 shows what we call a guide-restrained tipped disc, and Figure 3-12 shows what we call a seat-restrained tipped disc. These two figures illustrate the worst case tipping for each of the two cases. The tipping of the disc produces two effects that can contribute to atypical behavior: an increase in the mechanical interference between the disc and the guides and between the disc and the seat, and changes in the pressure distribution around the tipped disc.

Mechanical interference and the physical damage that sometimes accompanies it can contribute to atypical behavior by adding to the thrust required to operate the valve, particularly in the closing direction and under high flow conditions. This additional thrust, along with the other forces, can produce a peak stem force condition before flow isolation. If the angle of the tipping is large enough in the guide-restrained case, the guide contact area will be much smaller than normal. This results in an increase in the contact stress, which can lead to galling and plastic deformation. If the angle of the tipping is large enough in the seat-restrained case, mechanical interference between the leading edge of the disc and the edge of the seat will add to the thrust load in the stem. If the leading edge of the disc is sharp enough, the disc can shear stellite from the seat as it closes, resulting in loads that are likely to be even higher.

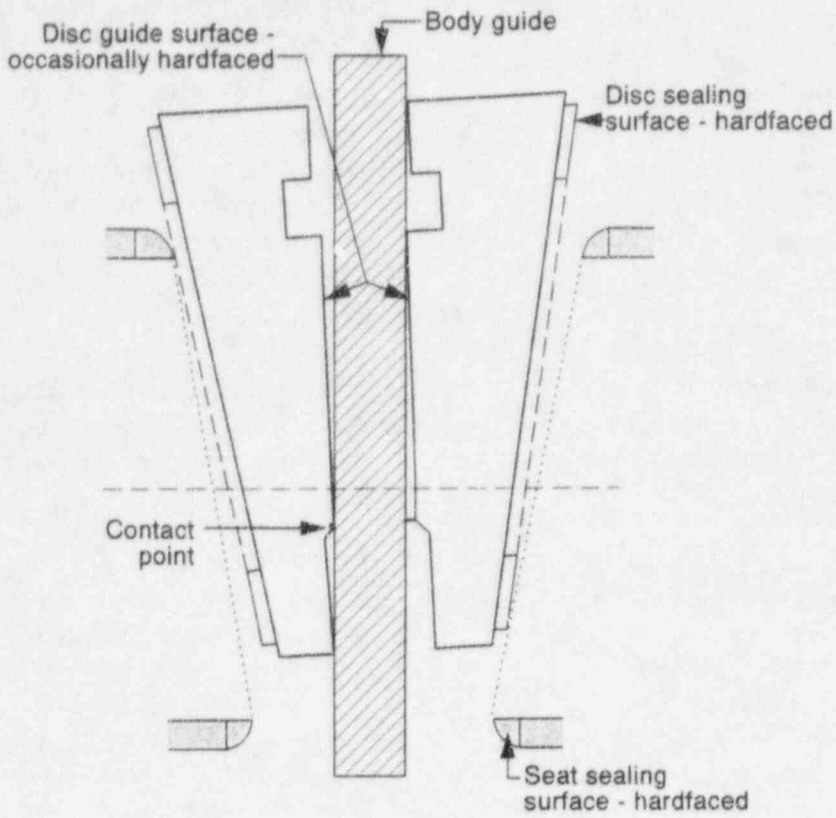
All of the anomalies described above have been observed in actual testing. Posttest inspections combined with careful data analysis have shown that most damage can be detected from the stem force history. Figures 3-13 and 3-14 are stem force histories from our full-scale valve testing. Valve damage is evident in the jagged appearance shown in the stem force histories. Figure 3-15^a is a stem thrust history from a valve closure in which the disc tipped (atypical response is evident), but no

damage occurred. These data are from the low-flow ambient temperature tests conducted as part of the Electric Power Research Institute (EPRI) performance prediction program. This valve and several other valves from industry test programs exhibited atypical responses in the closing direction, but without damage. We do not know the extent to which mechanical interference can contribute to an atypical response without causing damage. Moreover, in an atypical response without damage, it may be that only a small portion of the atypical response is due to mechanical interference.

The other factor that contributes to atypical valve response, and probably the more important of the two in most cases, is the change in the pressure distribution around the disc while it is tipped, before it comes in full contact with the seat. Full seat contact in this sense does not refer to wedging, but refers instead to the disc sliding in full contact with the downstream seat, before wedging begins. Full seat contact typically occurs after flow isolation in the closing direction (and after unwedging but before flow initiation in the opening direction). Figure 3-16 shows the area of the disc and the stem rejection area that the pressures act upon. These areas and the corresponding loads were the heart of the early industry gate valve sizing equation. These early industry equations were basically an area times a differential pressure times a fractional disc factor (typically 0.3), plus or minus the stem rejection load (depending on whether the valve was opening or closing), plus the packing friction load. The internal valve pressure is always trying to expel the stem, so the pressure load on the stem area assists the operator during opening and resists during closing. Except for the packing load, the stem rejection load was the only direct vertical load that was considered in the early gate valve sizing equations. The effect of the fractional disc factor was to account for disc-to-seat friction and any unknown variables.

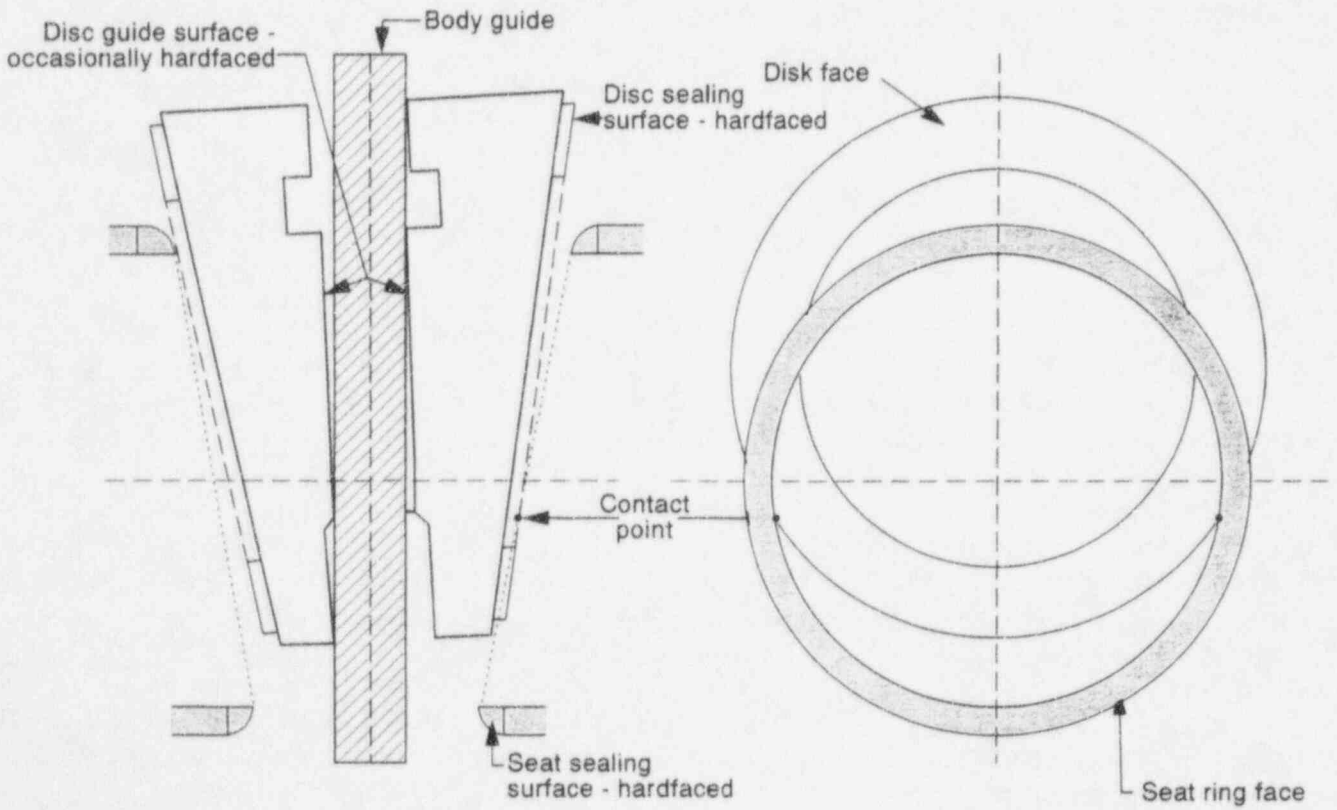
During the development of the INEL correlation, we identified an additional vertical area where pressure in the valve produces a load on the stem. That work is documented in NUREG/CR-5720 (1992). Figure 3-17 shows this additional area, defined as the elliptical area of

a. Nonproprietary, uncopyrighted data provided to the NRC by EPRI in a public meeting as part of a progress report.



Z191 rs-0394-03

Figure 3-11. A guide-restrained tipped disc.



Z191 rs-0394-04

Figure 3-12. A seat-restrained tipped disc.

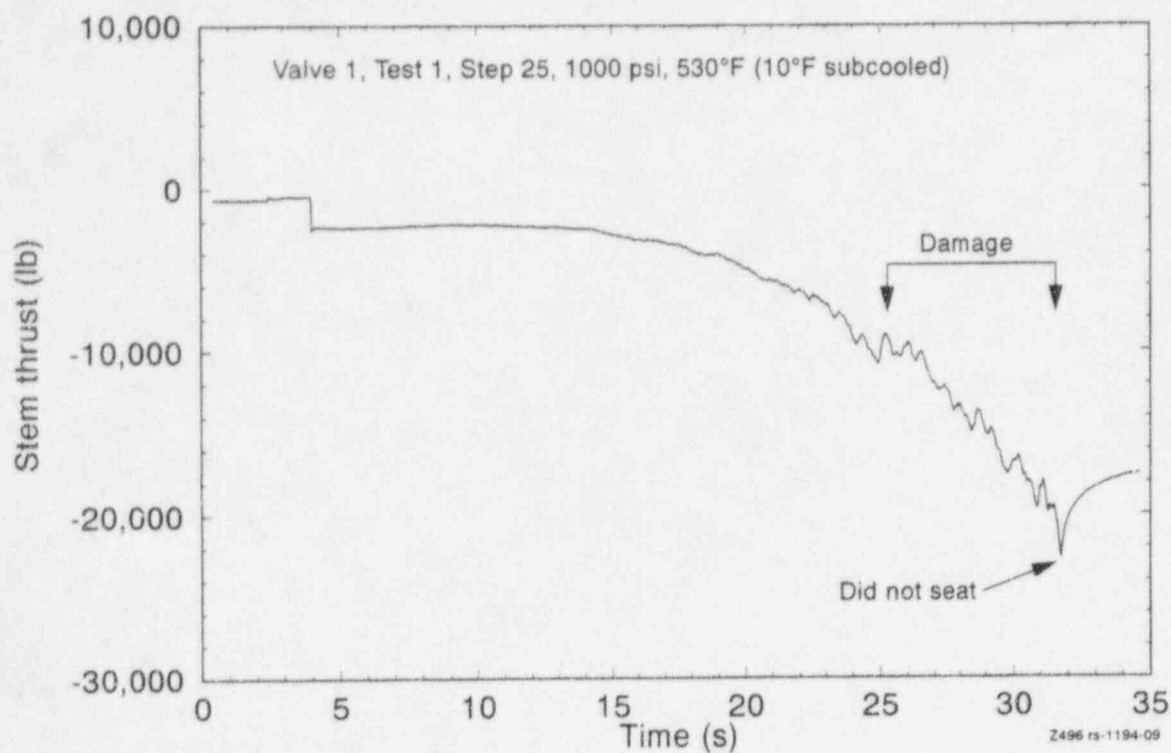


Figure 3-13. Stem thrust trace showing a jagged shape, indicating valve damage.

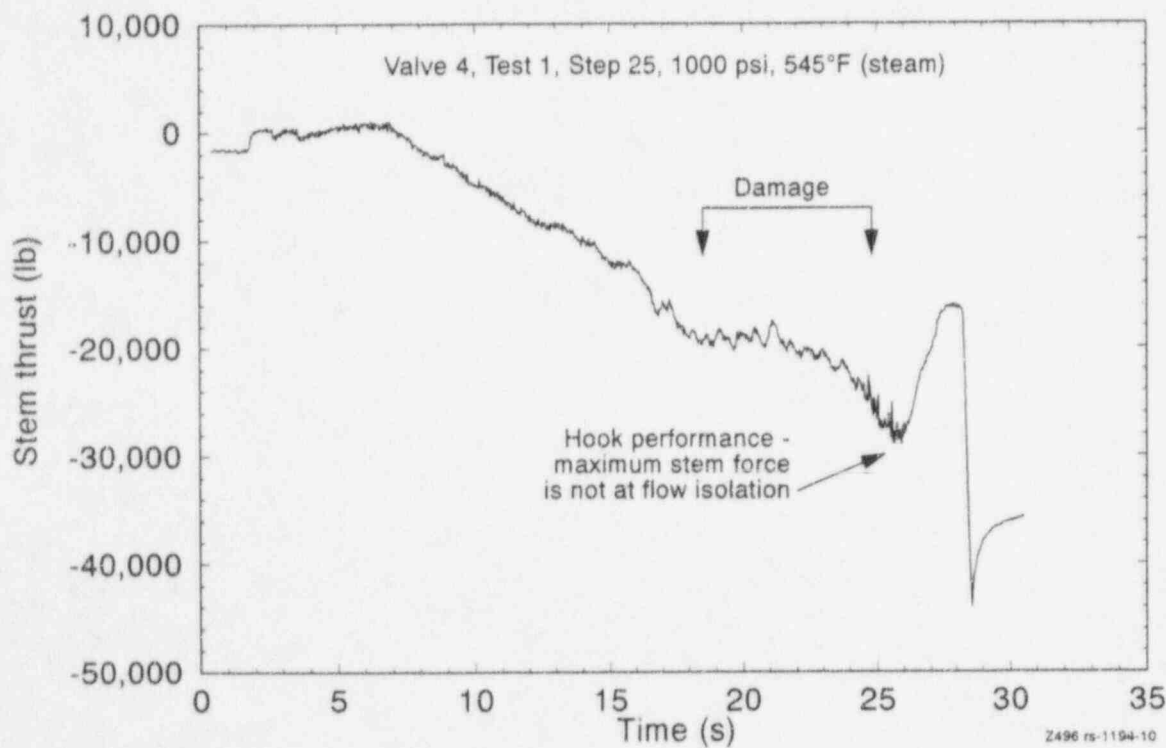


Figure 3-14. Stem thrust trace showing a hook shape in the response and showing evidence of valve damage.

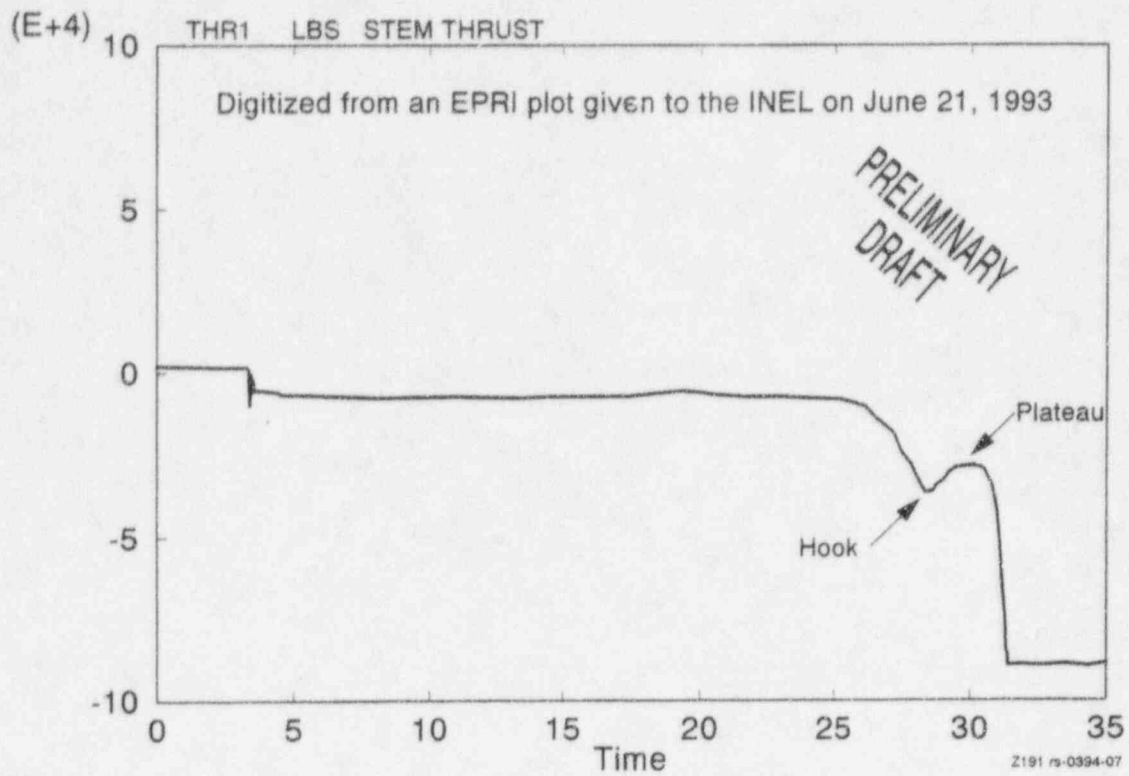


Figure 3-15. Stem thrust trace from testing of a 6-in. service water valve closing against design basis flow. The trace shows an atypical response, but no damage occurred.

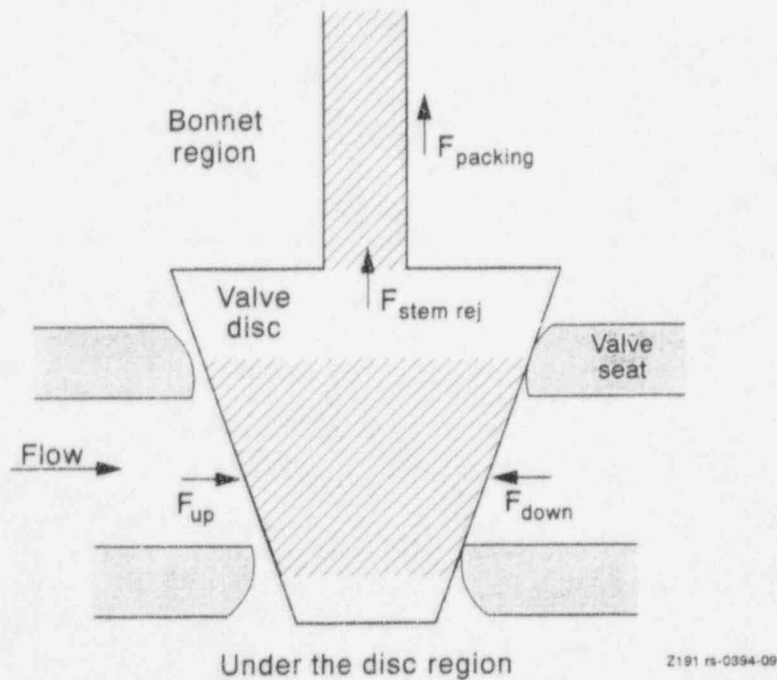


Figure 3-16. Valve disc cross-section showing horizontal and vertical forces acting on the disc and stem, as identified by the standard industry equation.

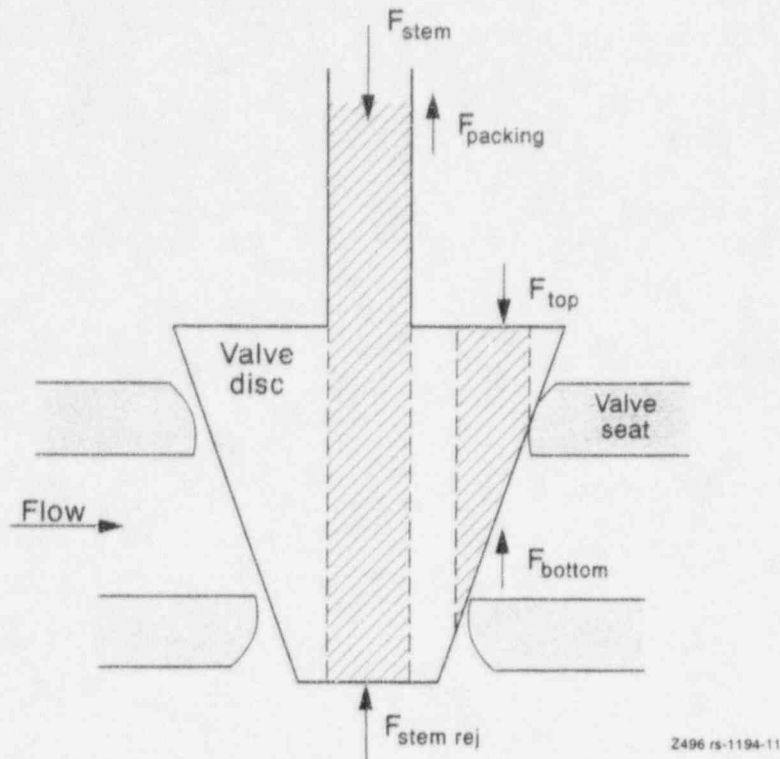


Figure 3-17. Valve disc cross-section showing additional vertical forces acting on the disc, identified as F_{top} and F_{bot} in the INEL correlation.

the seat orifice when viewed from the axis parallel to the stem. This area is a result of the angle of the seat (nominally 5 degrees) in a wedge-type gate valve. The bonnet pressure acts on this area from above, and the downstream pressure from below. These two pressures produce a net downward load that assists the operator during closing and resists during opening. Thus, this load tends to offset the stem rejection load. Typically, the stem rejection load dominates in valves smaller than 6 in., and the vertical disc load dominates in larger valves. All of these loads (including those discussed in the previous paragraph) maintain their relationships as long as the disc is closing or opening in an untipped condition. The result is a classic, typical response.

However, most valve discs will tip on the guides before coming into full contact with the downstream valve body seat, and some will tip enough to produce an atypical response. Figure 3-18 shows how the pressure distribution loads change with the disc tipped. The net down-

ward load shown in Figure 3-17 gets smaller. The effect of this change is to increase the stem thrust needed to close the valve. In addition, a tipped disc area term appears, acted upon by the difference between the upstream pressure and the bonnet pressure. This area becomes larger the more the disc tips. The result is another net vertical loading that resists valve closure. These two changes in the disc loads either modify or add to the loads in a classic, typical response, and along with mechanical interference, they contribute to the peak thrust seen before flow isolation in the atypical valve response. The decrease from the peak thrust point to the plateau at flow isolation, as shown in Figure 3-14, is caused by the disc coming into full contact with the seat and straightening up. This reorientation of the disc changes the pressure distribution around the disc back to normal and changes the mechanical interference loads back to simple sliding friction.

The propensity for a valve disc to tip is not associated with a single valve manufacturer.

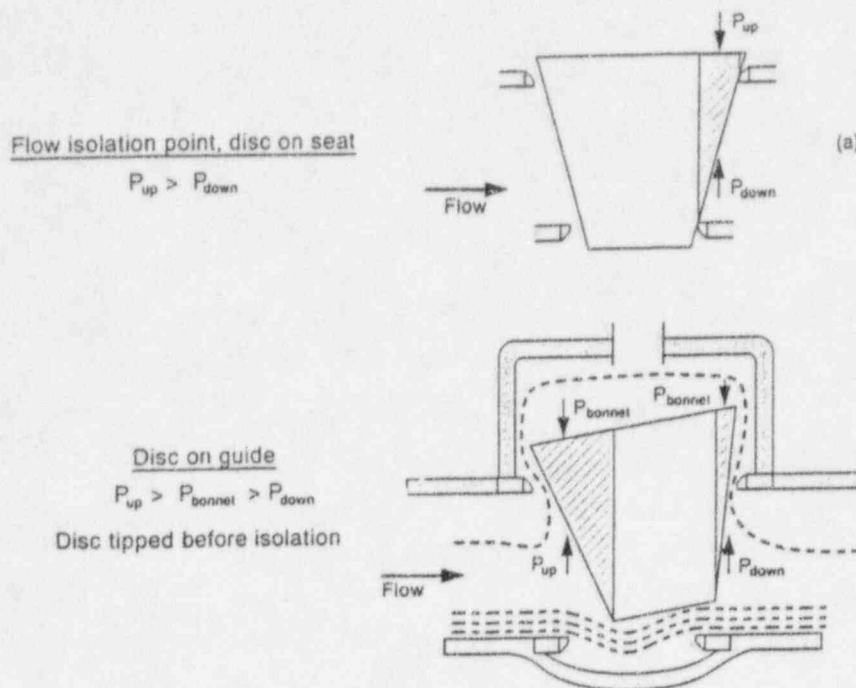


Figure 3-18. Disc areas that the various pressures act on; as the disc tips, these areas and pressures change.

According to the manufacturers' published tolerances, it is possible for the disc of almost any valve of any manufacturer to tip enough to result in atypical behavior, depending on how the tolerances stack up. In addition, no two valves can be expected to exhibit the same atypical response, even if the valves are of the same manufacturer and model. With measurements of individual clearances in the guides and seats, it might be possible to predict how much the disc will tip. However, the relationships between disc tipping, the flow paths through the bonnet region and under the disc, and the pressure distribution around the disc entail so many unknowns that any prediction of the resulting stem load would by its very nature require considerable conservatism.

3.2.2 Best Effort Flow Test. The alternative to blind predictions and the extra conservatism that they entail is testing. This does not mean that every valve that closes or opens against differential pressure must be tested at design basis conditions. However, some best effort differential pressure test should be performed to determine whether a

valve performs with a classic/typical or an atypical response. Our analysis of test data indicates that a valve tested at a reasonable differential pressure load in relation to its design basis differential pressure is sufficient for this purpose. We recommend 200 psid or 50% of the design basis load (whichever is lower) as a minimum. This minimum differential pressure loading should establish a disc response pattern for both typical and atypical valve performance. With the response pattern thus established, the analyst can select a method for predicting or extrapolating the design basis response. At this minimum loading, a valve with a propensity for atypical behavior will exhibit all of the signs of its atypical response, provided that the fluid temperature and fluid conditions are somewhat representative of the design basis conditions. (If the valve is tested in ambient temperature water, the resulting disc factor will probably be higher than it would be if the valve had been tested with higher temperature fluid.) Additionally, the flow must be sufficient that the disc is loaded to the minimum differential pressure before flow isolation. Under these conditions, the

tipping of the disc, the pressure distribution, and the fluid effects will all be exhibited. This means that bounding the design basis response should be a matter of a simple linear extrapolation, provided that valve damage is not a concern.

If the best effort flow test indicates that the valve has a classic, typical response, one of the conventional seating models can be used to evaluate the response. If an atypical response is evident, the next step is to examine the stem thrust history for evidence of damage. Figures 3-13 and 3-14 (Valve 1, a 6-in. 900-lb-class flex-wedge gate valve, and Valve 4, a 10-in. 900-lb-class flex-wedge gate valve, respectively) show stem thrust histories where damage occurred during the closing stroke, as indicated by the jagged appearance of the traces. Figure 3-15 shows a stem thrust history from a test of a service water valve in which no damage occurred. In our full-scale test programs, we were almost always able to correlate irregularities in the stem thrust traces with the occurrence of damage during the closure. Some of the more subtle damage, such as bent guides, was identified after testing through posttest inspection.

That response, too, is evident in the thrust history, now that we know what to look for (see Figure 3-19, closing portion of the trace). Following a flow test, a seat leakage test can also help identify damage. Such a test might be particularly important if the flow test is repeated and the hook is smaller in the second test. This usually indicates that the disc machined the seat during the first test, rounding the corners, so that there is less mechanical interference during the second test. (The first test removes the sharp edges from the valve body seat and rounds the matching area on the disc seat.) Figure 3-20 (upper plot, closing stroke) is a good example of a thrust trace where the hook is less pronounced in the second test than in the first test (Figure 3-20, lower plot).

3.2.3 Extrapolation of Atypical Responses. If no damage is observed, one can assume that the hooked response will increase linearly with pressure as the valve is exposed to higher pressure loadings. This being the case, the response at higher flow loads can be bounded with a linear extrapolation. This assumption is based on the fact that in the best effort flow test,

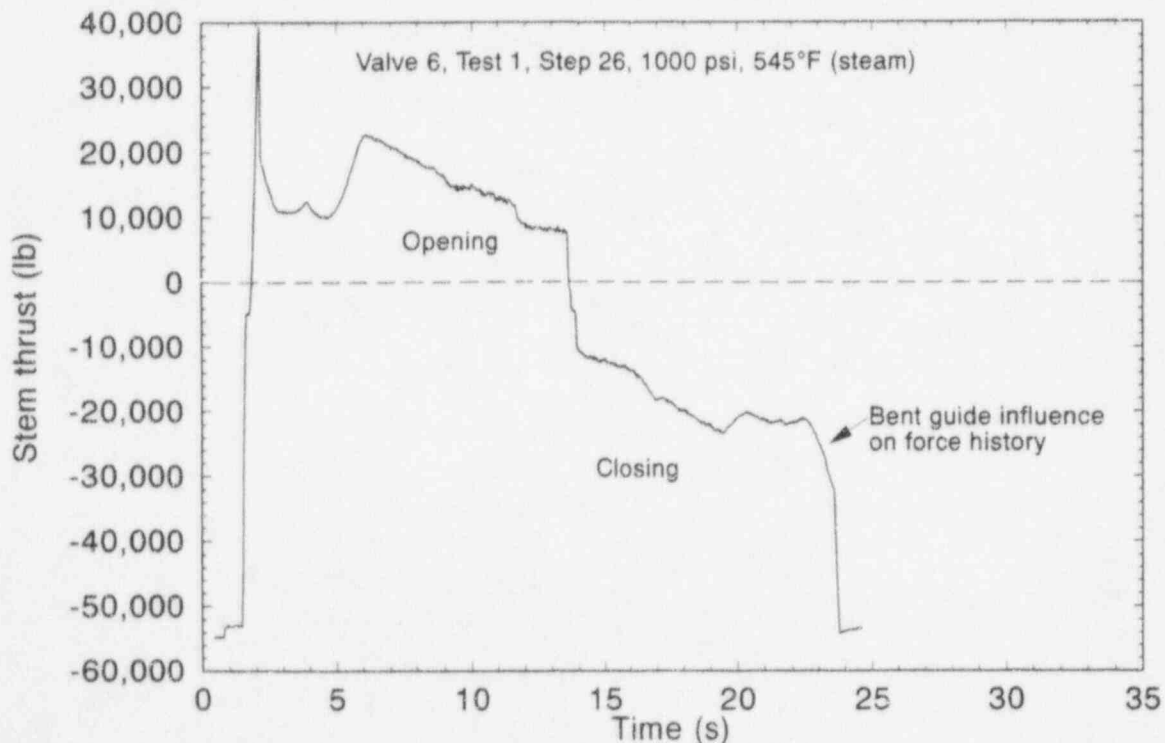


Figure 3-19. Stem thrust trace for partial opening and reclosing. The closing trace shows evidence of a bent guide.

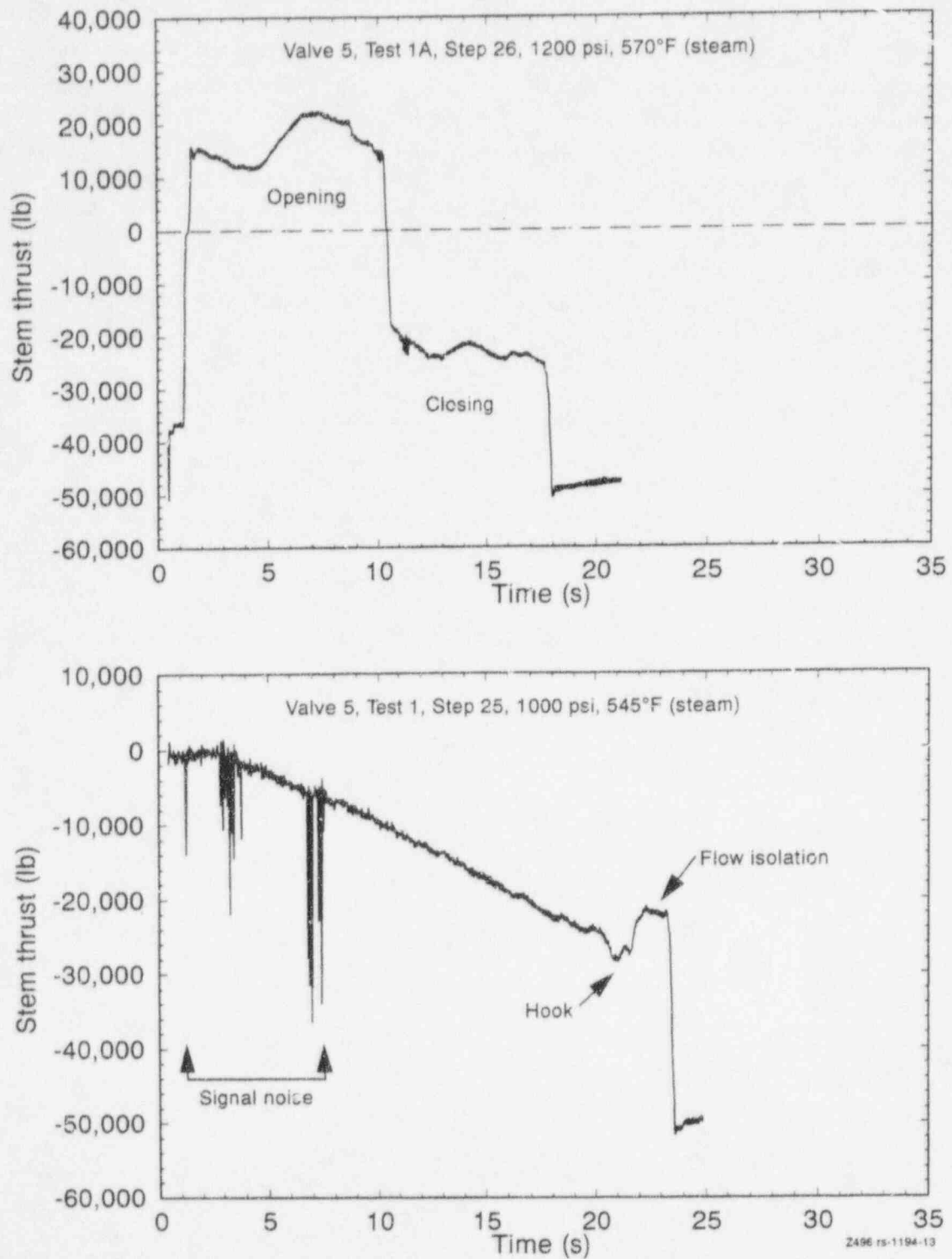


Figure 3-20. Stem thrust traces showing how the hook shape was less pronounced during the second test (upper plot, closing stroke) than during the first test (lower plot). Note also that during the partial opening stroke (upper plot), the peak thrust occurs after unwedging and unseating.

the disc is tipped as far as it can tip, so the pressure distribution around the disc and the resistance due to mechanical interference have been established. Thus, all of the load effects due to geometry, disc tipping, disc area, and mechanical interference are present in the best effort flow test. The area, tipping, and geometry will be the same in the higher pressure case; only the disc factor may change. We expect any change in the disc factor to be a downward change; the friction term is typically less at higher loads. Valve testing and laboratory single effects testing have confirmed that less thrust is required per pound of differential pressure at higher disc pressure loads. Because of differences among individual valves, this technique cannot be used in a grouping application, nor can the results of testing one valve be extended to other valves; this technique is valid only for the tested valve. Once best effort test data are obtained, the following equation can be used to extrapolate the results to the design basis differential pressure load:

$$F_{stem} = C_{hooking} \Delta P + P_{up} A_{stem} + F_{packing}$$

where

F_{stem}	= stem thrust
$C_{hooking}$	= hooking factor
ΔP	= differential pressure
P_{up}	= upstream pressure
A_{stem}	= stem area
$F_{packing}$	= packing drag

Use the data from the best effort flow test as input to calculate the hooking factor. The hooking factor is a term that accounts for both the disc factor and the disc area term. Because the peak force is measured before flow isolation, the disc area (the area of the disc exposed to flow and differential pressure forces) is unknown. (In the laboratory, it is possible to use stem position data to estimate the exposed area of the disc, but in the field this would be difficult, and for the purposes of the evaluation described here, it is unnecessary.)

Once the hooking factor is determined from the best effort flow test, the hooking factor is used along with the design basis pressure and differential pressure to estimate the design basis stem thrust. We believe that this procedure will bound the stem thrust at design basis conditions; as explained in the previous paragraph, the ratio of actual stem thrust (the force required to move the disc) to differential pressure decreases as the differential pressure across the disc increases, all other parameters remaining the same. Thus, the actual stem thrust required for valve operation will be lower than the stem thrust predicted using this procedure.

3.3 Opening Requirements

Although there are some similarities between opening and closing, there are also some important differences. The stem rejection load, which resists during closure and adds to the stem load, assists during opening. Likewise, the F_{top} load, identified during our development of the INEL correlation and mentioned earlier in this report (see Figure 3-17), assists during closure but adds to the stem load during opening. As with closing responses, we observed the occurrence of atypical as well as typical opening responses. Figure 3-21 shows the typical opening response. As expected, a classic, typical opening response shows the highest load (after unwedging) to occur while the disc is sliding on the downstream valve body seat but before flow initiation. This point in the opening stroke corresponds with the point of interest in the typical closing stroke, that is, where the full area of the disc is exposed to the full differential pressure. Because of this similarity, one might expect that the closing correlation could be modified (with sign changes for the stem rejection load and the F_{top} load) to predict typical opening responses. However, we found it necessary instead to develop a new correlation with a different disc friction factor that fits the test data.

We found atypical responses to be more common during opening than during closing. In some instances and under some conditions, valves that exhibited typical responses during closing exhibited atypical responses during opening. The

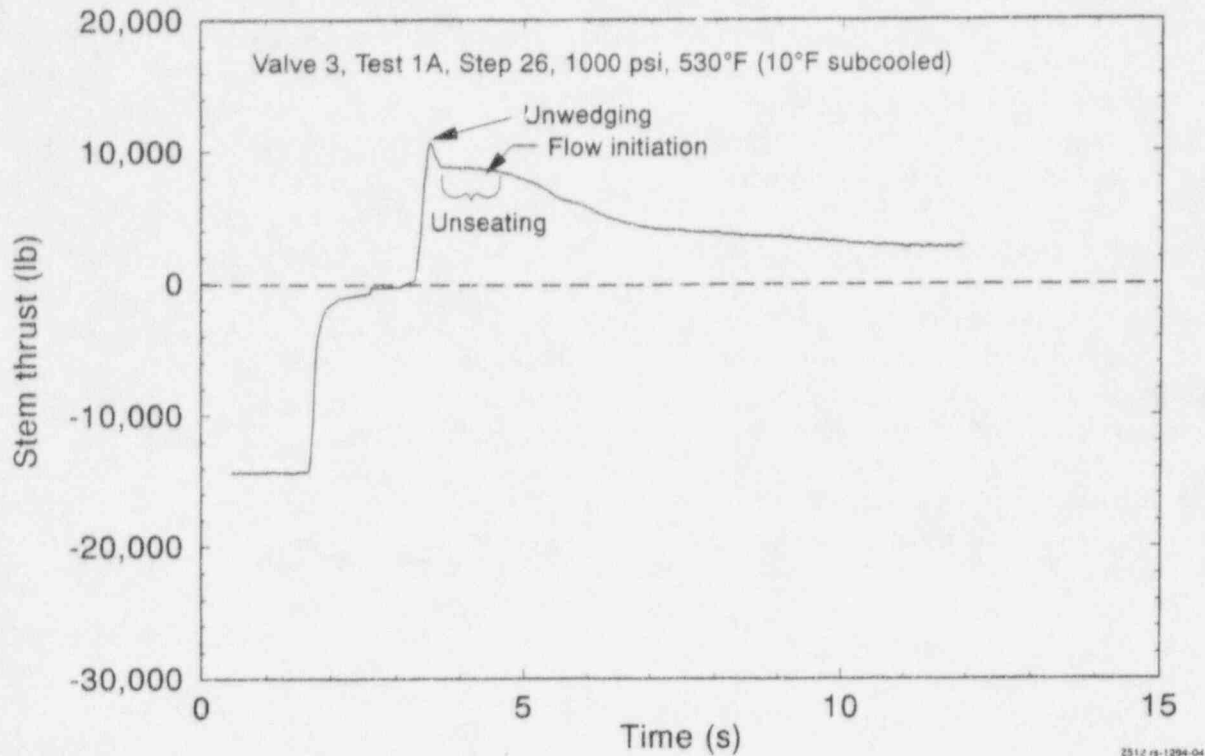


Figure 3-21. Stem thrust trace recorded during an opening test, showing the classic, typical response.

atypical response appeared in the stem force history as a hump in the trace after flow initiation, indicating an increase in the load instead of the expected decrease. After a careful study of the atypical opening responses from the NRC/INEL full-scale valve tests, we determined that the opening correlation we developed for typical responses also applies to atypical responses.

The following discussion first examines atypical opening responses observed in the NRC/INEL full-scale test results. Next, we present a new correlation for evaluating valve opening responses and predicting opening requirements. Then we address the applicability of the new correlation to atypical opening responses.

3.3.1 Analysis of Full-Scale Test Results.

Before the NRC-sponsored INEL valve testing program was conducted in 1988-89, not many high-energy gate valve test results were available in the public domain. Virtually no results were available from valves tested in the opening direction. Most of the analysis presented in the following discussion is based on the results of the

NRC/INEL valve test program. We have also reviewed a number of recent industry test programs, and the results of that work do not conflict with the results presented here.

In our early analysis of data from opening tests in the NRC/INEL Phase 2 full-scale test programs (reported in NUREG/CR-5558, 1990), we observed that with the larger (10-in.) valves tested with steam, the flow loads after unseating were higher than the loads during unseating. Figure 3-20 (upper plot, opening stroke) is an example of such a response. This result initially gave us the impression that for valves exhibiting atypical behavior, there was possibly not only a hook in the closing direction, but also a corresponding hump in the opening direction.

On closer examination, we found the atypical opening response to be more complicated than that. For both opening and closing, there are several mechanisms at work, each contributing to or subtracting from the total stem load. One of these mechanisms is mechanical interference between the disc and the seat, which adds resistance in the closing direction but not in the opening direction.

In addition, we found that in the opening direction, the atypical response is affected more by fluid condition and fluid pressure than in the closing direction. Separating these individual forces and influences was a different challenge for the opening direction than for the closing direction. The responses changed with pressure, test fluid (cold water, hot water, steam), degree of subcooling, and valve size. After analyzing some of the other data from the smaller valves and observing the results of industry testing, we determined that the atypical opening response occurred only with some single-phase fluids.

After a preliminary analysis, during which we tried to analyze the data by separating the forces and solving for the friction factor, we created a computer model that represented what we thought should be going on within the valve in the opening direction and then analyzed all of our close-to-open-to-close test data against this model. The model was based on the INEL closing equation, refitted for the opening direction, with the added capability to address the tipping of the disc. The model was designed to estimate the stem thrust responses using actual valve dimensions and real-time test pressures recorded in the bonnet and under the disc as well as upstream and downstream of the valve. It was not our intent during this effort to tweak the model until it provided accurate predictions of the valves' responses, but rather to check all our high-flow reopening and reclosing data against a common set of predictions based on what we thought was going on.

We made some simplifying assumptions. For example, we assumed a constant disc area throughout the stroke. This simplifying assumption causes the model to overestimate the stem thrust when the valve is open more than the 1.5-in. stem position (approximately). However, the model still met our needs, because we were interested primarily in the response during the initial portion of the opening stroke and the last part of the closing stroke, when most or all of the disc is exposed to the differential pressure.

Figures 3-22 and 3-23 show the responses of two of our 10-in. valves during the opening and closing cycle discussed above. The test medium

is steam. The upper trace in these figures represents the valve opening stroke, traveling left to right, whereas the lower trace represents the valve closing stroke, traveling right to left. The stem thrust traces have been plotted against stem position, so the fully closed position for both the opening stroke and the closing stroke is on the left. The zero stem position corresponds to the disc position where the visual flow path is barely blocked. With the data plotted in this manner, it is easy to see how closely the opening response mirrors the closing response.

Figure 3-22 shows the stem thrust during the opening and reclosing cycle for Valve 5, a 10-in. Wm. Powell flexwedge gate valve, and Figure 3-23 shows the same information for Valve 6, a 10-in. Velan flexwedge gate valve. As explained above, the calculated traces on the plots are the responses estimated by our simple model, based on the actual test pressures, assuming a specific disc friction, and adding the effects of slight tipping of the disc after the disc comes off the seat.

Except for the beginning of the opening responses, the estimates for both opening and closing are close to the actual measured values. The traces for both valves show slight hooks in the closing direction. (This atypical or "hooking" response during closure is discussed earlier in this section of the report.) For both valves, the thrust measured at the beginning of the opening stroke, while the disc is still riding on the downstream seat, is very low compared to the estimate. However, once the disc moves off the seat and after flow is initiated, the opening thrust recovers and matches the prediction quite well. Without this kind of comparison of measured versus predicted response, it would be easy to mistakenly assume that the load before flow initiation is a normal, expected load, and that the hump after flow initiation indicates an anomalous, unexpected load. With the comparisons shown in Figures 3-22 and 3-23, what we see instead is the reverse: the load before flow initiation is unexpectedly low, and the hump represents the increase of the load to the level predicted by the model. We tested three 10-in. valves; all three were tested only with steam, and the responses of two of the valves are

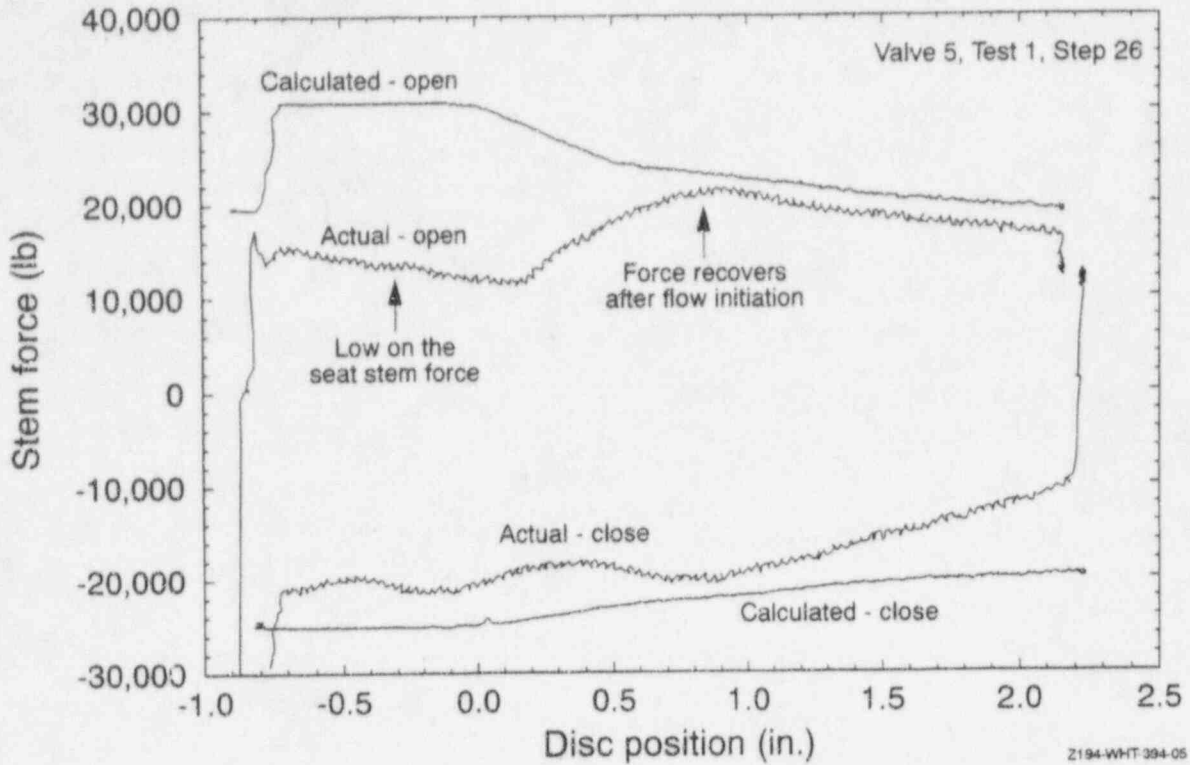


Figure 3-22. Valve 5 stem thrust traces compared to calculations for both opening and closing.

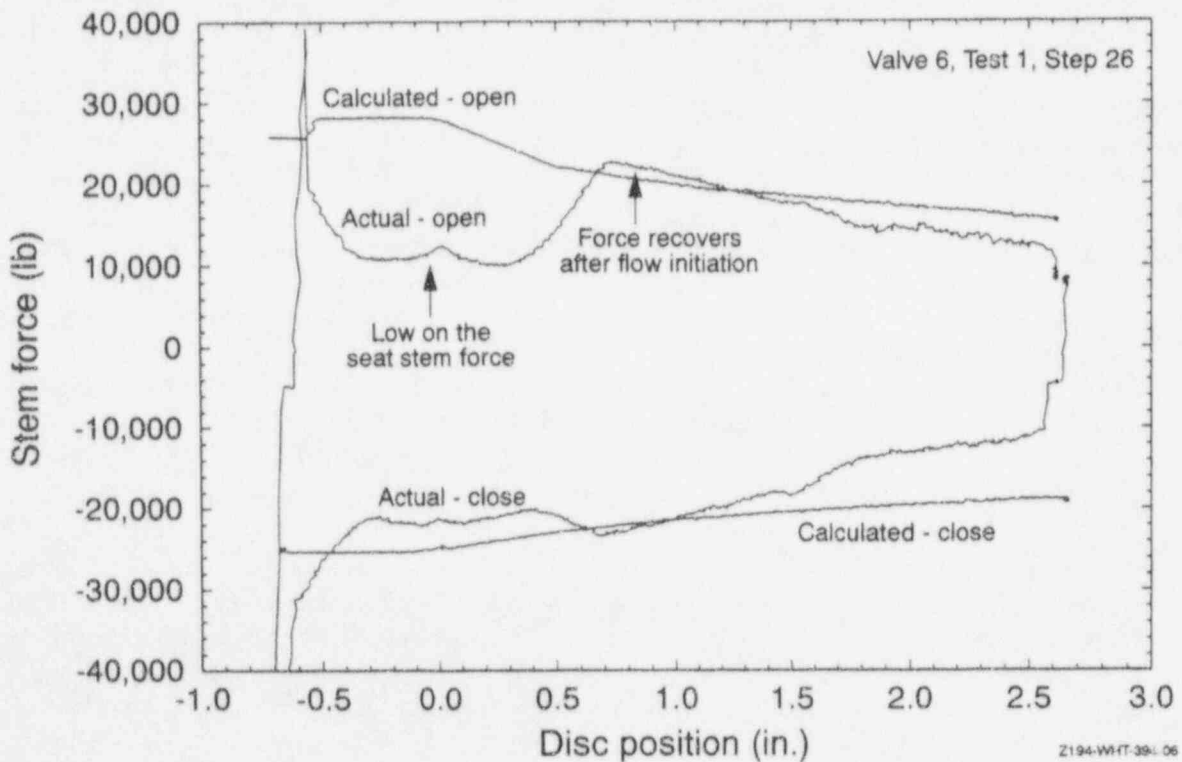


Figure 3-23. Valve 6 stem thrust traces compared to calculations for both opening and closing.

represented by the examples shown here. The one valve whose response we have not shown here is Valve 4, the Anchor/Darling valve; the response included extensive valve guide damage, so we did not include it in this comparison.

The smaller 6-in. valves were subjected to a number of parametric tests with various pressures and temperatures, with fluid conditions ranging from cold water to steam. The unexpectedly low on-the-seat response observed in the 10-in. valves during opening is also present in the 6-in. valves, but only with single-phase fluids (high velocity cold water and steam blowdown). These results are shown in Figures 3-24 and 3-25 for Valve 2, a 6-in. Velan flexwedge gate valve.

In contrast, Figure 3-26 shows the responses of Valve 2 while opening and closing against hot water at about 1000 psid with 10°F subcooling. In this case, the opening response is much closer to being a mirror image of the closing response. Figures 3-27 and 3-28 are from tests of Valve 2 opening and closing against hot water with 100°F subcooling. The conditions for these two tests were almost the same (the second test was a retest because the subcooling was slightly out of specification in the first test). We present both figures here to demonstrate the repeatability of the results. With the fluid at 100°F subcooling, the response is similar to the response shown in Figure 3-26 with the fluid at 10°F subcooling; the opening response looks like a mirror image of the closing response. Figures 3-29 and 3-30 are from two other tests of Valve 2 operating with fluid at 100°F subcooling, but the test pressure is higher. We observe that at higher test pressures, the model overestimates the stem thrust in the opening direction as well as the closing direction. This result is typical of data we have seen from valve closure tests; the higher the normal load on the disc, the lower the friction factor.

Figures 3-31 and 3-32 are stem thrust histories for Valve 3, a 6-in. Walworth flexwedge gate valve, opening and closing with water at 10°F subcooling. Figure 3-31 is from the test with the lower pressure of the two. These results, like those shown in Figures 3-28 through 3-30, show that

when a fluid can flash in a high-energy test, the opening direction develops a response that is nearly a mirror image of that seen in the closing direction. The pressure effect observed for Valve 2 in Figures 3-29 and 3-30 is also observed for Valve 3; the model tends to overestimate the stem thrust at higher test pressures.

3.3.2 A Correlation for Evaluating MOV Opening Requirements. The pressure effects and fluid condition effects on thrust in the opening direction are not unexpected. We observed pressure and subcooling effects in the closing direction; that analysis is reported in NUREG/CR-5720 (1992). However, the pressure effects and fluid condition effects we observed in the closing direction are not as great as those we see for opening.

The fluid condition effect in the closing direction was significant, requiring the INEL closing correlation to have two different disc friction factors, one for fluids with less than 70°F subcooling, and another for fluids with more than 70°F subcooling. The most significant fluid condition effect in the opening direction is the low on-the-seat friction factor for the high-pressure single-phase fluids. The cause of this phenomenon has not yet been identified, either by us or by other industry researchers investigating this issue. While this phenomenon is a curiosity, the fact remains that once flow starts, the thrust recovers to a more predictable value. This dictates that we predict the response without regard for the unexplained low friction while the disc is on the seat.

The pressure effects during closing are also built into the original INEL closing correlation. The net effect in both the opening and closing directions is that as the differential pressure increases, it takes less thrust per unit of differential pressure to move the disc.

Once we understood that the fluid condition and pressure effects were greater in the opening direction than in the closing direction, and that the hump in the opening direction did not represent a new flow load, but only an increase to the expected level, we were able to start developing

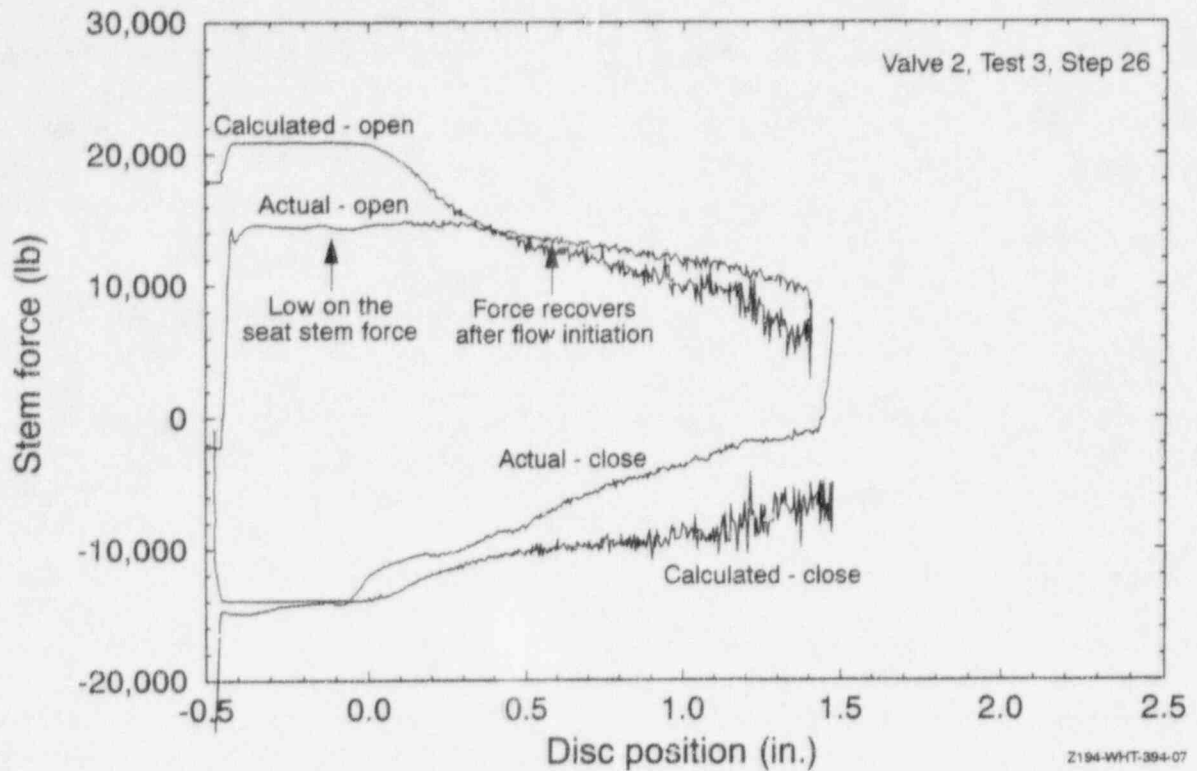


Figure 3-24. Valve 2 stem thrust traces compared to calculations for both opening and closing for a single-phase fluid, cold water.

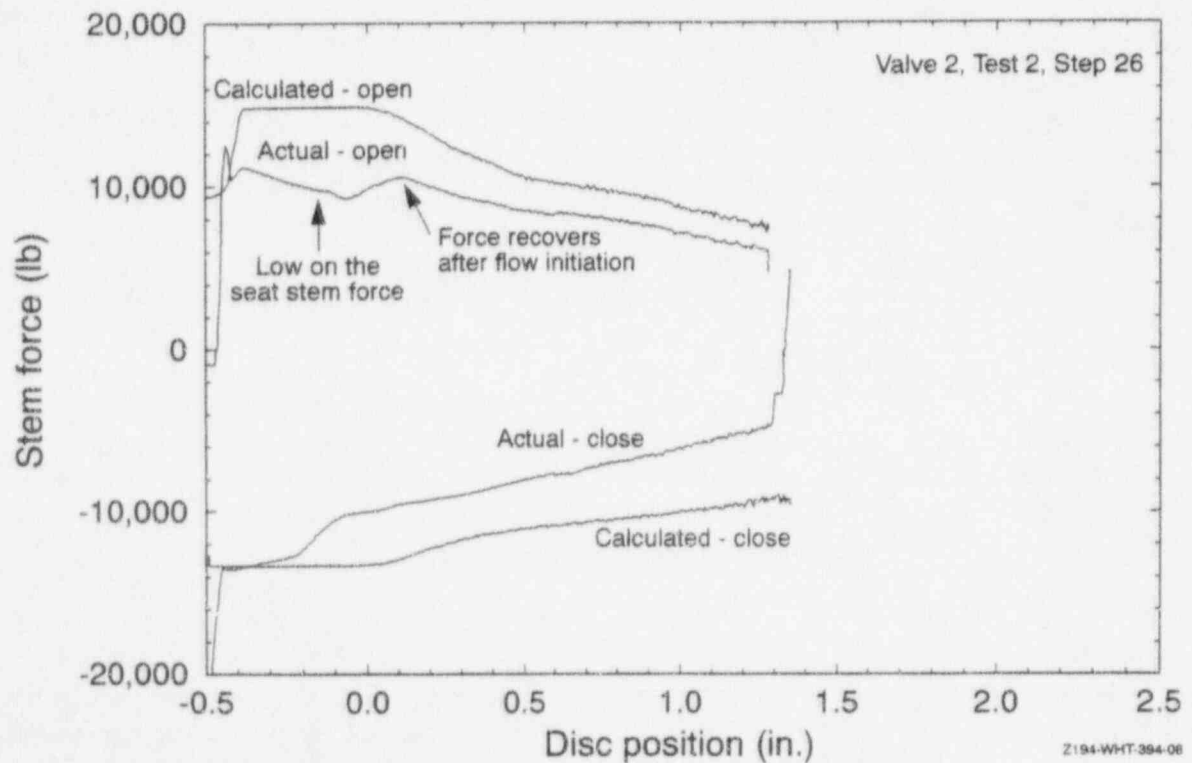


Figure 3-25. Valve 2 stem thrust traces compared to calculations for both opening and closing for a single phase fluid, steam.

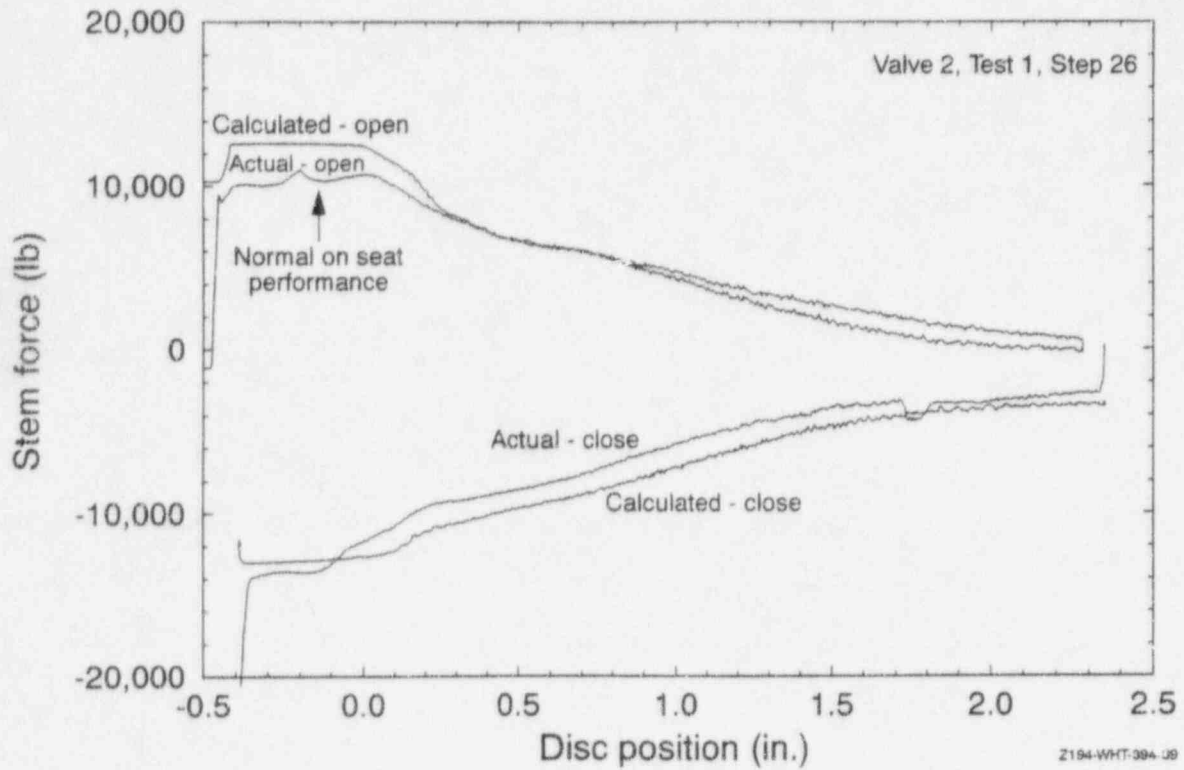


Figure 3-26. Valve 2 stem thrust traces compared to calculations for both opening and closing for 10°F subcooled water.

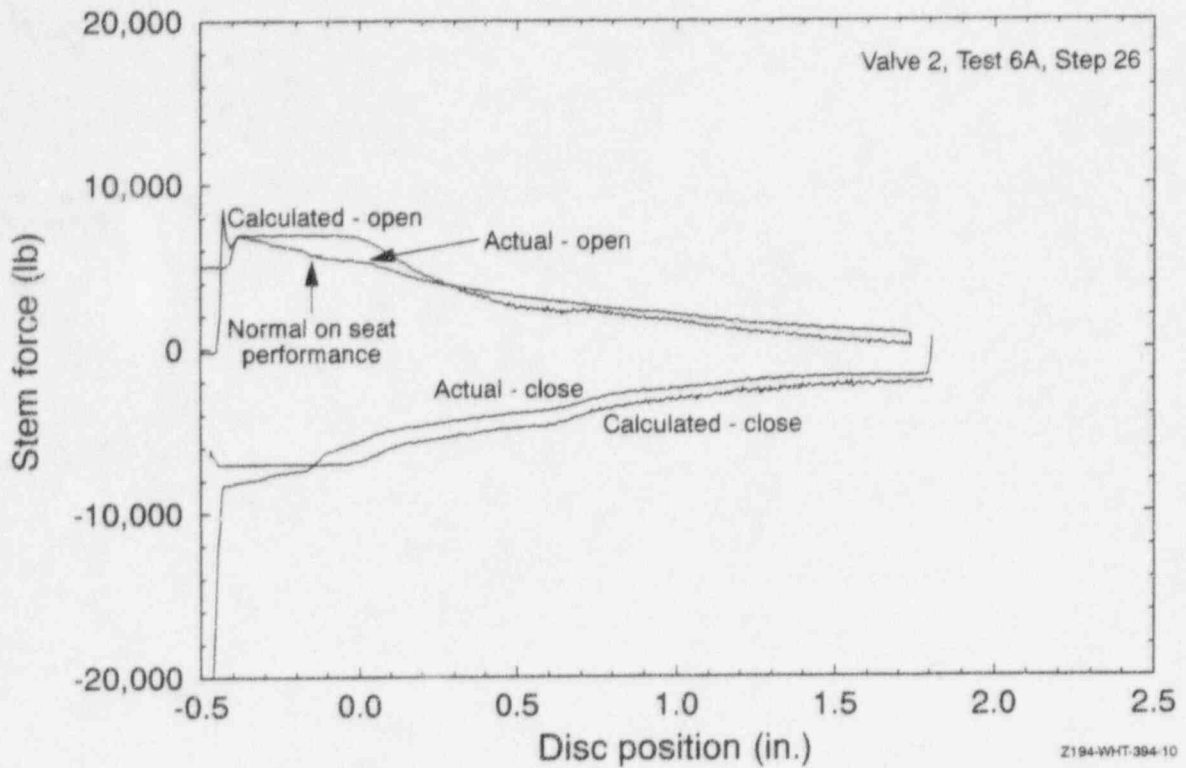


Figure 3-27. Valve 2 stem thrust traces compared to calculations for both opening and closing for 100°F subcooled water.

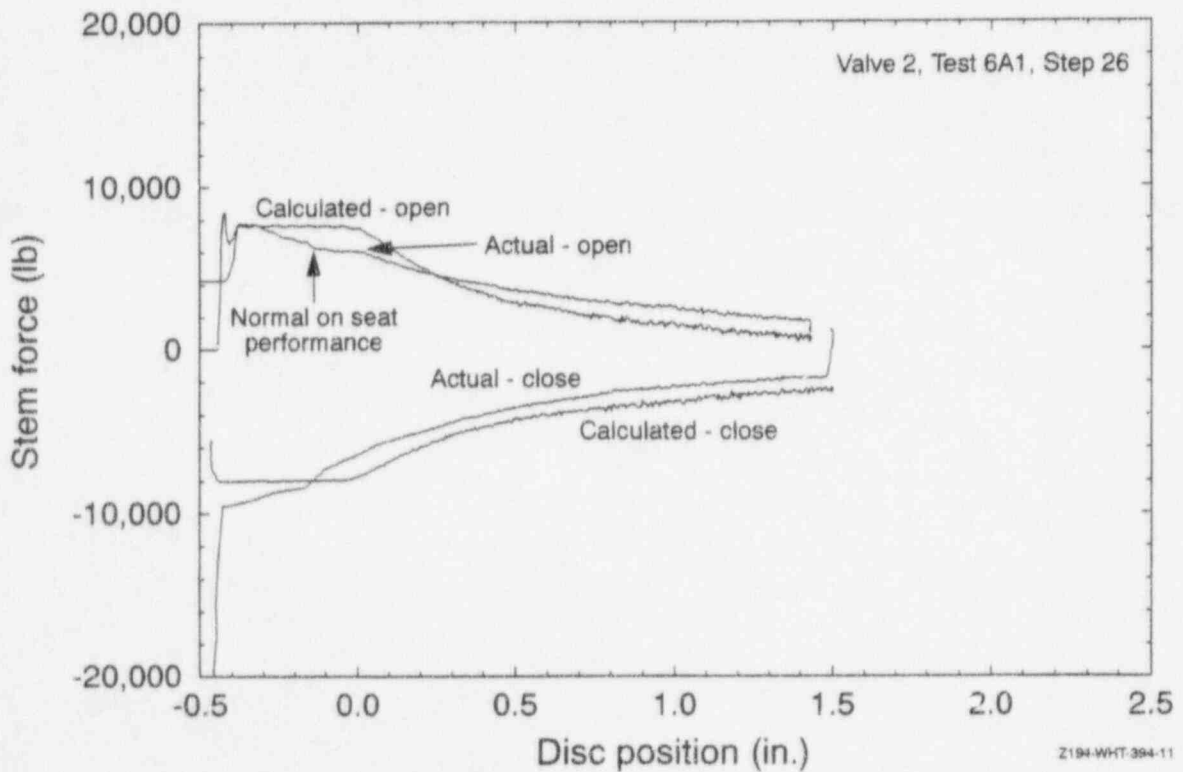
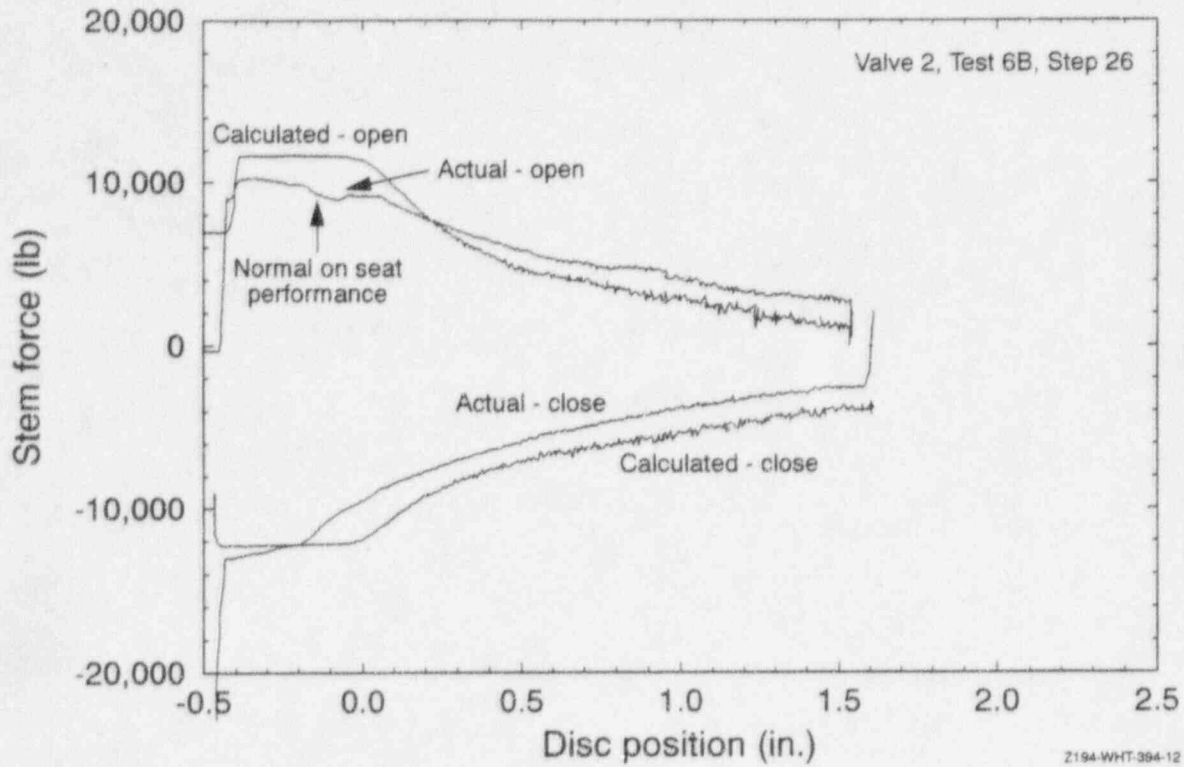
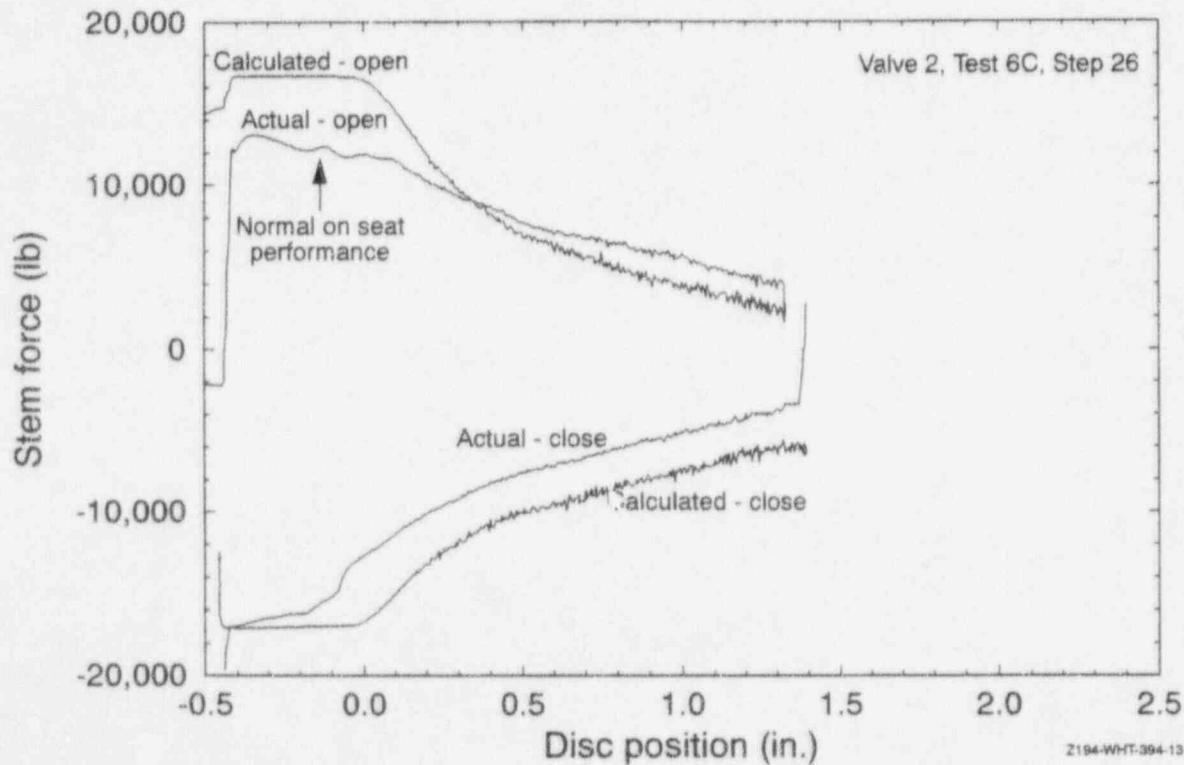


Figure 3-28. Valve 2 stem thrust traces compared to calculations for both opening and closing for 100°F subcooled water.



Z194-WHT-394-12

Figure 3-29. Valve 2 stem thrust traces compared to calculations for both opening and closing for 100°F subcooled water.



Z194-WHT-394-13

Figure 3-30. Valve 2 stem thrust traces compared to calculations for both opening and closing for 100°F subcooled water.

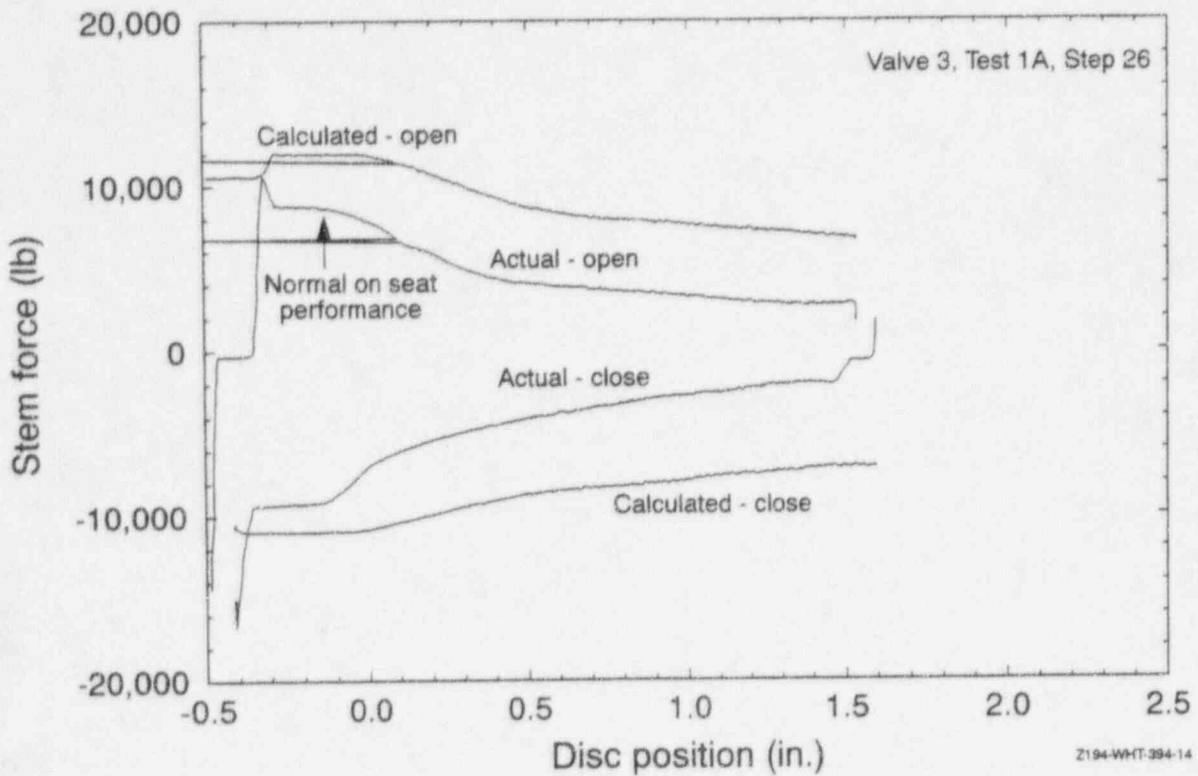


Figure 3-31. Valve 3 stem thrust traces compared to calculations for both opening and closing for 10°F subcooled water.

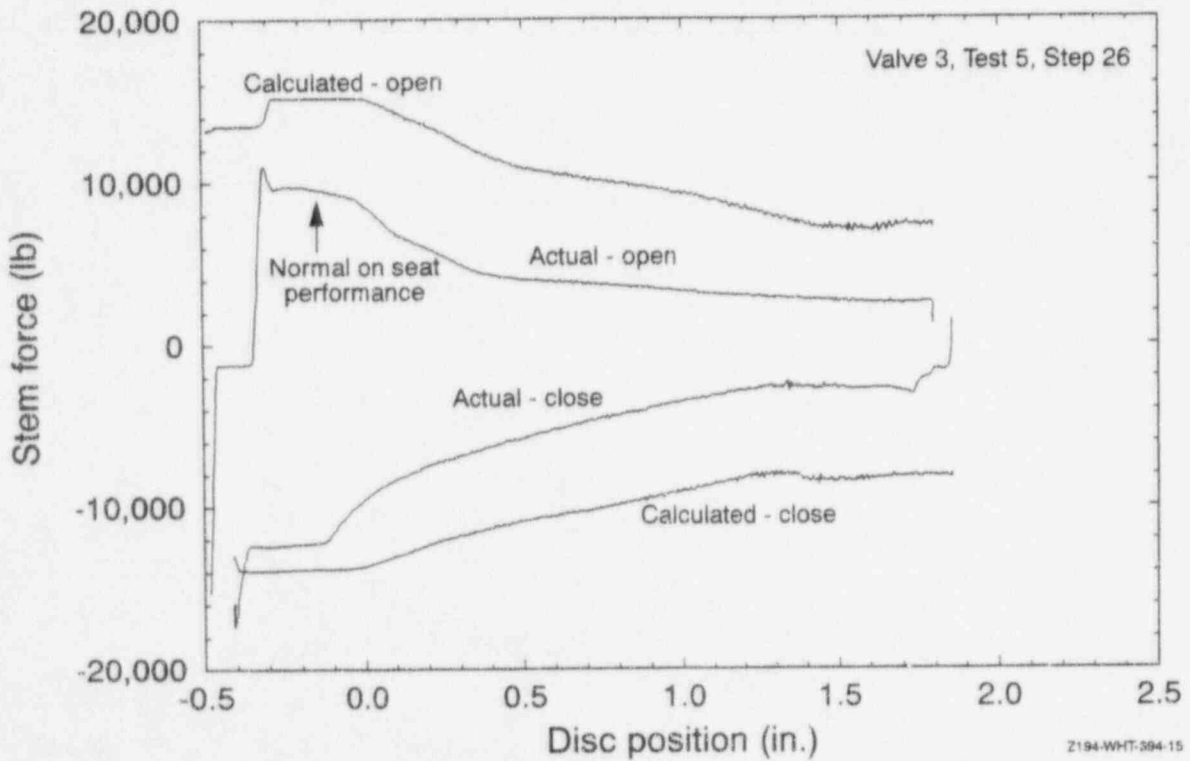


Figure 3-32. Valve 3 stem thrust traces compared to calculations for both opening and closing for 10°F subcooled water.

a method to estimate the opening response. After examining the NRC/INEL and industry valve test results in light of the effect fluid subcooling has on the peak opening response of the valve, we extracted the results of those tests where the fluid could flash (tests that produced typical responses). These results bound all the observed responses, and the use of these results avoids the difficulties of dealing with the unexpectedly low apparent friction during unseating and the subsequent increase in the stem thrust upon flow initiation, as seen in the atypical responses. Using the data thus extracted, we were able to estimate the normal and sliding loads acting on the disc and to correlate them over a wide range of differential pressure conditions. Figure 3-33 is a plot of the normalized normal versus normalized sliding loads for opening a gate valve. As with the original INEL correlation for closing, the slope of the trace represents the friction factor.

Based on this effort, we suggest that one of the following two correlations be used to estimate the peak stem thrust demands of a valve during open-

ing. Above a normalized normal load of approximately 350 psi, the first correlation should be used, whereas below this load, the second correlation should be used. The correlations are presented on page 3-32.

Unlike the INEL's linear correlation for closing, the opening correlations are quadratic. The effect is that the friction factor is larger when the valve is lightly loaded [the nominal (best fit) value is about 0.63], and the friction factor decreases as the valve load increases. Another difference between the closing correlation and the opening correlation can be seen in the limits of the data scatter at higher loadings. The closing correlation bounded the response with a ± 50 psi band, whereas the opening correlation bounds the data with a ± 60 psi band. These values represent the term necessary to bound actual valve performance. However, for all the differences between the opening and closing methodologies, the on-the-seat typical responses are quite similar. This fact adds to our confidence that the opening correlations are valid.

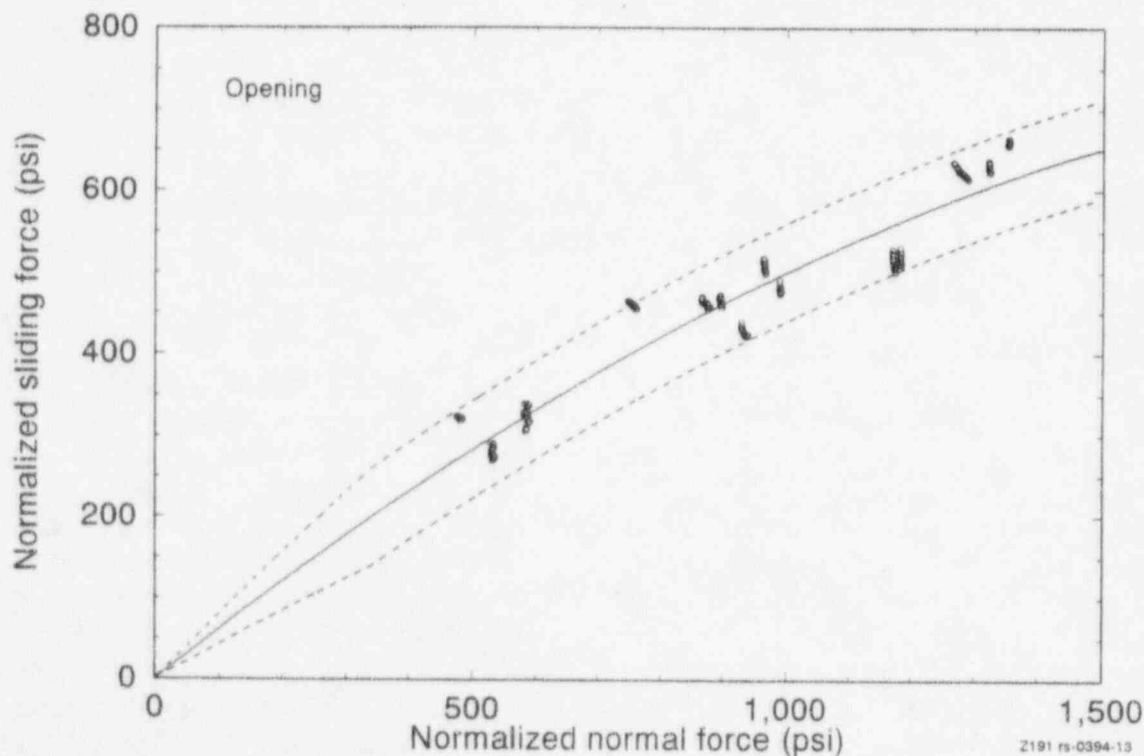


Figure 3-33. Normalized sliding loads versus normalized normal loads for the opening stroke for gate valves.

Disc Load

For $F_n \geq 350$ psi:

$$F_{stem} = F_{packing} + F_{top} - F_{bot} - F_{sr} + \frac{(\sin \alpha + f_o \cos \alpha)(F_{up} - F_{dn}) - \frac{ff_o \cos^2 \alpha}{A_{ms}} (F_{up} - F_{dn})^2 \pm 60 A_{ms}}{(\cos \alpha - f_o \sin \alpha) + \frac{2ff_o \cos \alpha \sin \alpha}{A_{ms}} (F_{up} - F_{dn})}$$

For $F_n < 350$ psi:

$$F_{stem} = F_{packing} + F_{top} - F_{bot} - F_{sr} + \frac{[\sin \alpha + (1.0 \pm 0.3)f_o \cos \alpha](F_{up} - F_{dn}) - \frac{(1.0 \pm 0.3)ff_o \cos^2 \alpha}{A_{ms}} (F_{up} - F_{dn})^2}{[\cos \alpha - (1.0 \pm 0.3)f_o \sin \alpha] + \frac{2(1.0 \pm 0.3)ff_o \cos \alpha \sin \alpha}{A_{ms}} (F_{up} - F_{dn})}$$

where

F_{stem}	=	stem thrust
$F_{packing}$	=	packing drag
F_{sr}	=	stem rejection load = $P_{up} * A_{stem}$
F_{top}	=	$P_{up} * A_{ms} * \tan \alpha$
F_{bo}	=	$P_{dn} * A_{ms} * \tan \alpha$
α	=	valve seat angle
F_{up}	=	$P_{up} * A_{ms}$
F_{dn}	=	$P_{dn} * A_{ms}$
A_{ms}	=	mean seat area = $1/4 \pi$ (mean seat diameter) ²
A_{stem}	=	stem area = $1/4 \pi$ (stem diameter) ²
P_{up}	=	upstream pressure
P_{dn}	=	downstream pressure
f_o	=	0.63
ff_o	=	0.00013

We know from our closing correlation that below a disc loading of about 400 psi, the data scatter becomes dominant. In the extension of the closing correlation to lower loads (discussed in a previous subsection), we used the data we received from utility testing, along with the publicly available data we have reviewed from other industry testing. All these data for low-pressure, low-flow testing indicate that when the disc is lightly loaded, the data scatter can be expected to

fall within the bounds specified in the previous paragraph. Based on those test results, we believe that test results that fall outside the specified bounds represent valve performance that is not characteristic of the responses we have observed.

The opening correlation can be used to evaluate the test results and the opening requirements of valves that can be tested in situ at conditions less severe than design basis conditions. We propose a method similar to the one we recommend in the use of the INEL correlation for closing requirements. With this method, the results of the in situ test are not used directly in an extrapolation. Instead, the test data are evaluated to determine whether the results fall within the bounds defined by the correlation. If so, it can be assumed that the response of the valve in question is represented by the data used to develop the correlation, and that the correlation is applicable. Once applicability has been demonstrated, the upper bound of the correlation is used to estimate the stem thrust requirements at design basis conditions.

All the results of NRC/INEL valve testing and all the industry valve testing we have reviewed show that the closing thrust requirements typically exceed the opening requirements, particularly in smaller valves. In our examination of the various loads that contribute to the total stem loads for opening and closing, we have found that the only load that causes an increase in the opening load compared to the closing load is the load due to the pressure on the top of the disc (F_{top} in Figure 3-17). This load assists during closing and resists during opening. In valves smaller than about 6 in., the effect of this load is offset by the stem rejection load, which resists closing and

assists opening. In addition, any tipping of the disc will reduce the F_{top} load.

A first principles evaluation of the normal versus sliding loads reveals another difference between opening and closing. Theoretically, if the force and the friction were operating on the same plane, the sliding friction during closure after flow isolation should be the same as the friction during opening after unwedging but before flow initiation, because either way, the disc is riding totally on the downstream seat. However, for wedge-type gate valves, the angle on the wedge and the seat relative to the plane of the stem is such that the valve is harder to close than it is to open. Figuratively speaking, in the closing direction the stem is pushing the disc uphill, while in the opening direction the stem is pulling the disc downhill. The effect of this phenomenon is always to increase the load during closing and decrease the load during opening. An exception to this analysis would be where the guides carry the disc up to very near wedging, such that the "uphill/downhill" effect is minimized.

Another difference between opening and closing involves the occurrence of any type of mechanical interference. Typically, the effects of mechanical interference are greater during closing than during opening, because the leading edge of the tilted disc contacts the valve seat more aggressively during closure.

According to the data we have evaluated, the overall effect of these various differences between opening and closing seems to be that for valves smaller than about 14 inches (nominal diameter), closing requirements exceed opening requirements. In our opinion, if an opening test cannot be performed but a closing test can, the results of the closing test can be used to bound the opening requirements, provided that the valve is smaller than 14 in.

3.3.3 Estimating an Atypical Opening Response. The atypical opening response that we have seen most often is where the disc load after the initiation of flow is higher than the disc load on the seat (see Figure 3-20, upper plot,

opening stroke). We do not fully understand the cause of this response. It is most likely to appear in high-pressure applications and single-phase fluids. We have not observed this type of response at loads less than about 400 psi differential pressure on the disc.

We know of no way that this response can be extrapolated. However, we do know that the increase after flow initiation is an increase from an unexpectedly low load to the expected level, not an increase to an unexpectedly high load. We recommend that the opening correlation presented above be used to estimate the design basis requirements for valves shown to have an atypical opening response. After flow is initiated, the stem thrust increases to the level we would expect for the loading just off the seat. Because the unexpected response is lower than the expected response, the best way to bound the valve's overall response is to ignore the unpredictable low response that can occur before flow initiation.

Occasionally an opening stem force history will have a dip or a reduction in the force trace momentarily after flow is initiated. Figure 3-34 is an example. This response is the opening equivalent to the hook that occurs in an atypical closing response. As the disc comes off of the seat, flow forces cause it to tip. The tipping of the disc changes the pressure distribution around the disc, and the stem force reflects that change. In this instance, some of the forces that cause an increase in the thrust during closure cause a decrease during opening. The apparent effect of these forces is usually smaller than in the hook seen in the closing direction, perhaps because the effects of other forces mask it. This drop in stem force after the disc comes off the seat is not a consideration in estimates of valve opening requirements, because the thrust at that point is lower than the on-the-seat peak thrust being estimated.

3.4 Conclusions

Atypical behavior, whether in the opening direction or the closing direction, is a manageable condition if valve damage is not a consideration.

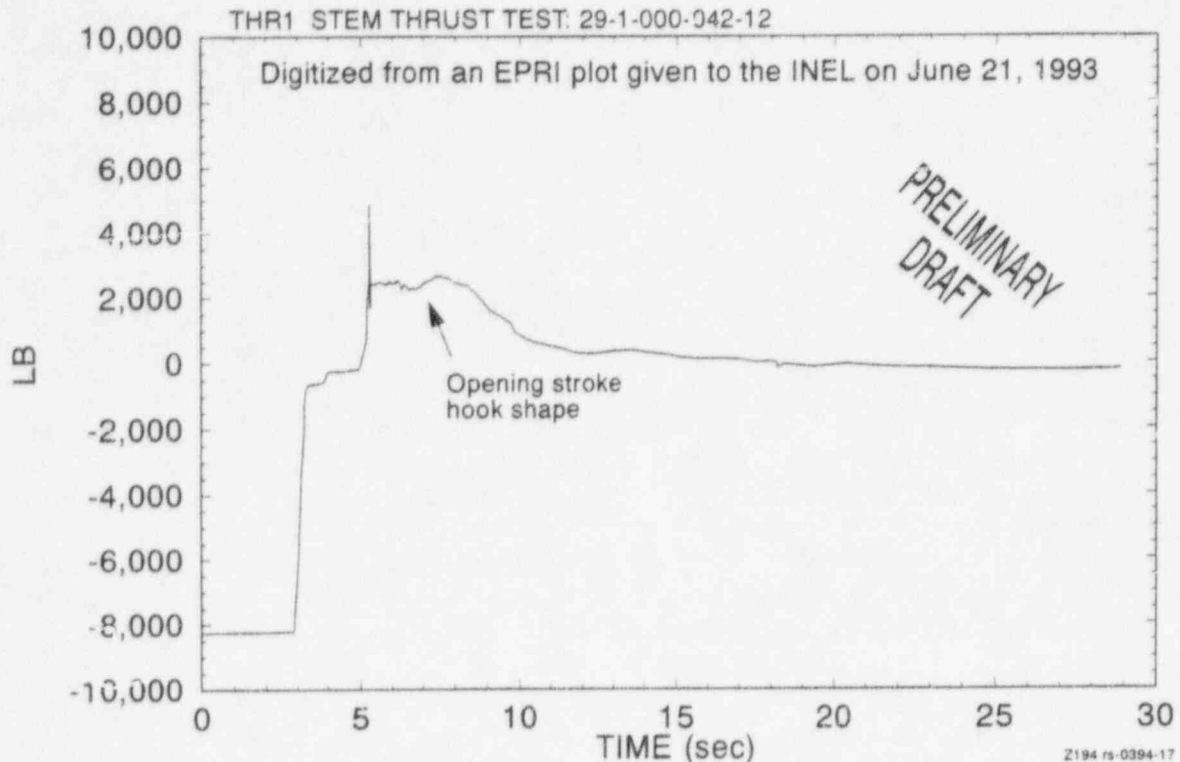


Figure 3-34. Stem thrust trace from testing a 6-in. service water valve opening against design basis flow; the trace shows indications of an atypical response just after flow initiation.

Establishing the tilted disc as the primary cause of atypical behavior makes it possible to understand this behavior.

Performing a best-effort differential pressure flow test in the direction of concern (open or close) provides important information for evaluating a valve's ability to perform its design basis function. For a valve that must open against a design basis load, the results of the best-effort test provide assurance that the INEL opening correlation is applicable. (The correlation is considered applicable if the peak force after unwedging in the best-effort test falls within the bounds of the correlation. This verifies that the valve being evaluated is similar in its operating characteristics to the test valves that were used to develop the correlation.) If so, the opening correlation can be used to estimate the valve's design basis requirement.

For a valve that must close against design basis loads, the best-effort flow test determines whether the valve's behavior is typical or not. For

a valve that demonstrates atypical behavior during closure (stem thrust *before* flow isolation is higher than the thrust *at* flow isolation), information provided by the best-effort test can be used in the INEL extrapolation method, described in Section 3.2.3 of this report, to make a reasonably accurate estimate of the valve's design basis requirement. If the best-effort test shows that the valve's behavior is typical (stem thrust *at* flow isolation is higher than the thrust *before* flow isolation), the results of the best-effort test provide assurance that the INEL closing correlation is applicable. (The correlation is considered applicable if the peak force before wedging in the best-effort test falls within the bounds of the correlation. This verifies that the valve being evaluated is similar in its operating characteristics to the test valves that were used to develop the correlation.) If so, the closing correlation can be used to estimate the valve's design basis requirement.

The estimates produced by these methods are much better than blind predictions, because they

are based on performance testing, i.e., the best-effort flow test.

The extension of the original INEL closing correlation to lower loads, the adaptation of the disc

factor equation for extrapolating atypical closing responses, and the development of the new opening correlation are advances in MOV research that provide technical support in areas where little or no such support previously existed.

4. STEM FACTOR

One of our research objectives for this reporting period was to develop a consistent and uniform method for evaluating motor-operated valve margins. At this stage in MOV research, one of the toughest hurdles to get past in developing the method was understanding the phenomena that influence the stem factor, which represents the conversion of operator torque to stem thrust in rising-stem motor-operated valves (torque divided by thrust equals stem factor).

Determining the design basis stem factor is important because it is the key to determining the operating margin of a specific valve. We know that for a specific valve stem and stem nut, the only variable in the conversion of torque to thrust is the coefficient of friction. We also know that the coefficient of friction changes with changes in the load. If the valve can be tested at design basis conditions and diagnostically monitored in situ, determining the operating margin is not difficult. However, some motor-operated valves cannot be tested in the plant at design basis conditions. The ability of these valves to perform their design basis function (typically, to operate against specified flow and pressure loads) must be ensured by analytical methods or by extrapolating from the results of tests conducted at lower loads. Because the stem factor tends to vary in response to load and lubrication phenomena that occur during running and wedging, such analytical methods and extrapolation methods have been difficult to develop and implement.

Early investigations into variability in the stem factor tended to look only at the tip of the iceberg; they focused on what was happening at torque switch trip, which usually occurs at full wedging (in torque-controlled wedge-type gate valves). In many stem and stem nut combinations, the stem factor is better (lower) at torque switch trip than during the running portion of the stroke before wedging, so working with torque switch trip data alone led many researchers to false conclusions about the relationship between stem factor and load. From our experience with testing of full-scale valves at design basis conditions, we under-

stood that it was important to take a close look at what happens during the running portion of the closing stroke as well. This shift in focus is important, because a valve's failure to close consists of failure to isolate flow, not failure to achieve full wedging. Thus, the stem factor that must be determined for the sake of a valve's design basis closing requirements is the stem factor that corresponds with the highest running load before wedging.

Calculations involving the conversion of torque to thrust use the industry's power thread equations. As stated above, for a given stem/stem-nut combination and for a given value of torque, the only variable in the conversion of torque to thrust is the coefficient of friction at the stem/stem-nut interface. Results of tests conducted at the INEL indicate that for at least two lubricants, the stem/stem-nut coefficient of friction determined in a test conducted at specific conditions less severe than design basis conditions provides consistent, useful information about the friction coefficient that can be expected at design basis loads. This result provided the insight for the initial development of two straightforward methods for determining the stem factor for a valve that cannot be tested at design basis conditions. Both methods require that torque and thrust be measured directly. The first method (we call it the *threshold method*) would require that a specified minimum stem load (usually a lower load than the design basis load) be imposed on the valve stem during the running portion of the stroke before wedging begins. The coefficient of friction determined from such a test could be used directly to calculate the valve's design basis torque requirement. The second method (the *fold line method*) estimates a bounding coefficient of friction from the wedging load in a test with a running load below that required for the threshold method. The threshold method is the more accurate of the two, but a stem factor determined using either of these methods is likely to be more accurate than some default values or extrapolation methods currently in use. This section of the report explains both methods and provides the

research results that support them. The data that support these methods were developed from limited research consisting of tests of a small sample (8 stems) with two lubricants. We encourage industry to continue the research and validate the methods.

The information presented here was derived from tests conducted in the closing direction. The results do not apply to the opening direction. At this stage of our research, we expect that the threshold method might work in the opening direction, but only if the differential pressure load were sufficient to exceed the stem rejection load by the minimum threshold stem thread pressure; however, at this time we do not have any data to substantiate this theory. Because the mating surfaces in the stem and stem nut are different for opening than for closing, stem factors developed from closing tests should not be used to determine operating margins for opening requirements.

The following discussion briefly describes the full-scale testing and the valve stem testing that contributed to our research. The discussion then describes the initial development of the two methods, mentioned above, for estimating the design basis stem factor from the results of tests conducted at conditions less severe than design basis conditions.

4.1 Results of Full-Scale Valve Testing

Figure 4-1 shows the stem force measurements for four tests of the same valve at four different flow and pressure loads. These results are from the NRC/INEL full-scale valve tests conducted in 1989 (as reported in NUREG/CR-5558, 1990). The torque switch setting was the same in all four tests. The long vertical line at the end of the low-load trace indicates the sudden increase in stem thrust at wedging; the running load before wedging was fairly low. In the design-basis-load test,

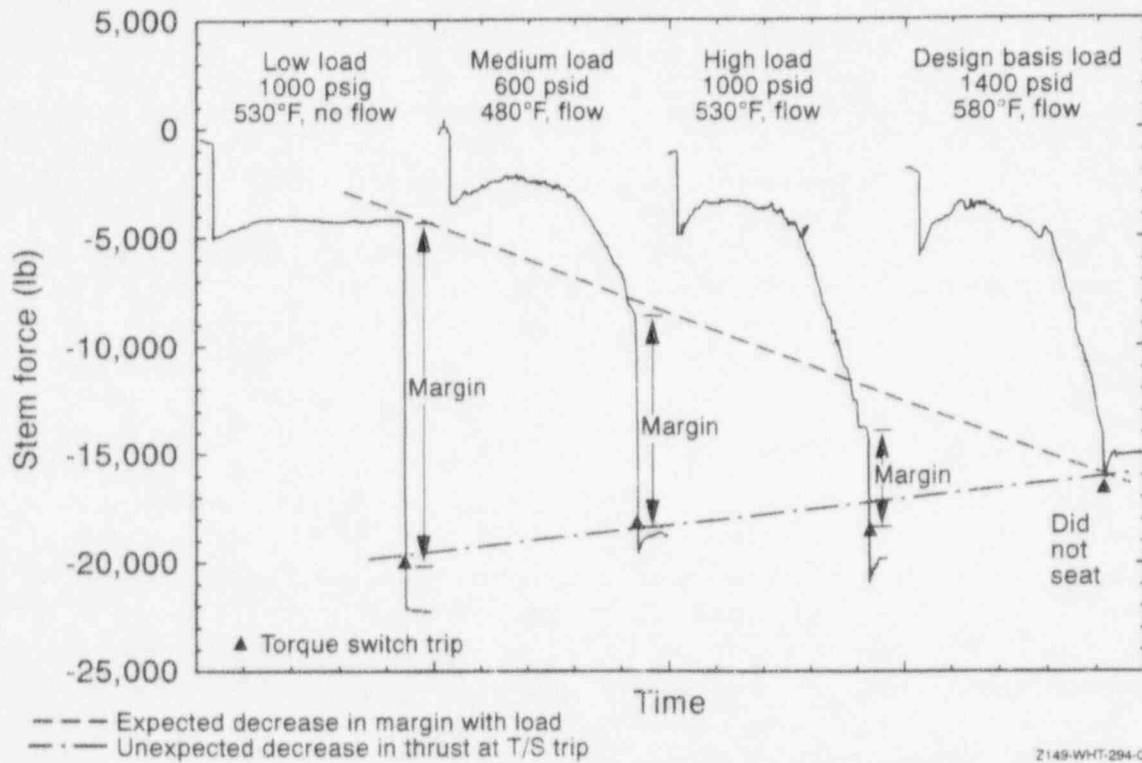


Figure 4-1. Four valve tests at the same torque switch setting. At the design basis flow and pressure loads, the valve failed to completely close.

the valve did not seat. Note that in the low-load test, the thrust measured at torque switch trip is considerably higher than in the design-basis-load test. This change in the thrust is due to a change in the stem factor. We call this phenomenon *load-sensitive behavior*. Some valve researchers refer to it as the *rate-of-loading effect*. We had always expected that the thrust margin at torque switch trip would decrease with load (as indicated in Figure 4-1), but we had not expected the thrust value to decrease at torque switch trip for a given value of operator torque. This decrease in the thrust value at torque switch trip converges with the decrease in margin due to load, resulting in failure to close at the design basis load for the valve being tested. The failure to close in the design-basis-load test demonstrates the seriousness of the problem: if an in situ test is conducted at low-load conditions, and if the thrust measured at torque switch trip is sufficient to overcome the calculated design basis load acting on the disc, there is still no assurance that the valve will fully close at design basis conditions. Changes in the stem factor must be accounted for.

4.2 Testing on the MOVLS

In preparation for the full-scale MOV flow tests conducted at Kraftwerk Union (KWU) in Germany in 1989, we built a MOV load simulator (MOVLS). The purpose of the MOVLS was to test MOV instrumentation techniques and data acquisition methods. After the tests in Germany were completed, we further developed the MOVLS so we could use it to conduct additional tests to address the stem factor issue and other motor-operator issues. The MOVLS, shown in Figure 4-2, uses motor-operators, valve yokes, and stems just as they are assembled on the valves. The flow load is simulated as the valve stem compresses a hydraulic cylinder that discharges to an accumulator. The specific valve load profile is controlled by the water level and gas charge in the accumulator, set up before testing. The MOVLS is instrumented to take all the measurements (direct and indirect measurements) that are used by the commercially available valve diagnostic systems, as well as a few measure-

ments unique to the MOVLS. Stem thrust is measured by a load cell mounted in the stem, and torque is measured in the stem by a calibrated torque arm. The simulator also has a torque cell mounted between the electric motor and the gear box to provide a direct measurement of real time motor torque. Motor speed is also measured directly.

Figure 4-3 shows the stem force traces for three tests conducted on the MOVLS at the same torque switch setting but at different simulated valve loads. The same load-sensitive behavior we observed in full-scale flow testing (Figure 4-1) is evident here.

As previously stated, but repeated here for continuity, the stem factor for a rising-stem MOV is the operator output torque (or stem torque) divided by the stem thrust. Figure 4-4 is a simplified diagram showing the important motor-operator mechanical components involved in the conversion of torque to thrust. Except for very small variations (due, for example, to worm/spline friction), an operator with a given torque switch setting will deliver a certain amount of torque to the stem nut. For a particular valve with a given stem/stem-nut combination, the only first order variable in the stem factor equation (assuming a constant value for the torque) is the coefficient of friction between the stem and the stem nut; the other components of the equation (for a given stem and stem nut) are constants (stem diameter, stem pitch and lead, etc.). Thus, any change in the relationship between operator torque and stem thrust is the result of a change in the stem/stem-nut coefficient of friction. This statement is based on INEL research and review and consultation with industry researchers and in-plant test results.

As part of this year's research, we conducted a comprehensive test program on the MOVLS. We tested eight typical acme threaded valve stems. Seven of the stems were provided by nuclear suppliers, and the eighth stem was built by Teledyne Engineering as part of their Smart Stem™ development program. (The Smart Stem™ is a valve stem that has been equipped with strain gages and

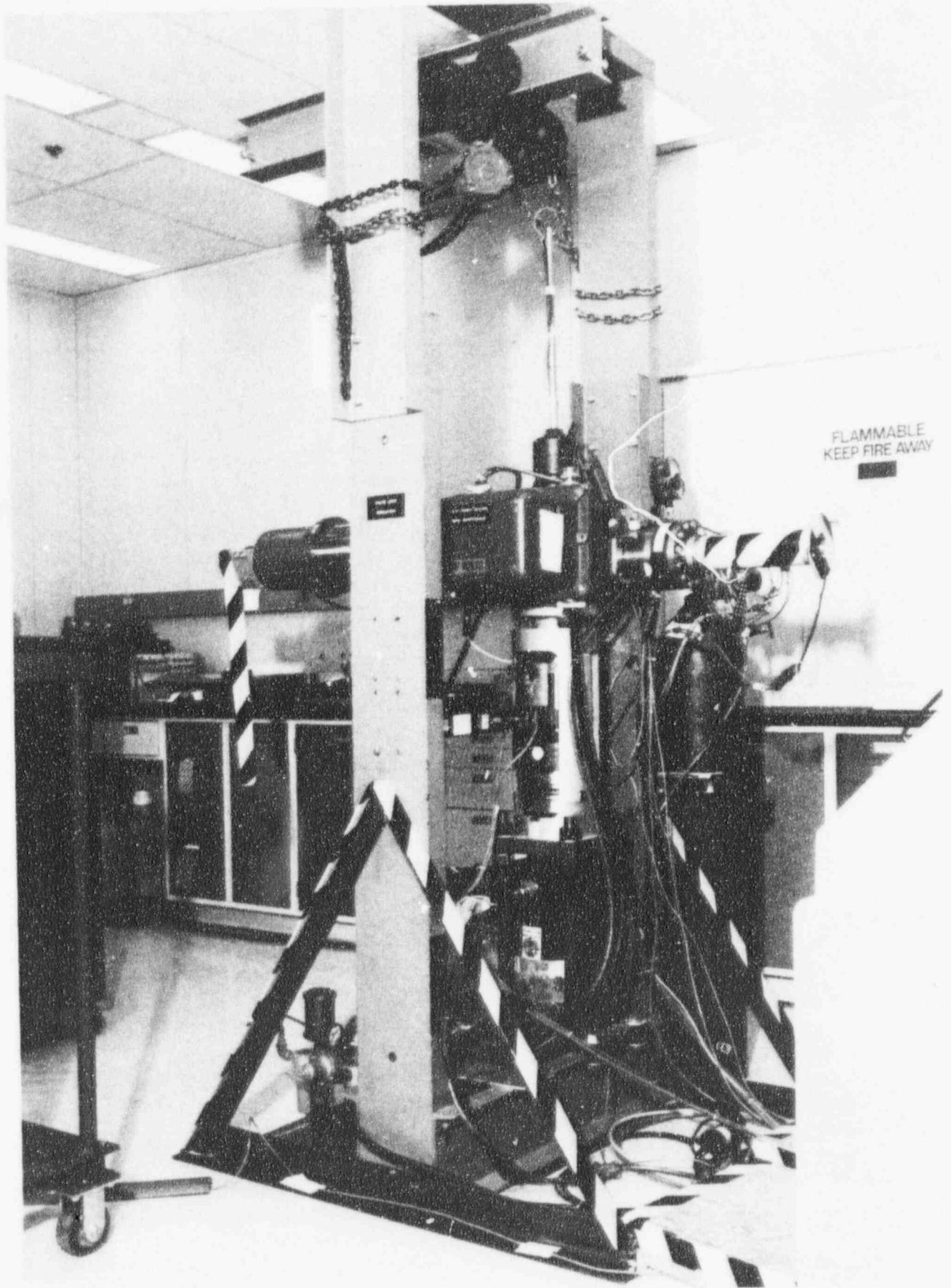


Figure 4-2. The INEL's load simulator for testing valve stems (the MOVLS).

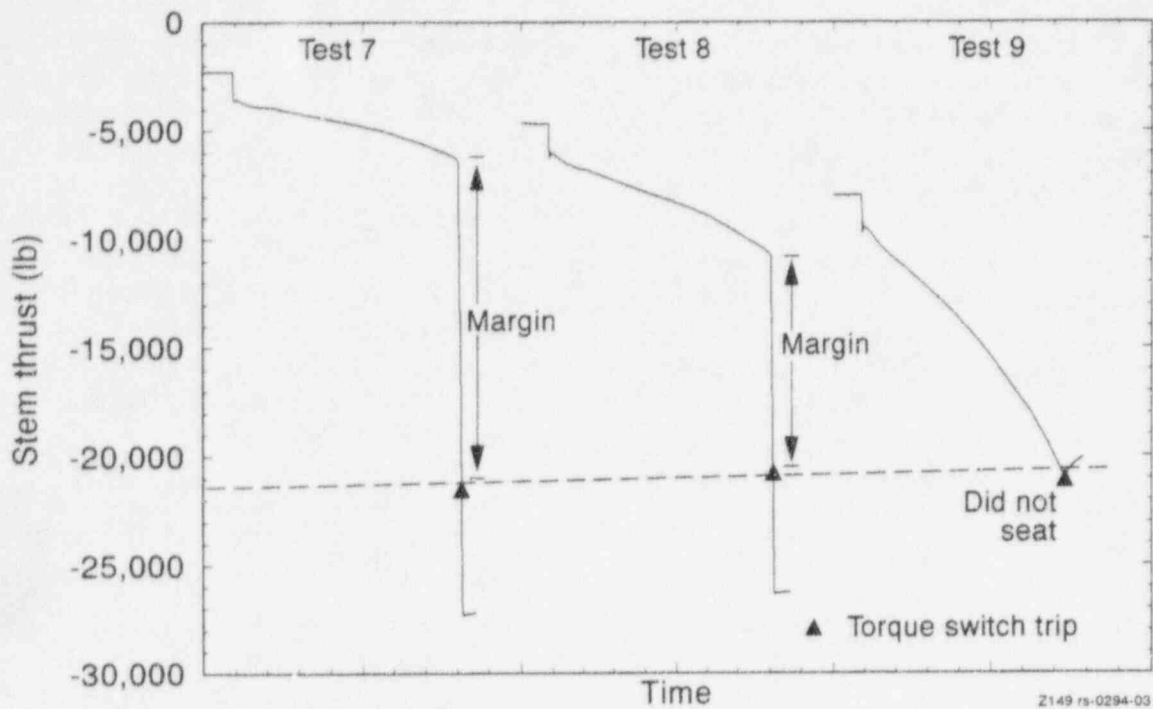


Figure 4-3. Load-sensitive behavior is simulated on the MOVLS.

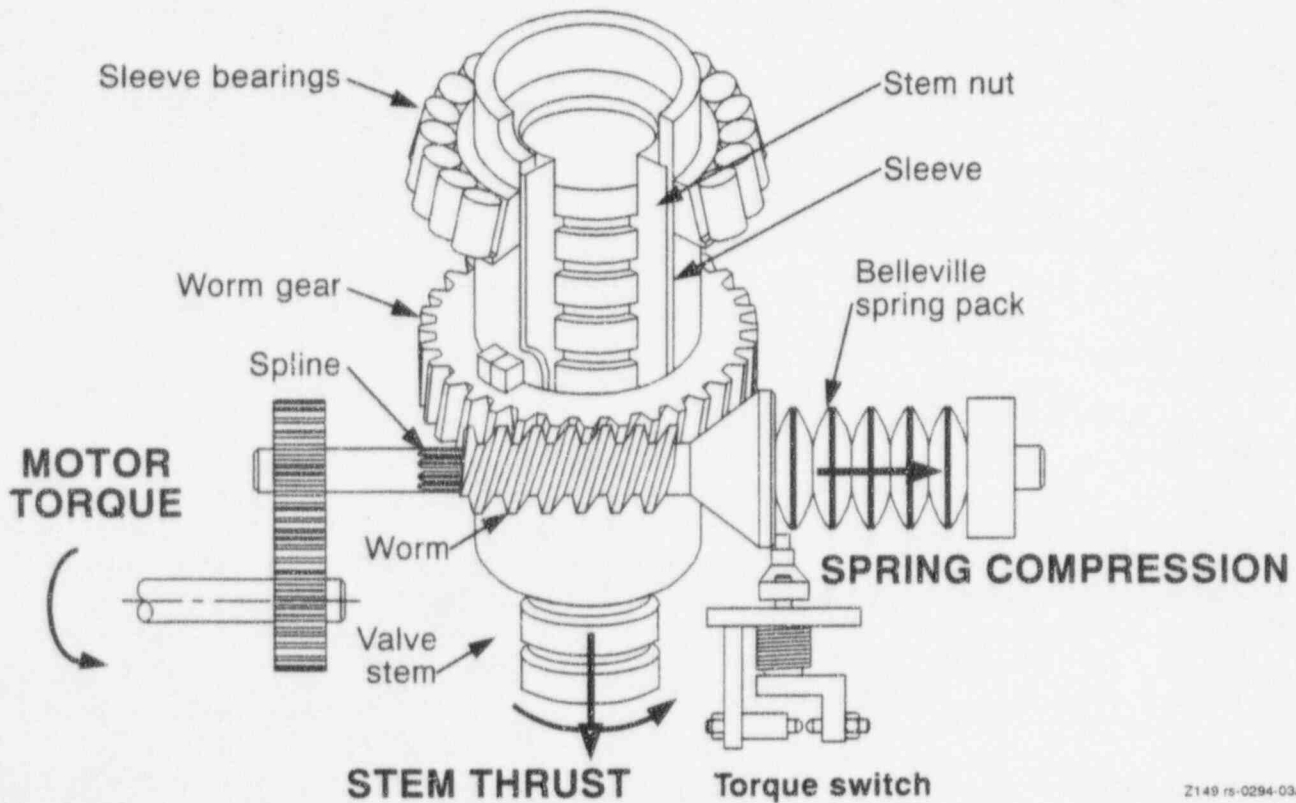


Figure 4-4. Simplified diagram showing the key components of a Limitorque motor-operator.

calibrated to measure both thrust and torque directly in the stem.) Three different sizes of Limitorque motor-operators were used in the test program. The technical details of the test hardware can be found in Table 4-1. The test program included two tests of each stem at each of three different torque switch settings. In each case, the first test was a static test (simulating a valve closure against packing load only), and the second test was a dynamic test (simulating valve closure against flow and pressure loads). Each stem was loaded in the range it would be expected to experience in the plant; that is, we did not load the 1.25-in. stems to the same load as the 2-in. stems. The test results were analyzed using the industry's power thread equations. (We have reviewed these equations both mathematically and from the evaluation of very accurately measured test results and found them to be valid.) By using the measured stem thrust and the measured stem torque, together with the power thread equations, we can calculate the stem/stem-nut coefficient of friction for any point of interest during the closing stroke.

The entire test sequence was repeated with each of the two lubricants: SWEPCO Moly 101, and Nebula EP-1. The purpose here was not to conduct a lubricant test, but simply to find out if the lubricant influenced the results. Cleaning of the stems and stem-nuts between changes from one lubricant to the other was performed very carefully. Each stem and stem-nut was washed in three different fluid baths, the last one being previously unused. The stems were also subjected to a light abrasive (Scotch-Brite™) surface scrubbing between the second and third baths to ensure that the previous lubrication film was broken. Several stems were lubricated, cleaned, lubricated with the other lubricant, then recleaned, relubricated with the original lubrication, and retested. The repeat test results were compatible with the first round of tests results, providing some assurance of repeatability with the entire process.

In a recent research report (NUREG/CR-5720, 1992), we discussed stem lubrication memory. This refers to the fact that the stem friction during a given closing stroke can be influenced by the

load imposed during the previous closing stroke. This effect can be prevented by running an unloaded valve stroke before running the loaded stroke. The effect of this unloaded stroke is to redistribute the lubrication on the working surfaces of the stem threads. For valves in the plant that are not regularly operated, this is the most likely condition that a valve will be left in after an ASME Section XI stroke time test. For the test results reported here, we were careful that lubrication memory did not influence the results. We avoided lubrication memory by running three unloaded strokes in a row as the preparation for the next set of tests.

Testing on the MOVLS has produced three important findings regarding the stem/stem-nut coefficient of friction:

- The coefficient of friction definitely varies with changes in the load. This is true of both the running portion of the closing stroke and the wedging portion.
- Different lubricants on the stem threads can produce different coefficients of friction, all other conditions being the same.
- Each individual stem/stem-nut combination is unique, with its own particular coefficient of friction profile. Some stems are more likely than others to exhibit load-sensitive behavior.

These findings underscore the difficulty valve researchers have experienced in attempting to analytically predict the coefficient of friction for any given valve; no two valves (even valves of the same size and model) can be expected to behave exactly alike, and the same valve can behave very differently, depending on either the lubricant or the load. One way to address this difficulty is to assign a value for the coefficient of friction that is high enough to bound the worst possible case; for example, Limitorque's sizing manuals recommend a value of 0.2. The problem with this solution is that in some cases such a value is too high; using too high a value in the analysis might require unnecessary replacement of valve motor-operators with more powerful ones, and it might cause yokes and

Table 4-1. Technical data for eight stems and three operators used in the MOVLS test program.

Operator stem	SMB-00	SMB-0				SMB-1		
	S7	S1	S2	S3	S8	S4	S5	S6
Motor set ratio	22/43	37/35	37/35	25/47	37/35	21/51	32/40	27/45
Overall ratio	87.8	34.96	34.96	69.56	34.96	82.55	42.50	56.64
Running efficiency	0.50	0.55	0.55	0.50	0.55	0.50	0.50	0.50
Stall efficiency	0.50	0.55	0.55	0.50	0.55	0.50	0.50	0.50
Pull out efficiency	0.40	0.40	0.40	0.40	0.40	0.40	0.40	0.40
Application factor	0.90	0.90	0.90	0.90	0.90	0.90	0.90	0.90
Motor rpm	1800	1800	1800	1800	1800	1800	1800	1800
Motor rated torque (ft-lb)	5	25	25	25	25	60	60	60
Motor stall torque (ft-lb)	6.6	29	29	29	29	67	67	67
Operator rated torque (max) (ft-lb)	250	500	500	500	500	850	850	850
Operator torque (motor rated) (ft-lb)	220	481	481	870	481	2477	1275	1699
Operator torque (motor stall) (ft-lb)	290	558	558	1009	558	2765	1424	1897
Stem diameter (in.)	1.25	1.5	1.75	1.25	1.75	2	2.5	2.125
Stem pitch	0.333	0.25	0.25	0.25	0.25	0.333	0.333	0.250
Stem lead	0.667	0.25	0.25	0.5	0.25	1.000	0.667	0.500
Stem force (max rated) (lb _f)	14000	24000	24000	24000	24000	45000	45000	45000
Stem force (rated torque) (lb _f)	15308	40642	35941	35198	35941	32956	35056	42958
Stem force (motor rated) (lb _f)	13441	39073	34554	61209	34554	96018	52585	85876
Stem force (motor stall) (lb _f)	17742	45325	40082	71003	40082	107220	58719	95895

valves to be subjected to unnecessarily high loads (too high a torque switch setting), with a potential to contribute to fatigue failures in the operator and valve. Another possible solution is to test all valves in situ at their design basis conditions so that no analytical predictions would be needed. In many cases, however, such testing is simply impossible. Some utilities have attempted to address this issue by testing a valve at static conditions (packing load only), deriving a coefficient of friction from the results at torque switch trip, and using that value in calculations to predict the operator torque needed for the design basis case. As our test results have shown, a single value of the coefficient of friction obtained during wedging can be artificially low, so using such a value without adjusting it to account for load-sensitive behavior is unreliable.

Although any single value of the coefficient of friction derived from a static test tends to differ significantly from the design basis running coefficient, results from testing on the MOVLS show that it is possible to get reliable, useful information from static and low-load tests. The following discussion proposes two new methods that use data from tests conducted at conditions less severe than design basis conditions to either predict or bound the design basis coefficient of friction. The methods are based on the results of our testing of eight stems. We believe that with additional validation, these two methods represent a major breakthrough in stem factor research. Use of these methods will make the stem factor portion of the determination of MOV margins simpler and more accurate.

4.3 The Threshold Method

The appropriate coefficient of friction to use in a design basis calculation is one that corresponds with the highest stem load during the running portion of the stroke (throughout this discussion, the word *running* is used to refer to the running portion of the closing stroke before wedging, and the word *wedging* is used to refer to that portion of the valve stroke when the disc comes to a stop as it wedges between the seats). In valves that exhibit typical responses, this highest running load occurs just before wedging, at a point that corresponds with

flow isolation. This is the point where the entire area of the disc is exposed to the maximum differential pressure. Some valves exhibit what we call atypical responses. In these valves, the highest stem force occurs before flow isolation, a phenomenon that is due to internal valve clearances and flow and pressure effects. In either case, the coefficient of friction at the highest stem force before wedging is the one that is important. Figure 4-5 is a scatter plot of such data from tests on the MOVLS with Moly 101 lubricant on the eight stems. Running data just before wedging are included for all eight stems and all three torque switch settings for each stem. Repeated tests for some stems are also included. The coefficients of friction were calculated using direct measurements of stem torque and stem thrust.

Coefficient of friction is plotted against stem thrust in Figure 4-5. We found that stem thrust is not the best variable to use in a study of stem friction with stems of different sizes and thread geometries. A 10,000-lb thrust is a very different condition for a 1-in. stem versus a 2-1/2-in. stem. We found the most appropriate variable that includes thrust and also normalizes the effect of thrust on stems of various sizes was stem thread pressure. We calculated thread pressure (in pounds per square inch) using the measured thrust and an approximate thread area based on one stem thread revolution, as shown in the equation below. Coefficient of friction is plotted against thread pressure in Figure 4-6. Although the envelope of the data hasn't changed dramatically, the relative position of data for the various stems has shifted somewhat.

$$TP = \frac{2 F_{stem}}{\pi SP (D_{stem} - \frac{1}{2} SP)}$$

where

TP	=	thread pressure, psi
F _{stem}	=	stem thrust, lb _f
SP	=	stem pitch
D _{stem}	=	stem diameter at the stem nut, inches

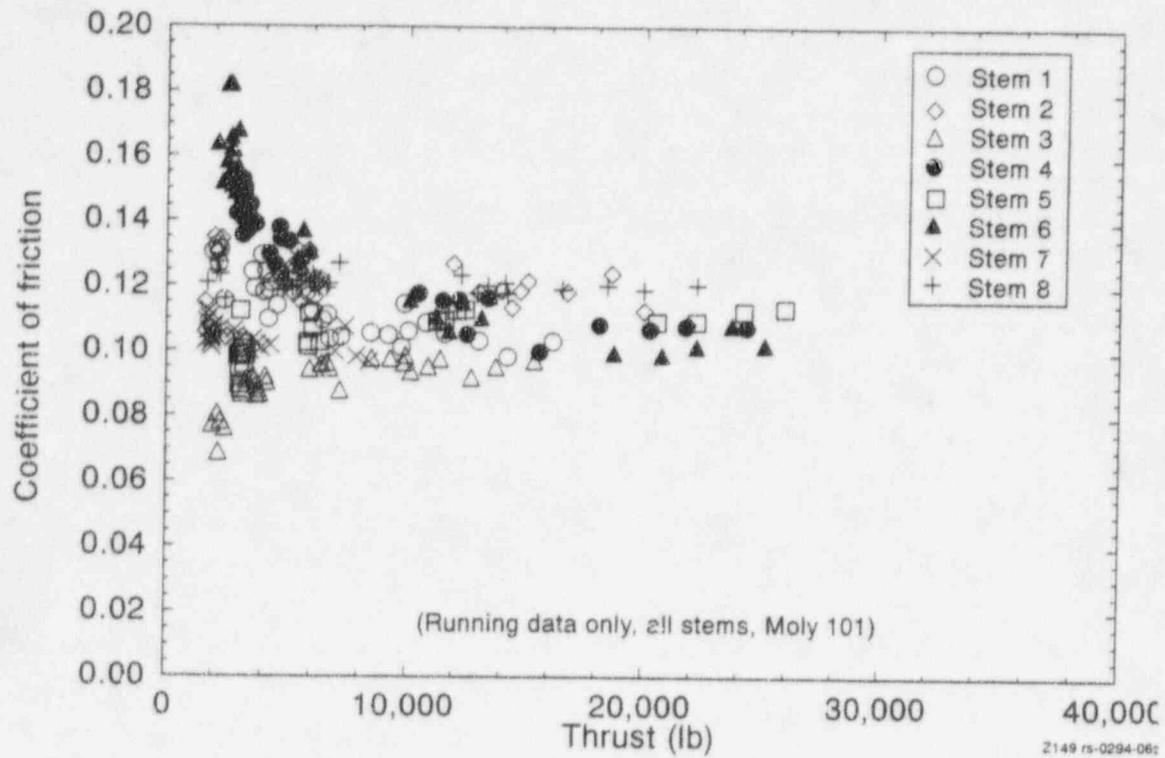


Figure 4-5. Coefficient of friction versus stem load for tests with Moly 101 lubricant; the data scatter decreases as the load increases.

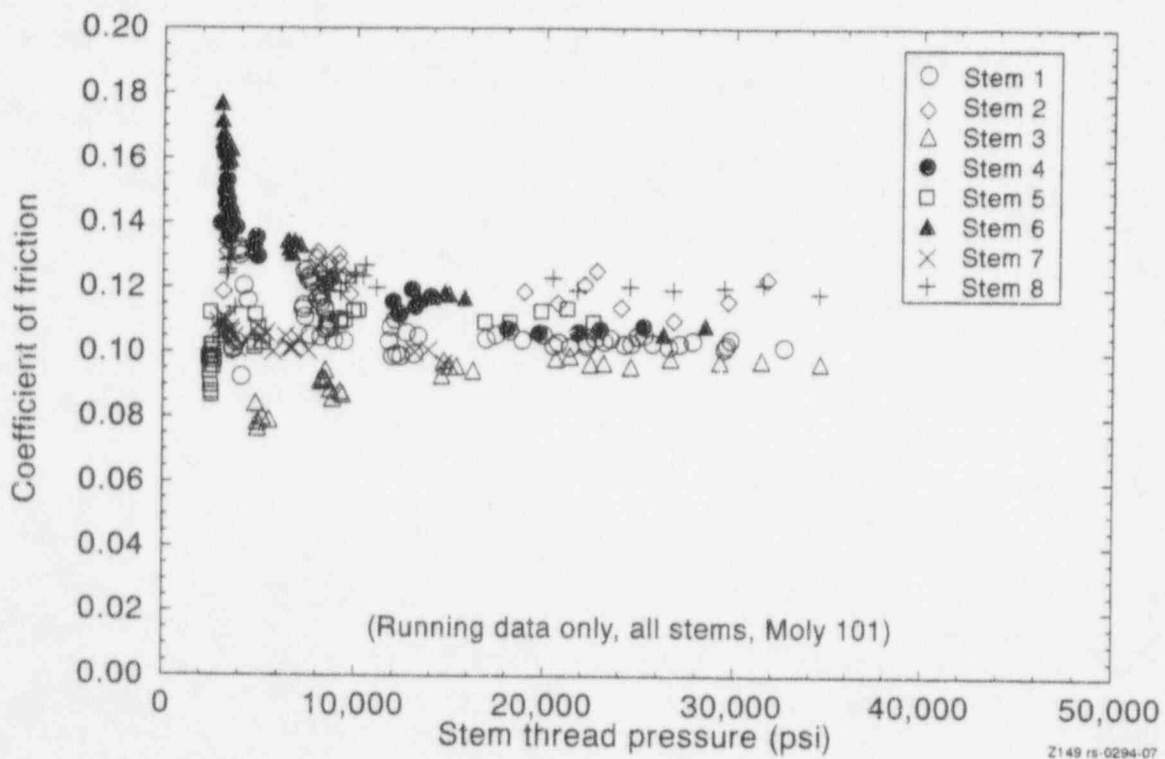


Figure 4-6. Friction data plotted against a normalized load, with coefficient of friction versus stem thread pressure for tests with Moly 101 lubricant.

A careful review of Figure 4-6 shows that there is a lot of scatter in the coefficient of friction data at low thread pressures, but the trends for the individual stems flatten out above a thread pressure of about 10,000 psi. This is the key to what we call the *threshold method* of using the results of a low-load test to predict the design basis coefficient of friction for a given stem. In practice, if a valve test can be set up to yield a running stem thread pressure above the stem thread pressure threshold, the coefficient of friction (or the stem factor) derived from the test at the maximum running load measured during the test can be treated as the design basis value and used directly in the calculation to determine the valve's design basis torque requirement. (Design basis stem thrust times design basis stem factor equals required torque.) For many valves, the load that achieves this threshold stem thread pressure is significantly lower than the design basis load; for example, it might consist of the packing load combined with a pressure load (stem rejection load), or a combination of the packing load, a pressure load, and a low flow load. Normally the packing load alone is not enough to achieve the minimum threshold pressure.

The data shown in Figure 4-6 are from tests with the stems lubricated with Moly 101 grease. All of the stems we tested on the MOVLS were also tested with EP-1 grease. A presentation of the EP-1 data is included in Appendix A. The thread pressure scatter plot for EP-1 is shown here as Figure 4-7. The threshold method works as well with EP-1 as it does with Moly 101. The absolute values for coefficient of friction are slightly higher for most stems, but some stems performed better with EP-1 than with Moly 101. Figure 4-8, derived from testing of Stem 3, compares Moly 101 data with EP-1 data. Not all the stems exhibited the constant offset shown here for Stem 3. Note that although the coefficients of friction are different for the two greases, the results are consistent with our understanding of the basis of the threshold method; both traces reach a plateau, and the plateau occurs at about the same stem force threshold.

The work in developing the threshold method is not done yet. This method is based on empirical

data from a sample of eight valve stems. Before the method is put to use, it will be necessary to increase the sample size to ensure that the method works for a larger population of stems. In addition, more data are needed to determine the exact threshold for stems in general, especially for smaller stems.

However, the threshold method appears to be very promising for those valves where a partial differential pressure test can be run. It is certainly an improvement over the use of default coefficients; it takes advantage of the observation that the coefficient of friction in most stems is somewhere near 0.12, as compared with the best default value of 0.15 or the higher default value of 0.2.

4.4 The Fold Line Method

Predicting a design basis stem factor from the results of a packing load test (static test) is very attractive because this is the best that can be done in situ for some valves. Such a prediction has been difficult to develop because the behavior of the coefficient of friction is different during wedging compared to that during the running portion of the closing stroke. It is also difficult because each stem/stem-nut combination behaves uniquely inside the larger envelope of the population. This is generally shown in Figure 4-6 in the overall responses of the individual stems. Figure 4-9 shows examples of responses that make up Figure 4-6. These are typical coefficients of friction derived from the running portion of dynamic tests, just before wedging, for three individual stems. These three responses represent all the observed responses of running coefficients of friction: increasing with load, decreasing with load, and relatively constant with load.

Consistent with what we know about load-sensitive behavior in many stems, the coefficient of friction at torque switch trip in a static test is lower than the running coefficient of friction just before wedging in a dynamic test. This phenomenon is probably the result of lubrication performance at the stem/stem-nut interface. This difference is shown in Figure 4-10. Note that

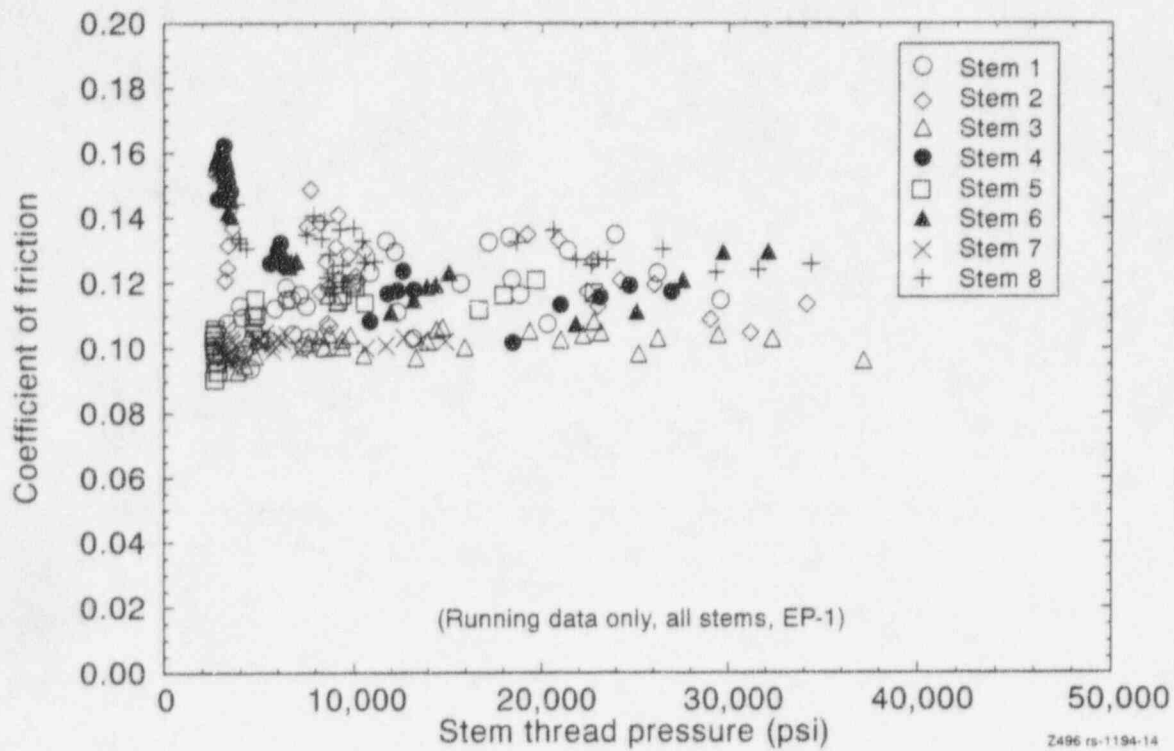


Figure 4-7. Coefficient of friction versus stem thread pressure for tests with EP-1 lubricant.

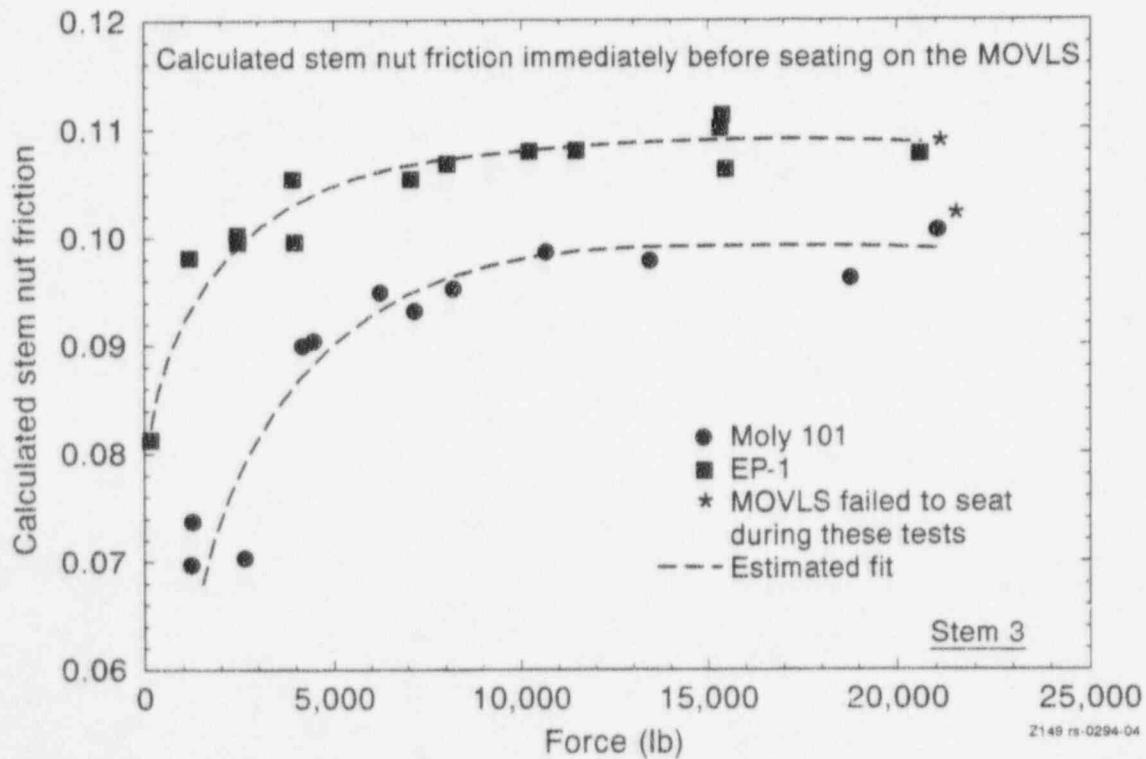
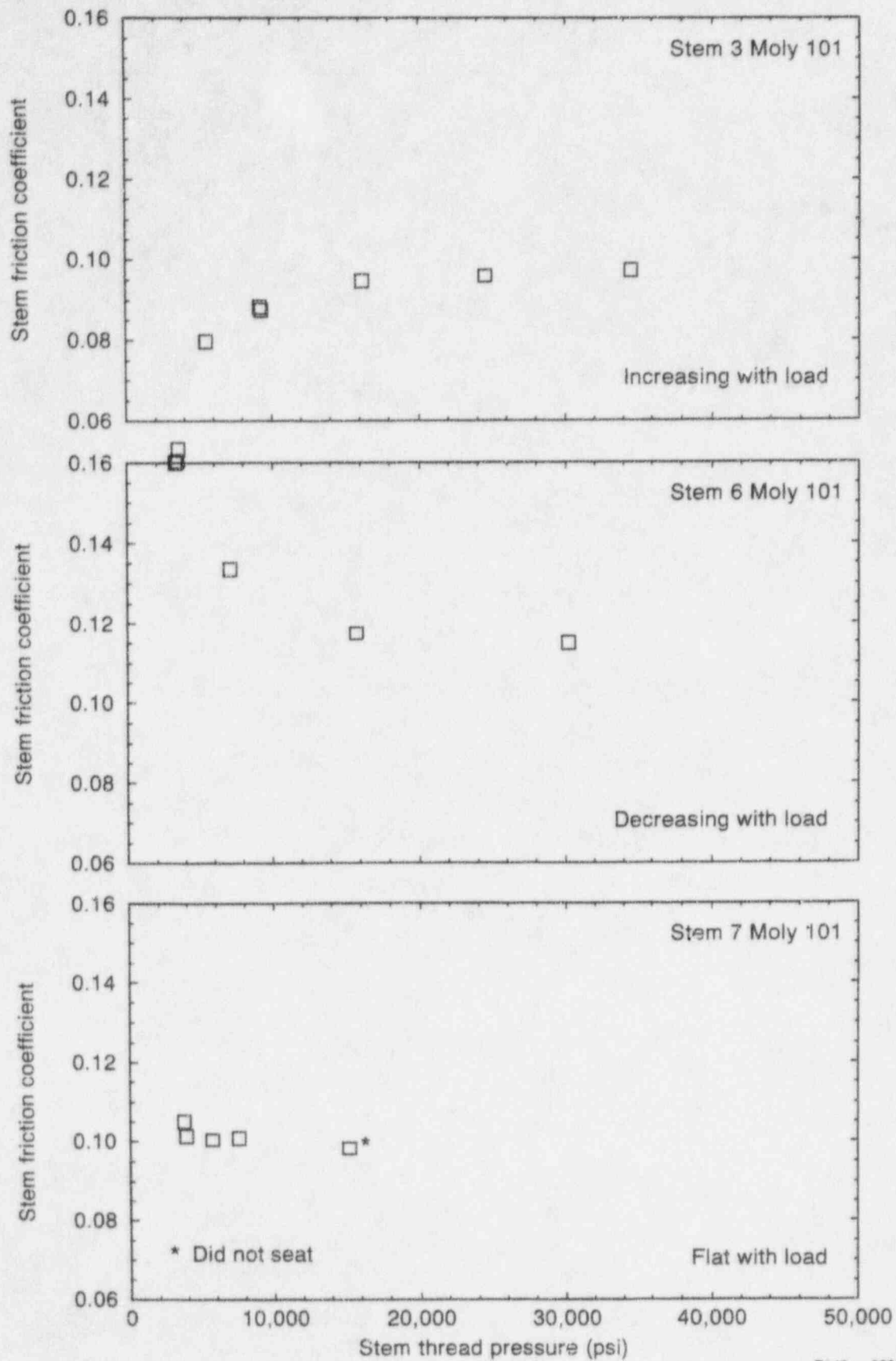


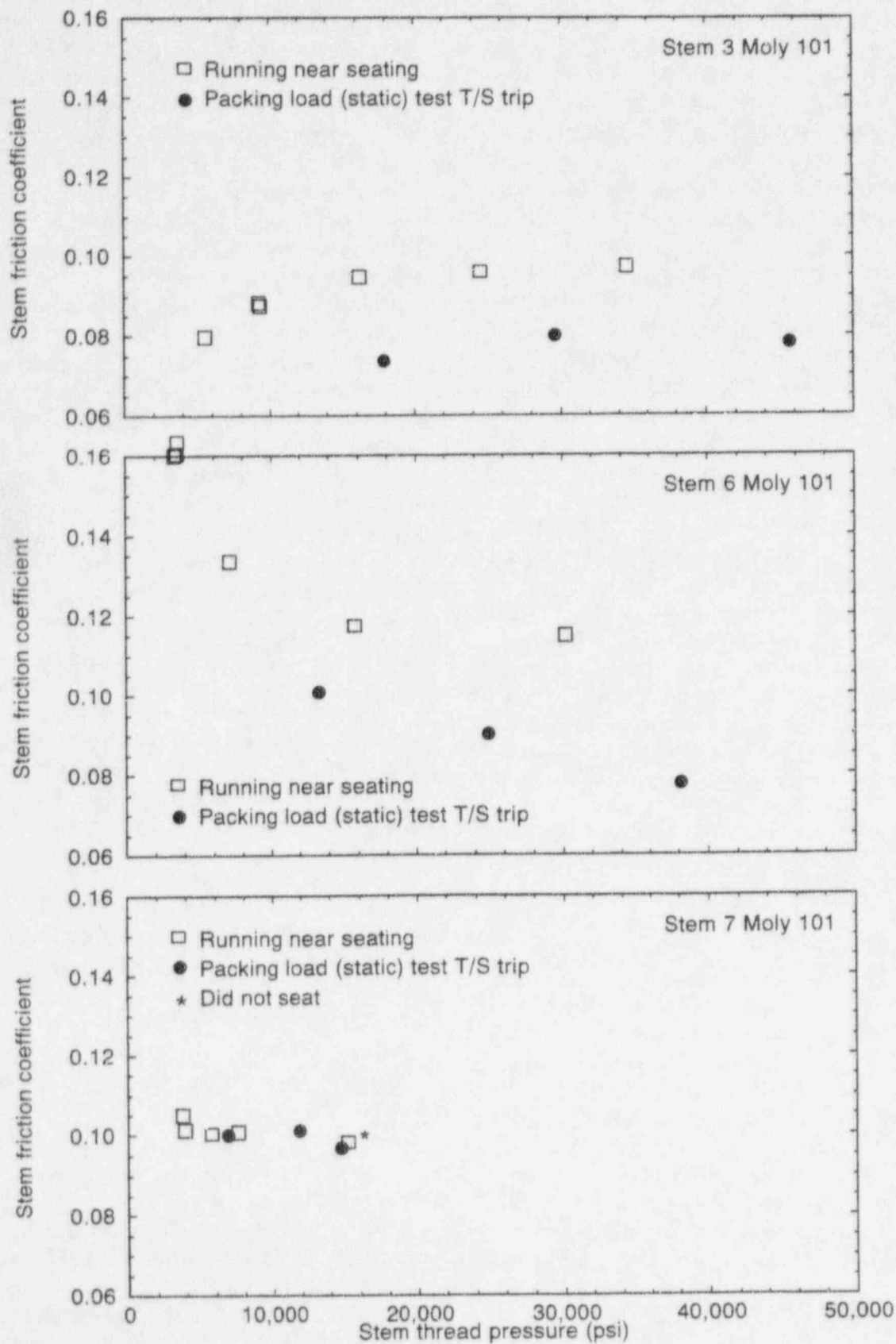
Figure 4-8. Coefficient of friction versus load comparing two greases on the same stem.

Stem Factor



Z149 rs-0294-08

Figure 4-9. Running coefficients of friction (just before wedging) versus stem thread pressure for three representative stems.



Z149 rs-0294-09

Figure 4-10. Running and wedging (torque switch trip) coefficients of friction versus stem thread pressure for three stems.

although they are lower, the single data points for torque switch trip in the static tests generally follow the trend observed in the running data from the dynamic tests: increasing, decreasing, or a nearly flat response. This insight provided the first clue that there might be a link between wedging and running friction coefficients.

Although the single value for coefficient of friction taken at torque switch trip does not tell us what we need to know about the design basis coefficient, a close look at the entire wedging transient does provide some important information. The transient in this case consists of a small interval of time from initiation of wedging (at about 5000 psi thread pressure) through torque switch trip to the final maximum thrust. Figure 4-11 plots stem/stem-nut coefficient of friction against stem thread pressure during the wedging transient derived from the static test of Stem 6 at the highest torque switch setting. This trace represents the value calculated from the measured stem thrust and the measured stem torque during the small interval of time in which wedging occurs. This figure shows how the coefficient of friction changes as the load in a static test suddenly increases at wedging.

A comparison of the Stem 6 wedging transient (shown in Figure 4-11) with the Stem 6 running and wedging data is presented in Figure 4-12. These Stem 6 data points represent the friction coefficients just before wedging and at torque switch trip for the dynamic and the static tests at three torque switch settings. Note that this wedging transient generally models the trends in the wedging data from the static tests, and it roughly models the shape of the running data. This similarity provided the second clue to a link between running data and wedging data. It also appears that the variation in the coefficient of friction during the single wedging transient for the highest torque switch setting represents the total variability among the single data points for the static tests at torque switch trip for all three torque switch settings.

To better understand the nature of the wedging transient, we plotted a family of wedging transient curves for each of the three representative

stems (Stem 3, Stem 6, and Stem 7) for dynamic as well as static tests, as shown in Figure 4-13. For Stem 3, the top three traces are the dynamic wedging transients, increasing in load from left to right. The bottom three are the static wedging transients; the longest is from the test with the high torque switch setting, and the shortest is from the test with the low setting. The six traces represent three pairs of tests (a dynamic test and a static test) for each of three torque switch settings. For Stem 6 there are only two traces from the dynamic tests (Stem 6 did not seat in the dynamic test with the highest load and the highest torque switch setting, so there is no wedging transient for that test). For Stem 7, the traces are on top of each other, and it is difficult to distinguish which is which. This is because Stem 7 has a very flat response with almost no tendency toward load-sensitive behavior. Notice, however, that in a given family plot, the shape of all the traces is the same, regardless of the load before wedging or the torque switch setting.

We observed that these wedging transients provide a snapshot of the characteristic behavior of each stem. For each stem, the absolute value of the friction coefficient during the transient varies according to the load the stem experiences just before wedging, but the shapes are the same. For a given stem, the range of variation in the friction coefficient during a wedging transient is influenced by the duration of the transient, which is determined by the load just before wedging and by the torque switch setting. In addition, this range of variation is different from one stem to the next. The stem with the greatest range of variation in a single trace also has the greatest variation among the absolute values from one trace to the next.

This last observation is shown more clearly in Figure 4-14. The upper plot is the same as Figure 4-12, showing the wedging transient and the individual data points for running and torque switch trip for Stem 6. Compare these data with the lower plot, which shows the same data for Stem 8. Note that in the upper plot, the large change in the friction coefficient during the wedging transient corresponds with large differences between the running data points and the

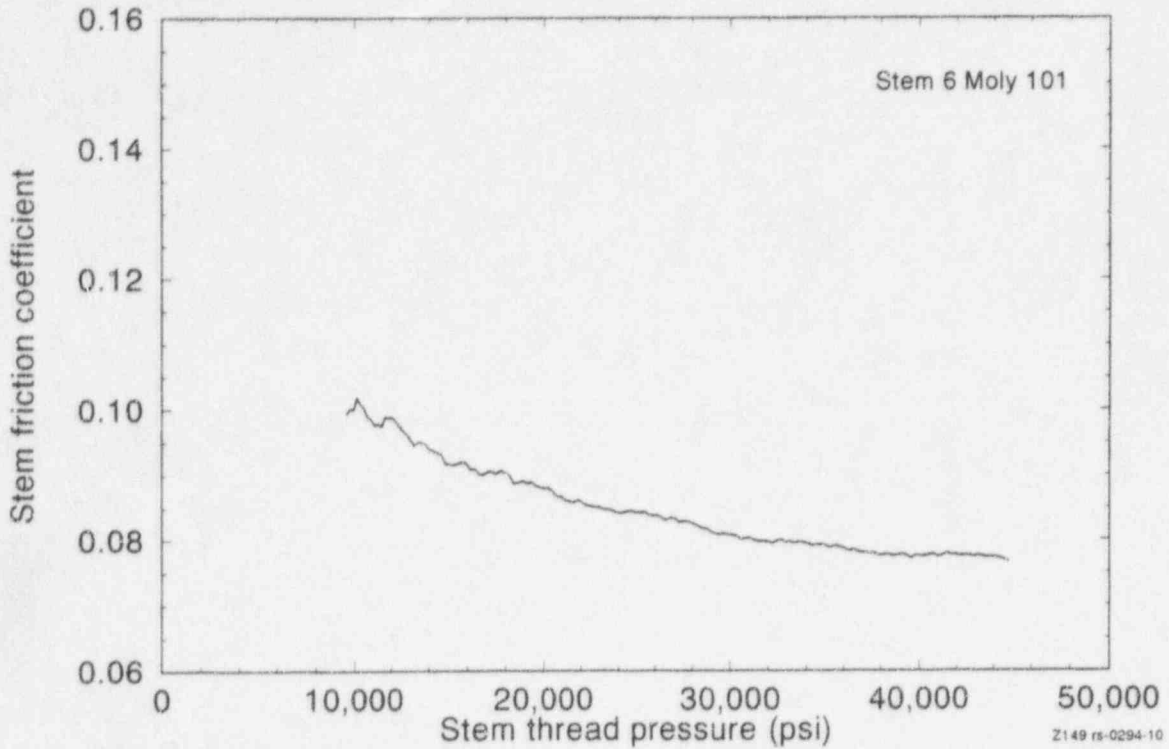


Figure 4-11. Wedging transient for Stem 6 (static test, high torque switch setting), with coefficient of friction plotted against thread pressure.

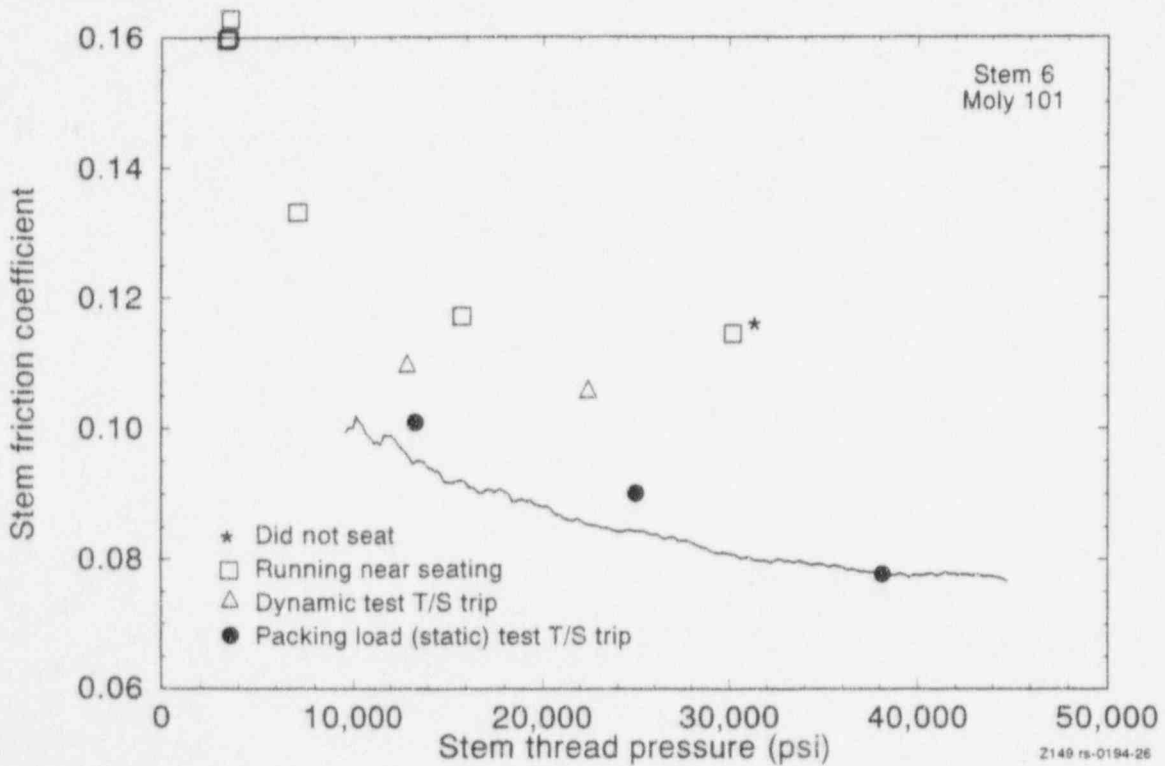
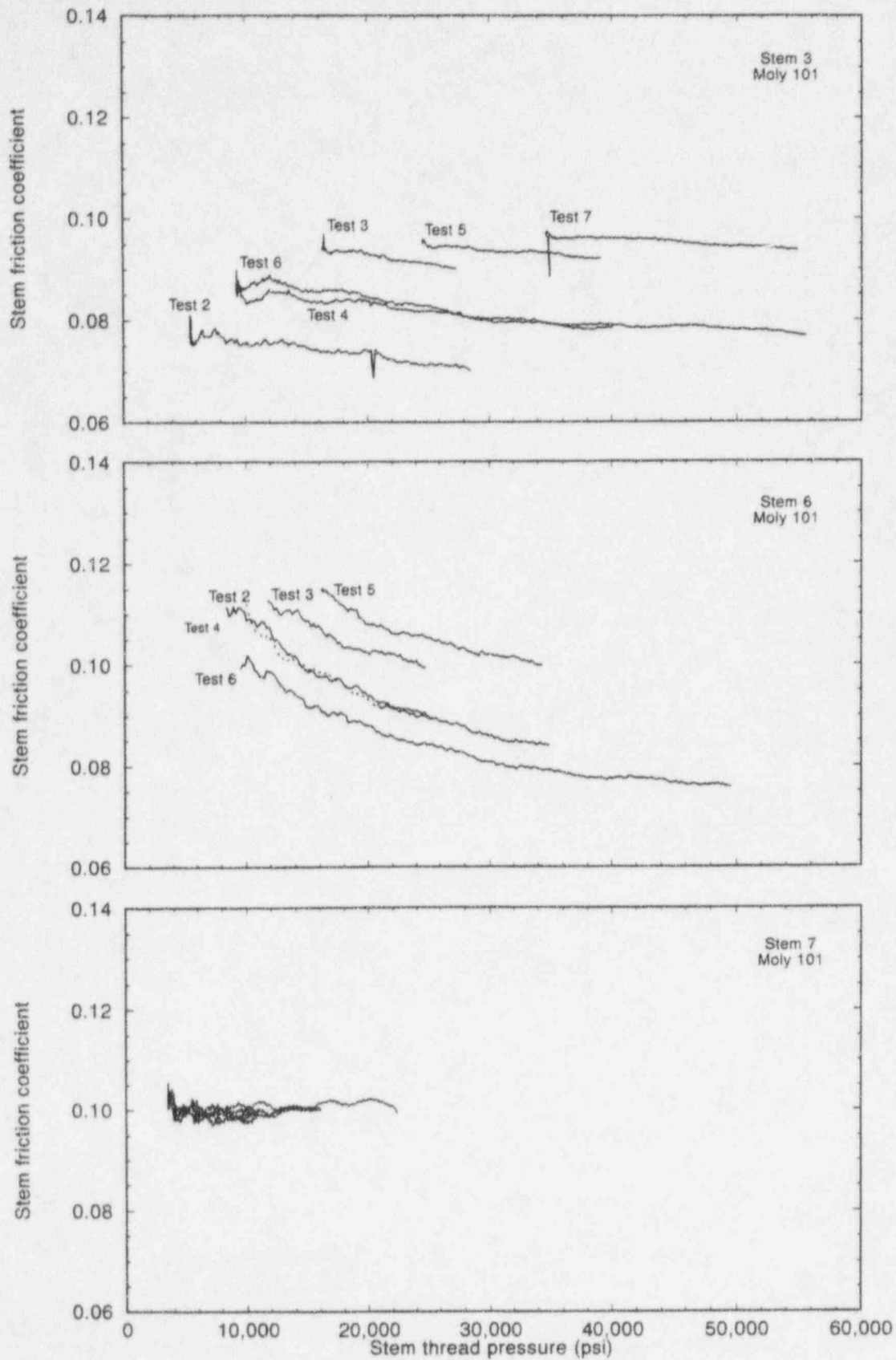


Figure 4-12. Coefficient of friction during the wedging transient for Stem 6, compared to individual data points for running and for torque switch trip.

Stem Factor



Z149 rs-0294-27

Figure 4-13. Wedging transients for three representative stems.

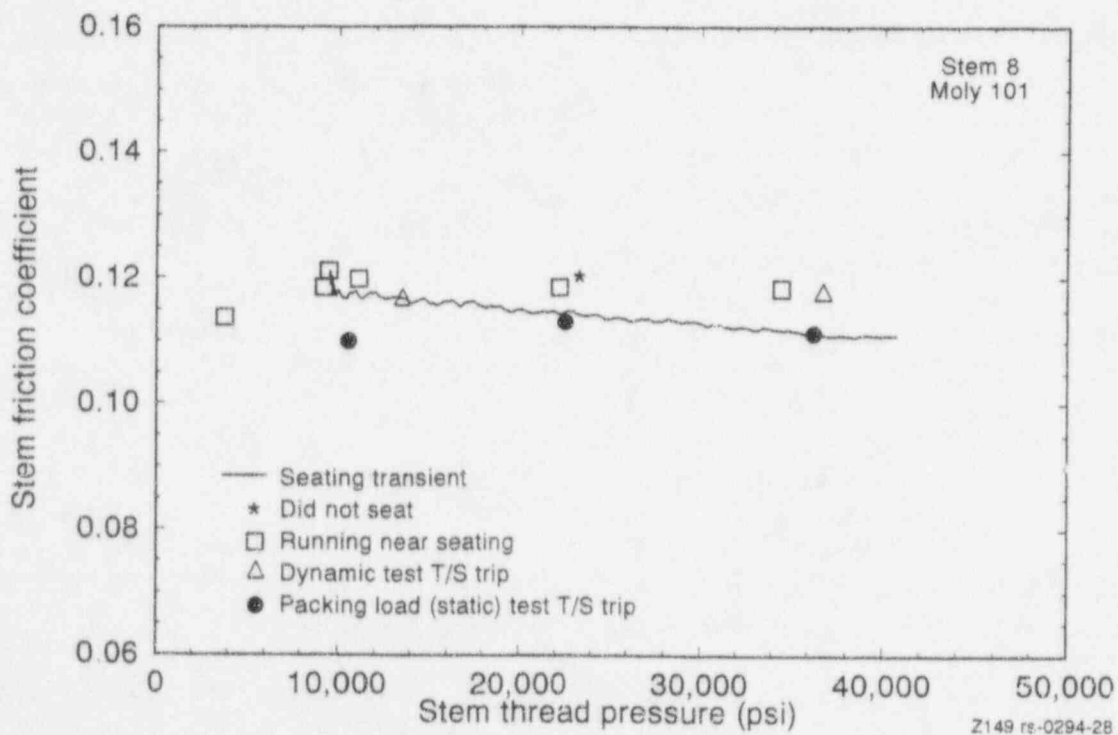
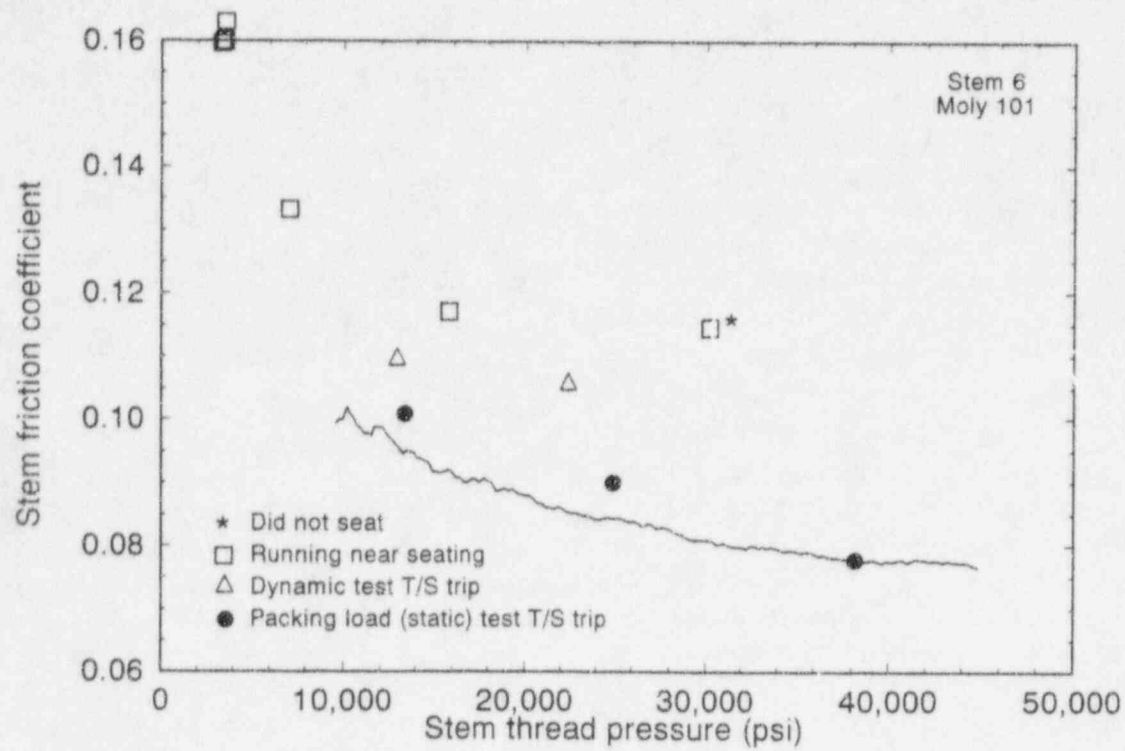


Figure 4-14. Stem 6 data compared with Stem 8 data.

torque switch trip data points, while in the lower plot, the small change during the wedging transient corresponds with small differences. It is evident that the wedging transient tells a lot about the stem's propensity for load sensitive behavior; the greater the change in friction during the wedging transient, the more load-sensitive behavior is seen in the comparison between the static torque-switch-trip data and the dynamic running data. This observation provided the third clue about the relationship between running data and wedging data, and it provided the basis for what we call the *fold line method* for bounding the design basis friction coefficient from the results of a static test.

We also observed that the friction coefficient at the beginning of the wedging transient (in the static test) provides a bench mark from which to anchor the bounding methodology. This is true of all eight of the stems we tested. (One stem's coefficient of friction did not improve during the wedging transient, but the methodology is still applicable; that performance is discussed later in this section.) By coupling this knowledge with the friction coefficient's expected variability, as defined by the wedging transient, we can now bound the design basis running coefficient of friction.

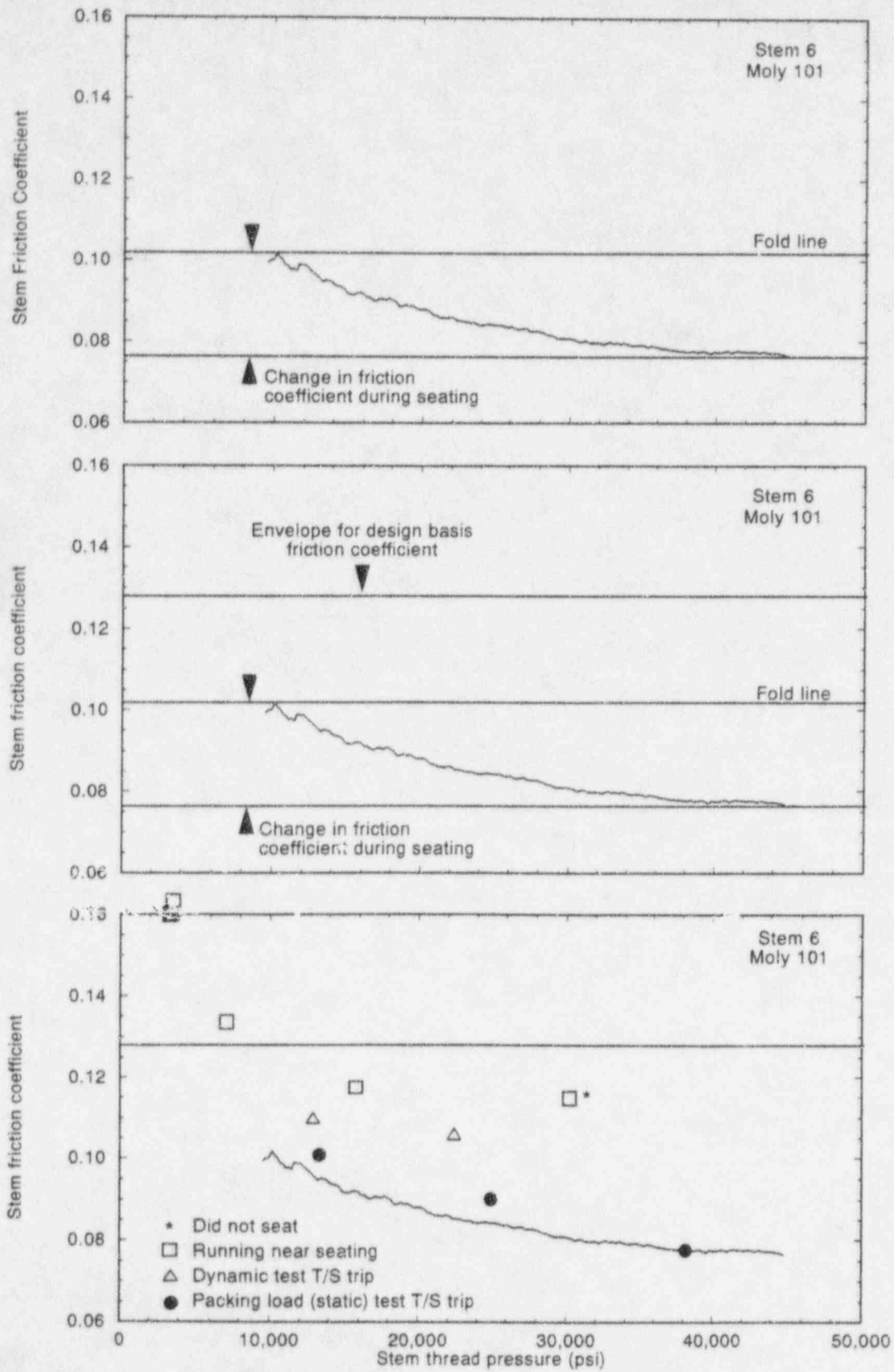
The following exercise demonstrates how the *fold line method* works. The upper plot in Figure 4-15 is the same as Figure 4-11, except that we have drawn two horizontal lines to mark the variation in the friction coefficient during the wedging transient. The top line represents the bench mark or *fold line* from which we intend to extrapolate, and the difference between the top line and the bottom line represents the range of variability in the friction coefficient we expect for that stem. By folding on the *fold line*, we can identify the location of a third line that will envelope the running data. The effect is to use the variability below the bench mark to bound the expected variability above the bench mark. This effort is demonstrated in the middle plot in Figure 4-15. The lower plot shows that the result bounds the running coefficients of friction near wedging and the coefficients at torque switch trip for all thread pressures above 10,000 psi. This

completes the basis of the *fold line method* for bounding the design basis friction coefficient.

Figure 4-15 demonstrates the fold line method for Stem 6. Figures 4-16 through 4-18 provide the same information (in a slightly condensed format) for Stems 1 through 4 and Stems 7 and 8. (Stem 5 is discussed below.) In each case, the dotted lines identify the variability in the coefficient of friction during the wedging transient, and the solid line identifies the bound that envelopes the running data. These results show that the fold line method consistently provides appropriate results for all seven stems.

The fold line method also provides appropriate results for Stem 5, but the analysis is a little different. As stated earlier, most stems experience a decrease in the coefficient of friction during the wedging transient of the static test. Stem 5 is the exception. With Stem 5, the friction coefficient increases during the wedging transient. The cause of this behavior is probably that the roughness of the metal surfaces in the stem/stem-nut interface precludes the improvement in lubrication performance that occurs in the other stems at wedging. However, even though the wedging behavior of Stem 5 is different from that of the other stems, the running data for Stem 5, like those for the other stems, reach a plateau at about 10,000 psi stem thread pressure (Figure 4-6). Note also that the fold line method applied to Stem 5 still bounds the response. This result is shown in Figure 4-19. As with the other stems, the wedging transient provides a snapshot of the stem's overall behavior, and we can use the wedging transient to define the expected variability in the friction coefficient. As with the other stems, we place the fold line (the bench mark) at the highest value observed during the wedging transient. The only difference is that for Stem 5, this highest value occurs at the end of the wedging transient instead of at the beginning.

The data plots shown in Figures 4-9 through 4-19 are from tests with the stems lubricated with Moly 101 grease. As mentioned earlier in this discussion, all of the stems we tested on the MOVLS were also tested with EP-1 grease, and a



Z149 rs-0294-29

Figure 4-15. The fold line method demonstrated in three successive plots of Stem 6 data.

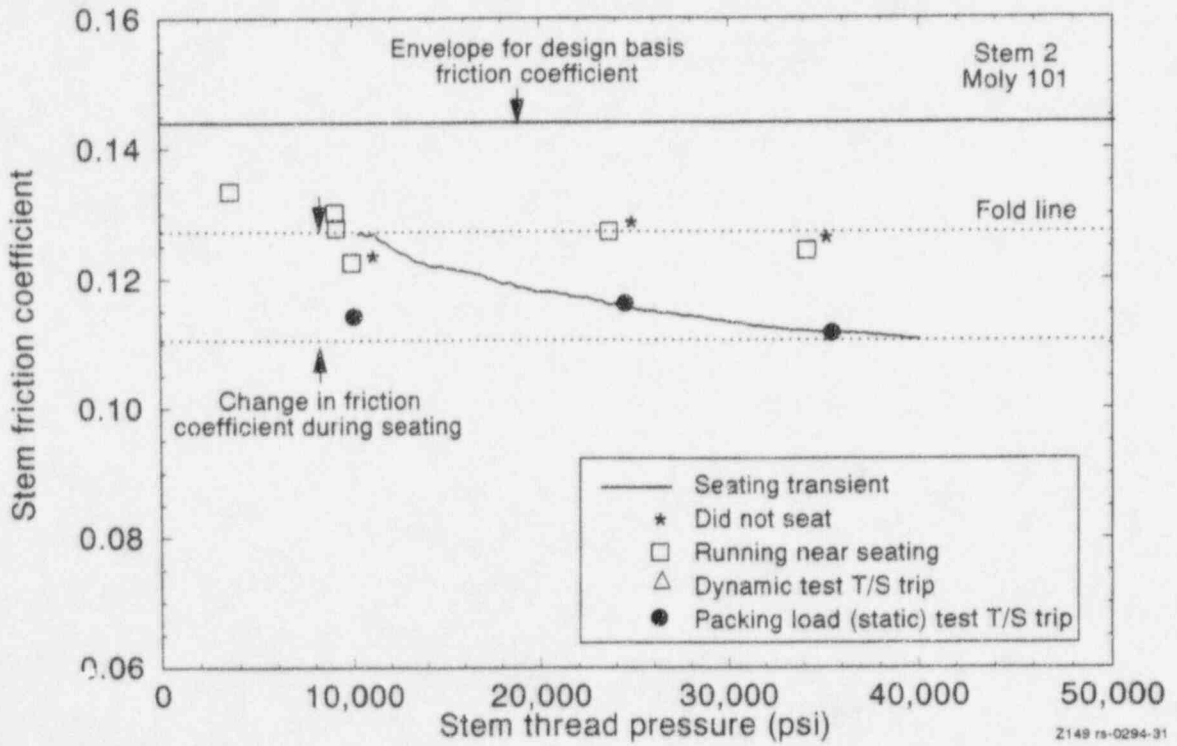
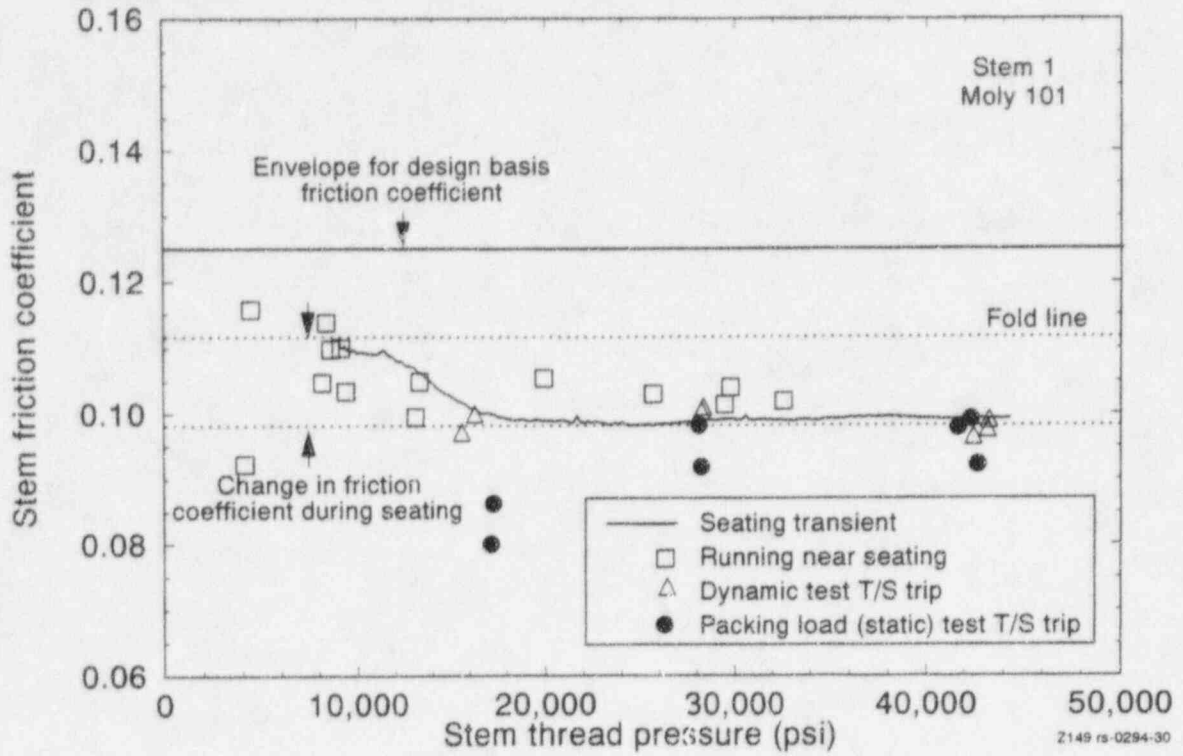


Figure 4-16. The fold line method bounds the performance of Stems 1 and 2.

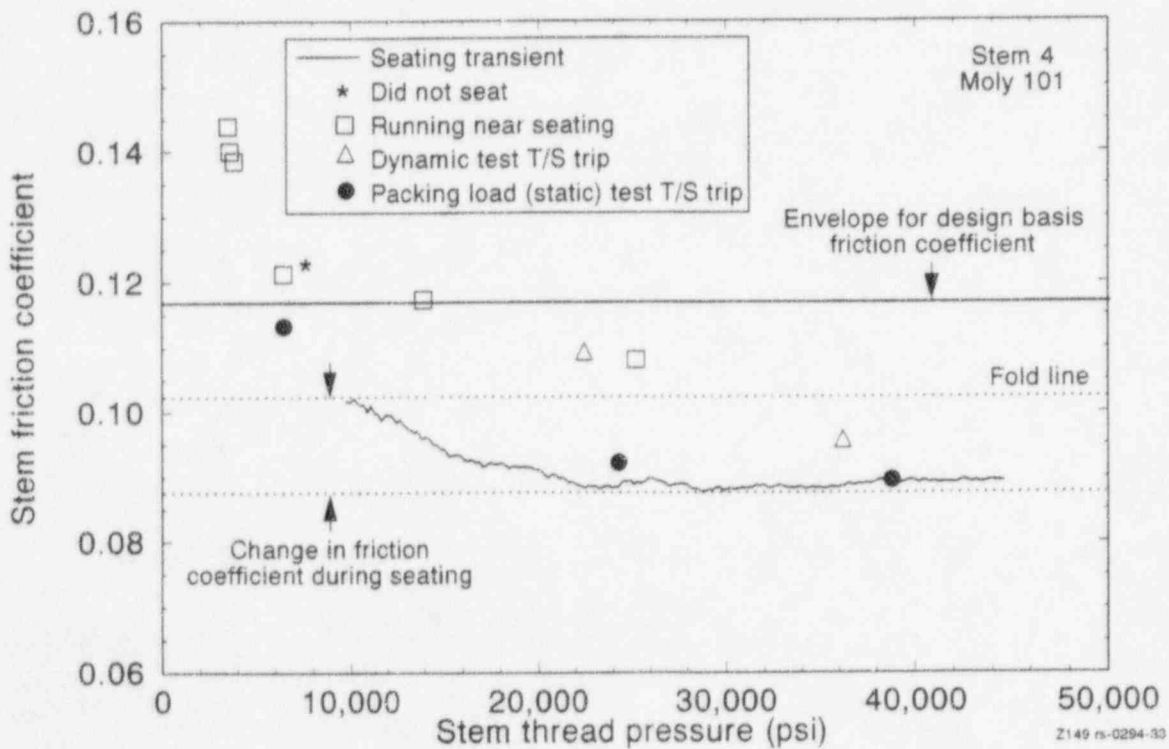
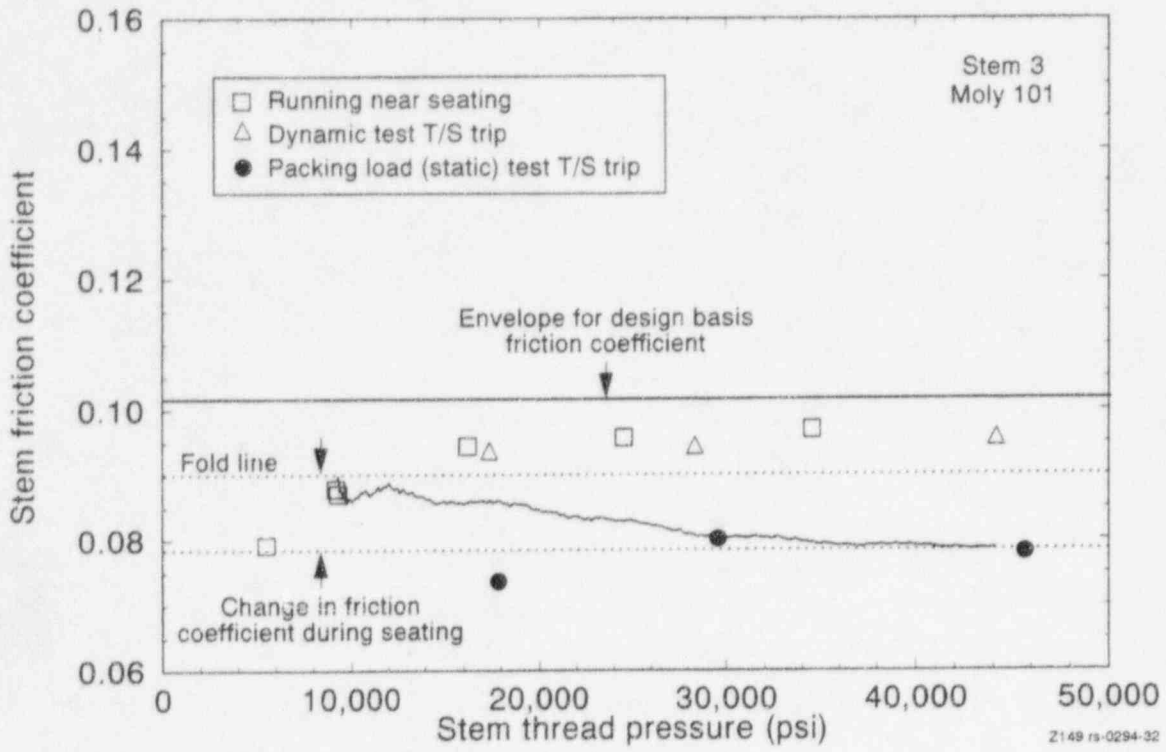


Figure 4-17. The fold line method bounds the performance of Stems 3 and 4.

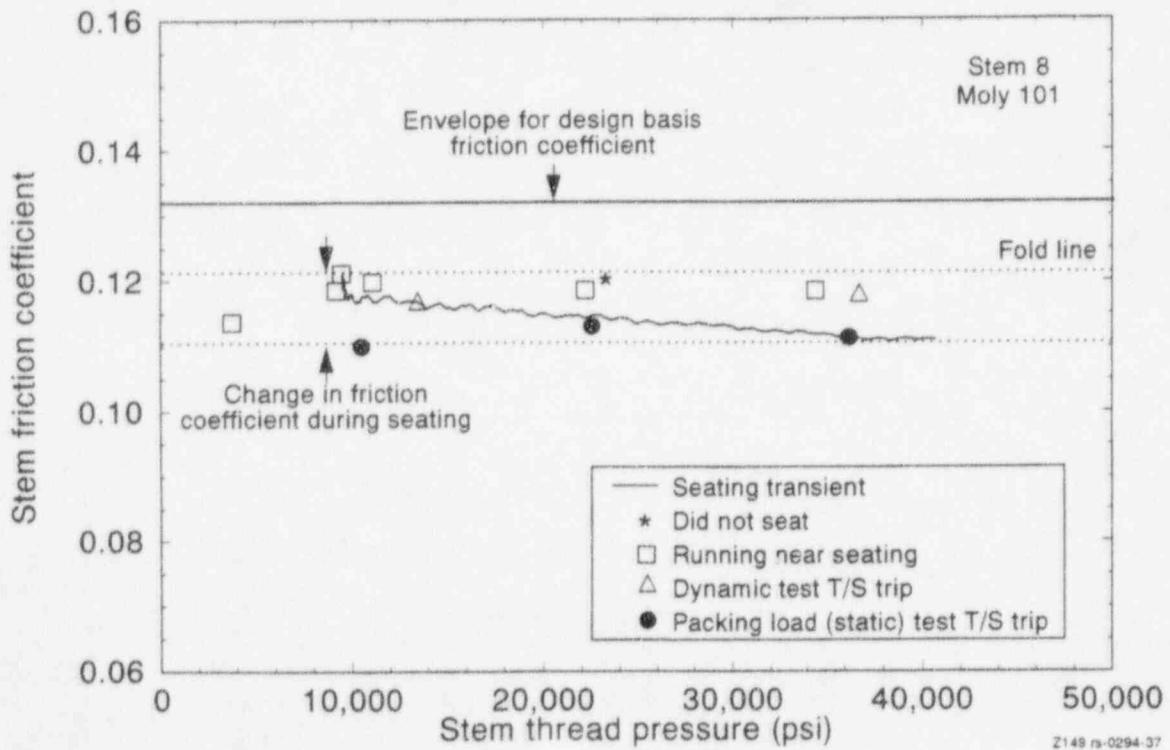
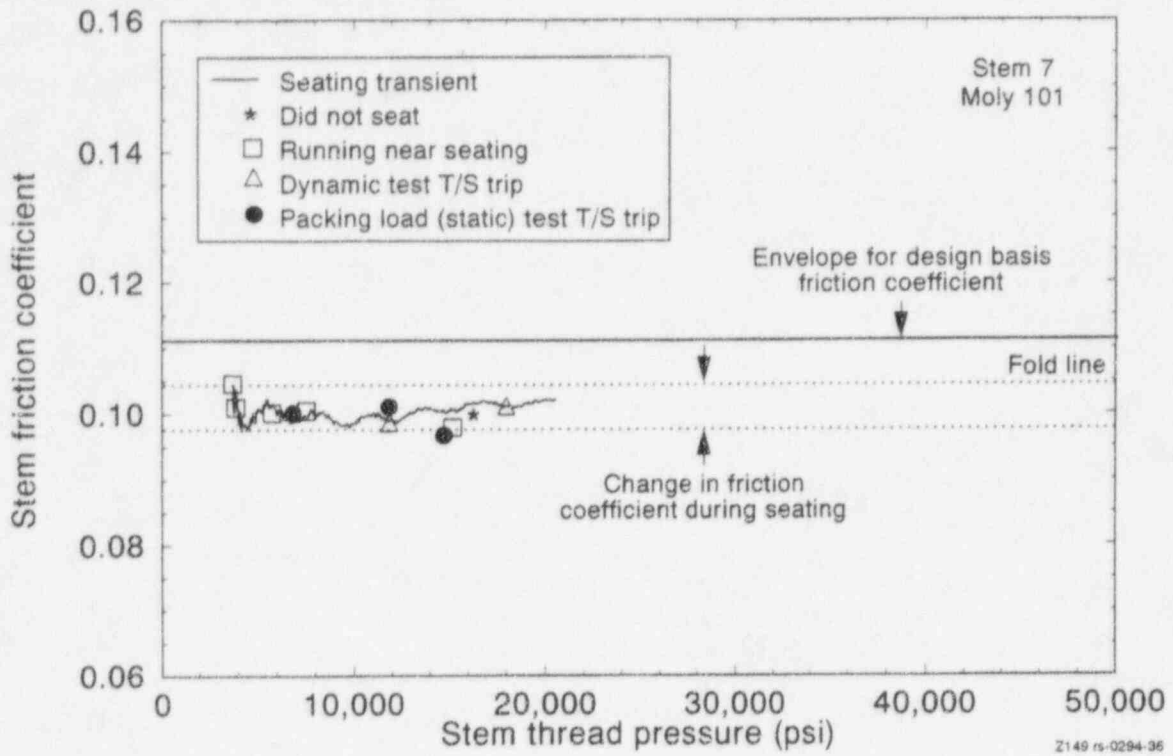


Figure 4-18. The fold line method bounds the performance of Stems 7 and 8.

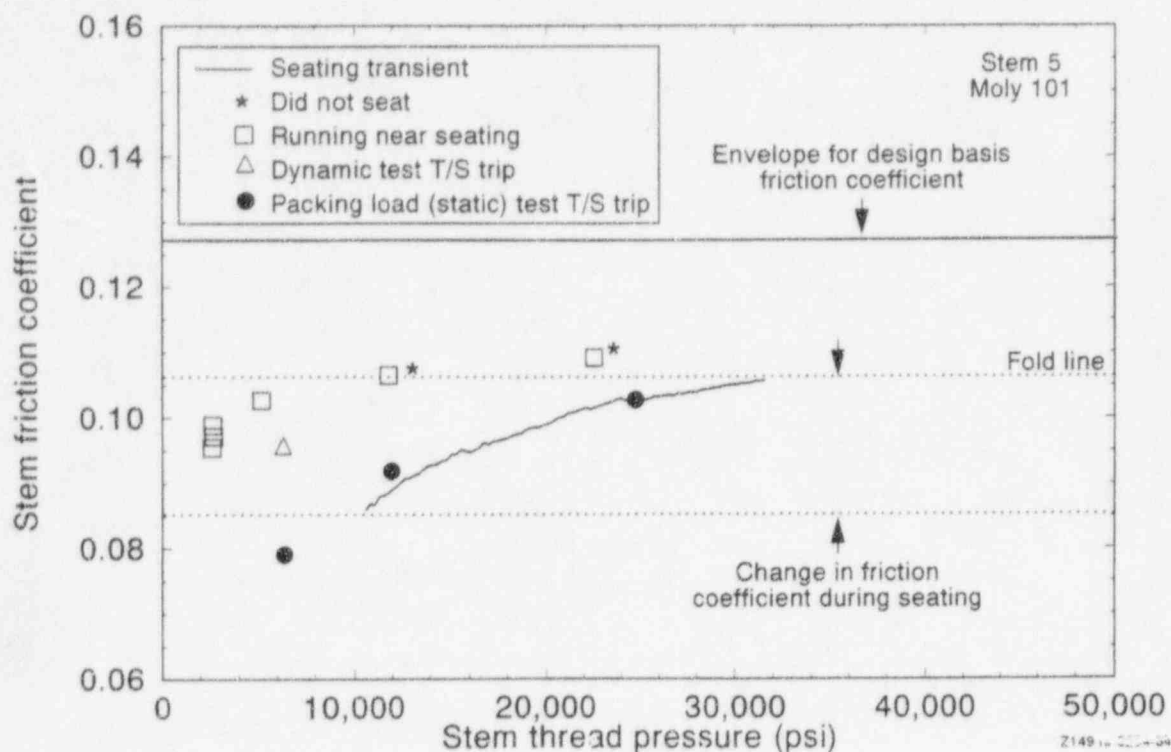


Figure 4-19. The behavior of Stem 5 is different from that of the other stems, but the fold line method still bounds its response.

similar analysis of those data has been performed. The results are presented in Appendix A. From that analysis, we have determined that the fold line method works as well with EP-1 as it does with Moly 101. Figure 4-20 is a representative example, showing the results of testing of Stem 3 with EP-1. Note that although the friction coefficients are slightly higher than those for Moly 101 (compare to Figure 4-17), the fold line method nevertheless bounds the responses.

Our sample is small, 8 stems, but we believe that with further validation and refinement, the *fold line method* will be a useful tool for valves that can be tested only at static conditions. It provides the most accurate bound of all the methods we have studied to date for predicting design basis response using data from static tests. It may also provide results that are lower than the default values for the coefficient of friction.

With further development and validation, an analysis using the *fold line method* might not

always require that the coefficient of friction be plotted against stem thread pressure, or that the wedging transient be plotted as we have plotted it in this presentation. Figure 4-21 is an ordinary plot of the friction coefficient over time for Stem 3 for two pairs of tests: a static test and a dynamic test at the low torque switch setting and at the medium torque switch setting. For Stem 3, it is easy to identify the wedging transient in the static test and to use the fold line method to draw the bounding line. Note also that in each case, this line bounds the design basis running coefficient just before wedging in the dynamic test. (The last 20% of the trace from the dynamic test represents the value that needs to be bounded.)

The data presented in Figures 4-15 through 4-19 demonstrate the method using the wedging transient from static tests with high torque switch settings. In contrast, the fold line method as demonstrated in Figure 4-21 uses the wedging transient from static tests at the low and medium torque switch settings. We performed a

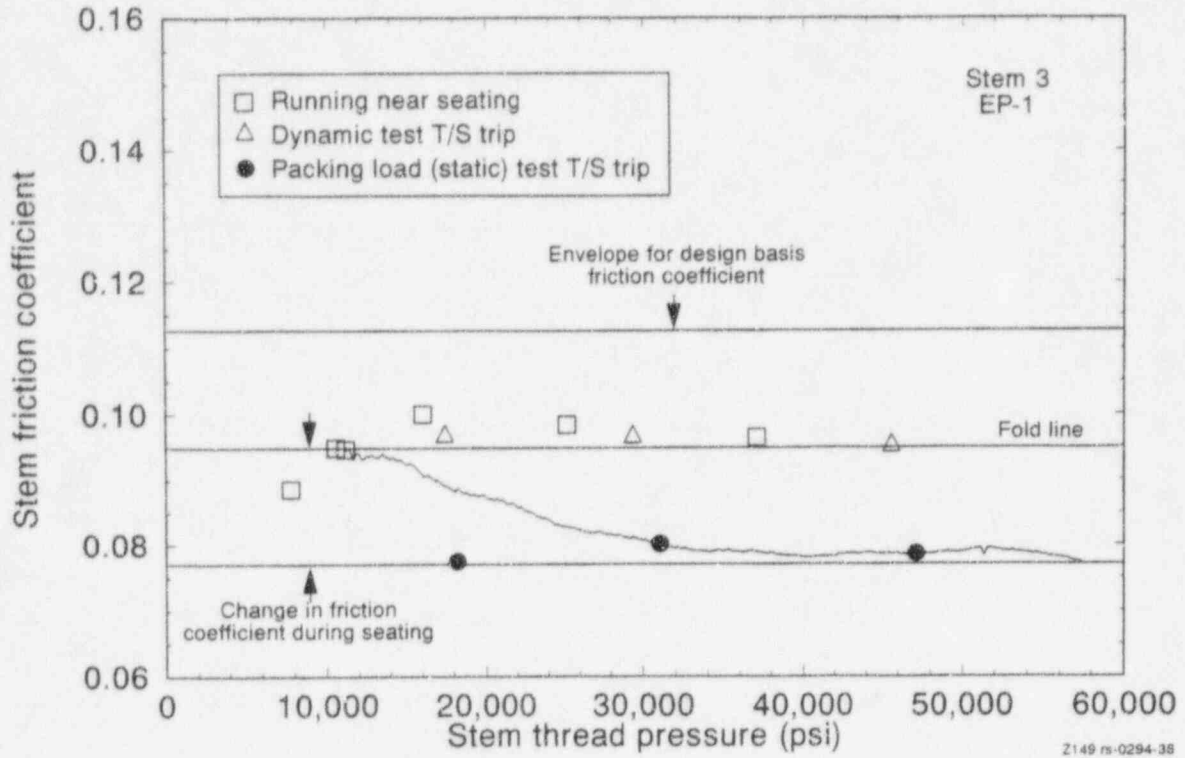


Figure 4-20. The fold line method bounds the performance of Stem 3 in tests using EP-1 lubricant instead of Moly 101.

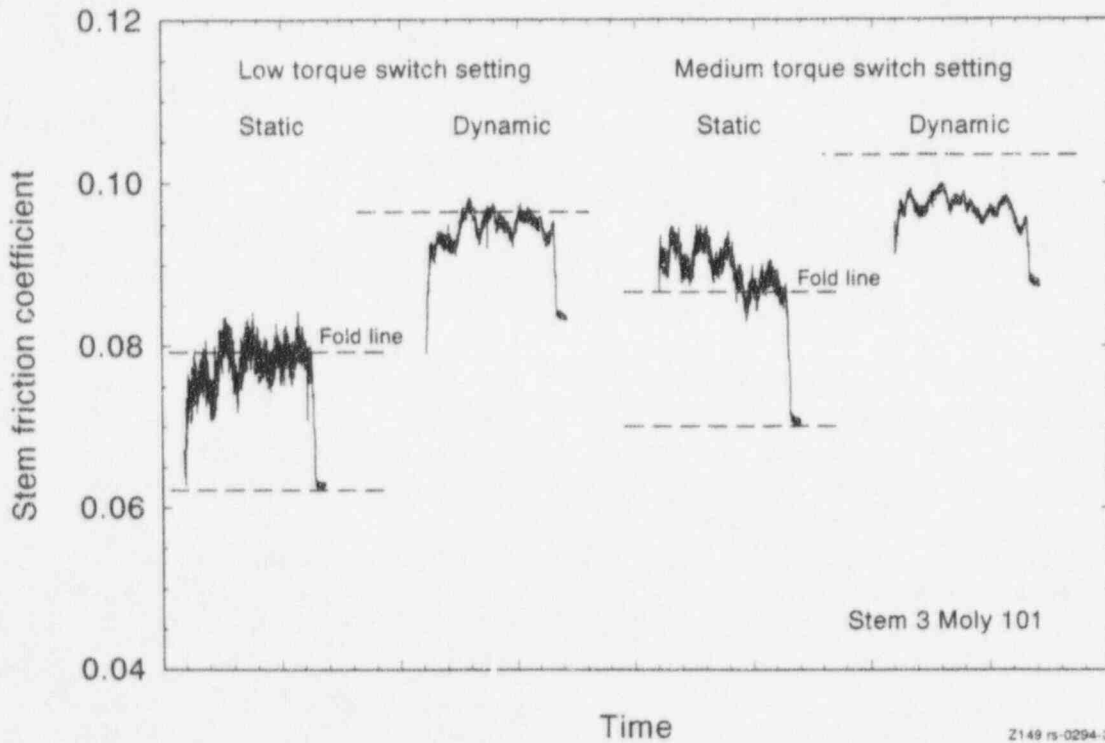


Figure 4-21. Real-time coefficient of friction data from two pairs of tests at two torque switch settings for Stem 3.

similar comparison of the other pairs of tests for the other stems and the other torque switch settings. In each case, the fold line method based on the wedging transient in the static test bounded the running friction coefficient in the corresponding dynamic test. This result lends confidence that the fold line method is applicable not only at high torque switch settings, but also at lower torque switch settings.

4.5 Conclusions

The research described here has provided the basis for two possible methods for determining a valve's design basis stem factor from the results of tests less severe than design basis tests. We present these methods here with the intent that industry may choose to develop them further.

There are several possible explanations as to why the stem/stem-nut friction reaches a plateau at a certain stem thread pressure. Similarly, there are several possible explanations for the relationship between the wedging friction in a static test and the running friction in a dynamic test. Tribology experts who are currently investigating the stem factor issue do not concur on an explanation. We have not endeavored to precisely identify the friction and lubrication phenomena that produce the effects that are evident in the data. We have endeavored instead to perform the initial development of methods that are supported by test data. So far, the data show that these methods work. Both methods are based on tests that can be performed in situ, and both methods use simple, straightforward analyses. Both methods provide appropriate results without imposing excessive conservatism.

Additional research is needed in several areas. More data are needed for a wider range of stems to more closely define the threshold value to be used in the threshold method. Additional running data for a wider range of stems would also increase confidence that the uniform flat response above the threshold is a universal characteristic.

The data used to develop the methods discussed here were taken with ideal lubricant conditions.

Stems were carefully cleaned before lubricant was applied, and the tests were conducted shortly afterwards. Aging, dirt degradation, and dry-out degradation need to be addressed.

The data used to develop both the threshold method and the fold line method were obtained from direct measurement of torque and thrust in the stem. For valve diagnostic tools that determine operator torque indirectly, using either spring pack force or spring pack displacement, additional validation would be necessary.

The range of variability in the coefficient of friction for a given stem, as obtained during the wedging transient of a static test, appears to depend on the thread pressure achieved during running and on the duration of the wedging transient. As presented in this discussion, the fold line method uses static tests with low running loads (simulated packing drag loads) and typical torque switch settings to define the variability in the friction coefficient. More study is needed with very low packing loads and very low torque switch settings to determine if the fold line method is still applicable at those conditions. If there are lower limits to the packing load and the torque switch setting, additional research may be able to fine-tune the fold line method to make it applicable below those limits.

Of the two lubricants we used in the tests, Moly 101 had the lower overall coefficient of friction, but on some stems EP-1 had the lower friction coefficient. The reason probably has to do with surface finish and lubricant performance relative to that surface finish. Future research might undertake to identify which surface finish characteristics lower the coefficient of friction and limit load-sensitive behavior, and to determine which lubricants are best for a stem with a given surface finish.

Further development might include a normal versus sliding correlation for the stem/stem-nut coefficient of friction. We have done a little preliminary work on such a correlation, and it shows promise. We will report more on possible refinements when more data are available.

5. ELECTRIC MOTOR TESTING

During this past reporting period we tested three of the five motors that are scheduled for testing in this test series. The purpose of the electric motor testing is to answer questions about degraded voltage, elevated ambient temperature, stall characteristics, inrush current, unbalanced voltage (ac only), and motor momentum. The MOVLS is an integrated test device where motor loads are achieved by loading the motor-operator. Motor torque is measured directly by an in-line torque cell mounted between the motor and the gearbox. Operator output torque is measured directly in the valve stem. Thus, along with the motor test results, we are able to look at gearbox efficiencies (discussed at the end of this section). Motor temperature was measured using a combination of thermocouples and an infrared sensor, allowing us to monitor the air gap between the rotor and stator. Table 5-1 lists the test matrix for the entire test series, indicating the motors and operators included in the tests. The table also indicates which parts of the test series have been completed.

The only data available at this time are quick look data. However, some interesting results are already apparent. One of these results involves the ac voltage square calculation, which is used extensively in the industry to predict motor output at degraded voltage conditions. According to the voltage square calculation, the theoretical relationship of torque to voltage at constant speed is

$$T_{act} = T_{rat} \left(\frac{V_{act}}{V_{rat}} \right)^2$$

where

T_{act} = actual torque

T_{rat} = rated torque

V_{act} = actual voltage

V_{rat} = rated voltage.

Output at degraded voltage is one of the first things we looked at after completing testing of

each of the three ac motors. In this initial evaluation, we also compared the actual motor torque/speed curve with the curve provided by the manufacturers, and we compared locked rotor starting current with stall current. All these evaluations are important in evaluating motor margins.

We used a three-phase, 60-amp-per-leg auto transformer to perform the degraded voltage tests. In the elevated temperature tests, we wrapped the motor with three separate sections of heat tape, placed on the front, center, and back of the motor. Each section had its own thermocouple and variable voltage control. The motor was also insulated, creating a custom oven on each motor. Environmentally qualified motors were heated to 300°F. Because of insulation concerns, the other motors were heated only to 250°F. All testing at normal temperature was conducted with an internal motor temperature between 70 and 80°F. RMS (root mean square) voltage was measured between phases 1 and 2 and between phases 2 and 3. Current was measured peak to peak on all three phases. Motor power and phase angle were also measured.

5.1 Motor Performance Curves

Figure 5-1 presents the manufacturer's torque/speed and torque/current curves for the 5 ft-lb ac motor. (All the manufacturers' motor torque/speed and torque/current curves were digitized from those published by Limitorque.) We extrapolated the current trace on this plot from the point of the asterisk through the published stall current value to approximate what we thought might occur. Figure 5-2 shows the actual torque curves derived from our test data. These curves are produced by running the motor at normal speed and then applying a constantly increasing load until the load causes the motor to stall. The major difference is the shape of the knee of the curve. The manufacturer's curve indicates that there is usable torque down to about 1000 rpm, while the curve derived from testing shows that the motor will stall at about 1200 rpm. After the motor speed drops below 1200 rpm, the increase in the current (from about 3.0 amp to almost 4.5 amp) does not

Table 5-1. Matrix for testing of operators and stems on the MOVLS.

Operator	Stem	Test	Lubricant	Comments	Complete	
SMB-0-25 ac	Stem 3	LSB ^a	EP-1		Y	
		LSB	Moly 101		Y	
	Stem 1	LSB	Moly 101		Y	
		LSB	EP-1		Y	
	Stem 8	LSB	Moly 101	SMART STEM	Y	
		LSB	EP-1		Y	
	Stem 2	LSB	Moly 101		Y	
		LSB	EP-1		Y	
		Low Volt	EP-1	Low voltage LSB test	Y	
		ac Dyn ^b	EP-1	Includes stall tests	Y	
	Stem 9	LSB		Ball screw stem/stem nut	Y	
	SMB-00-5 ac	Stem 7	LSB	Moly 101		Y
			LSB	EP-1		Y
Low Volt			EP-1	Low voltage LSB test	Y	
ac Dyn			EP-1	Includes stall tests	Y	
SMB-1-60 ac	Stem 4	LSB	Moly 101		Y	
		LSB	EP-1		Y	
	Stem 6	LSB	Moly 101		Y	
		LSB	EP-1		Y	
	Stem 5	LSB	Moly 101		Y	
		LSB	EP-1		Y	
		Low Volt	EP-1	Low voltage LSB test	Y	
		ac Dyn	EP-1	Includes stall tests	Y	
SMB-1-40 dc	Stem 5	Low Volt	EP-1	Low voltage LSB test		
		dc Dyn	EP-1	Includes stall tests		
SMB-0-25 ac	Stem 3	LSB ^a	EP-1		Y	
SB-1-40 ac (3600 rpm)	Stem 5	LSB	EP-1			
		Low Volt	EP-1	Low voltage LSB test		
		ac Motor	EP-1	Includes stall tests		
		ac Motor	EP-1	Elevated temp. 200°F		
		ac Motor	EP-1	Elevated temp. 300°F		

a. Refers to a load-sensitive behavior test sequence (described in Section 4 of this report), consisting of three pairs of tests (a static test and a dynamic test) at low, medium, and high torque switch settings.

b. Refers to dynamometer tests.

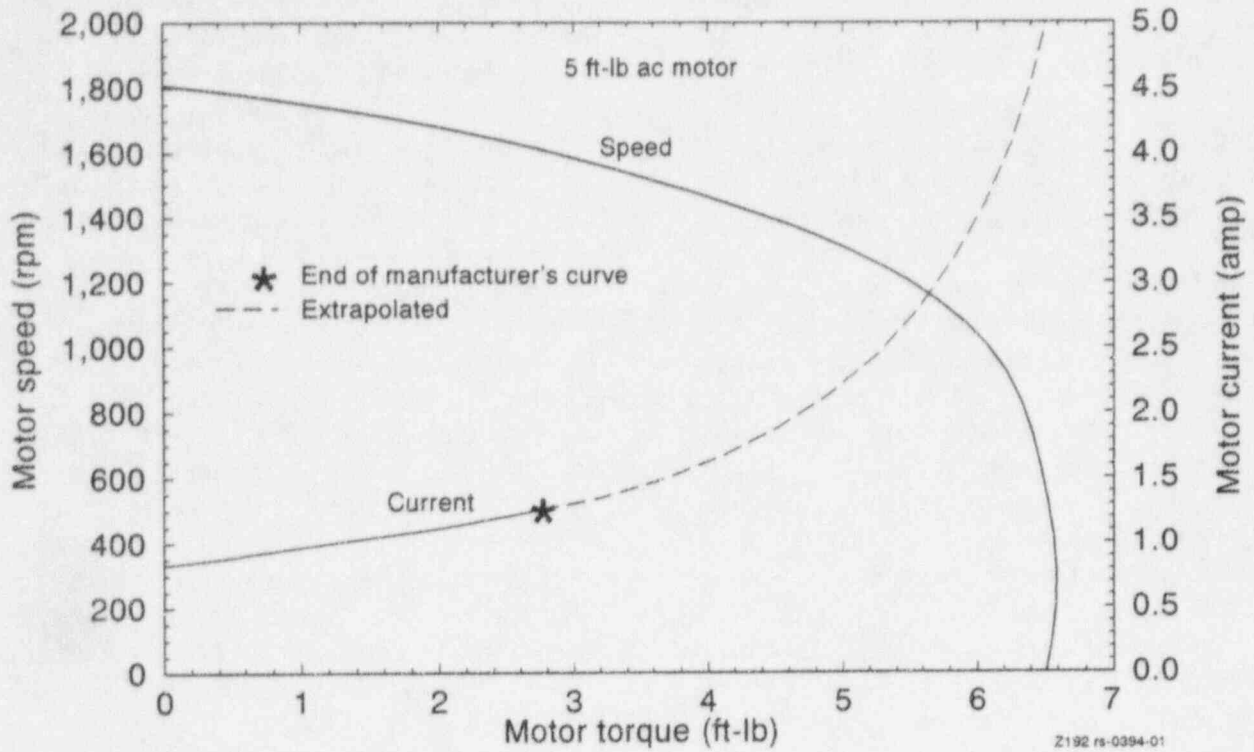


Figure 5-1. Manufacturer's motor performance curves for the 5 ft-lb 460-volt ac motor.

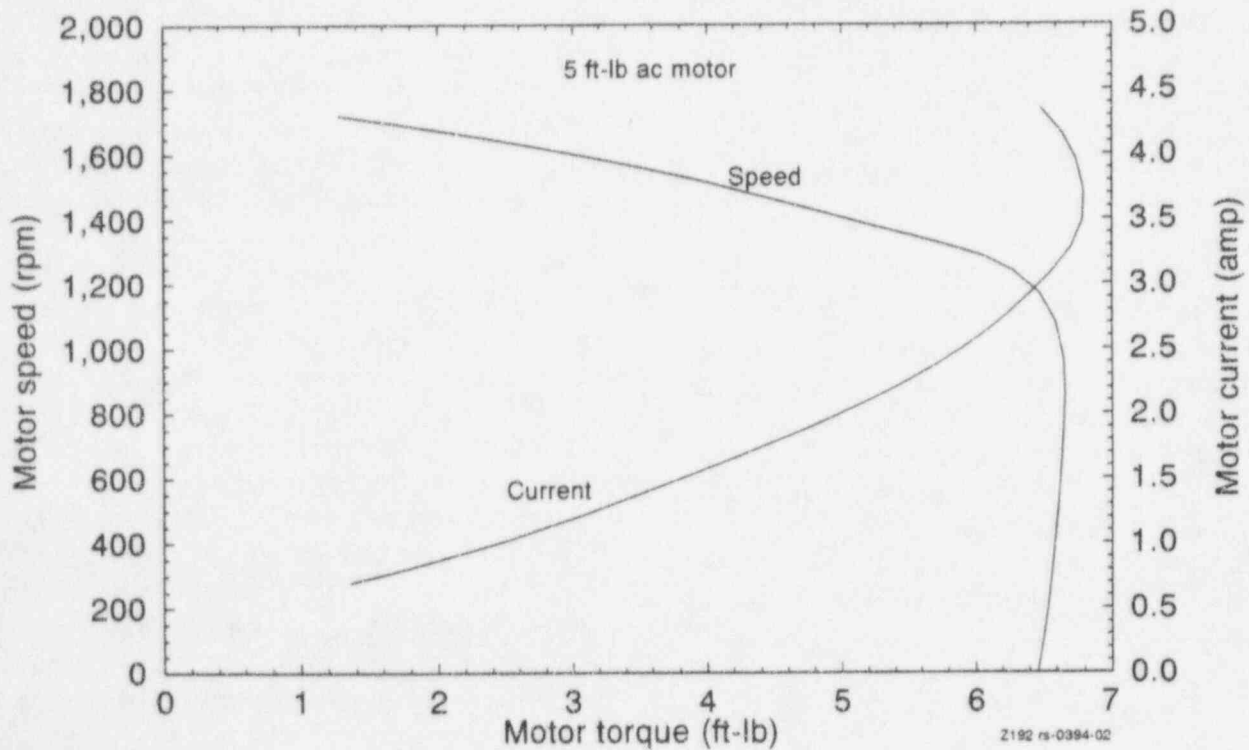


Figure 5-2. Actual motor performance curves for the 5 ft-lb 460-volt ac motor.

produce any additional torque. However, note that this particular motor is rated at 5.0 ft-lb and it produces nearly 6.5 ft-lb of torque.

Figure 5-3 presents the manufacturer's torque curves for the 25 ft-lb ac motor. The asterisk on the current trace marks the end of the manufacturer's curve, and the two Xs are test points from earlier field testing. The remainder of the curve is extrapolated through the published locked rotor current. Figure 5-4 presents the actual torque curves for the motor. As with the 5 ft-lb motor, the knee of the speed curve derived from testing is much sharper than shown on the manufacturer's curve. There is no increase in torque after the motor speed drops below about 1200 rpm. Both curves show the motor to be capable of delivering 30 ft-lb of torque.

Figure 5-5 presents the manufacturer's torque curves for the 60 ft-lb ac motor. Again, we extrapolated the current from the asterisk through the published locked rotor stall current. Figure 5-6 presents the actual curves derived from test data. As with the other two motors, the knee of the actual speed curve is much sharper than the manufacturer's curve; no additional torque is gained after the motor speed drops below about 1000 rpm. This motor's output torque is close to its 60 ft-lb rating, and the manufacturer's curve slightly overestimates the actual performance at stall.

This comparison of published data versus test data yielded two findings: (a) in general, the test data show that the load threshold at which the motor will drop to a stall occurs at a higher speed than is indicated by the published data, and (b) there is some variation between the published rated torque and the measured torque at stall. All three motors exceeded their rated output torque. This result indicates that for these motors, using the rated output torque in the margins calculations would be appropriate.

5.2 Degraded Voltage

Figure 5-7 shows motor torque/speed curves for the 5 ft-lb motor at degraded voltages down to

60% of the nominal 460 vac. The results of using the voltage square calculation to predict a single value of the running torque (near the knee of the curve) and the stall torque at degraded voltage are also shown. These predicted values are calculated from the actual output at 100% voltage, not the rated output. As shown in Figure 5-7, the voltage square calculation overestimates the actual stall torque at degraded voltage by 0.2 to 0.4 ft-lb. With the 25 ft-lb motor, the voltage square calculation overestimates the torque by 1 to 1.5 ft-lb (Figure 5-8), and with the 60 ft-lb motor the calculation overestimates by 2 to 6 ft-lb (Figure 5-9). These preliminary results challenge the appropriateness of using the voltage square method to predict motor torque at degraded voltage. Using the motor's actual output torque as the basis for the calculation does not always provide appropriate results. Using the rated motor torque instead of the actual motor torque for the 5 and 25 ft-lb motors would provide appropriate degraded voltage predictions, but only because the actual torque at 100% voltage is higher than the rated torque. For the 60 ft-lb motor, using the rated torque in the calculation does not provide appropriate results.

The small delta symbols at the bottom of the plot in Figure 5-7 are the locked rotor starting torques. These individual data points are produced by energizing the motor with the output shaft locked so it cannot turn. Note that the speed curves at motor stall end at the locked rotor starting torques, indicating that the motor torque at stall and the starting motor torque with a locked rotor for these motors are the same. Figure 5-10 shows the torque/current traces for the 5 ft-lb motor (these torque/current traces correspond with the torque/speed traces shown in Figure 5-7). Again, the locked rotor starting currents match very well with the stall current traces. Figure 5-11 shows the same data for the 25 ft-lb motor, and Figure 5-12 shows the data for the 60 ft-lb motor. (Figure 5-12 does not show locked rotor starting data; locked rotor starting tests were not performed in the initial tests of the 60 ft-lb motor.)

Considering that locked rotor starting torques and locked rotor starting currents match very well

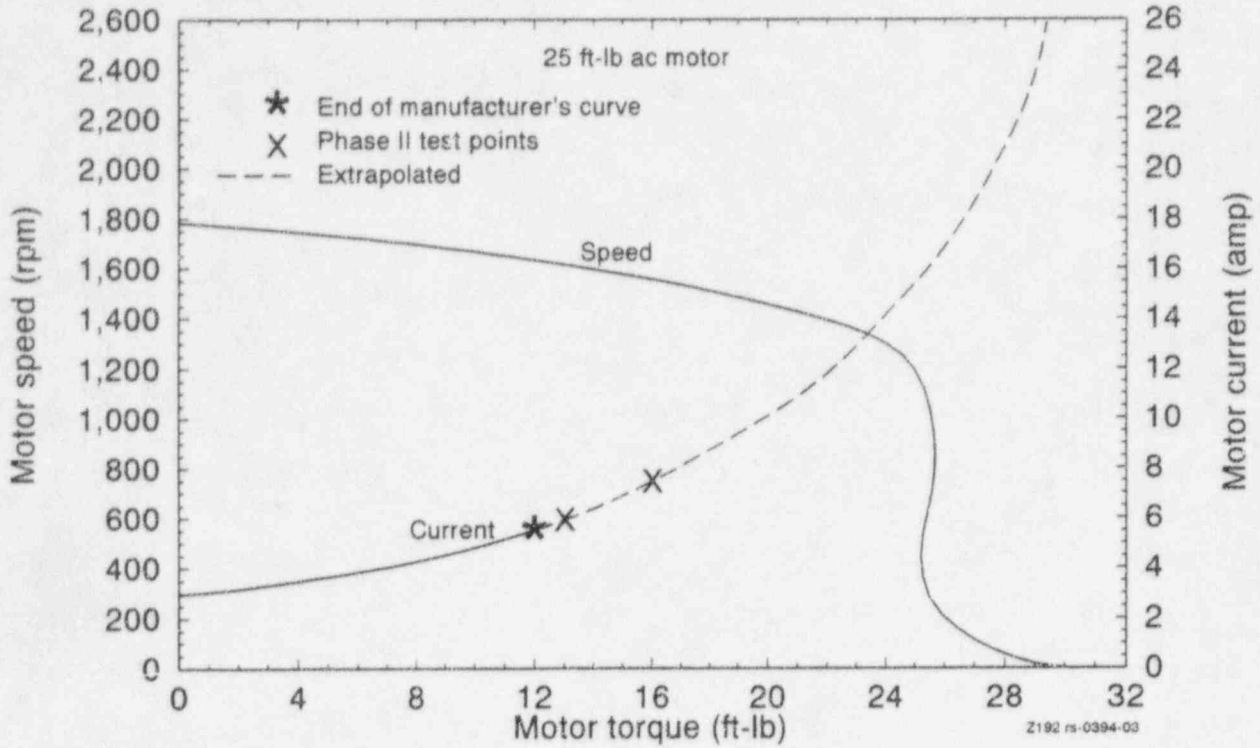


Figure 5-3. Manufacturer's motor performance curves for the 25 ft-lb 460-volt ac motor.

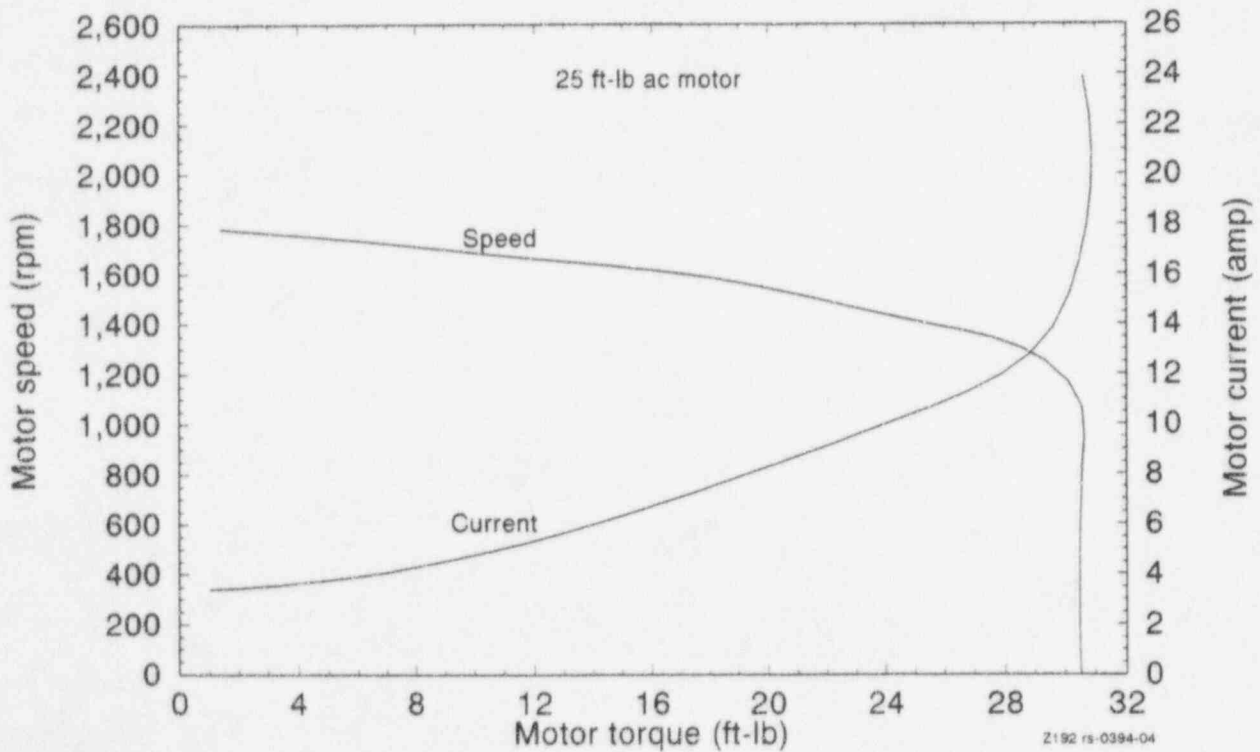
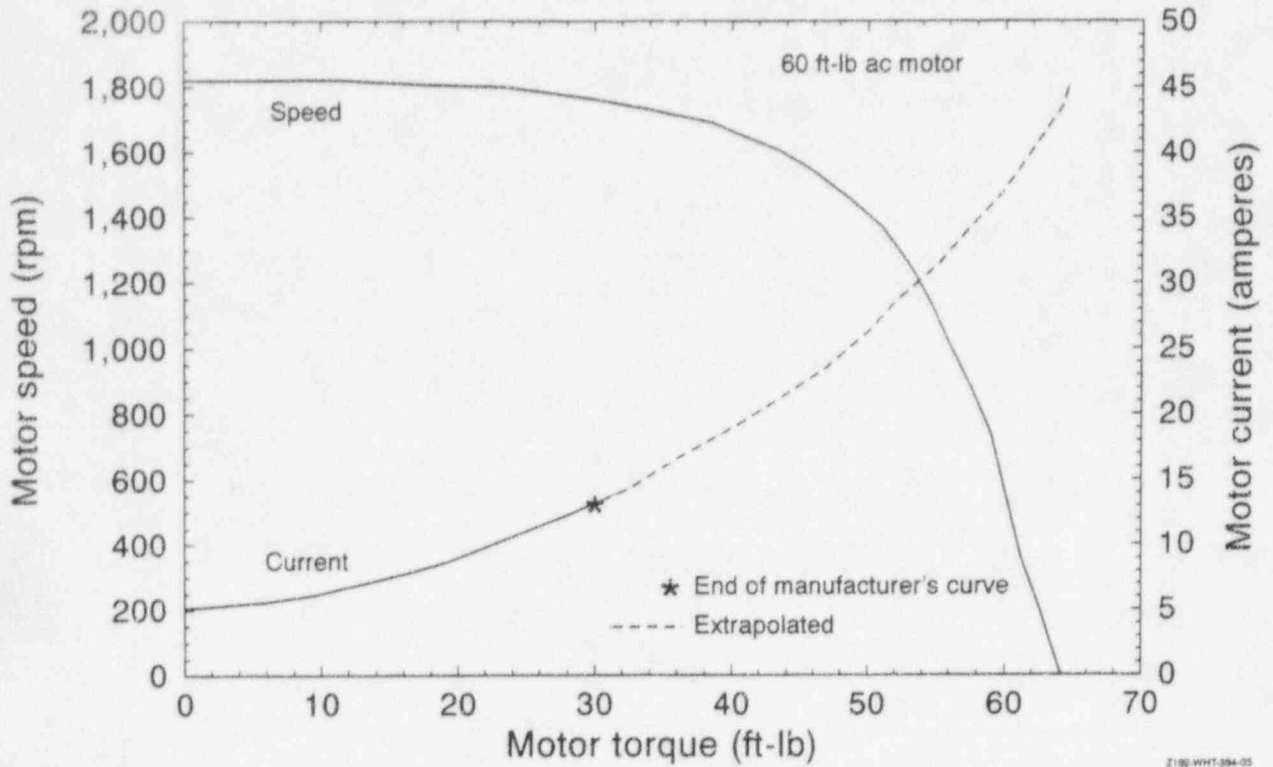
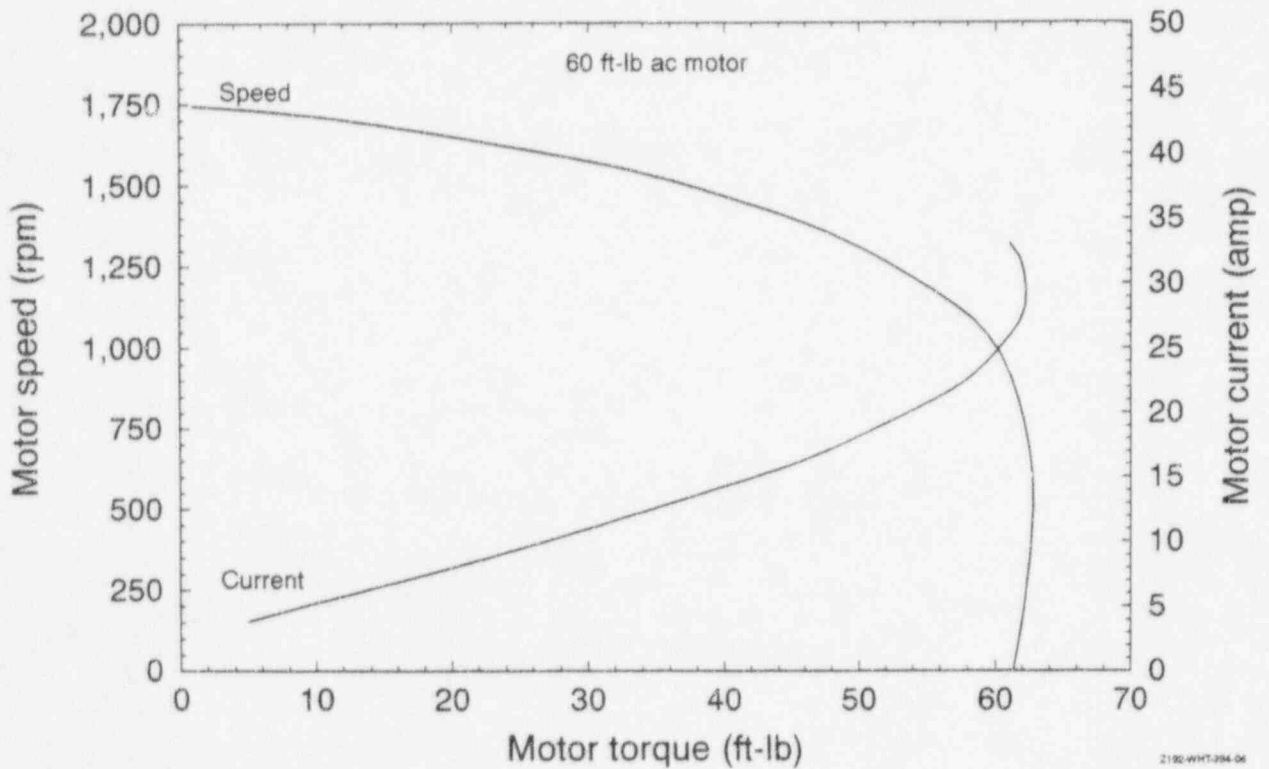


Figure 5-4. Actual motor performance curves for the 25 ft-lb 460-volt ac motor.



2192-WHT-394-05

Figure 5-5. Manufacturer's motor performance curves for the 60 ft-lb 460-volt ac motor.



2192-WHT-394-06

Figure 5-6. Actual motor performance curves for the 60 ft-lb 460-volt ac motor.

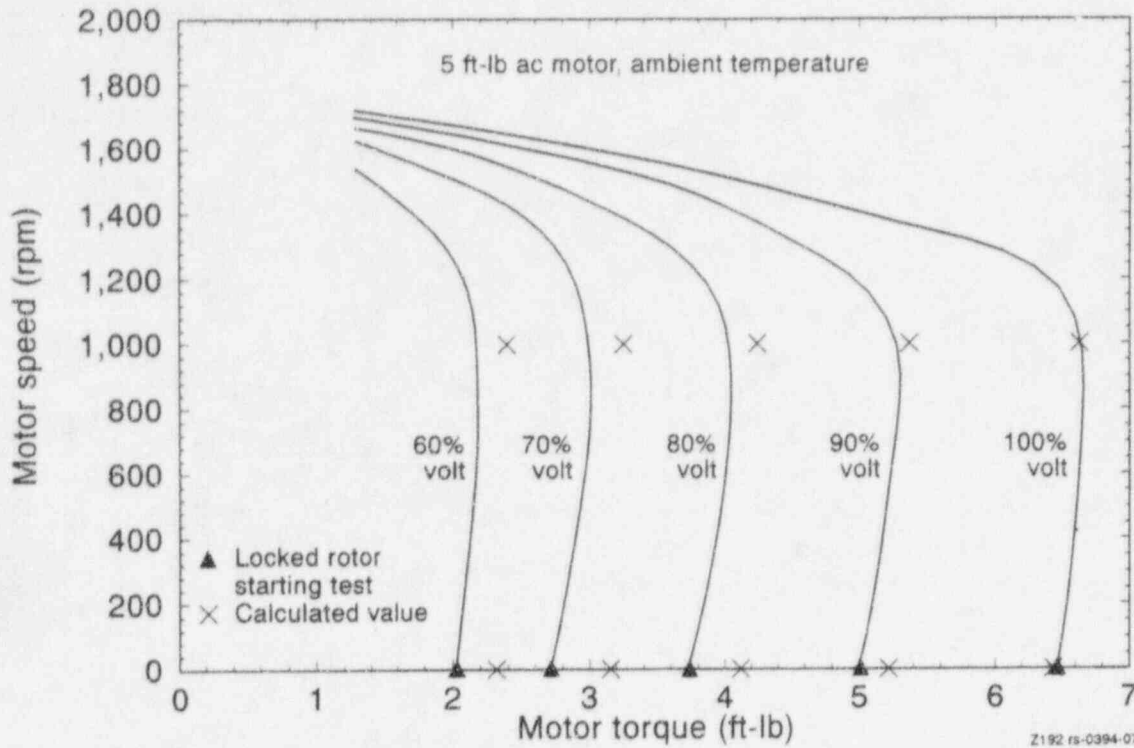


Figure 5-7. Actual motor speed versus torque, derived from testing of the 5 ft-lb motor at degraded voltage.

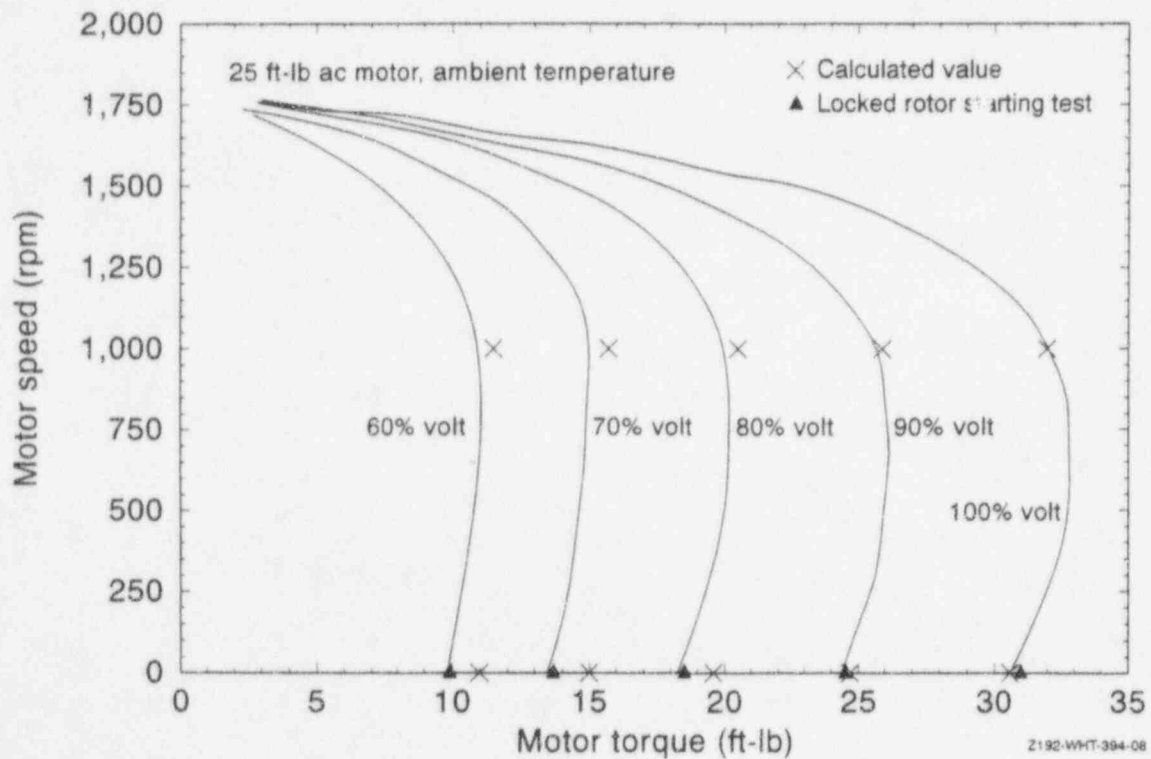


Figure 5-8. Actual motor speed versus torque, derived from testing of the 25 ft-lb motor at degraded voltage.

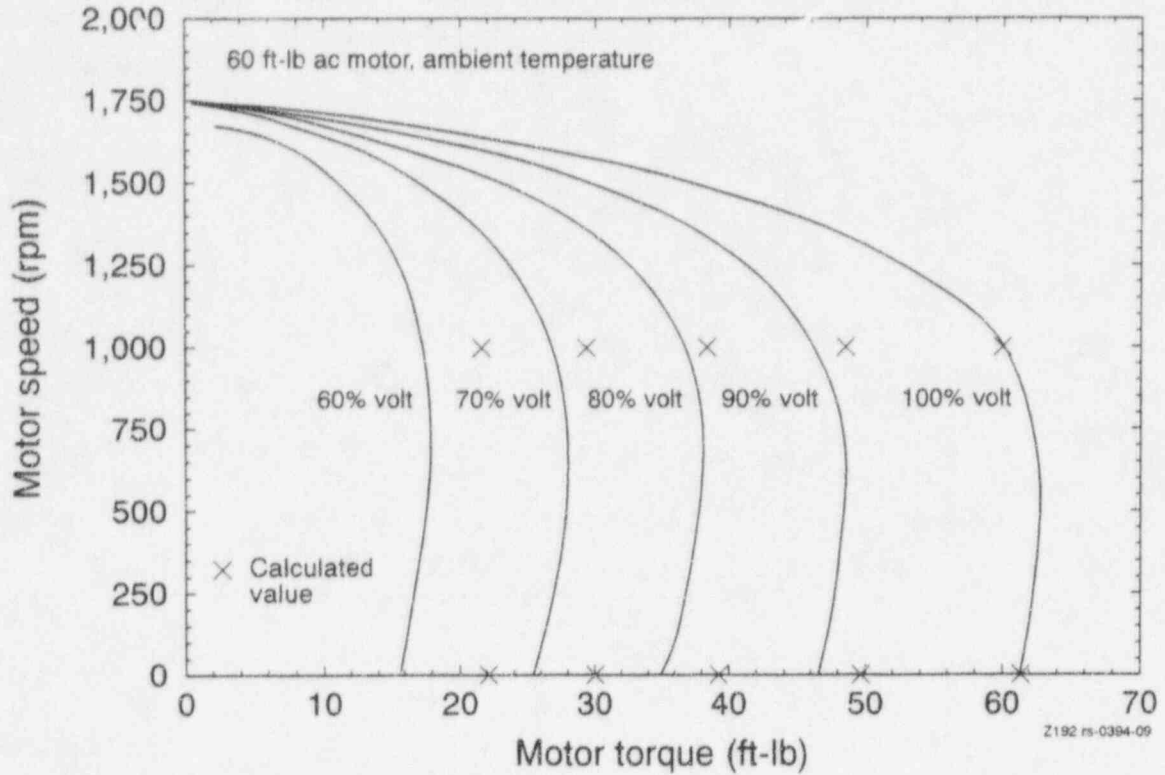


Figure 5-9. Actual motor speed versus torque, derived from testing of the 60 ft-lb motor at degraded voltage.

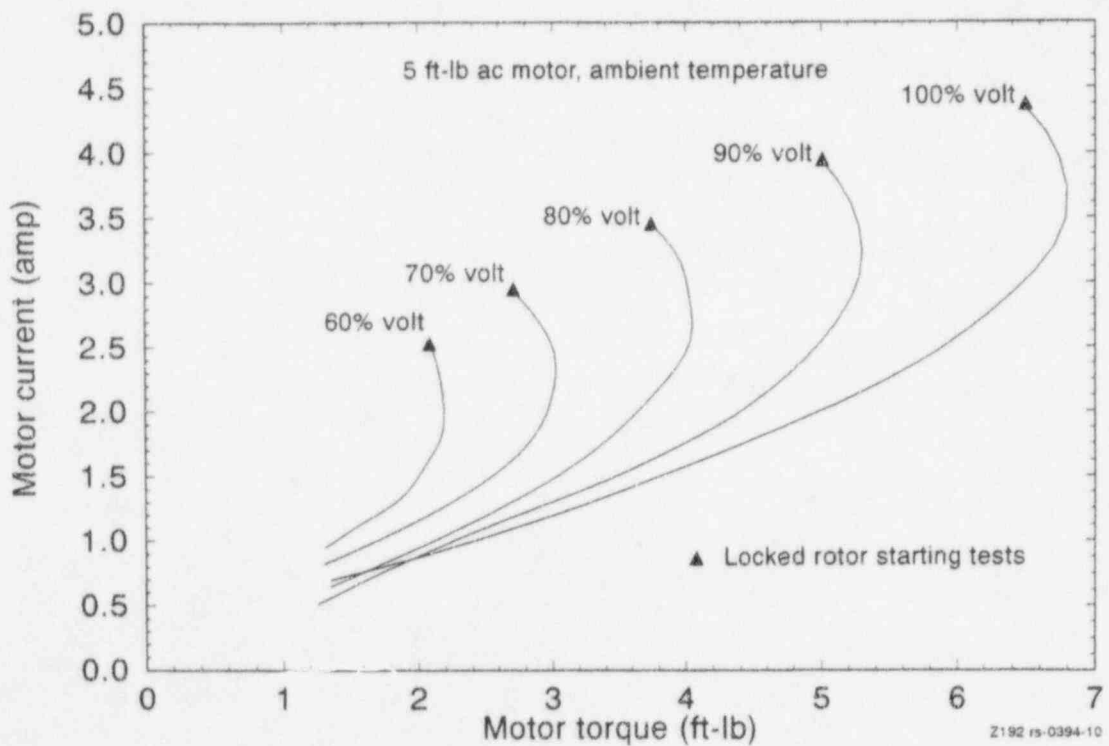


Figure 5-10. Actual motor current versus torque, derived from testing of the 5 ft-lb motor at degraded voltage.

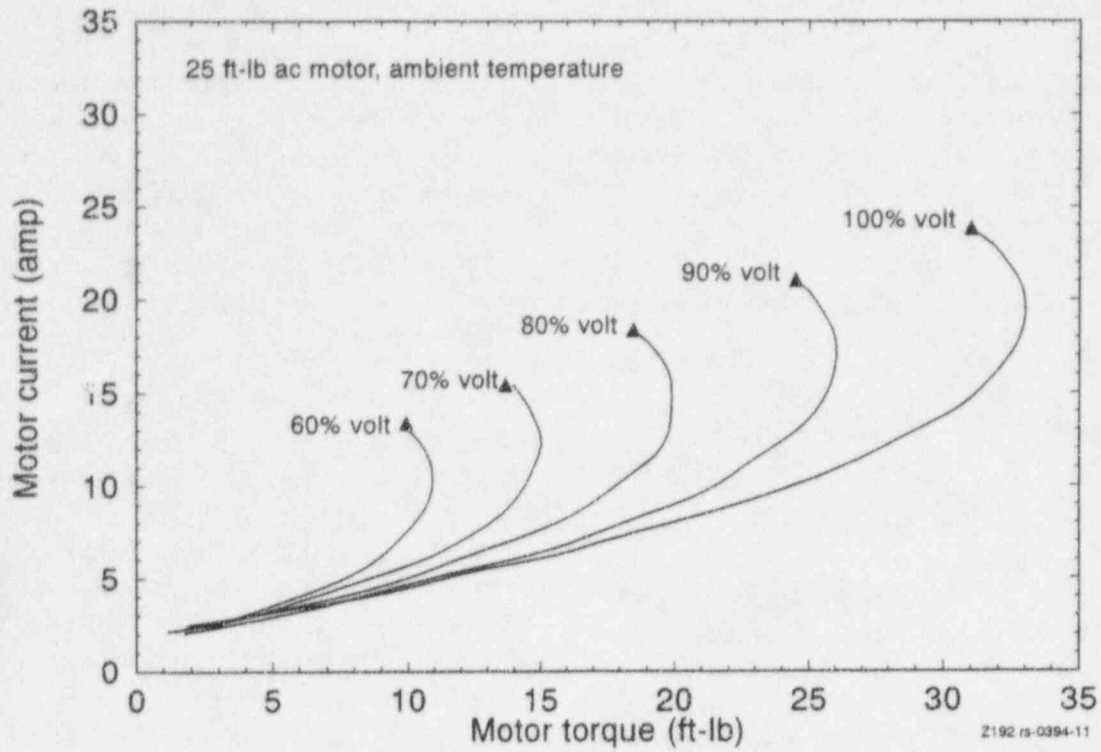


Figure 5-11. Actual motor current versus torque, derived from testing of the 25 ft-lb motor at degraded voltage.

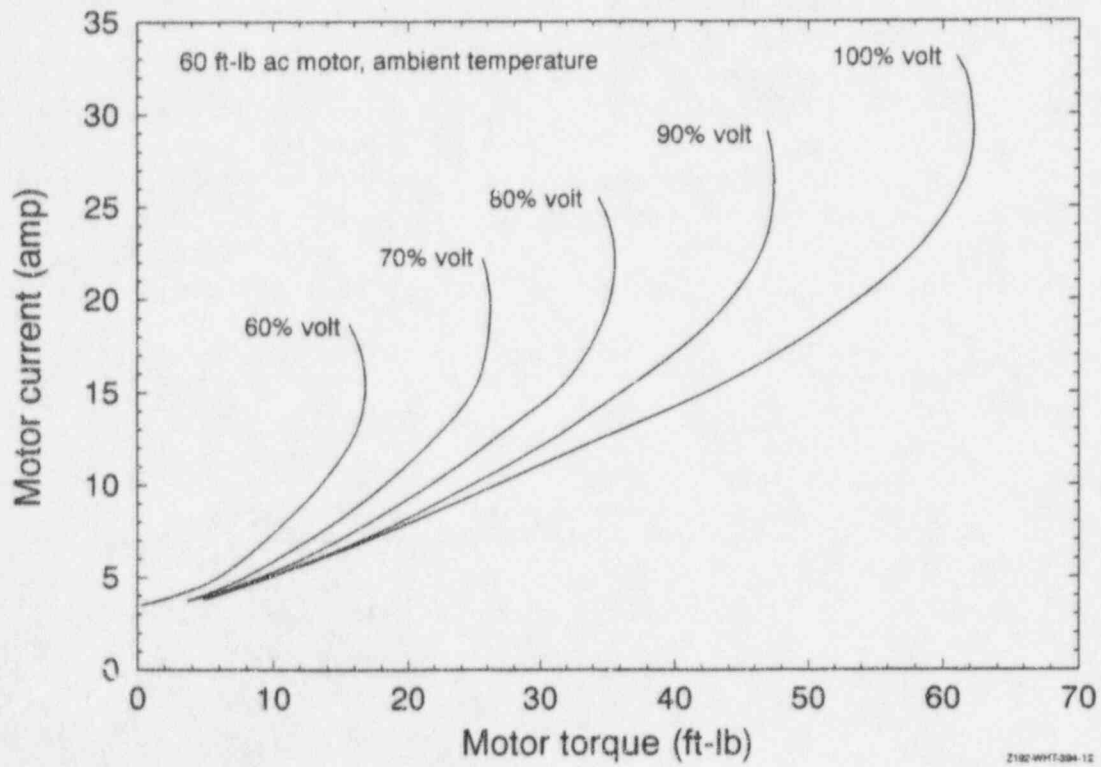


Figure 5-12. Actual motor current versus torque, derived from testing of the 60 ft-lb motor at degraded voltage.

with the stall torques and stall currents, the locked rotor starting test might be a good test for determining where a specific motor is with respect to its rating. Since the output of these motors can vary from their ratings, such a determination could be important if there is not much margin in a specific application. A very simple fixture can be used in a locked rotor starting test; these tests are much easier to conduct than the dynamometer tests that would typically be used to determine stall torque and stall current.

5.3 Elevated Temperatures

Figures 5-13 and 5-14 show the performance of the 5 ft-lb ac motor during the elevated temperature testing at 100 and 80% voltage, respectively. The 5 ft-lb motor is an environmentally qualified motor, so we heated it to 300°F. The motor was tested at both voltage conditions at room temperature, at 100°F, and at increments of 50°F up to 300°F.

Figure 5-14 includes two marks on the torque axis that indicate the results of using the voltage square calculation to predict the performance of the motor at reduced voltage at 300°F and at 80°F. The prediction is more accurate for the 300°F case than for the 80°F case. Taken together, the reduction caused by both the reduced voltage (80%) conditions and the elevated temperature (300°F) conditions amounts to about half of the

motor's capability, compared with normal voltage and room temperature conditions.

Figures 5-15 and 5-16 are the elevated temperature plots for the 25 ft-lb ac motor. This motor is not qualified for service in a harsh environment, so it was heated only to 250°F. With this motor, the voltage squared calculation overestimates the torque at reduced voltage for both the low-temperature (80°F) case and the high-temperature (250°F) case.

Figures 5-17 and 5-18 are the elevated temperature plots for the 60 ft-lb motor. This motor is not qualified for service in a harsh environment, so it was heated only to 250°F. As with the 25 ft-lb motor, the voltage square calculation applied to this motor overestimates the actual torque at elevated temperature conditions (250°F) by about the same margin as at normal temperature conditions. Motor torque would be predicted at 33.5 ft-lb at 80% voltage and 250°F, and it is only 30 ft-lb. This approximately 10% discrepancy at both ambient and elevated temperature challenges the use of the voltage square calculation for this motor.

Figures 5-19 and 5-20 are the current/torque plots that correspond with the torque/speed plots shown in Figures 5-17 and 5-18. We used these data to evaluate the actual degraded performance of the motor for comparison with the data shown in Table 5-2. Table 5-2 is based on the 10 CFR Part 21 notification issued recently by Limitorque

Table 5-2. Limitorque Part 21 predictions for loss in performance with increased temperature.

Motor temperature	Current loss (%)				Torque loss (%)			
	5 ft-lb motor	25 ft-lb motor	60 ft-lb motor	40 ft-lb motor	5 ft-lb motor	25 ft-lb motor	60 ft-lb motor	40 ft-lb motor
77°F (25°C)	0	0	0	0	0	0	0	0
100°F (38°C)	1.80	1.90	1.71	1.34	1.81	1.91	1.72	0.97
150°F (66°C)	5.70	6.04	5.44	4.24	5.73	6.07	5.47	3.09
200°F (93°C)	9.61	10.18	9.17	7.14	9.65	10.23	9.21	5.20
250°F (121°C)	13.52	14.32	12.90	10.05	13.58	14.39	12.96	7.32
300°F (149°C)	17.42	18.46	16.63	12.95	17.50	18.54	16.71	9.43
356°F (180°C)	21.8	23.1	20.8	16.2	21.9	23.2	20.9	11.8

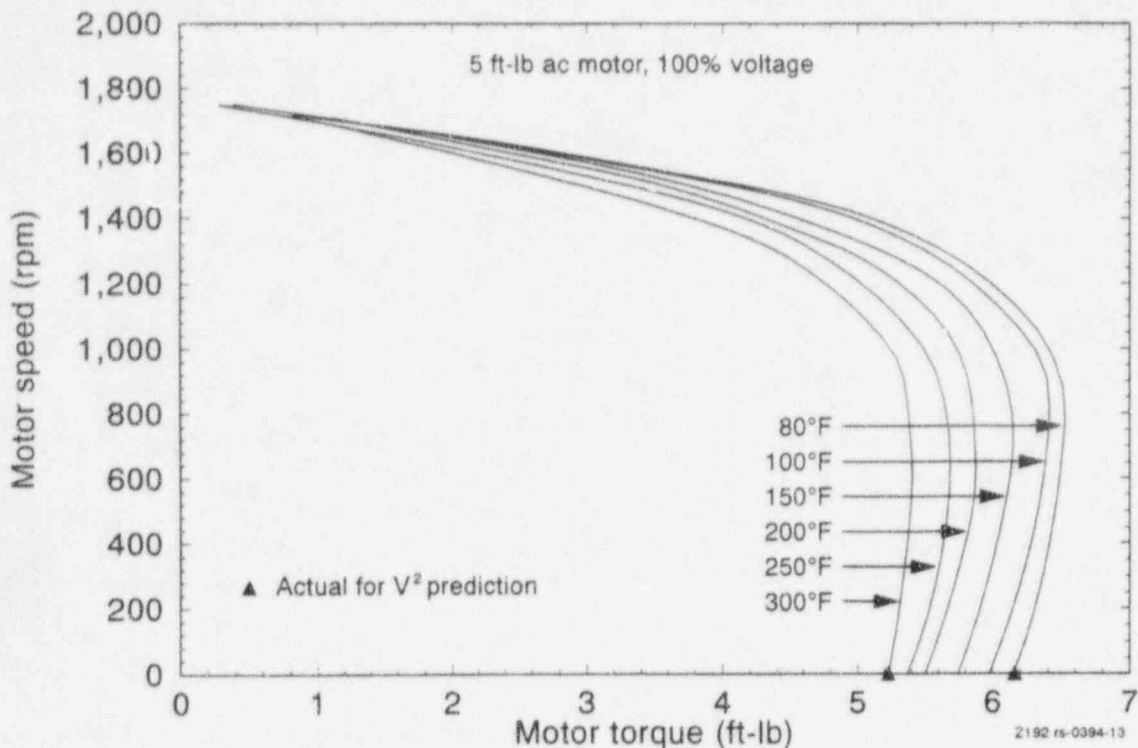


Figure 5-13. Actual motor speed versus torque, derived from elevated temperature testing of the 5 ft-lb motor at 100% voltage.

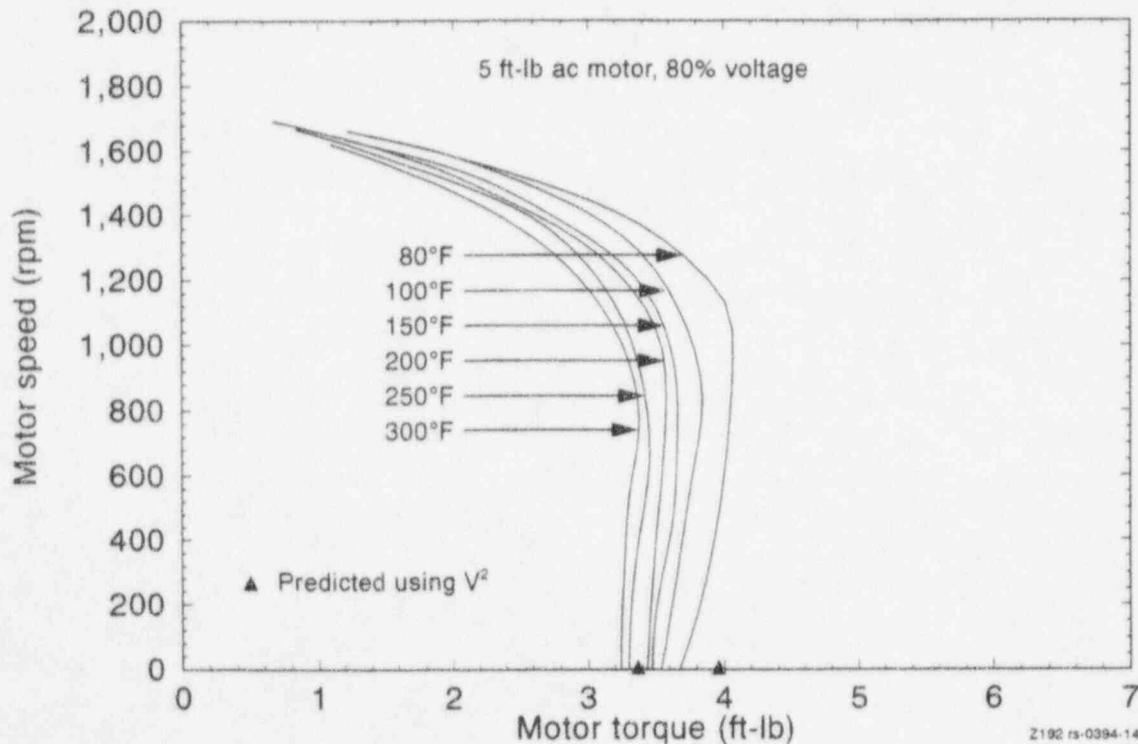


Figure 5-14. Actual motor speed versus torque, derived from elevated temperature testing of the 5 ft-lb motor at 80% voltage.

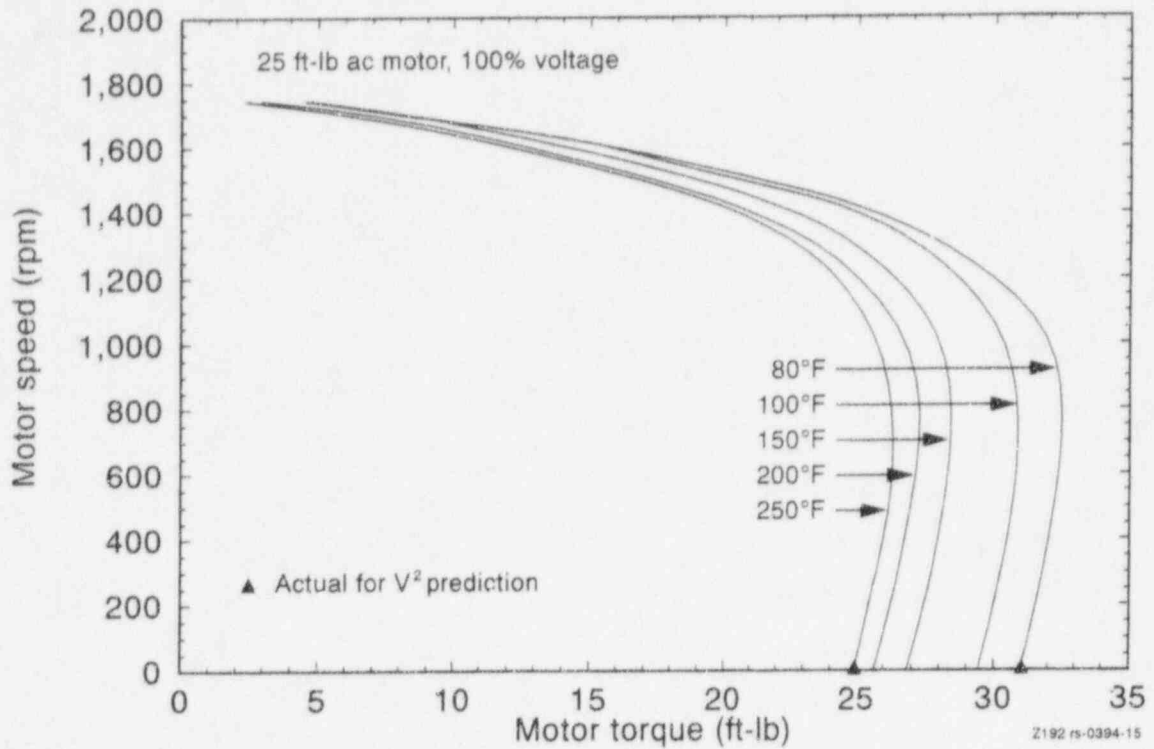


Figure 5-15. Actual motor speed versus torque, derived from elevated temperature testing of the 25 ft-lb motor at 100% voltage.

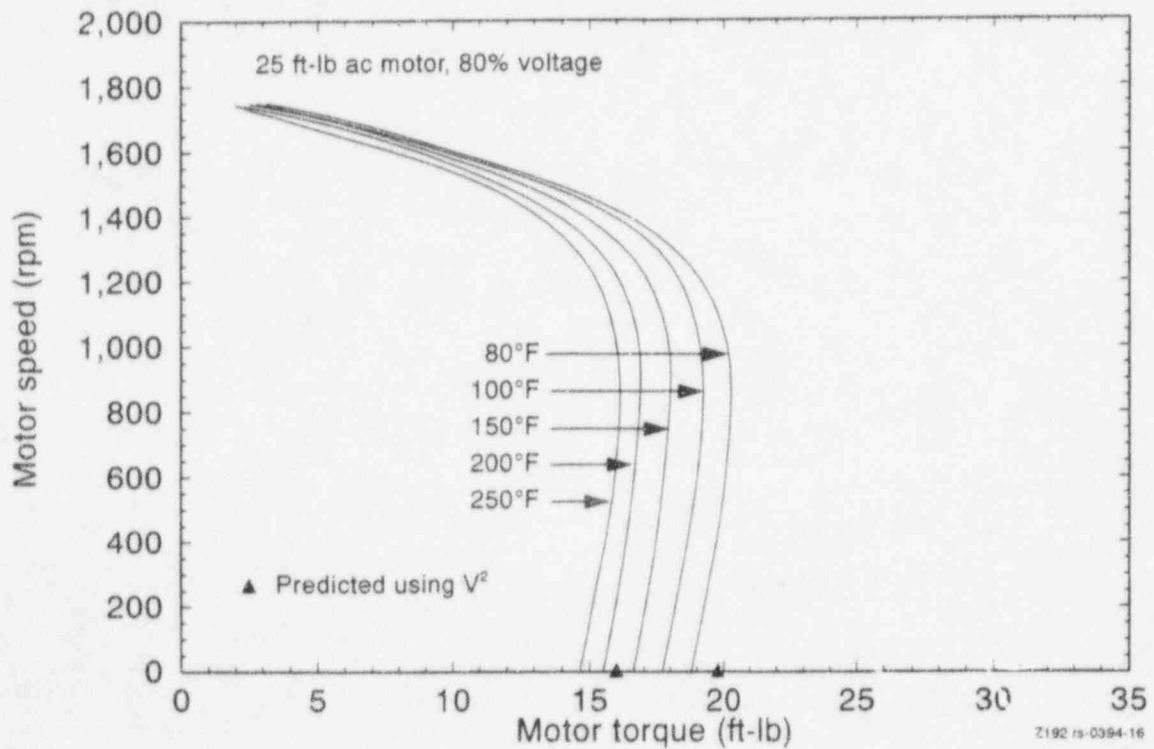


Figure 5-16. Actual motor speed versus torque, derived from elevated temperature testing of the 25 ft-lb motor at 80% voltage.

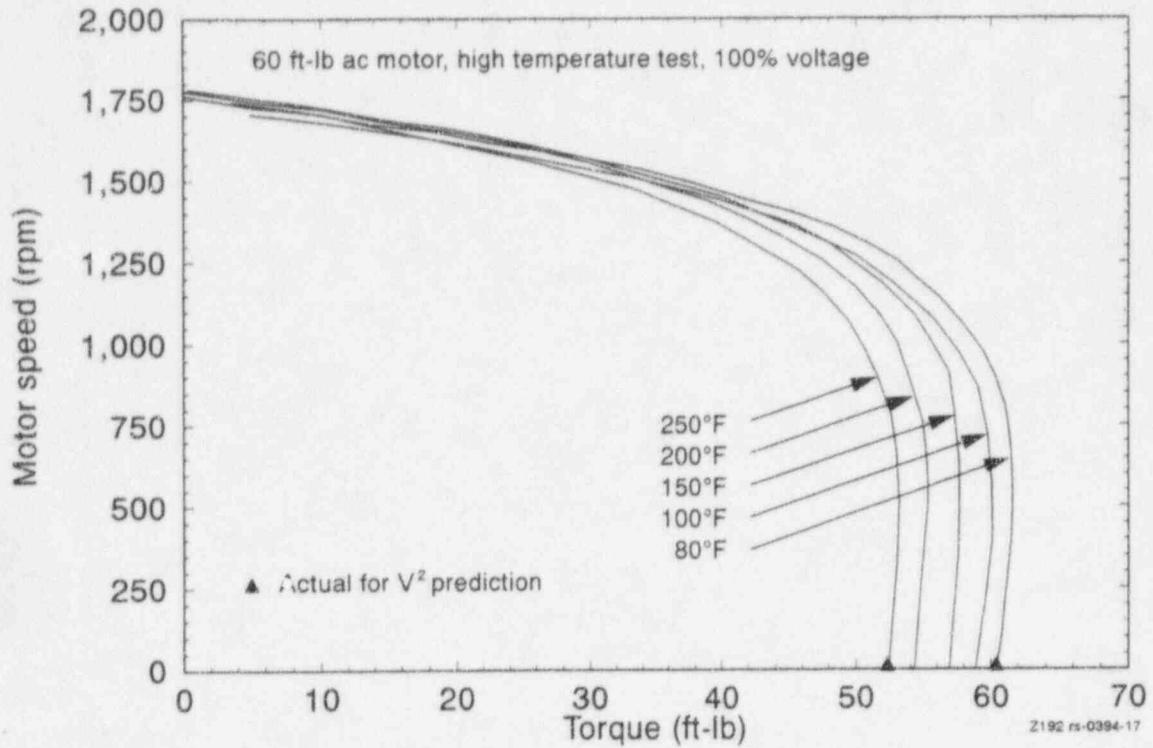


Figure 5-17. Actual motor speed versus torque, derived from elevated temperature testing of the 60 ft-lb motor at 100% voltage.

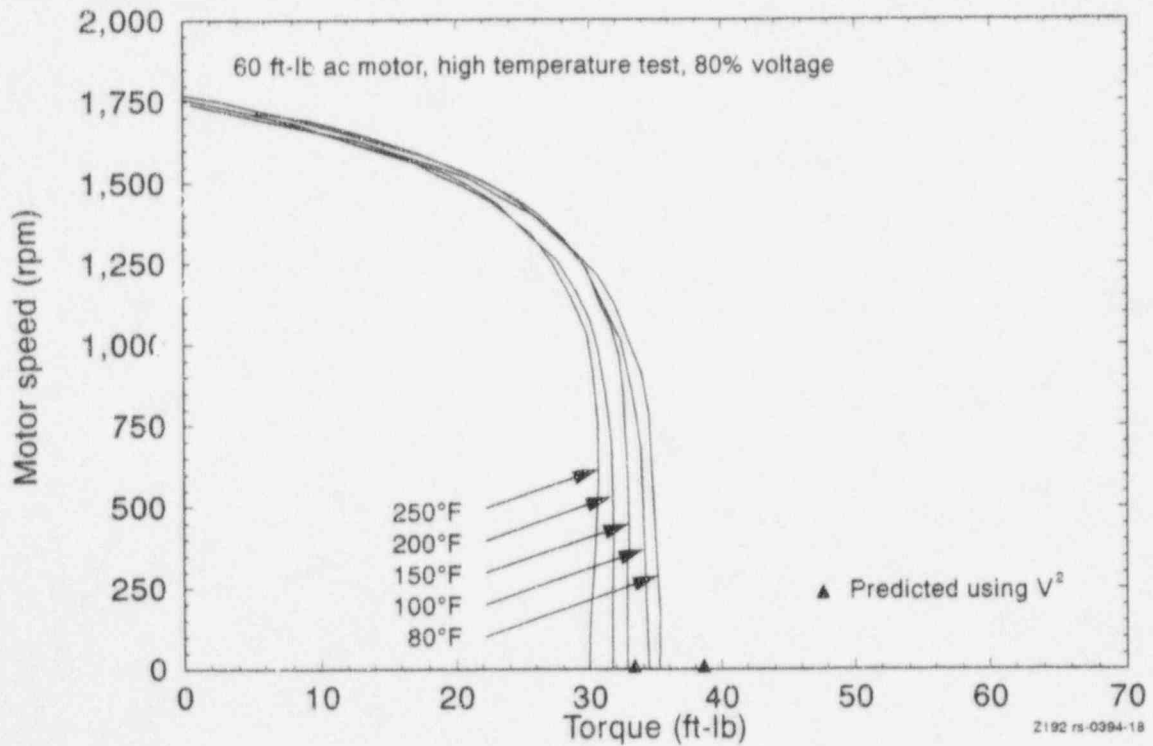


Figure 5-18. Actual motor speed versus torque, derived from elevated temperature testing of the 60 ft-lb motor at 80% voltage.

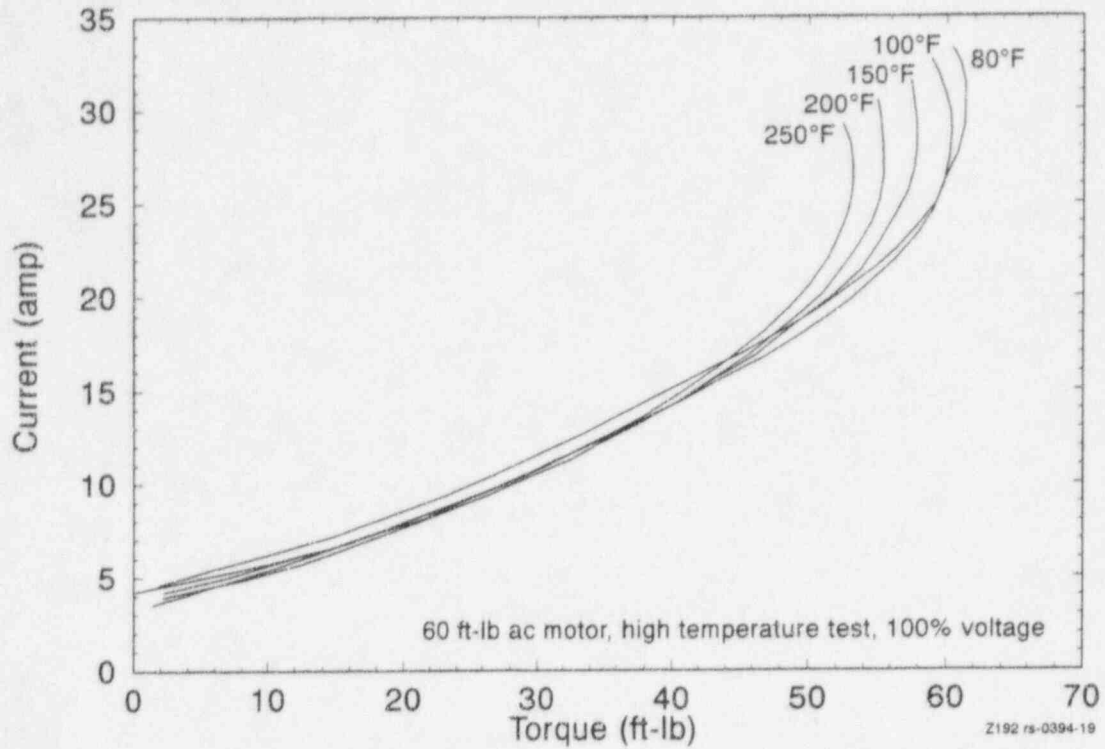


Figure 5-19. Actual motor current versus torque, derived from elevated temperature testing of the 60 ft-lb motor at 100% voltage.

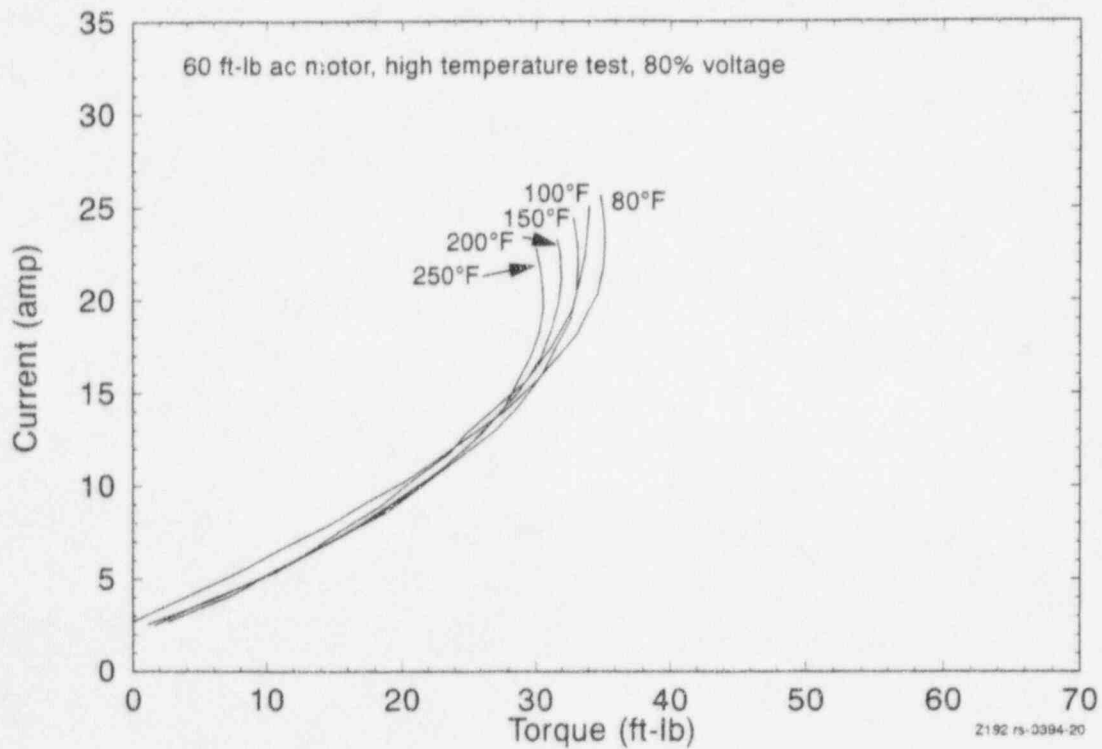


Figure 5-20. Actual motor current versus torque, derived from elevated temperature testing of the 60 ft-lb motor at 80% voltage.

on the subject of degraded motor performance at elevated ambient temperatures. The table shows the data for the four motors we are testing. Figures 5-21 and 5-22 show the actual motor torque and motor current measured at elevated temperature for both 100% voltage and 80% voltage for the 60 ft-lb motor. The figures also show the Limitorque Part 21 predictions for that motor. The test results follow the Part 21 predictions very well.

The results reported here are preliminary; additional motor tests will be performed, and all the data will be analyzed according to uniform criteria. However, these preliminary results raise some questions about applying the voltage square calculation for the motors we tested. On the positive side, the elevated temperature results appear to support the Part 21 information issued by Limitorque on motor performance at elevated temperature.

5.4 Motor-Operator Gearbox Performance

Motor-operator gearbox performance is measured in terms of percent efficiency. Operator gearbox efficiency is a calculation of the input (electric motor) torque versus the output (stem-nut) torque. There are three efficiency factors: pullout efficiency, stall efficiency, and running efficiency. The pullout efficiency is the lowest of the three; it applies when the motor is lugging at very low speed under a load or starting up against a load without the aid of the unloaded run before the hammer blow. The stall efficiency is higher than the others because it includes consideration of motor inertia during a sudden stall; it is typically used in evaluations of possible overload problems. The running efficiency is the efficiency of the gearbox at normal motor speed.

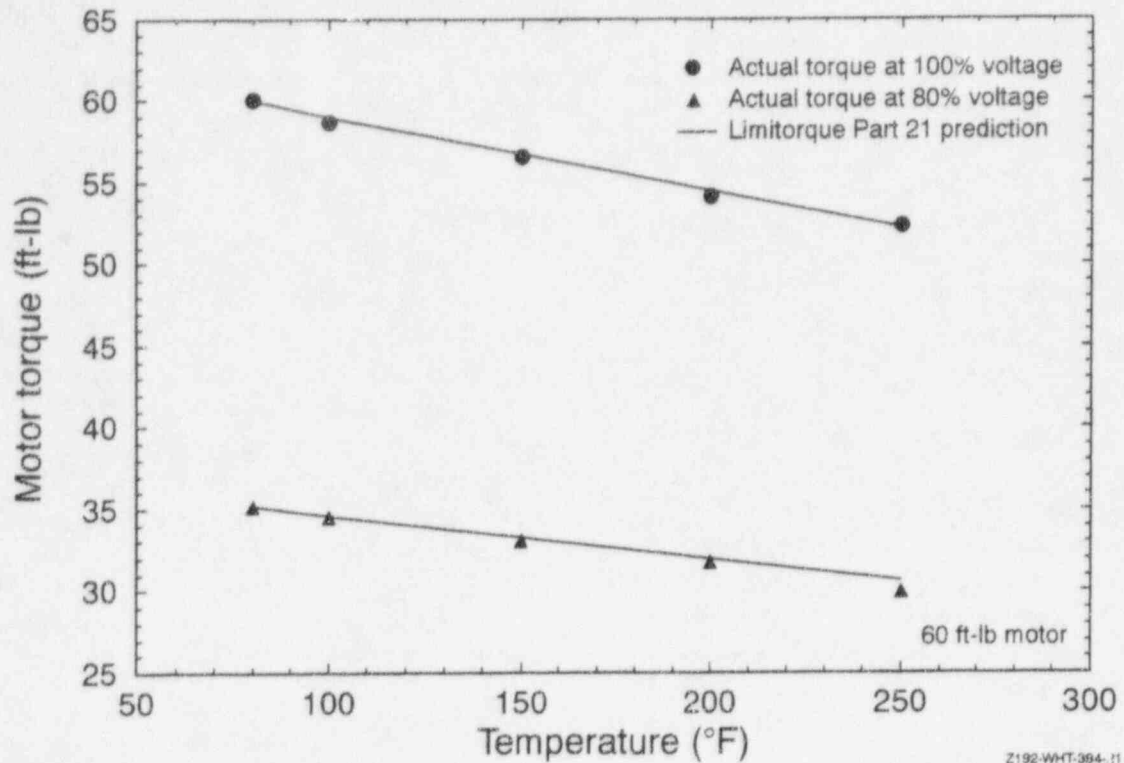
Most of the operators tested in this test series are rated to be about 50% efficient. That is, it takes about half the input motor power to overcome losses (primarily friction) in the gear box. We have not yet completed all the efficiency evaluations, but we do have preliminary information on

running efficiencies from full motor speed to near stall for the three operator/motor combinations tested to date. We calculated operator efficiency from measurements of the actual electric motor (input) torque and the actual stem-nut (output) torque.

The published running efficiencies of the operators vary between 50 and 55%, as shown previously in Table 4-1. These efficiency values were obtained from Limitorque engineering data published in November 1989. The SMB-0 operator has more than one published efficiency. This is because we installed more than one helical gear set in the operator to get the stem speed we needed with the various stems we used with that operator. We also changed gear sets in the SMB-1 operator, but these changes did not influence the operator's published efficiency.

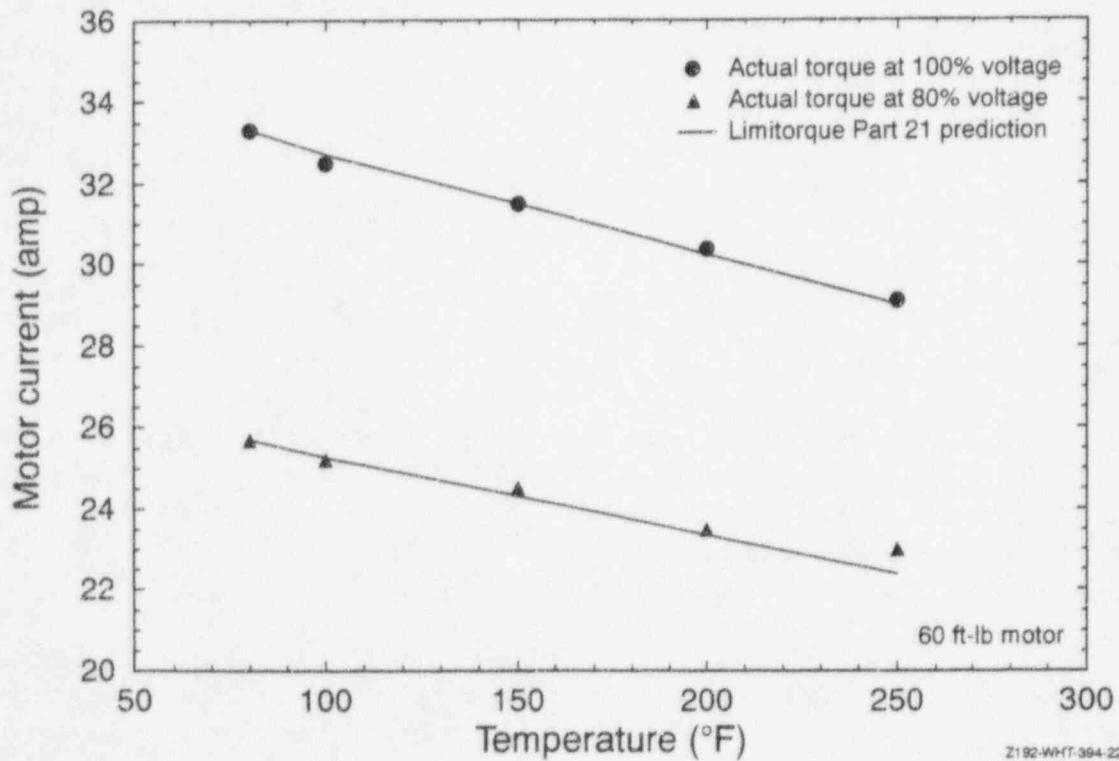
Figure 5-23 is an example of the actual efficiency for the SMB-00-5 operator that we tested. The plot was derived from a test in which the load on the operator was gradually increased until the motor stalled. Thus, the trace represents efficiency values that correspond with the definitions of running efficiency and pullout efficiency, as well as the transition from one to the other. Motor torque (input torque) is plotted against operator torque (output torque), and the gearbox efficiency is represented by the slope of the trace. The plot includes diagonal lines representing Limitorque's published running and pullout efficiencies, along with the application factor reduction calculation for each. The tested SMB-00-5 should have had a running efficiency of 0.5; the actual running efficiency from our tests averaged near 0.36, the value of the published pullout efficiency times the application factor (0.4 times 0.9). Figure 5-24 presents the same data for the SMB-0-25 operator, and Figure 5-25 presents the data for the SMB-1-60 operator.

From this preliminary look at the data, we infer that actual efficiencies can differ from those published by the operator manufacturer. It also appears that using the running efficiency for available torque calculations may not be appropriate; the pullout efficiency was more



Z192-WHT-394-11

Figure 5-21. Motor torque versus elevated temperature at 100% voltage and 80% voltage, compared with the Limitorque Part 21 prediction.



Z192-WHT-394-22

Figure 5-22. Motor current versus elevated temperature at 100% voltage and 80% voltage, compared with the Limitorque Part 21 prediction.

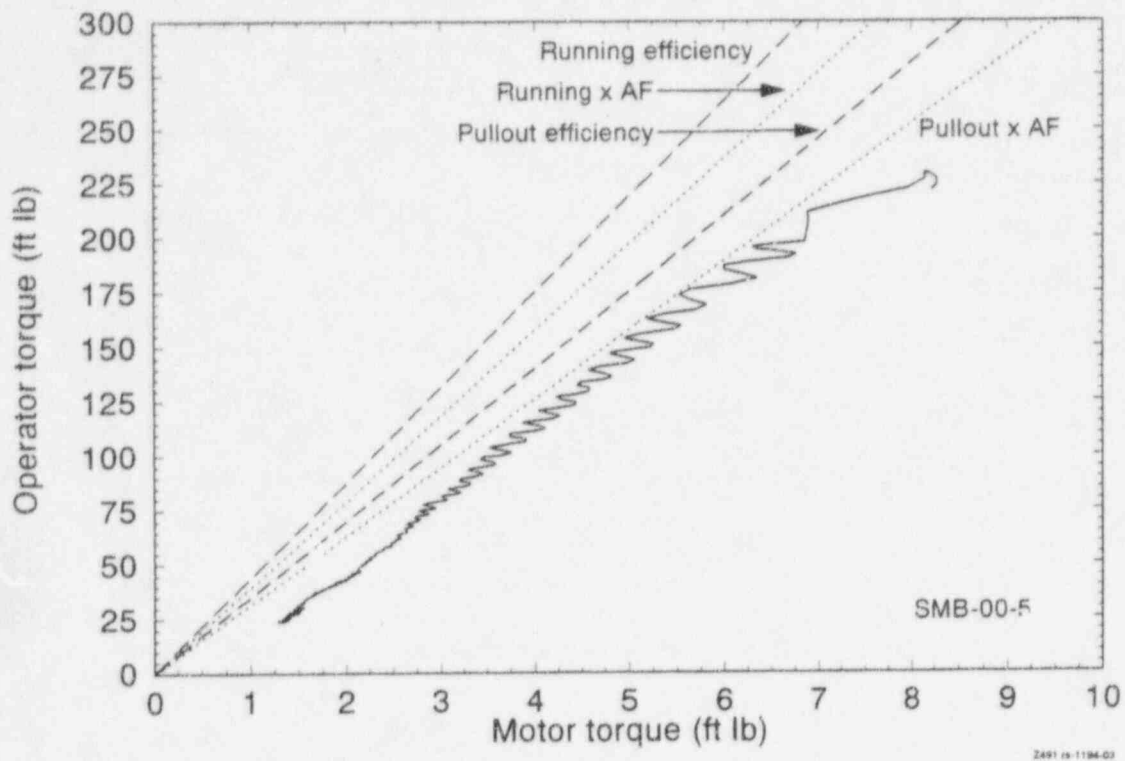


Figure 5-23. Actual gearbox efficiency measured during stall testing of the SMB-00 motor operator.

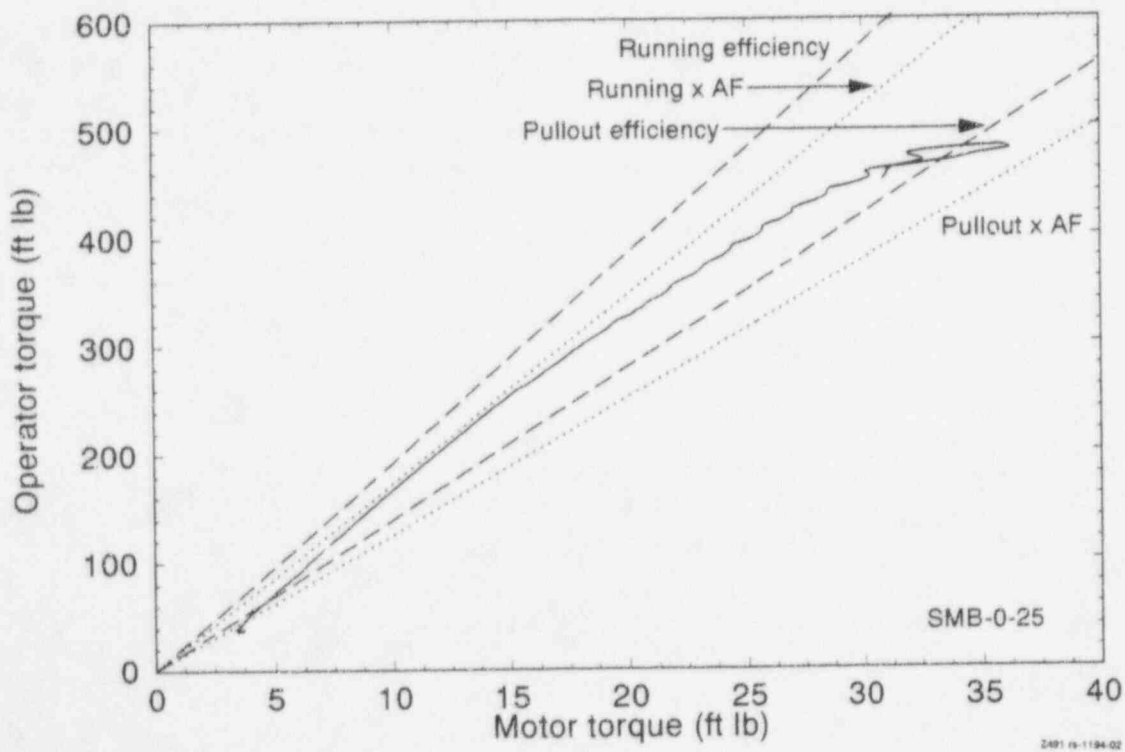


Figure 5-24. Actual gearbox efficiency measured during stall testing of the SMB-0 motor operator.

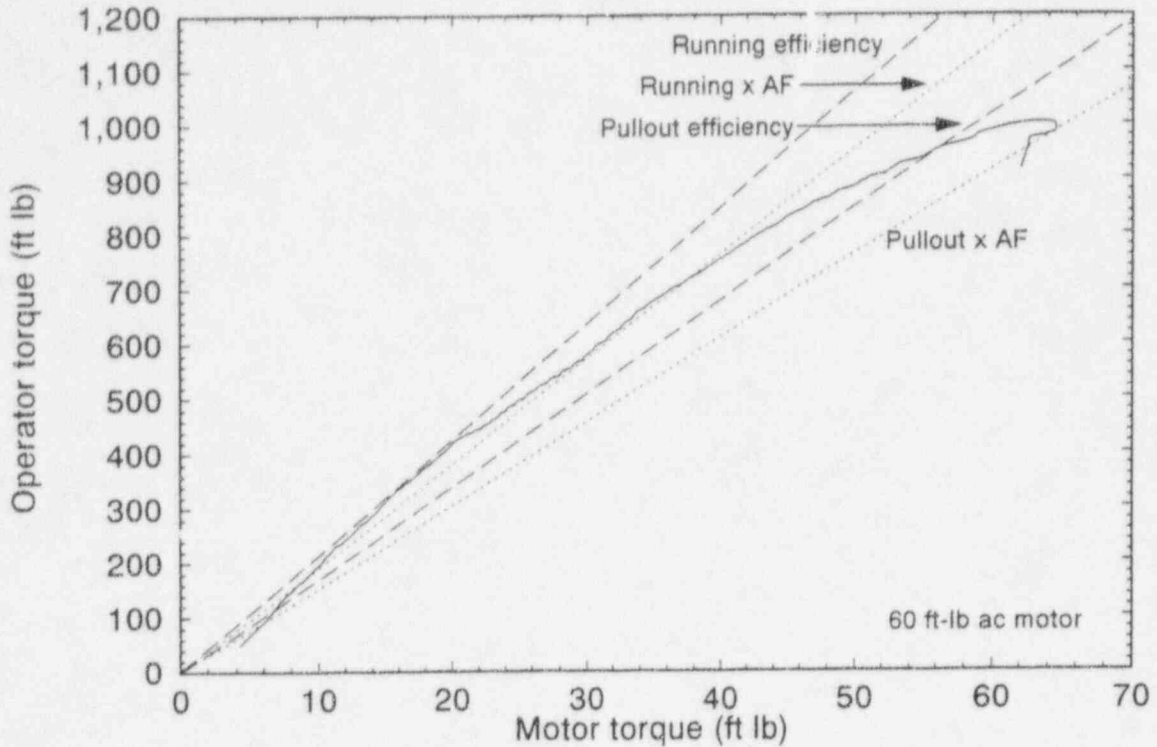


Figure 5-25. Actual gearbox efficiency measured during stall testing of the SMB-1 motor operator.

appropriate for the operators that we tested. This was particularly true when the motor-operator was operated at higher loads. Because of the potential for widespread use of running efficiency in evaluations of valve requirements in the closing direction, we thought it was important to present even this preliminary information as early as possible.

5.5 Conclusions

Conclusions would be premature in this section addressing electric motor and operator performance. The quick-look review points to the need to examine these issues very closely before coming to any conclusions, because of potential implications to MOV margins calculations.

6. GENERAL CONCLUSIONS

This report includes guidelines for an approach for determining operating margins for MOVs. The methodology and the findings presented in this report describe how many of the variables in the margins evaluation can be quantified.

Our full-scale MOV test programs together with in situ testing performed by utility and industry test programs, have identified three types of gate valve responses to flow and differential pressure loadings: (1) those that perform with a classic, typical response that is consistent with prediction models, (2) those that perform with an atypical response, but without damage, and (3) those that perform with an atypical response and experience damage.

For valves that perform in the classic or typical manner, this report presents some new approaches for determining design basis stem loads. Embedded in these approaches is the hypothesis that as the differential pressure load on the disc increases, the disc friction factor decreases. This hypothesis is supported by almost all the test results we have seen. The decrease is more pronounced in the opening direction than in the closing direction. For both opening and closing, the new approaches establish a maximum friction factor allowed at low loads. Test experience indicates that friction factors less than 0.65 will not degrade to higher values when the valve is retested at higher loads. It appears that friction factors greater than 0.65 in low-load tests are

probably not the result of sliding friction alone. By establishing this value as a maximum low-pressure-load friction factor, we should be able to eliminate any real outliers and provide a sound basis for bounding design basis loads.

For valves with atypical responses, the mechanical interference (due to tipping of the disc) and the changes in pressure distribution around the disc generally constitute most of the atypical portion of the loading. Except for valve closure against blowdown loads, valve damage appears to play a less significant role. All tipped discs experience some mechanical interference, increasing the value we commonly call a friction factor or a disc factor. Short of a design basis test, atypical loads cannot be predicted with certainty, but reasonable results can be obtained by running a best effort flow test and then extrapolating the results.

Our research results indicate that the stem factor can be determined from tests conducted at conditions less severe than design basis conditions. Our results also indicate that stem factors thus determined are usually lower than default values. Using this approach can improve the margins calculations and may prevent unnecessary replacement or overstressing of components.

Our analysis of electric motor performance and operator efficiency is preliminary. More complete results will be reported in the next update.

7. REFERENCES

- Grant, W. and R. Keating, (1990), *Application Guide for Motor-Operated Valves in Nuclear Power Plants*, NP-6660-D, prepared by MPR Associates, Inc. for the Nuclear Maintenance Application Center.
- NUREG/CR-5720 (1992), R. Steele, Jr., J. C. Watkins, K. G. DeWall, M. J. Russell, *Motor-Operated Valve Research Update*, EGG-2643.
- NUREG/CR-5558 (1990), R. Steele, Jr., K. G. DeWall, and J. C. Watkins, *Generic Issue 87 Flexible Wedge Gate Valve Test Program, Phase II Results and Analysis*, EGG-2600.
- NUREG/CR-5406 (1989), K. G. DeWall and R. Steele, Jr., *BWR Reactor Water Cleanup System Flexible Wedge Gate Isolation Valve Qualification and High Energy Flow Interruption Test*, EGG-2569.
- Watkins, J. C., R. Steele, Jr., and K. G. DeWall (1994), *Isolation Valve Assessment (IVA) Software*, Version 4.1, INEL-94/0094 .

Appendix A
Nebula EP-1 Lubricant Analyses for the
Eight Tested Stems

Appendix A

Nebula EP-1 Lubricant Analyses for the Eight Tested Stems

The eight stems that we tested with Moly 101 lubricant were also tested with EP-1 lubricant. Figure A-1 shows the running data for those tests, with the friction coefficient plotted against stem thread pressure. These data points represent the friction coefficients derived from measurements taken during the running portion of the closing stroke, immediately before wedging. Fig-

ures A-2 through A-5 show the analysis for the *fold line method* for Stems 1 through 8, with the stems lubricated with EP-1. The analysis process is explained in Section 4 of this report. These figures are presented here for those who may want to compare the response of the stems using EP-1 lubricant with the Moly 101 response, also presented in Section 4 of this report.

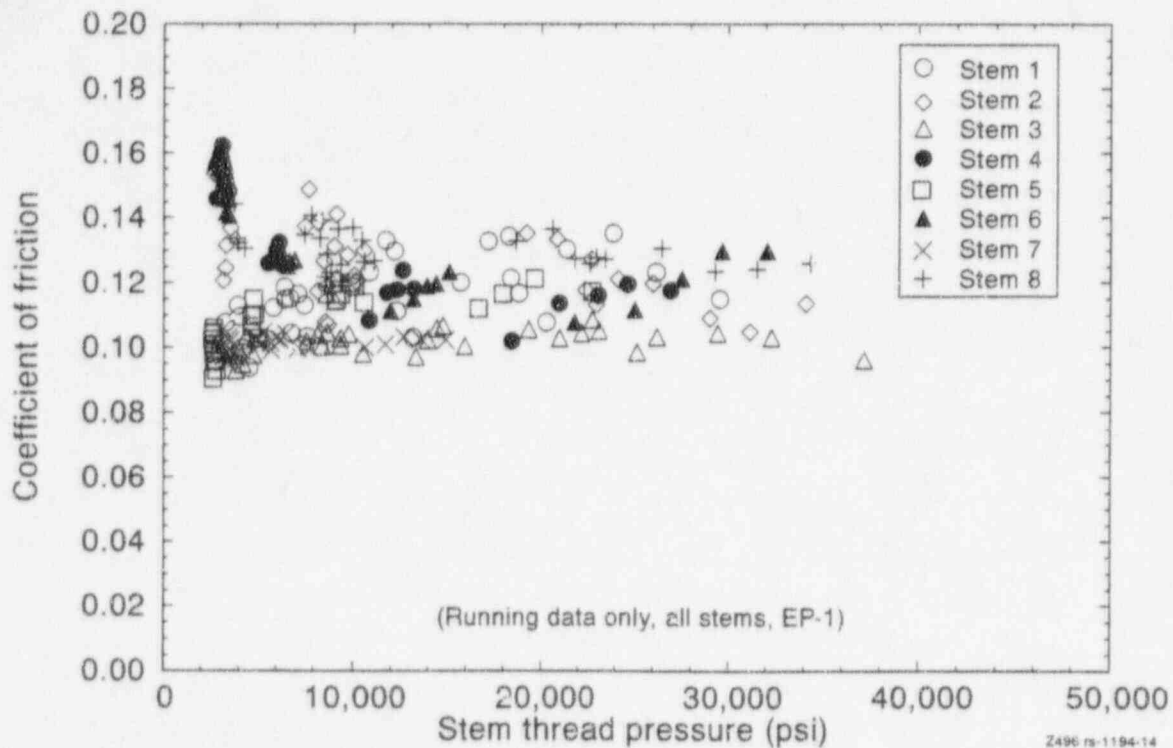


Figure A-1. Coefficient of friction versus stem thread pressure for tests with Nebula EP-1 lubricant. With the data thus normalized, it is evident that the friction coefficient for each of the eight stems is stable above a load of about 10,000 psi.

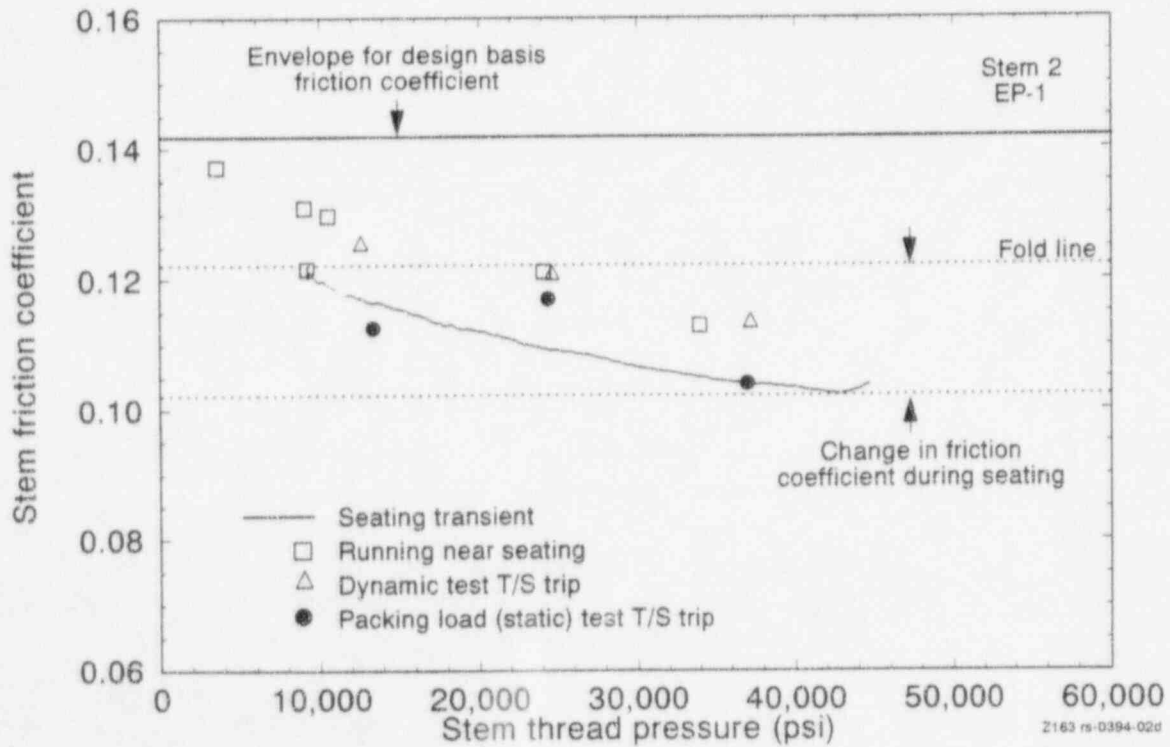
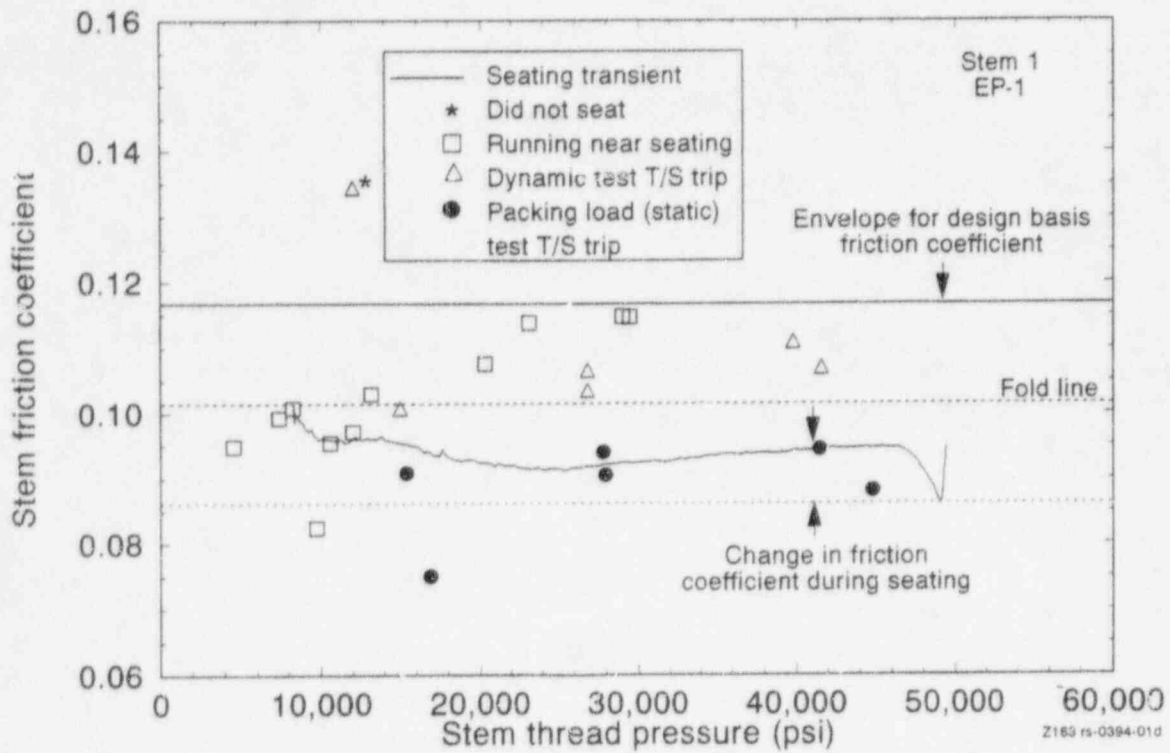


Figure A-2. The fold line method bounds the performance of Stems 1 and 2.

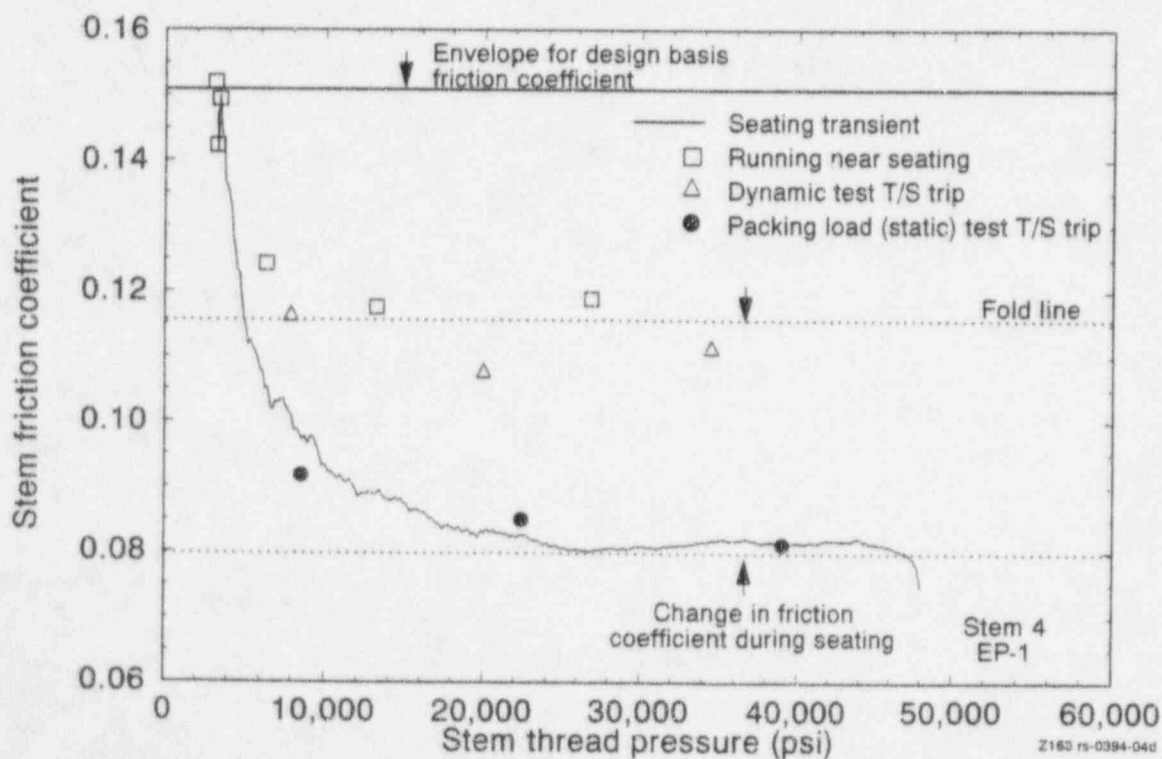
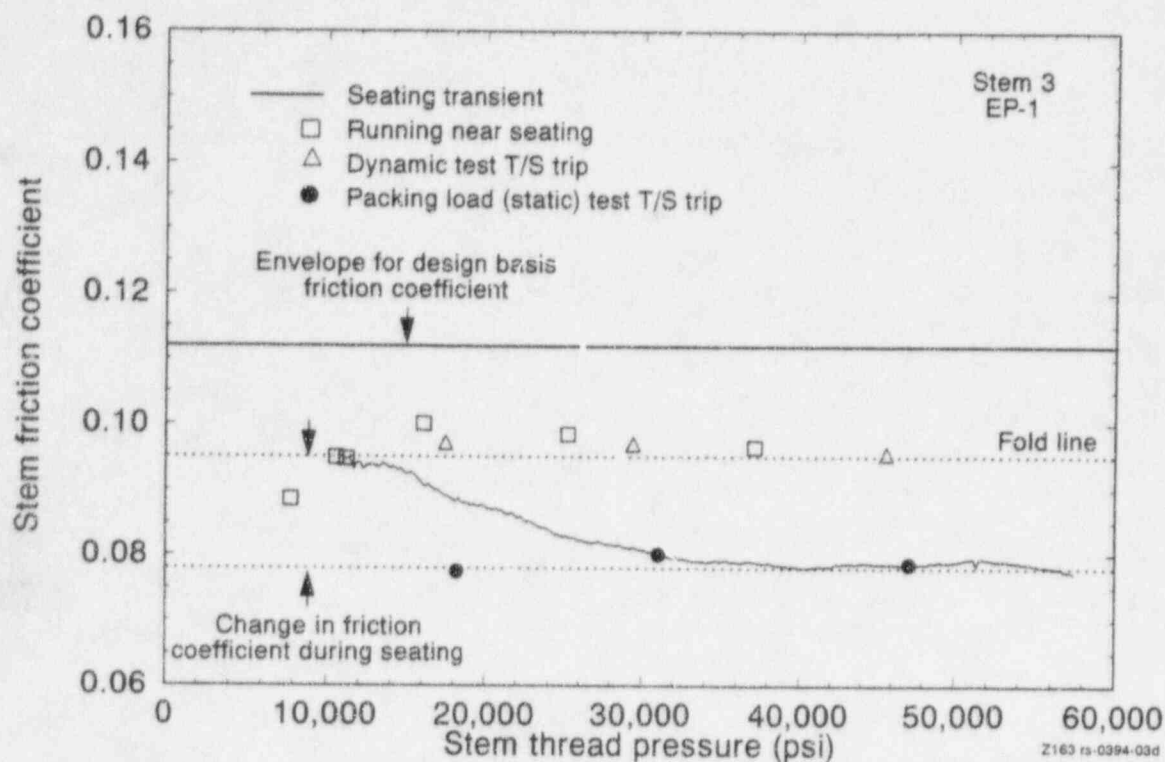


Figure A-3. The fold line method bounds the performance of Stems 3 and 4.

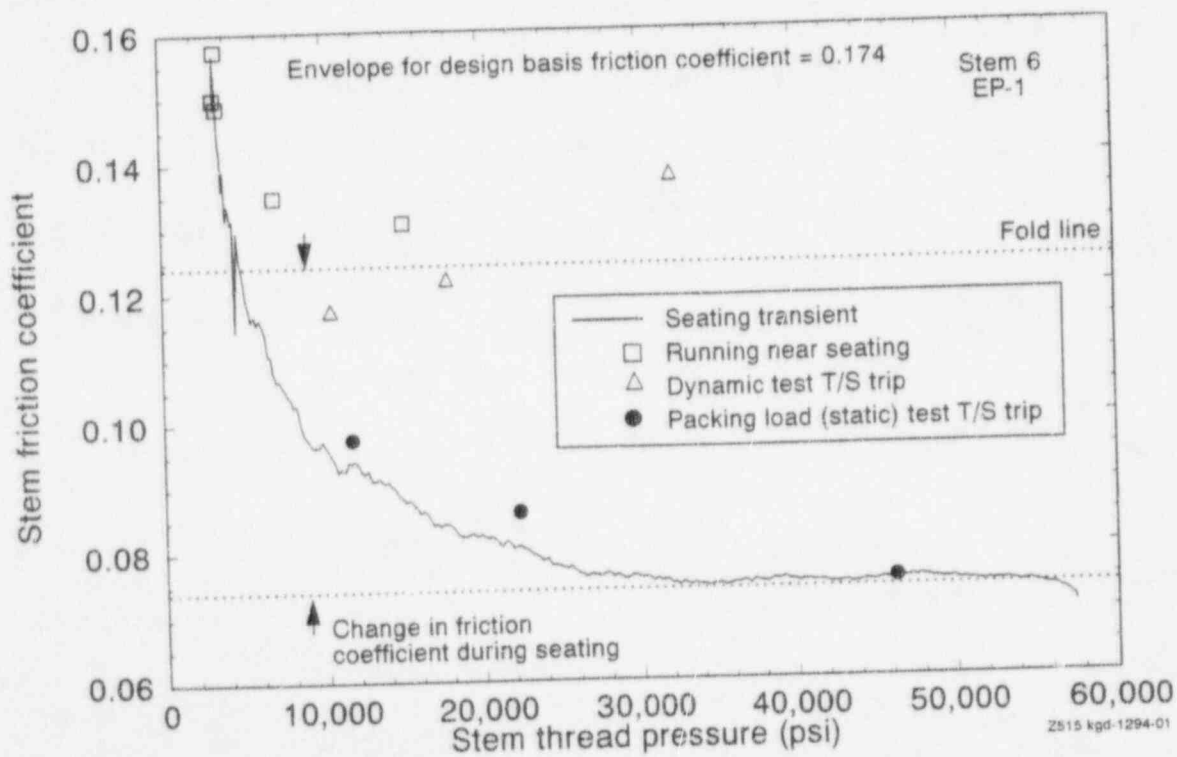
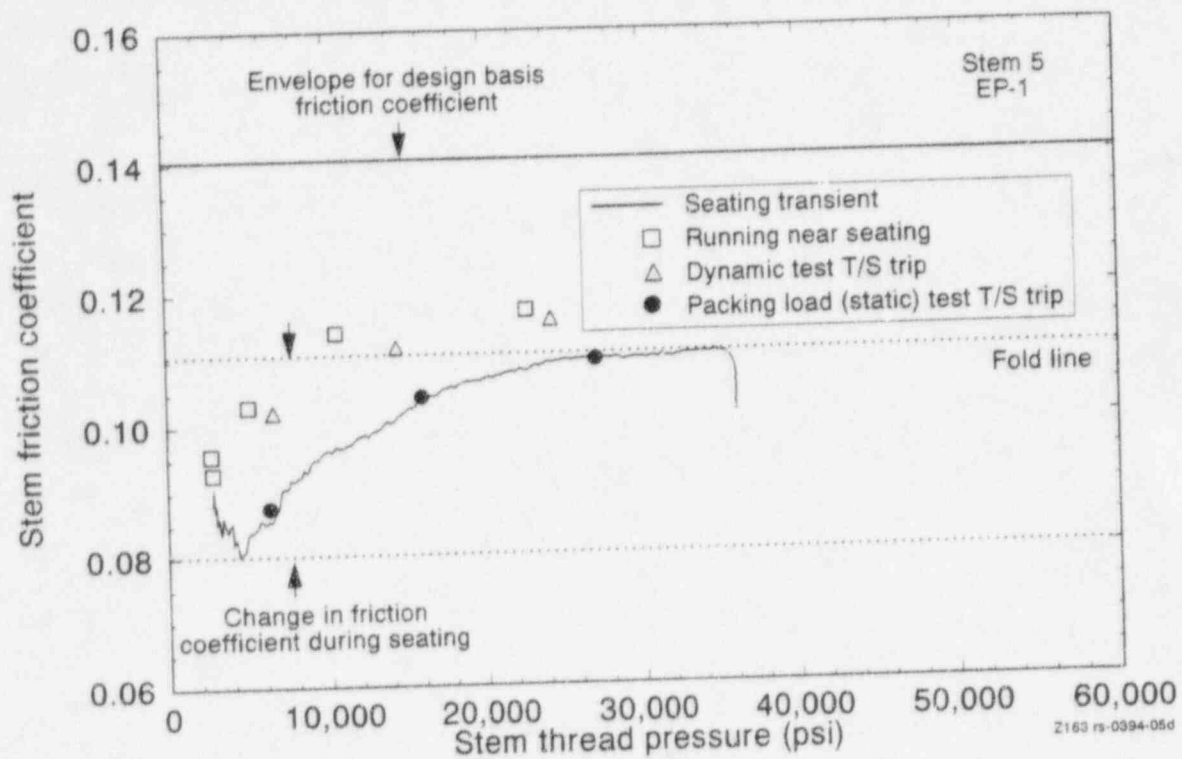


Figure A-4. The fold line method bounds the performance of Stems 5 and 6.

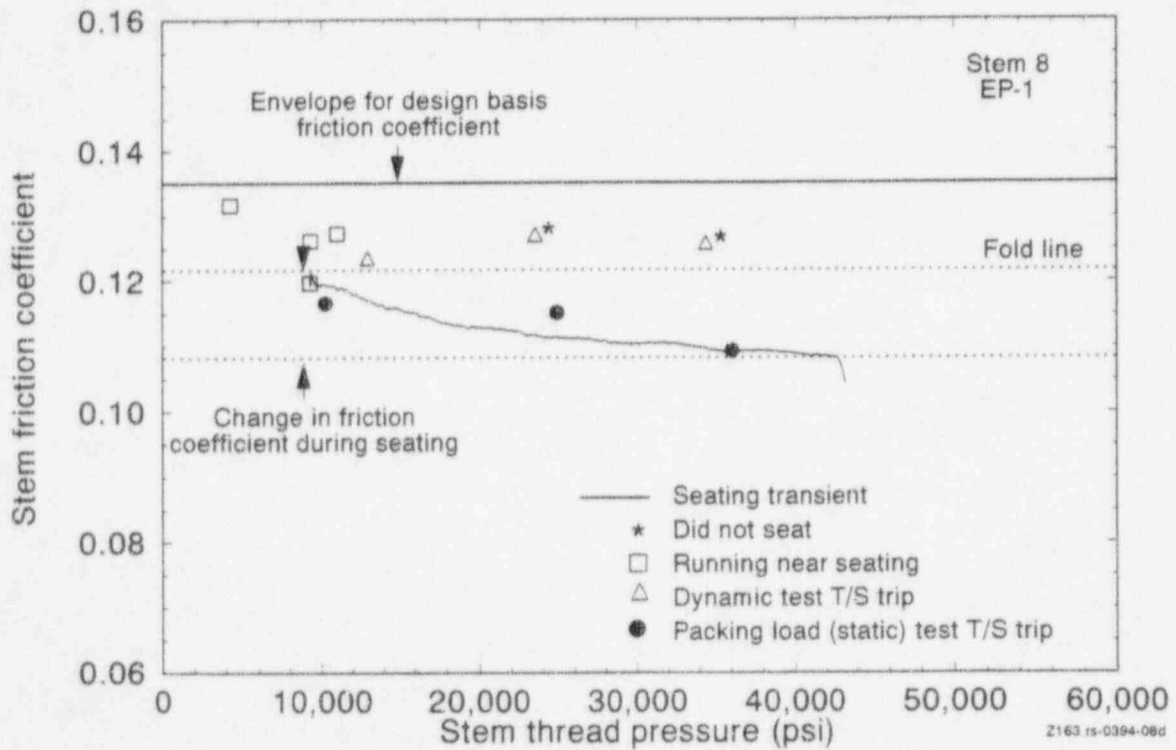
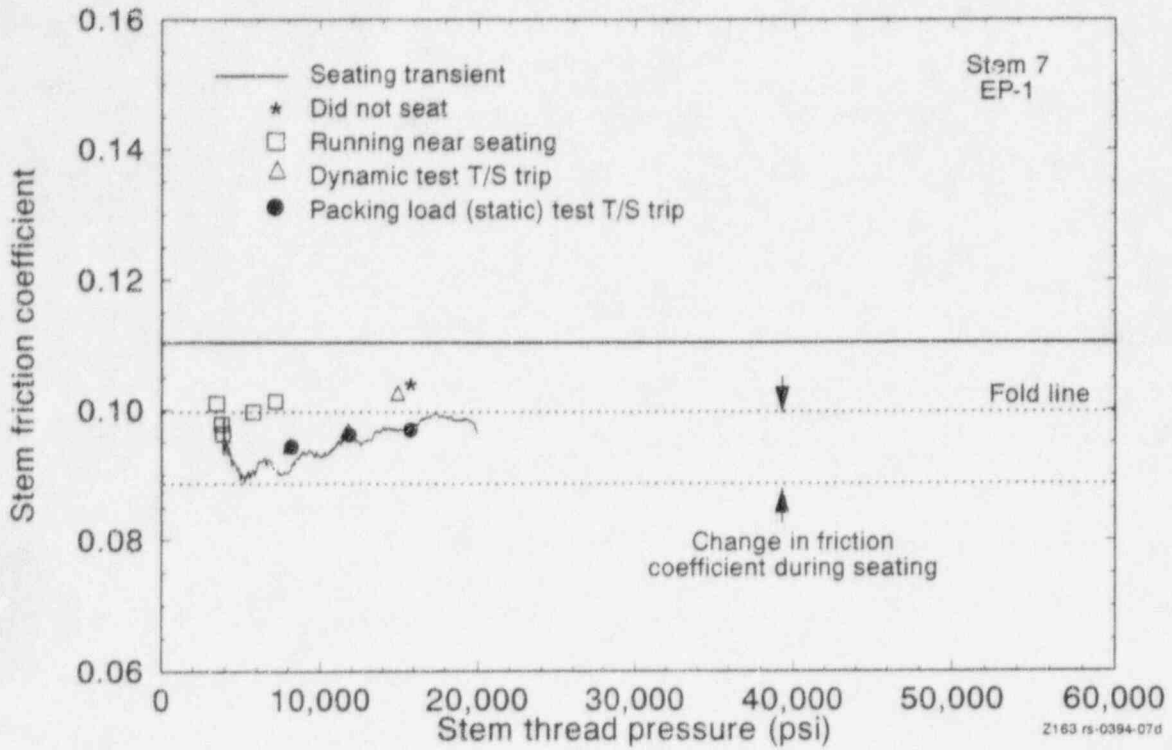


Figure A-5. The fold line method bounds the performance of Stems 7 and 8.

BIBLIOGRAPHIC DATA SHEET

(See instructions on the reverse)

1. REPORT NUMBER
*(Assigned by NRC. Add Vol., Suppl., Rev.,
and Addendum Numbers, if any.)*

NUREG/CR-6100
INEL-94/0156

2. TITLE AND SUBTITLE

Gate Valve and Motor-Operator Research Findings

3. DATE REPORT PUBLISHED

MONTH YEAR
September 1995

4. FIN OR GRANT NUMBER

A6857

5. AUTHOR(S)

R. Steele, Jr., K. G. DeWall, J. C. Watkins, M. J. Russell, D. Bramwell

6. TYPE OF REPORT

Technical

7. PERIOD COVERED *(Inclusive Dates)*

8. PERFORMING ORGANIZATION - NAME AND ADDRESS *(If NRC, provide Division, Office or Region, U.S. Nuclear Regulatory Commission, and mailing address. If contractor, provide name and mailing address.)*

Idaho National Engineering Laboratory
Lockheed Idaho Technology Company
P.O. Box 1625
Idaho Falls, Idaho 83415-0001

9. SPONSORING ORGANIZATION - NAME AND ADDRESS *(If NRC, type "Same as above" if contractor, provide NRC Division, Office or Region, U.S. Nuclear Regulatory Commission, and mailing address.)*

Division of Engineering Technology
Office of Nuclear Regulatory Research
U.S. Nuclear Regulatory Commission
Washington, D.C. 20555-0001

10. SUPPLEMENTARY NOTES

11. ABSTRACT *(200 words or less)*

This report provides an update on the valve research being sponsored by the U.S. Nuclear Regulatory Commission (NRC) and conducted at the Idaho National Engineering Laboratory (INEL). The research addresses the need to provide assurance that motor-operated valves can perform their intended safety function, usually to open or close against specified (design basis) flow and pressure loads. This report describes several important developments: (a) two methods for estimating or bounding the design basis stem factor (in rising-stem valves), using data from tests less severe than design basis tests; (b) a new correlation for evaluating the opening responses of gate valves and for predicting opening requirements; (c) an extrapolation method that uses the results of a best effort flow test to estimate the design basis closing requirements of a gate valve that exhibits atypical responses (peak force occurs before flow isolation); and (d) the extension of the original INEL closing correlation to include low-flow and low-pressure loads. The report also includes a general approach, presented in step-by-step format, for determining operating margins for rising-stem valves (gate valves and globe valves) as well as quarter-turn valves (ball valves and butterfly valves).

12. KEY WORDS/DESCRIPTORS *(List words or phrases that will assist researchers in locating the report.)*

Motor-operated valve (MOV)
Gate valve—disc load
Rising-stem valve—stem friction
MOV operating margin

13. AVAILABILITY STATEMENT

Unlimited

14. SECURITY CLASSIFICATION

(This Page)

Unclassified

(This Report)

Unclassified

15. NUMBER OF PAGES

16. PRICE



Federal Recycling Program

UNITED STATES
NUCLEAR REGULATORY COMMISSION
WASHINGTON, DC 20555-0001

SPECIAL FOURTH-CLASS MAIL
POSTAGE AND FEES PAID
USNRC
PERMIT NO. G-67

OFFICIAL BUSINESS
PENALTY FOR PRIVATE USE, \$300

120555139531 1 1AN1RM1R111S
US NRC-OADM
DIV FOIA & PUBLICATIONS SVCS
TPS-PDR-NUREG
2WFM-6E7
WASHINGTON DC 20555